



Universitetet
i Stavanger

DET TEKNISK-NATURVITENSKAPELIGE FAKULTET

MASTEROPPGAVE

Studieprogram/spesialisering: 2-årig master, Konstruksjoner og Materialer Fordypning Offshorekonstruksjoner	Vårsemesteret, 2015 Åpen / Konfidensiell
Forfatter: Anders Lysø Kleven (signatur forfatter)
Fagansvarlig: S. A. Sudath C. Siriwardane Veileder(e): Ole Gabrielsen, DNVGL Stavanger Andreas Aaslid, DNVGL Stavanger	
Tittel på masteroppgaven: Evaluering av SCFer for Avstivede Knutepunkt av Rørprofiler Engelsk tittel: Evaluation of SCFs for Stiffened Tubular Joints	
Studiepoeng: 30	
Emneord: Sveiste knutepunkt Hot spot spenning Utmatting FEM analyse Abaqus	Sidetall: 116 + vedlegg/annet: 81 Stavanger, 29.06.2015 dato/år

Abstract

In this thesis the field of stress concentration factors for use in fatigue analysis is explored. The focus is on stiffened tubular joints, which are common on offshore structures. An analysis methodology is established following a literature study of the subject. Shell and solid analysis is performed for different joint geometries, as well as determination of SCFs by use of parametric flume. Verification of the analysis methodology was performed on two types of joints. One of the joints is a verification specimen from DNVGL-RP-0005 [1]. The other is a simple tubular T-joint from a flare tower. Two case studies are then performed, to compare performance between a simple tubular joints and a stiffened tubular joint. The first case study compares two types of T-joints, one which is simple and one which is stiffened. The second case study is for tubular KT-joints. The first joint geometry is simple and the second is a stiffened joint. SCFs obtained through solid and shell FEM analysis are compared, as well as SCFs determined from parametric formulae.

Acknowledgements

Thanks to DNV GL Stavanger, dept. Offshore Structures, for giving me the opportunity to write about this interesting topic at their offices. Special thanks to Ole Gabrielsen and Andreas Aaslid for their theoretical, practical and technical assistance throughout the process of working with the thesis.

Thanks to my supervisor at the University of Stavanger, Sudath C. Siriwardane for his guidance and academic competence.

I would also like to thank my employer, Aibel Haugesund, for allowing me to use their software licenses and computer in my thesis work.

Finally I would like to thank my wife and family for their continued support through the demanding process of writing my master thesis in combination with working. This has taken up most of my spare time this half year, and I look forward to spend more time with my family.

Table of Contents

Abstract	iii
Acknowledgements	iv
1 Introduction	1
1.1 Background.....	1
1.2 Objective.....	1
1.3 Content.....	2
1.4 Abbreviations.....	3
2 Fatigue.....	4
2.1 General.....	4
2.2 Fatigue design approaches.....	4
2.3 S-N curves	5
2.4 Safety factors	6
2.5 Fatigue assessment methods.....	7
2.6 Stress Concentration Factors	9
2.6.1 Definition of stress concentration factor	9
2.6.2 Parametric SCF equations for simple tubular joints.....	9
2.6.3 Efthymiou SCF equations for simple tubular joints.....	10
2.6.4 Short chord effects	13
2.6.5 Types of hot spots	14
2.6.6 FEM analysis.....	14
2.6.7 Extrapolation of stresses.....	15
2.6.8 Derivation of hot spot stress.....	17
3 Finite element method.....	20
3.1 General.....	20
3.2 Shape functions.....	20
3.3 Isoparametric elements	21
3.4 Extrapolation with shape functions	21
4 Methodology	25
4.1 Purpose	25
4.2 Recommended practice.....	25
4.3 Extents of model and validity range	25
4.4 Modelling and assembly	26

4.5	Constraints	26
4.6	Boundary conditions	26
4.7	Loading and analysis steps	27
4.8	Meshing	27
4.8.1	Read out of stresses	28
4.9	Extrapolation procedure	28
4.9.1	Method A.....	28
4.9.2	Method B.....	30
4.10	Shell element selection	30
4.11	Solid element selection.....	30
4.12	Weld geometry	30
4.13	Mathcad extrapolation program for shell elements	31
4.14	Check of FEM model	31
4.15	Extraction of analysis output	32
5	Analysis of joints.....	33
5.1	Overview	33
5.1.1	Joint 1 – Verification specimen.....	33
5.1.2	Joint 2 – Simple T-joint.....	33
5.1.3	Joint 3 – Simple tubular T-joint with $\beta = 1$	33
5.1.4	Joint 4 – Stiffened tubular T-joint with $\beta = 1$	33
5.1.5	Joint 5 – Simple tubular KT-joint with $\beta = 1$	33
5.1.6	Joint 6 – Stiffened tubular KT-joint with $\beta = 1$	33
5.2	Joint 1 – Verification specimen 1	34
5.2.1	General	35
5.2.2	Joint 1 model overview	35
5.2.3	Joint 1 - Model I.....	36
5.2.4	Joint 1 – Model II.....	38
5.2.5	Joint 1 – Model III.....	40
5.2.6	Joint 1 – Model IV	42
5.2.7	Joint 1 – Model V.....	44
5.2.8	Result summary – Joint 1	46
5.3	Joint 2 – Simple T-joint.....	47
5.3.1	Introduction	47
5.3.2	General geometry	48
5.3.3	Comparison of chord lengths	48

5.3.4	Efthymiou SCFs	49
5.3.5	Evaluation of Efthymiou SCFs	49
5.3.6	Loading and boundary conditions	51
5.3.7	Methodology	51
5.3.8	Joint 2 – Model overview	53
5.3.9	Joint 2 – Stress distribution	53
5.3.10	Joint 2 – Model I	55
5.3.11	Joint 2 – Model II	57
5.3.12	Joint 2 – Model III	59
5.3.13	Joint 2 – Model IV	61
5.3.14	Joint 2 – Model V	64
5.3.15	Comparison of results.....	67
5.3.16	Sources of errors.....	68
5.4	Joint 3 and 4 – Case study – Tubular T-joint	70
5.4.1	Introduction	70
5.4.2	General geometry	70
5.4.3	Efthymiou SCFs Joint 3	73
5.4.4	Loads and boundary conditions.....	73
5.4.5	Assembly	73
5.4.6	Methodology	74
5.4.7	Joint 3 and 4 – Model overview	74
5.4.8	Stress distribution and screening.....	75
5.4.9	Joint 3 – Model I	79
5.4.10	Joint 4 – Model I to III	82
5.4.11	Joint 4 – Model IV	86
5.4.12	Comparison of results.....	87
5.5	Joint 5 and 6 – Case study – Tubular K-joint	89
5.5.1	Introduction	89
5.5.2	General geometry	89
5.5.3	Efthymiou SCFs joint 5.....	91
5.5.4	Loads and boundary conditions.....	91
5.5.5	Special load cases.....	92
5.5.6	Assembly	93
5.5.7	Methodology	93
5.5.8	Joint 5 and 6 – Model overview	93
5.5.9	Stress distribution and screening.....	94
5.5.10	Joint 5 – Model I	102

5.5.11	Joint 6 – Model I	104
5.5.12	Joint 6 – Model II	106
5.5.13	Comparison of results.....	108
6	Discussion	111
6.1	Efthymiou equations.....	111
6.2	FEM analysis results.....	111
6.3	Solid versus shell models	112
6.4	Design improvements of joints.....	112
6.5	Methodology for derivation of hot spot stress.....	113
7	Conclusion.....	114
8	References	116
Appendix A – Stress contours		1
A.1	Joint 1	1
A.2	Joint 2	6
A.3	Joint 3	18
A.4	Joint 4	20
A.5	Joint 5	36
A.6	Joint 6	40
Appendix B – Extrapolation spreadsheets		1
B.1	Joint 1	1
B.2	Joint 2	2
B.3	Joint 3	7
B.4	Joint 4	8
B.5	Joint 5	12
B.6	Joint 6	14
Appendix C – Efthymiou SCFs.....		1
C.1	Joint 2	1
C.2	Joint 3	2
C.3	Joint 5	3
Appendix D – Mathcad extrapolation program.....		1

1 Introduction

1.1 Background

Tubular joints are widely used in offshore structures, for example in jackets, bridges and flare towers. Some joints have a simple geometry while others have complex geometry. Offshore structures are in general subjected to fatigue due to environmental loads. Therefore it is important to properly estimate stress concentration factors at joints as these form the basis for fatigue life evaluations. Some parametric formulae exist for simple and ring-stiffened tubular joints, but most stiffened joints need separate FEM assessments to be made. The DNV GL Recommended Practice for Fatigue Design of Offshore Steel Structures, DNVGL-RP-0005, gives guidance on how to establish SCFs by use of the Finite Element Method.

1.2 Objective

The objective of this study is to explore how stress concentration factors for stiffened tubular joints may be established by use of the Finite Element Method. The scope of work consists of the following.

- Perform a literature study on current knowledge on how to establish SCFs for simple and complex tubular joints
- Study methodologies described in current knowledge
- Select joint geometries for which current SCF formulae are applicable
- Select joint geometries for which current SCF formulae are not applicable
- Establish FE models for both types of geometries, both using shell and solid elements
- Establish SCFs for axial, in-plane and out-of-plane loading
- Compare results from formulae (where applicable), shell models and solid models

Two case studies for simple versus stiffened tubular joints have been investigated to evaluate fatigue performance against each other.

Typically the investigated joints are from flare tower structures. Ring-stiffened tubular joints have been extensively investigated in several previous works, so the focus of this thesis is on tubular joints stiffened in other ways.

The joints are modelled in the FEM analysis software Abaqus.

1.3 Content

8 general geometries have been investigated in this thesis, named Joint 1 to 6. Joints 2-6 are all examples of joints found in flare towers on offshore structures.

Joint 1 is a verification geometry from DNVGL-RP-0005 [1], where the objective is to verify the FEM analysis methodology. A target SCF is listed in the standard, and we can compare the accuracy of our results against this SCF. Result accuracy is of course very dependent on geometry and what applications each element type is best suited for, but it gives some indication of element performance.

Joint 2 is also used as a form of verification. This joint is a simple tubular T-joint found on a flare tower structure. Efthymiou SCFs have been calculated and are used for comparison with FEM results. Shell models with identical geometry but other varying parameters have been analysed and compared to these results. Also solid models with the weld toe included in the analysis have been analysed. All results are compared against each other and against Efthymiou SCFs, as well as some evaluation of the Efthymiou SCFs according to HSE tables [2] which are comparing Efthymiou results against real world test results.

Joint 3 and 4 make up a case study where a simple tubular T-joint with brace and chord of the same diameter is compared to a stiffened tubular T-joint with the same geometry, except for the stiffener arrangement. The goal of this study is to evaluate the fatigue performance of the two different joints. By varying the plate thickness for the stiffeners, the design of the joint is investigated to try to obtain a balanced stress distribution, and as a result a longer fatigue life. Shell model analysis is performed for both joints, as well as a solid model analysis for joint 4. The study also includes a discussion of the practical advantages of each type of joint.

For joints 5 and 6 there is another case study, this one regarding simple tubular KT-joints with equal diameter chord and brace, against a stiffened tubular KT-joint with the same geometry. Again the objective is to compare fatigue performance for the two designs. Shell model analysis has been performed for both joints, as well as a solid model including weld geometry for joint 6.

1.4 Abbreviations

ABS	American Bureau of Shipping
DNV	Det Norske Veritas
BC	Brace Chord
BS	Brace Saddle
CC	Chord Crown
CS	Chord Saddle
DFF	Design Fatigue Factor
FE	Finite Element
FEM	Finite Element Method
HSS	Hot Spot Stress
HSSR	Hot Spot Stress Range
IIW	International Institute of Welding
IPB	In-plane bending
OD	Outer diameter
OPB	Out-of-plane bending
RHS	Rectangular Hollow Section
SCF	Stress Concentration Factor

2 Fatigue

2.1 General

Fatigue refers to the damage caused by repeated application of time-varying stresses at specific locations of a structure. These time-varying stresses are caused by variable actions, typically environmental loads.

All components of a structure are potentially sensitive to fatigue damage accumulation. In particular, every welded connection, every connection joined by other means than welding, every attachment, every structural discontinuity, and every place where some form of stress concentration is present is a potential location of fatigue cracking and can require individual consideration [3].

2.2 Fatigue design approaches

There are a few different approaches to fatigue design. Normally it is checked if the structural detail matches an existing classification of details. If this is the case, the so-called nominal stress approach is suitable. For these structural details, the nominal stress over the cross section is used. The classification of the structural detail then refers to a suitable S-N curve which is used for the fatigue design. This method has the advantage of simplicity, but the catalogue of classification limited in selection of structural details.

If there is no classification available for a structural detail the structural hot spot stress approach is an alternative. DNVGL-RP-0005 [1] refers to chapter 4 which involves FEM analysis and determination of local stress concentration factors. This involves modelling the local geometry in a sufficiently detailed manner, applying a nominal load, and reading out stresses to be used for calculation of the hot spot stress. Fatigue design based on the calculated hot spot stress performed, usually in conjunction with the D curve, or in case of a tubular joint the T curve. There are some exceptions to this choice of S-N curve which is noted later.

The effective notch stress approach is also available. This approach is mainly based on the computed highest elastic stress at the crack initiation points. In the FEM model, the notch itself is modelled, usually with a 1mm radius. The effective notch approach is included in [1,

4] as an alternative approach. The very fine mesh density required in this method requires significant modelling work, and can often produce larger models.

2.3 S-N curves

Fatigue design is based on the use of S-N curves, which are the obtained from fatigue tests. The S-N curves included in [1] are based on the mean-minus-two-standard-deviation curves for the relevant experimental data. This correlates to a 97.5% probability of survival.

For practical design, all welded joints are classified to a corresponding design S-N curve. All tubular joints are assumed to be class T. Other types of joint should be classified as one of the 14 other classes of details included in Appendix A of [1]. The class of the detail depends on geometrical arrangement of the detail, direction of the fluctuating stress and the method of fabrication and inspection of the detail.

The basic design S-N curve is given as [1]

$$\log N = \log \bar{a} - m \log \Delta\sigma$$

N = predicted number of cycles to failure for stress range $\Delta\sigma$

$\Delta\sigma$ = stress range with unit MPa

m = negative inverse slope of S-N curve

$\log \bar{a}$ = intercept of log N-axis by S-N curve

$$\log \bar{a} = \log a - 2s_{\log N}$$

where

$\log a$ = intercept of mean S-N curve with the log N axis

$s_{\log N}$ = standard deviation of log N

The fatigue strength of welded joints is also dependent to some extent on plate thickness. The thickness effect is taken into account by modifying the stress so the design S-N curves for thicknesses larger than reference thickness is altered to

$$\log N = \log \bar{a} - m \log \left(\Delta\sigma \left(\frac{t}{t_{ref}} \right)^k \right)$$

t_{ref} = reference thickness equal to 25mm for welded connections other than tubular joints.
For tubular joints t_{ref} is 32mm. For bolts t_{ref} is 25mm.

t = thickness through which a crack will most likely grow. $t = t_{ref}$ is used for a thickness less than t_{ref}

k = thickness exponent on fatigue strength

The effect of the weld notch is included in the S-N curves, which is why we can disregard the notch stress and linearize the structural stress when using the hot spot method.

Normally when using the hot spot stress methodology the D curve is used, or the T curve in case of a tubular joint. The structural stress concentration embedded in the details of these classes of S-N curves is 1.

This is not always the case however. For example for two RHS members joined with a full penetration weld, welded for the outside without a backing bar, the calculated hot spot stress would equal nominal stress since there is no change in the cross section. However if we see in Appendix A of [1] we observe that this type of detail is classed as an F3 detail, which implies the use of a lower S-N curve.

2.4 Safety factors

The mean-minus-two-standard-deviation S-N curve is part of what sets the safety level of the fatigue calculations. There are no load or partial factors from NORSOK applied to the fatigue calculations. Based on the failure consequences and the accessibility for inspection, maintenance and repair of a detail, a design fatigue factor (DFF) is applied. This can range from 1 for a readily accessible detail with no substantial consequences if failure occurs, to 10 if the consequences are substantial and it is not accessible for inspection.

The factor is applied to the number of load cycles, meaning the detail is designed for 1 to 10 times the estimated design life of the structure, depending on the magnitude of the DFF.

2.5 Fatigue assessment methods

Simplified analysis is an indirect fatigue assessment, based on limiting a predicted stress range to below a predicted stress range. This method is often used as basis of a fatigue screening technique. Failure of a detail using this method does not exclude verifying its adequacy with more sophisticated methods [5].

Deterministic analysis uses an artificial representation of the true random nature of the wave environment. This method has some similarities with conventional design wave analysis in that environmental actions and structural responses are calculated directly by periodic waves. This method is not recommended for final check of structures in a harsh fatigue environment however, but has some applications for screening purposes. The method requires less computational effort than the spectral analysis, but still significant work is required [3].

Spectral analysis is the method best able to represent the random nature of a wave environment, and as such is the most comprehensive and reliable assessment method for fatigue due to wave action. It accounts for the influence of the frequency of excitation on actions as well as on structural response. Fundamentally the task of a spectral fatigue analysis is the determination of the stress range transfer function $H_\sigma(\omega|\theta)$, which expresses the relationship between stress σ at a particular structural location per 'unit wave height', wave of frequency ω and heading θ . The spectral method is a complex and numerically intensive technique. A thorough explanation of this is found in references [3, 5].

In deterministic and spectral analysis the fatigue damage on the structures is calculated by adding the contributions from each individual load cycle. This is called the Palmgren-Miners rule [1] and is stated as

$$D = \sum_{i=1}^k \frac{n_i}{N_i} = \frac{1}{\bar{a}} \sum_{i=1}^k n_i \cdot (\Delta\sigma_i)^m \leq \eta$$

D = accumulated fatigue damage

\bar{a} = intercept of the design S-N curve with the log N axis

m = negative inverse slope of the S-N curve

k = number of stress blocks

n_i = number of stress cycles in stress block i

N_i = number of cycles to failure at constant stress range $\Delta\sigma_i$

η = usage factor (1 / DFF)

Many variables are involved with establishing the load and stress history of the structure, and uncertainties in fatigue analysis are often connected to this process as well.

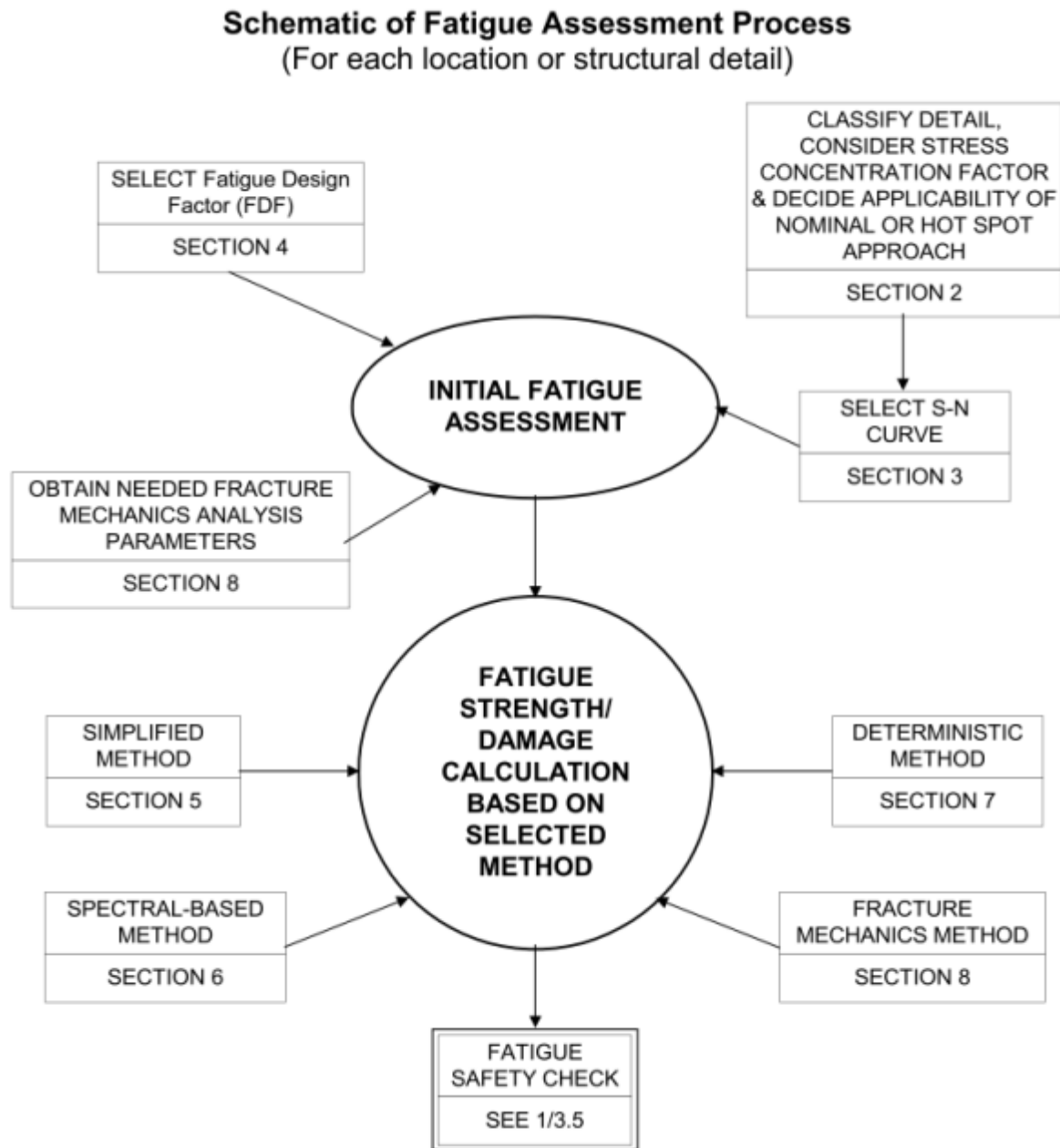


Figure 2-1: Schematic of fatigue assessment process [5]

2.6 Stress Concentration Factors

2.6.1 Definition of stress concentration factor

A SCF is defined as the ratio of hot spot stress range over nominal stress range. The SCF takes into account of the geometry of the detail, but excludes the notch stress due to the discontinuity at the weld toe. Hot spot stress is the sum of the membrane stress and the bending stress, but excludes the non-linear stress due to the weld notch.

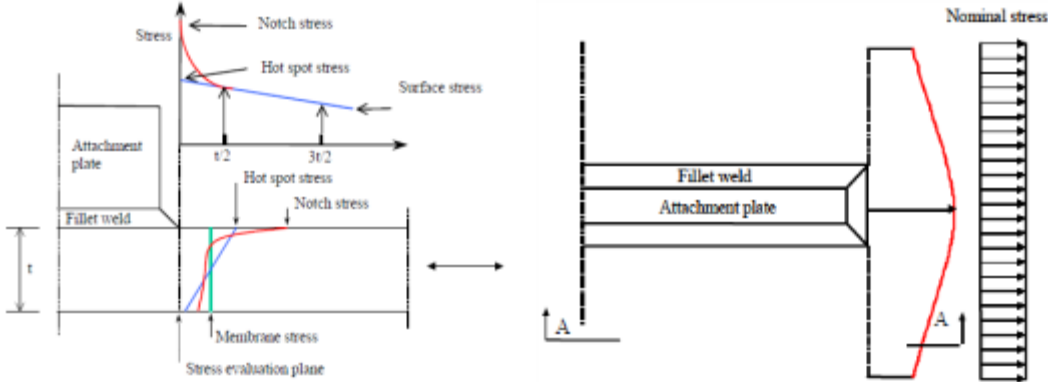


Figure 2-2: Stress distribution at a hot spot [1]

2.6.2 Parametric SCF equations for simple tubular joints

For design of simple tubular joints it is standard practice to use parametric equations for derivation of the stress concentration factors to obtain hot spot stress for the actual geometry. The commonly most recognized set of SCF equations for simple tubular joints are the Efthymiou equations. These are included in many design codes and recommended practices [1, 3, 6]. In a comparison studies performed by Lloyd's Register, the Efthymiou SCF equations were found to provide a good fit the SCF database, with bias of about 10% to 25% on the conservative side [2, 3].

The validity range of the Efthymiou equations

$$\begin{aligned}
 0.2 &\leq \beta \leq 1.0 \\
 0.2 &\leq \tau \leq 1.0 \\
 8 &\leq \gamma \leq 32 \\
 4 &\leq \alpha \leq 40 \\
 20^\circ &\leq \theta \leq 90^\circ \\
 \frac{-0.6\beta}{\sin \theta} &\leq \xi \leq 1.0
 \end{aligned}$$

2.6.3 Efthymiou SCF equations for simple tubular joints

2.6.3.1 Geometrical parameters

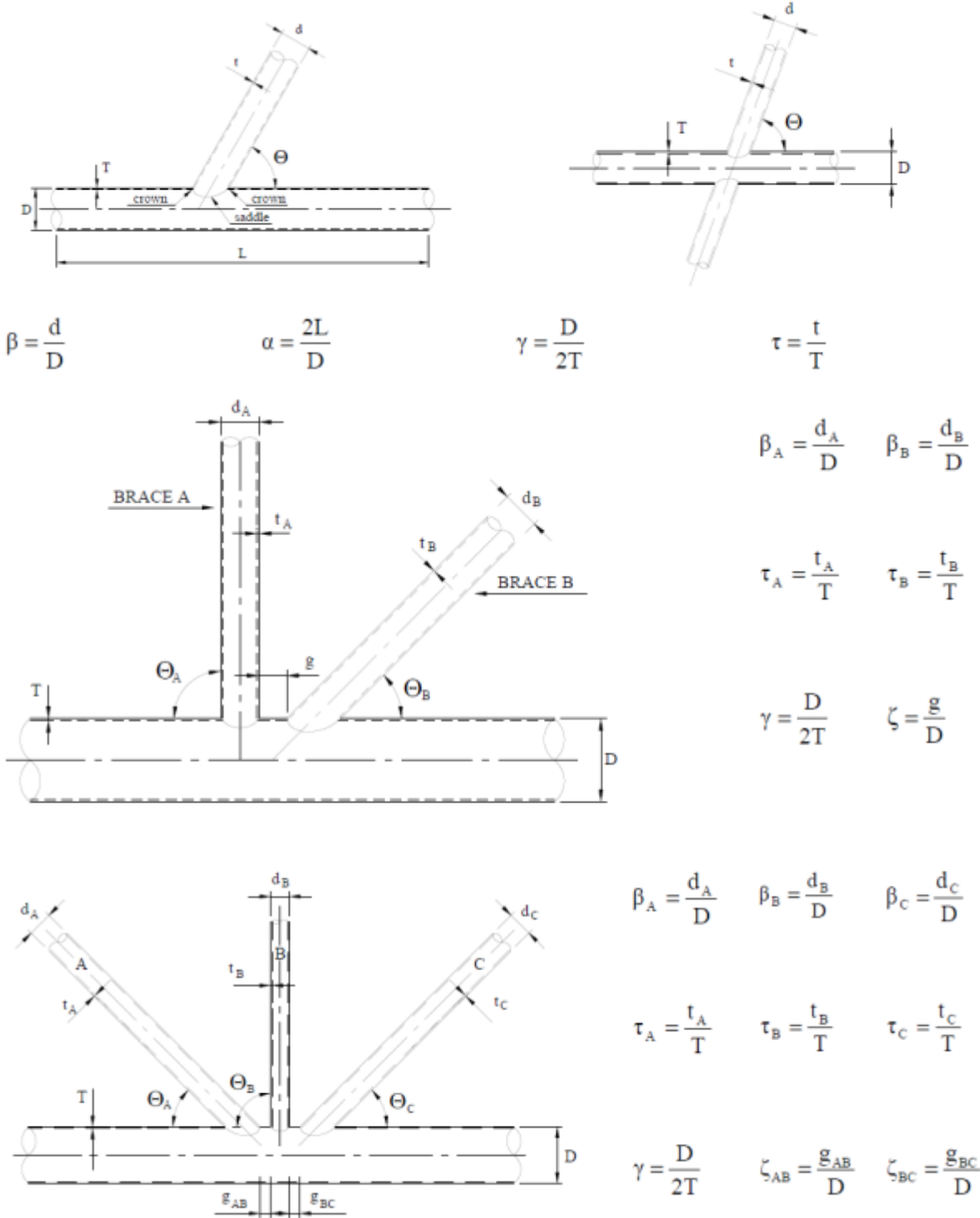


Figure 2-3: Description of geometrical parameters for tubular joints, Ref [1]

2.6.3.2 Parametric SCF equations for simple T/Y-joints

Of simple tubular joints only a T-joint has been investigated in this thesis. Only formulas used in this thesis is listed below, without short chord correction factor or chord end fixity parameter correction.

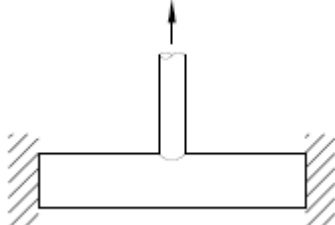
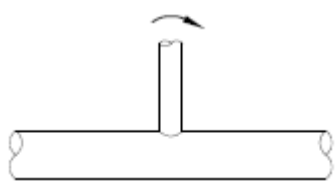
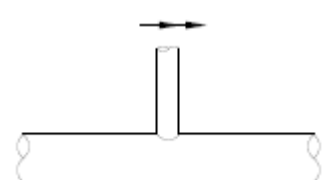
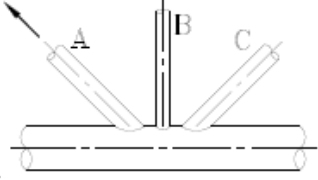
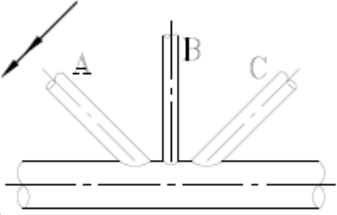
<p style="text-align: center;">Axial load Chord ends fixed</p> 	<p>Chord saddle: $\gamma\tau^{1.1}(1.11 - 3(\beta - 0.52)^2)(\sin\theta)^{1.6}$</p> <p>Chord crown: $\gamma^{0.2}\tau(2.65 + 5(\beta - 0.65)^2) + \tau\beta(0.25\alpha - 3)\sin\theta$</p> <p>Brace saddle: $1.3 + \gamma\tau^{0.52}\alpha^{0.1}(0.187 - 1.25\beta^{1.1}(\beta - 0.96))(\sin\theta)^{(2.7-0.01\alpha)}$</p> <p>Brace crown: $3 + \gamma^{1.2}(0.12e^{(-4\beta)} + 0.011\beta^2 - 0.045) + \beta\tau(0.1\alpha - 1.2)$</p>
<p style="text-align: center;">In-plane bending</p> 	<p>Chord crown: $1.45\beta\tau^{0.85}\gamma^{(1-0.68\beta)}(\sin\theta)^{0.7}$</p> <p>Brace crown: $1 + 0.65\beta\tau^{0.4}\gamma^{(1.09-0.77\beta)}(\sin\theta)^{(0.06\gamma-1.16)}$</p>
<p style="text-align: center;">Out-of-plane bending</p> 	<p>Chord saddle: $\gamma\tau\beta(1.7 - 1.05\beta^3)(\sin\theta)^{1.6}$</p> <p>Brace saddle: $\tau^{-0.54}\gamma^{-0.05}(0.99 - 0.47\beta + 0.08\beta^4)$ $* \gamma\tau\beta(1.7 - 1.05\beta^3)(\sin\theta)^{1.6}$</p>

Table 2-1: Efthymiou SCF formulas, Ref [1]

2.6.3.3 Parametric SCF equations for simple KT-joints

<p style="text-align: center;">Axial load on one brace only</p> 	<p>Chord saddle: $\gamma\tau^{1.1}(1.11 - 3(\beta - 0.52)^2)(\sin\theta)^{1.6} + C_1 * (0.8\alpha - 6)\tau\beta^2(1 - \beta^2)^{0.5}(\sin 2\theta)^2$</p> <p>Chord crown: $\gamma^{0.2}\tau(2.65 + 5(\beta - 0.65)^2) + \tau\beta(C_2\alpha - 3)\sin\theta$</p> <p>Brace saddle: $1.3 + \gamma\tau^{0.52}\alpha^{0.1}(0.187 - 1.25\beta^{1.1}(\beta - 0.96))(\sin\theta)^{(2.7-0.01\alpha)}$</p> <p>Brace crown: $3 + \gamma^{1.2}(0.12e^{(-4\beta)} + 0.011\beta^2 - 0.045) + \beta\tau(C_3\alpha - 1.2)$</p>
<p style="text-align: center;">In-plane bending</p>	<p>Chord crown: $1.45\beta\tau^{0.85}\gamma^{(1-0.68\beta)}(\sin\theta)^{0.7}$</p> <p>Brace crown: $1 + 0.65\beta\tau^{0.4}\gamma^{(1.09-0.77\beta)}(\sin\theta)^{(0.06\gamma-1.16)}$</p>
<p style="text-align: center;">Out-of-plane bending on one brace only</p> 	<p>Chord SCF adjacent to diagonal brace A: $\gamma\tau_A\beta_A(1.7 - 1.05\beta_A^3)(\sin\theta_A)^{1.6} \cdot (1 - 0.08(\beta_B\gamma)^{0.5} \exp(-0.8x_{AB})) \cdot (1 - 0.08(\beta_C\gamma)^{0.5} \exp(-0.8x_{AC}))$</p> <p>where</p> $x_{AB} = 1 + \frac{\zeta_{AB}\sin\theta_A}{\beta_A}$ $x_{AC} = 1 + \frac{(\zeta_{AB} + \zeta_{BC} + \beta_B)\sin\theta_A}{\beta_A}$

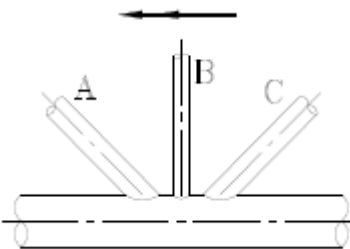
<p>Out-of-plane bending on one brace only</p> 	<p>Chord SCF adjacent to central brace B:</p> $\gamma\tau_B\beta_B(1.7 - 1.05\beta_B^3)(\sin\theta_B)^{1.6} \cdot$ $(1 - 0.08(\beta_A\gamma)^{0.5} \exp(-0.8x_{AB}))^{P_1} \cdot$ $(1 - 0.08(\beta_C\gamma)^{0.5} \exp(-0.8x_{BC}))^{P_2}$ <p>where</p> $x_{AB} = 1 + \frac{\zeta_{AB}\sin\theta_B}{\beta_B}$ $x_{BC} = 1 + \frac{\zeta_{BC}\sin\theta_B}{\beta_B}$ $P_1 = \left(\frac{\beta_A}{\beta_B}\right)^2$ $P_2 = \left(\frac{\beta_C}{\beta_B}\right)^2$
---	---

Table 2-2: Efthymiou SCF formulas, Ref [1]

Formulae for the cases of balanced axial load and unbalanced out-of-plane bending are also provided in [1], but are not used in this thesis.

2.6.4 Short chord effects

Certain effects come into play when $12 > \alpha$, this translates to a chord length less than 6 times the diameter of the chord. The boundary conditions will start restricting the ovalization of the chord at the joint intersection, causing disturbance in the stress field at the joint intersection, and effectively reducing the SCFs at the saddle position. Crown SCFs have been found not to be affected by a short chord. They are however heavily dependent on α because of the influence of beam bending at the crown position [7].

2.6.5 Types of hot spots

In the IIW recommendations [4], distinction is made between types a, b and c hot spots. Further, extrapolation method is determined by hot spot type. In DNVGL recommendations [1], different types of hot spots are described, but there is no mention of separate extrapolation method depending on hot spot type. It is mentioned that care should be given to possible stress underestimations particularly for hot spots of type b.

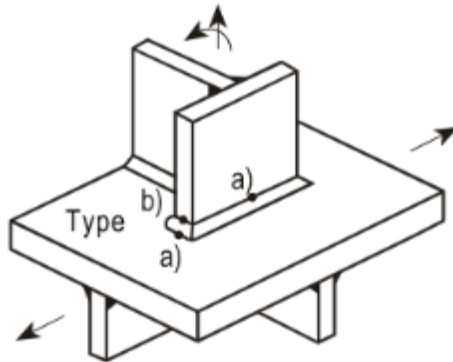


Figure 2-4: Types of hot spots [4]

2.6.6 FEM analysis

The methodology for determining SCFs by FEM analysis is described in the DNVGL recommended practice [1]. It is recommended to perform shell element analysis, but solid element analysis is an alternative. Element selected must be able to allow for steep stress gradients as well as plate bending.

For shell element analyses, 8-noded shell elements with reduced integration are recommended. Welds are not normally modelled, except for special cases where results are affected by high local bending. Here welds may be included by transverse plate elements having appropriate stiffness or by introducing constraints for coupled node displacements. Thickness equal to 2 times the thickness of the plates may be used for modelling the welds by transverse plates. Mesh size from $t \times t$ to $2t \times 2t$ may be used, and it is mentioned that larger mesh size at the hot spot location may produce a non-conservative result. For efficient read out of stresses a mesh of $t \times t$ is preferred.

For more complex cases solid elements may be used, and for solid element models an isoparametric 20-node solid element with reduced integration is recommended. Modelling of welds for solid element models is generally recommended and can be performed as shown in the figure below.

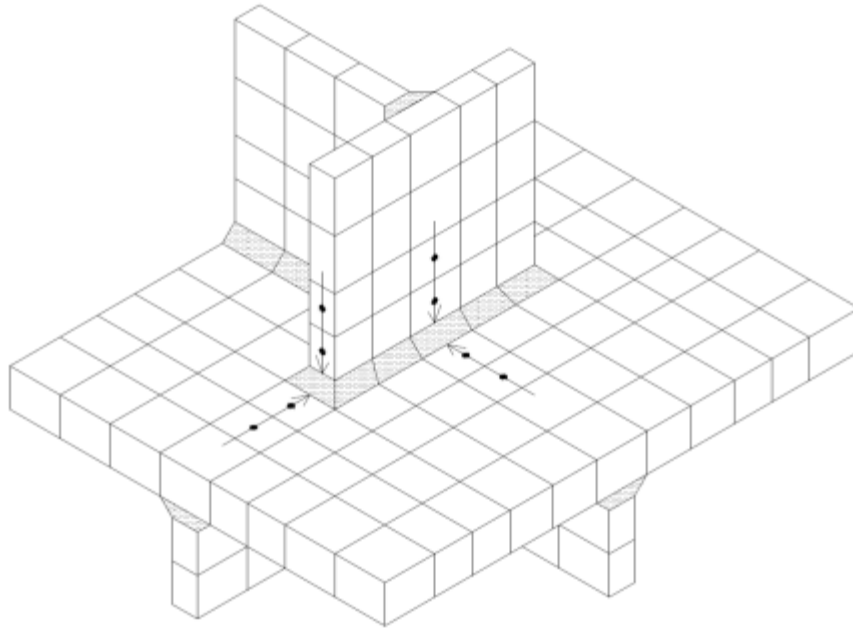


Figure 2-5: Plot of suggested modelling of welds for solid models and stress read out point locations [1]

2.6.7 Extrapolation of stresses

Stress components may be read out directly from mid side nodes for shell and solid elements, and averaged stresses can be used. The read out points are dependent on whether or not the detail is a tubular joint. For tubular joints read out points a and b are used, while for joints other than tubular joints, read out points 0.5t and 1.5t are used. See figure 2-4 for read out points for general joints, and figure 2-5 for read out points for tubular joints.

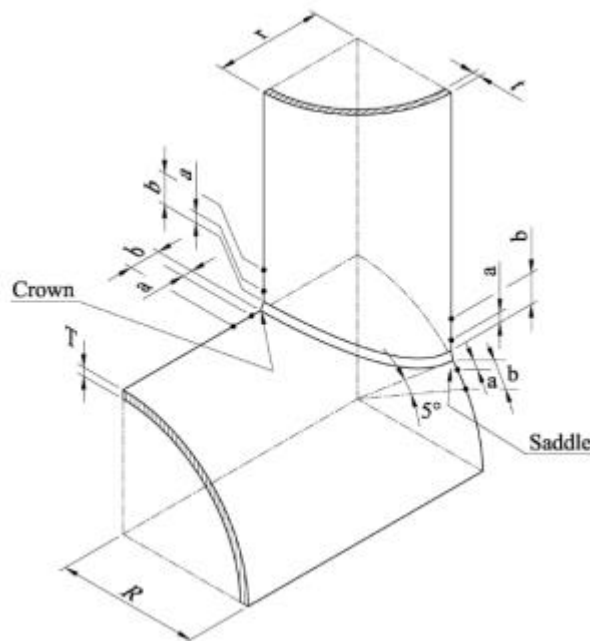


Figure 2-6: Stress read out points for a tubular joint [1]

Points a and b are dependent on radius and thickness of the member and chord.

For extrapolation of stress along the brace surface normal to the weld toe

$$a = 0.2\sqrt{rt}$$

$$b = 0.65\sqrt{rt}$$

For extrapolation of stress along the chord surface normal to the weld toe at the crown position

$$a = 0.2\sqrt{rt}$$

$$b = 0.4\sqrt[4]{rtRT}$$

For extrapolation of stress along the chord surface normal the weld toe at the saddle position

$$a = 0.2\sqrt{rt}$$

$$b = 2\pi R \frac{5}{360} = \frac{\pi R}{36}$$

IIW recommendations [4] states more options regarding stress read out points for regular joints. For example there is the option of having a finer mesh than $t \times t$, with read out points at $0.4t$ and $1.0t$. There are also separate stress read out locations for type b hot spots, since the stress distribution on the plate edge is not dependent on plate thickness. These are included for information, but are not used in the thesis.

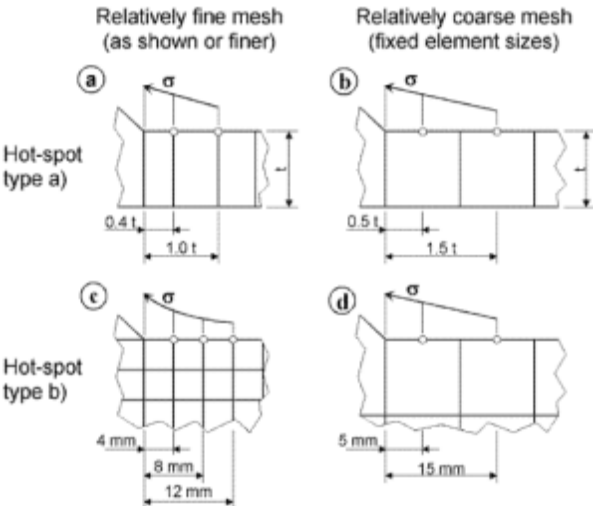


Figure 2-7: IIW [4] stress read out point locations

There is some dissent on the subject of which stresses to extrapolate. IIW [8] states that the strictly correct way of extrapolating stresses is to extrapolate component stresses to the hot spot and calculating the principal stress at the hot spot, but proposes that extrapolating principal stresses is an acceptable method. ABS [5] suggests read out of component stresses for extrapolation and calculation of principal stress at the hot spot. DNVGL [1] provides no discussion of the methodology, but mentions stress components as the stresses sampled at read out points.

If extrapolation from integration points has to be performed manually, it should be done in the manner shown in the figure below

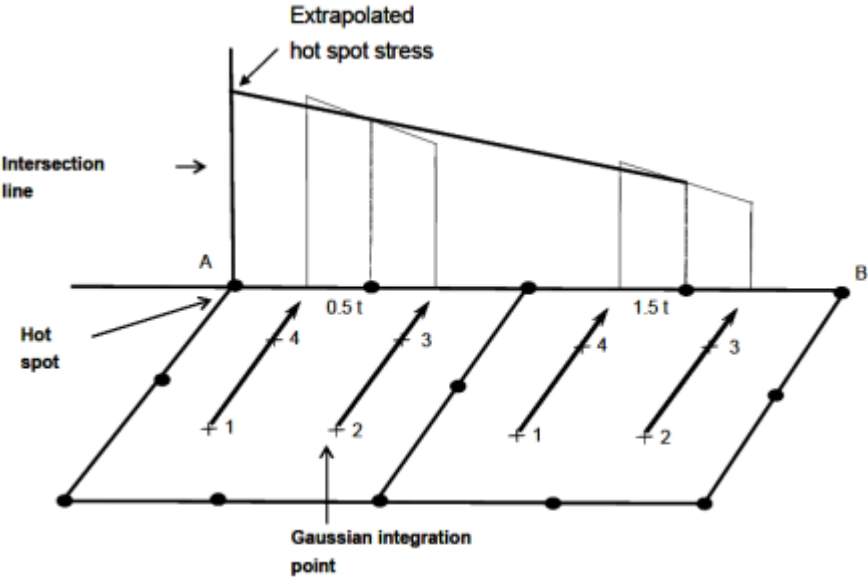


Figure 2-8: Extrapolation from integration points [1]

One should be mindful of the locations of the integration points when performing these extrapolations. Refer to software documentation [9] and FEM theory [10].

2.6.8 Derivation of hot spot stress

DNVGL [1] provides two options for derivation of hot spot stress, method A and method B. Both methods are perceived as equal to the reader as no recommendations are made on strengths or weaknesses of the two methods, or when to use any method over the other. It is clear that method B requires the least amount of manual work, and is typically preferred for daily use by many engineers.

2.6.8.1 Method A

For modelling with shell elements without any weld included in the model the stresses read out at from points 0.5t and 1.5t are to be extrapolated to the joint intersection. In the case of solid elements with the weld included the stresses are to be read out at 0.5t and 1.5t away from the weld toe, and extrapolated to the weld toe.

The linear extrapolation formula for 0.5t and 1.5t to hot spot location

$$\sigma_{hs} = 1.5\sigma_{0.5t} - 0.5\sigma_{1.5t}$$

Effective hot spot stress range to be used together with the hot spot S-N curve is derived as

$$\sigma_{eff} = \max \left\{ \begin{array}{l} \sqrt{\Delta\sigma_{\perp}^2 + 0.81\Delta\tau_{\parallel}^2} \\ \alpha|\Delta\sigma_1| \\ \alpha|\Delta\sigma_2| \end{array} \right.$$

where

$\alpha = 0.90$ if the detail is classified as C2 with stress parallel to the weld at the hot spot

$\alpha = 0.80$ if the detail is classified as C1 with stress parallel to the weld at the hot spot

$\alpha = 0.72$ if the detail is classified as C with stress parallel to the weld at the hot spot

The principal stresses for plane stress are calculated as

$$\sigma_1 = \frac{\sigma_{\perp} + \sigma_{\parallel}}{2} + \frac{1}{2}\sqrt{(\sigma_{\perp} - \sigma_{\parallel})^2 + 4\tau_{\parallel}^2}$$

$$\sigma_2 = \frac{\sigma_{\perp} + \sigma_{\parallel}}{2} - \frac{1}{2}\sqrt{(\sigma_{\perp} - \sigma_{\parallel})^2 + 4\tau_{\parallel}^2}$$

The equation for effective stress is made to account for the situation with fatigue cracking along a weld toe and fatigue cracking when the principal stress direction is more parallel with the weld toe [1].

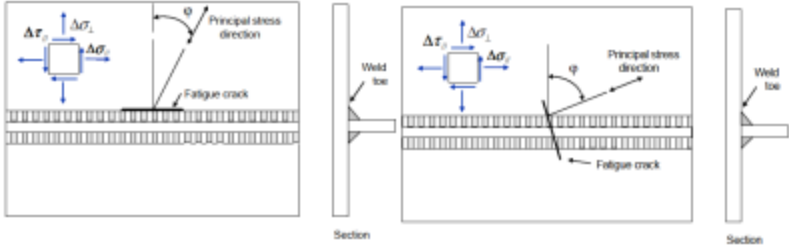


Figure 2-9: Fatigue cracking along weld toe (left), principal stress direction more parallel with weld toe (right) [1]

2.6.8.2 Method B

When using shell element models without the weld geometry included, the hot spot stress is taken as the stress read out point 0.5t away from the intersection line. For solid element models with the weld geometry included, the hot spot stress is taken as the stress read out point 0.5t away from the weld toe.

The effecting hot spot stress range is derived as

$$\sigma_{eff} = \max \left\{ \begin{array}{l} 1.12 \sqrt{\Delta\sigma_{\perp}^2 + 0.81\Delta\tau_{\parallel}^2} \\ 1.12\alpha|\Delta\sigma_1| \\ 1.12\alpha|\Delta\sigma_2| \end{array} \right.$$

Where

A, $\Delta\sigma_1$ and $\Delta\sigma_2$ are explained under method A [1].

3 Finite element method

3.1 General

Some concepts of the finite element method are applied directly in this thesis. In this chapter these concepts are explained briefly [10].

The general 4-node quadrilateral element is called a Q4 element. The 4-node quadrilateral element used in Abaqus is called S4.

3.2 Shape functions

Shape functions are used to interpolate coordinates or displacements over the element. This interpolation provides us with a single valued and continuous field of the field quantity. Since the stresses are extrapolated from the integration points to an element side we can use the shape functions to perform the extrapolations.

For a linear Q4 element, the shape functions are linear, and are as follows

$$\begin{aligned}
 N_1 &= \frac{(a-x)(b-y)}{4ab} & N_2 &= \frac{(a+x)(b-y)}{4ab} \\
 N_3 &= \frac{(a+x)(b+y)}{4ab} & N_4 &= \frac{(a-x)(b+y)}{4ab}
 \end{aligned}$$

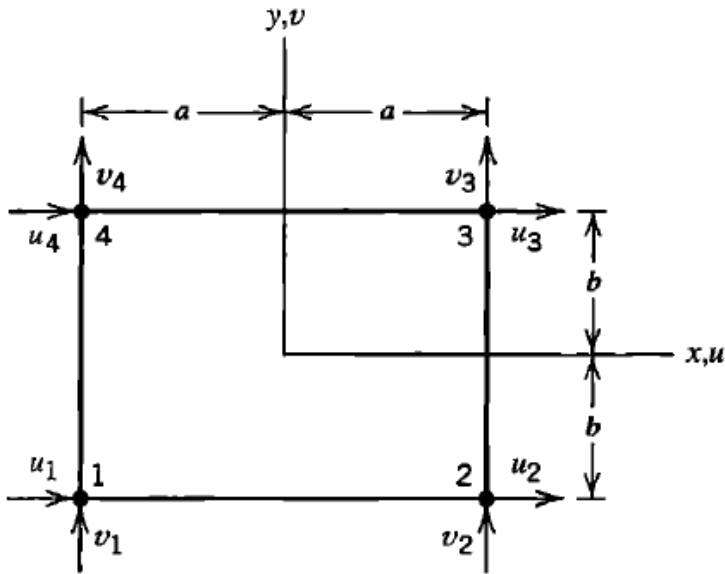


Figure 3-1: Bilinear quadrilateral Q4 and its eight nodal d.o.f. [10]

3.3 Isoparametric elements

Isoparametric formulation allows quadrilateral and hexahedral elements to have non-rectangular shapes and even curved sides in the case of a quadratic element formulation. They use reference coordinates to map the physical element into a reference element that has the shape of a square, or a cube for solid elements. In element formulation the price paid for a general shape is having to deal with transformation of coordinates. The shape functions for isoparametric S4 elements are used to interpolate both the displacement field and the element geometry. The shape functions are as follows

$$N_1 = \frac{1}{4}(1 - \xi)(1 - \eta) \quad N_2 = \frac{1}{4}(1 + \xi)(1 - \eta)$$

$$N_3 = \frac{1}{4}(1 + \xi)(1 + \eta) \quad N_4 = \frac{1}{4}(1 - \xi)(1 + \eta)$$

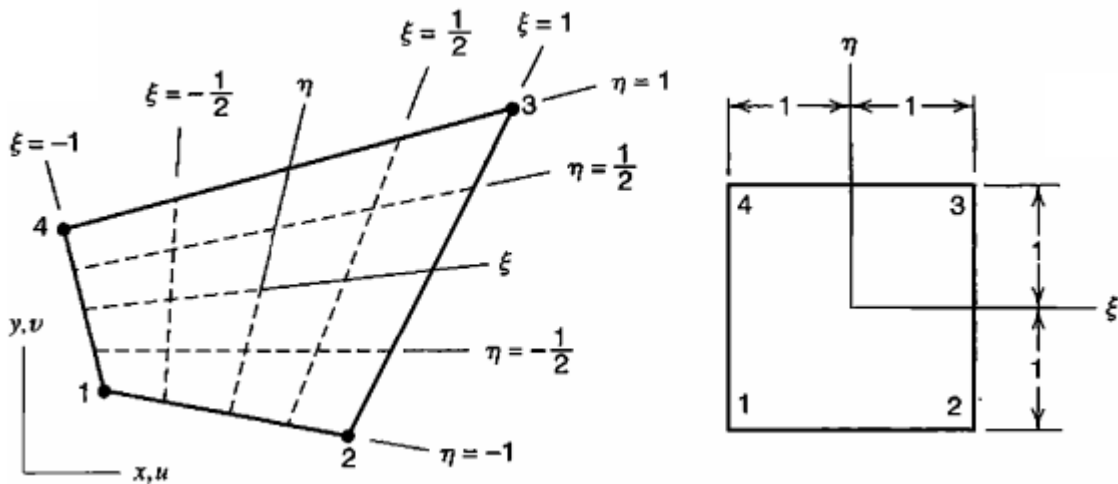


Figure 3-2: Four node plane element in physical space (left) and in $\xi\eta$ space (right) [10]

3.4 Extrapolation with shape functions

Extrapolation for isoparametric S4 elements has been performed by use of shape functions. This is due to the elements not having a mid-side node, so for a $t \times t$ mesh stresses must be extrapolated from the integration points to the side, and interpolated between to obtain stress at $0.5t$ and $1.5t$. For a quadratic element shape this is fairly straight forward, but for a general element shape it becomes more work.

The integration points are positioned at $\xi = \pm \frac{1}{\sqrt{3}}$ and $\eta = \pm \frac{1}{\sqrt{3}}$ when gauss rules of 2nd order are used.

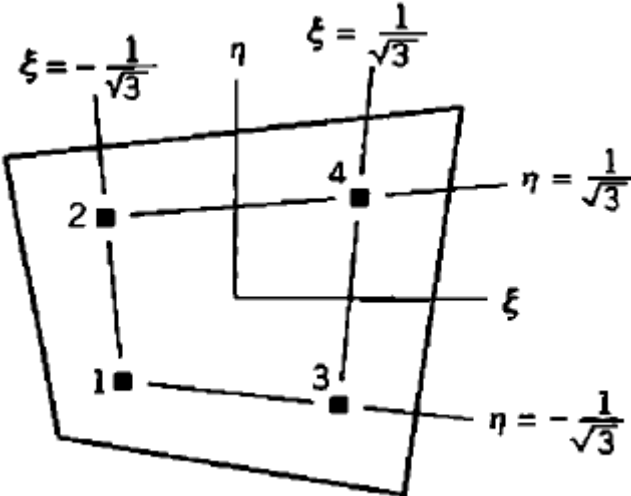


Figure 3-3: Sampling point locations for gauss integration of 2nd order [10]

Imagine the left side in this picture to be the side where stress read outs are to be performed. It has been made to be 1t long, as per a t x t mesh scheme, it can be seen that stresses must be extrapolated to the position $\xi = -1, \eta = 0$ to obtain the stress at 0.5t.

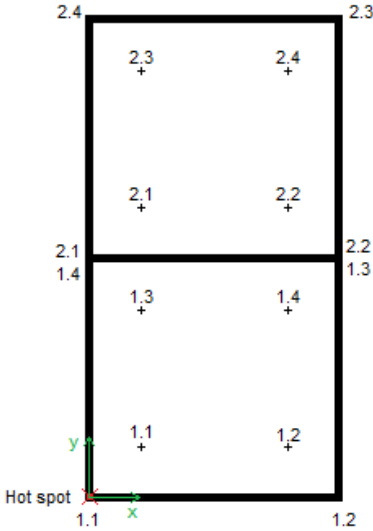


Figure 3-4: 2 closest elements to hot spot, integration point numbering and corner node numbering

Global coordinates of the corner nodes of the relevant elements can be found from the model joint geometry, and input in the Mathcad extrapolation program. There is also an option for selecting quadratic element shape, where $t \times t$ mesh is assumed. This saves some manual work with having to input the global coordinates of the corner nodes. Determination of the global coordinates of the integration points is then possible by applying the following formulae.

$$\begin{Bmatrix} x \\ y \end{Bmatrix} = \begin{bmatrix} \sum_{i=0}^n N_i x_i \\ \sum_{i=0}^n N_i y_i \end{bmatrix}$$

where

$$c = [x_1 \quad y_1 \quad x_2 \quad y_2 \quad x_3 \quad y_3 \quad x_4 \quad y_4]$$

$$N = \begin{bmatrix} N_1 & 0 & N_2 & 0 & N_3 & 0 & N_4 & 0 \\ 0 & N_1 & 0 & N_2 & 0 & N_3 & 0 & N_4 \end{bmatrix}$$

When the global coordinates are known, extrapolation of stress components to the element side is performed by linear extrapolation.

Values at integration point 1 and 2 extrapolated to element side

$$\sigma_\eta = \sigma_1 + \frac{\sigma_1 - \sigma_2}{x_1 - x_2} \cdot (-x_1)$$

Repeated for integration points 3 and 4 to element side

$$\sigma_{-\eta} = \sigma_3 + \frac{\sigma_3 - \sigma_4}{x_4 - x_3} \cdot (-x_4)$$

where

$$\eta = -\frac{1}{\sqrt{3}}$$

In case of a non-rectangular shape of the element, the distance from the extrapolated stresses to the element side to the hot spot must be found. This is again done with the shape functions, but can be simplified somewhat since only the y-coordinate is of interest.

$$\begin{Bmatrix} y_\eta \\ y_{-\eta} \end{Bmatrix} = \begin{bmatrix} N_1(\xi, \eta) & N_2(\xi, \eta) & N_3(\xi, \eta) & N_4(\xi, \eta) \\ N_1(\xi, -\eta) & N_2(\xi, -\eta) & N_3(\xi, -\eta) & N_4(\xi, -\eta) \end{bmatrix} \begin{bmatrix} y_1 \\ y_2 \\ y_3 \\ y_4 \end{bmatrix}$$

where

$$\xi = -1$$

$$\eta = -\frac{1}{\sqrt{3}}$$

Stresses are then extrapolated to the point $0.5t$ along the element side.

$$\sigma_{0.5t} = \frac{\sigma_\eta - \sigma_{-n}}{y_\eta - y_{-\eta}} \cdot (0.5t - y_\eta) + \sigma_\eta$$

The same procedure is used for the next element to find the stress at $1.5t$ away from the hot spot. Once stress components at both points are known, extrapolation is performed in the normal manner as explained in chapter 2.6 and 4.9.

The full Mathcad program can be found in Appendix D.

4 Methodology

4.1 Purpose

The methodology was established in conjunction with doing the analysis of the two first joint geometries. Establishing the methodology is important in being able to verify the validity of the results, as well as serving as a general guideline when creating the analyses. The methodology includes information about the analysis procedure related to modelling, element selection, meshing, stress read out points and extrapolation techniques.

4.2 Recommended practice

The NORSOK standards are governing for all offshore structures on the Norwegian continental shelf. NORSOK N-004 “Design of steel structures” [11] refers to DNVGL-RP-0005 “RP-C203: Fatigue design of offshore steel structures” [1] in the chapter regarding fatigue. In the practical cases where [1] has a clear guideline, this should be followed. Other literature has also been studied in depth to see what alternative methods are available for deriving SCFs.

4.3 Extents of model and validity range

The chord length-diameter relation, α , is an important parameter for stress concentration factors in simple tubular joints. For brace axial loading, a bending moment is induced in the chord. This causes the chord to ovalize, and the ovalization decays as we move away from the intersection. If this natural decay is interrupted the SCFs at the joint intersection will be reduced. In the Efthymiou SCF equations, a short chord correction factor is applied if $\alpha < 12$. This implies that the chord length L must be over $6D$ to avoid short chord effect.

For cases where the joint geometry parameters are outside the validity range of the Efthymiou equations, the following recommendations are made. SCF calculations should be performed using the actual joint geometry parameters, then SCF calculation using the parameters at the edge of the validity range should be performed. The largest SCF calculated by the two methods should be used [7]. [1] notes that the upper limit on the α -parameter is removed with respect to validity of the SCF equations. This is relevant as Joint 2 has an α -value of 63.

The FEM model chords are modelled to the centre of neighbouring joints, and the chord ends are set as fixed. Length of the brace is of less significance, but the brace is also modelled to the neighbouring joint.

4.4 Modelling and assembly

FEM models are modelled as a single part if joint geometry allows it. For complex solid joints, the model may be comprised of several parts modelled and meshed individually. The parts are assembled in the Abaqus assembly module. This is done by using tie constraints and in some cases shell-to-solid couplings.

4.5 Constraints

3 types of constraints have been used in the analysis. Coupling constraints have been used to couple a reference point at the centre of the brace end cross section to the surface of the cross section. This allows for easy application of forces, where a concentrated force or a moment can be applied in the reference point. The coupling then redistributes the force or moment evenly over the cross section.

For solid models, an assembly of different parts are connected. The parts are connected by applying tie constraints over a matching area for two different parts. This locks the displacement of the surface nodes to follow each other. This has the advantage of allowing each part to be meshed individually, which means easier positioning of stress read out points.

Shell-to-solid couplings have also been used for solid models. This has been done to reduce computational effort. The areas of the model that are not near areas of interest are modelled as shell parts. The edge of the shell parts are then coupled to a surface of the solid parts by the shell-to-solid coupling.

4.6 Boundary conditions

The boundary conditions are set as fixed at chord ends. To avoid short chord effects $\alpha > 12$, this means that the chord length must be at least 6 times the diameter of the chord [7].

Some different boundary conditions have been utilized in the earlier research on simple tubular joints. Wordsworth [12] used pinned boundary conditions, which subsequently lead to high SCFs for the crown position in the axial load case. Efthymiou equations allow you to

adjust the stiffness of the chord ends, from pinned to fixed, through the chord end fixity parameter [7].

4.7 Loading and analysis steps

The analysis steps are the load cases defined for the model. A solution must be computed for each step. Axial load, in-plane bending and out-of-plane bending is specified for each of the braces.

Load as applied at the brace end to a reference points coupled with the brace end cross section. A coordinate system local to the brace is created to avoid converting the loads to the global coordinate system. The applied loads are of a magnitude such that nominal stress will be equal to 1MPa for each of the load components, for easier computation of SCF.

For KT-joints, additional load cases exist. These include balanced axial load and unbalanced out of plane bending. The impact of these additional load cases involve the influence the combination of the loads have on the SCF for the joint [13]. These cases have not been included in the work in this thesis, and is possible to investigate in future work.

4.8 Meshing

SCF determination from FEM analysis is highly mesh sensitive, so it is critical that a good mesh quality is obtained. This is especially true at the stress read out locations. As per [1] a mesh density or mesh adapted to the tubular joint stress read out points a and b is used. This is achieved through partitioning the model properly and using the best meshing algorithm available for the volume cell or shell surface in question. For complex models extensive partitioning may be required to be able to control the quality of the mesh to a sufficient degree. Most of the time spent on the FEM analyses is spent on partitioning the model and adapting the mesh to the stress read out points.

Certain rules regarding the quality of the mesh are recommended. It is important to have a continuous and not too steep change in the density of the element mesh in the areas where the hot spot stresses are to be calculated. The geometry of the elements should be evaluated carefully in order to avoid errors due to deformed elements. Corner angles between 60° and 120° and length/breadth ratio of less than 5 is recommended [1].

4.8.1 Read out of stresses

There are some different methodologies available in various literatures [1, 4]. The document referenced in NORSOK N-004 [11] is DNVGL-RP-0005 [1]. This means for the offshore structures on the Norwegian continental shelf, the recommendation in [1] should be followed.

Stress read out points for tubular joints are at positions "a" and "b". These are at different lengths from the joint intersection depending on the position stresses are extracted for. The chord crown, chord saddle and brace side have different distances to a and b, and they are dependent on the radius and thickness of the member. For easier read out of stresses the mesh is adapted so that nodes are placed at the a and b positions.

Stress read out points for joints other than tubular joints are at 0.5t and 1.5t from the joint intersection. A mesh density of txt locally at the joint intersection is recommended.

Following experimentation with averaged and non-averaged stress read outs for Joint 2, and the recommended practice in [1], stresses are read out as averaged stress components.

4.9 Extrapolation procedure

There are alternatives for derivation of hot spot stress available in [1], Method A and Method B. Whenever possible, both methods are used and results compared.

4.9.1 Method A

The extrapolation formula depends on the relative distances between the hot spot and the first and second stress read out point. The equations are found from the formula for a straight line.

For stress read out points at 0.5t and 1.5t the extrapolation formula is

$$\sigma_{hs} = 1.5\sigma_{0.5t} - 0.5\sigma_{1.5t}$$

The formulas for tubular joints are of the same format, but with different constant factors.

For method A, all stress components sampled from the two read out points are extrapolated to the hot spot. At the hot spot location the principal stresses are calculated, as well as a stress equation made to account for the situation with fatigue cracking along a weld toe. The effective hot spot stress range to be used together with the hot spot S-N curve is

$$\sigma_{eff} = \max \begin{cases} \sqrt{\Delta\sigma_{\perp}^2 + 0.81\Delta\tau_{\parallel}^2} \\ \alpha|\Delta\sigma_1| \\ \alpha|\Delta\sigma_2| \end{cases}$$

The principal stresses for plane stress are calculated as

$$\sigma_1 = \frac{\sigma_{\perp} + \sigma_{\parallel}}{2} + \frac{1}{2}\sqrt{(\sigma_{\perp} - \sigma_{\parallel})^2 + 4\tau_{\parallel}^2}$$

$$\sigma_2 = \frac{\sigma_{\perp} + \sigma_{\parallel}}{2} - \frac{1}{2}\sqrt{(\sigma_{\perp} - \sigma_{\parallel})^2 + 4\tau_{\parallel}^2}$$

For a three-dimensional stress state, which includes the stress components in a solid model, calculating the principal stresses is more time consuming. First the stress invariants must be determined, and then the principal stress can be calculated using the invariants [14].

$$\sigma_1 = \frac{I_1}{3} + \frac{2}{3}\left(\sqrt{I_1^2 - 3I_2}\right)\cos\phi$$

$$\sigma_2 = \frac{I_1}{3} + \frac{2}{3}\left(\sqrt{I_1^2 - 3I_2}\right)\cos\left(\phi + \frac{2\pi}{3}\right)$$

$$\sigma_3 = \frac{I_1}{3} + \frac{2}{3}\left(\sqrt{I_1^2 - 3I_2}\right)\cos\left(\phi + \frac{4\pi}{3}\right)$$

where

$$\phi = \frac{1}{3}\cos^{-1}\left(\frac{2I_1^3 - 9I_1I_2 + 27I_3}{2(I_1^2 - 3I_2)^{\frac{3}{2}}}\right)$$

$$I_1 = \sigma_{11} + \sigma_{22} + \sigma_{33}$$

$$I_2 = \sigma_{11}\sigma_{22} + \sigma_{22}\sigma_{33} + \sigma_{33}\sigma_{11} - \sigma_{12}^2 - \sigma_{23}^2 - \sigma_{31}^2$$

$$I_3 = \sigma_{11}\sigma_{22}\sigma_{33} - \sigma_{11}\sigma_{23}^2 - \sigma_{22}\sigma_{31}^2 - \sigma_{33}\sigma_{12}^2 + 2\sigma_{12}\sigma_{23}\sigma_{31}$$

Described above is the correct method of extrapolation. In practice it is usually sufficient to read the principal stress directly and extrapolate it to the hot spot [8]. If the principal stress direction changes direction near the hot spot, this method may produce wrong results.

4.9.2 Method B

Method B is a simplified method. It only requires a stress read out at 0.5t from the joint intersection, and does not require extrapolation. The stress gradient is represented by a factor 1.12 which is applied to the stresses read at 0.5t. In cases where the stress gradient is steep, this may lead to underestimation of the SCF. However, the method requires much less manual work than Method A, and in most cases it is within +/- 10% of the Method A SCF. Refer to chapter

4.10 Shell element selection

Element performance has been evaluated in Joint 1 and 2. The element selected for shell model analyses is the 8-node S8R thick shell element with reduced integration. Other shell elements experimented with for Joint 1 and 2 are the S4 4-node general purpose shell element, and the S8R5 8-node thin shell element with reduced integration. All of these elements have their 4 integration points in the same locations.

4.11 Solid element selection

For solid model FEM analysis, literature [1, 4, 8] uniformly recommends the use of 20-node solid elements with reduced integration. It is stated that 8-node elements can be used, but in this case at least 4 elements should be included through the thickness of the plate.

In all solid models the Abaqus solid element C3D20R (20-node brick with reduced integration) is used.

4.12 Weld geometry

For solid models the weld geometry has been included. The length of the weld toe is taken as half the thickness of the plate or member which is grooved for welding.

Some techniques are suggested in various literature [8] on how to represent the weld fillet in a shell model, but this has not been used in the work within this thesis.

4.13 Mathcad extrapolation program for shell elements

A Mathcad spreadsheet was created to assist with extrapolation of stresses from the integration points of the elements to arbitrary points on the element surface. This was done by using the element shape functions of a S4 element, as well as general FEM theory [10]. The spreadsheet had further capabilities to extrapolate the stresses to the hot spot, calculate principal stresses and SCF. The spreadsheet is most accurate for a S4 element, but can be used with any plane shell element with 4 integration points as long as the sides of the element are not curved.

Due to utilizing the capabilities of the Abaqus program, in combination with the selection of the S8R element, the use of this Mathcad program was limited. Ultimately it was only used to extrapolate stresses for Joint 4 – Model I (S4 elements).

4.14 Check of FEM model

Some checks are performed to verify the FEM analysis output. Nominal stress in the brace is controlled to be 1MPa. This indicates correct thicknesses used for elements, as well as correct load.

Visual inspection of the non-averaged stress contours of the model is also performed. This gives an indication of the quality of the mesh. If the stress contours are discontinuous there is an indication that the mesh quality could be bad.

The stiffness of the shell and solid models are compared by checking displacements at the brace ends.

For shell models the shell orientation is checked to get the stress read out from the correct side of the element.

Solid models connected by constraints are visually checked for gaps or missing couplings or ties. This is done by scaling the displacement plot to exaggerate the displacements and inspecting regions which are coupled with constraints. Also the stress contours in areas near constraints are checked to see if any odd behaviour is present.

4.15 Extraction of analysis output

The extraction of the analysis output takes place in the Abaqus visualization module. An absolute max principal stress contour is applied to locate the areas where the stress concentrations are highest. Stresses are then probed at the appropriate read out locations, and if there are several possible node couples that could produce the highest hot spot stress, they are all checked and compared.

Stress components sampled at 0.5t and 1.5t are manually entered into an Excel spreadsheet which performs the extrapolation to the hot spot.

5 Analysis of joints

5.1 Overview

5.1.1 Joint 1 – Verification specimen

Joint 1 can be found in section D.12 of [1]. It is designed to calibrate or compare FEM models of similar details to an experimentally determined SCF which is listed in table D-9. 5 different analyses were performed for this joint.

5.1.2 Joint 2 – Simple T-joint

This joint is found on a flare tower structure, and is used to test the performance of different methodologies, as well as some comparison the SCFs found by parametric equations. 6 different models were created for this joint.

5.1.3 Joint 3 – Simple tubular T-joint with $\beta = 1$

This is a simple tubular T-joint where brace and chord has same diameters and thicknesses. It has been analysed with a shell model, and the parametric SCF values has been calculated and compared to the results.

5.1.4 Joint 4 – Stiffened tubular T-joint with $\beta = 1$

Together with Joint 3 this forms a case study of tubular T-joints with $\beta = 1$. Joint 4 is a stiffened tubular T-joint with equal dimensions as Joint 3, but at the joint intersection a stiffener plate arrangement is used. The joint is analysed with both shell and solid models and compared to the results of Joint 3.

5.1.5 Joint 5 – Simple tubular KT-joint with $\beta = 1$

Joint 5 is a simple tubular KT-joint where brace and chord has equal diameters and thicknesses. The member dimensions and extents of the joint are the same as for Joint 3. Analyses are performed with a shell model, and parametric SCF values have been calculated and compared.

5.1.6 Joint 6 – Stiffened tubular KT-joint with $\beta = 1$

Joint 6 is a stiffened tubular KT joint with the same geometry as Joint 5, except for a stiffener arrangement being used at the joint intersection. Shell and solid models have been analysed and results are compared to the results of Joint 5.

5.2 Joint 1 – Verification specimen 1

This is the detail “Specimen 1”, found in DNVGL-RP-0005 [1] section D.12, and is typically used for verification of analysis methodology. An analysis of this detail is useful to observe differences between the different elements and meshing method used.

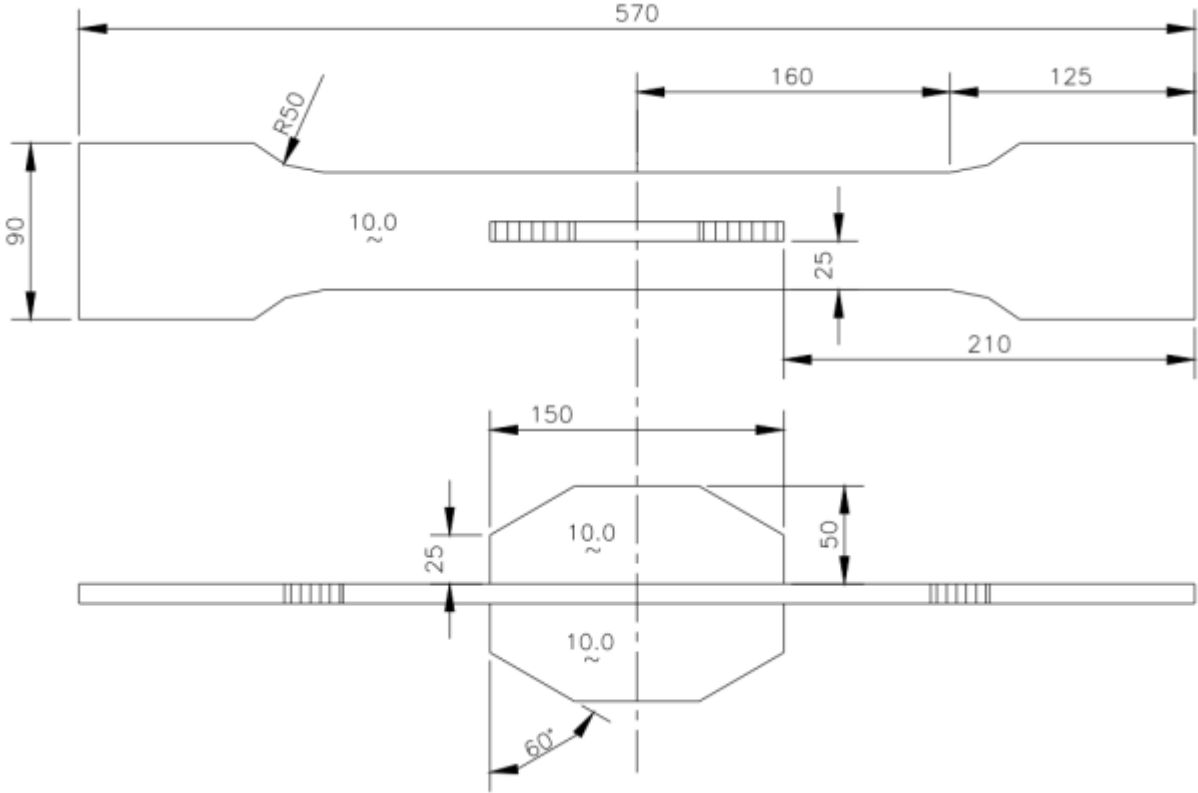


Figure 5-1: Geometry of Specimen 1, Ref [1]

5.2.1 General

Experimentally determined SCF for the joint is 1.32. It is loaded with an axial stress over the end area of 0.667MPa, this yields a nominal stress of 1.0 MPa over the narrower cross section. Since the detail is symmetric and is symmetrically loaded, the model uses symmetry as a boundary condition in the mid cross section of the detail (symmetry plane shown as dotted line in figure 5-1). Stress extrapolation procedure follows DNVGL-RP-0005 [1], thus stress read out points are 0.5t and 1.5t.

5.2.2 Joint 1 model overview

The following models of this joint has been made and analysed

- I. Shell model using S4 elements, txt mesh.
- II. Shell model using S8R elements, txt mesh
- III. Shell model using S8R5 elements, txt mesh.
- IV. Solid model using C3D20R with one element through thickness, txt mesh.
- V. Solid model using C3D20R with four elements through thickness, 0.25t x 0.25t mesh.

5.2.2.1 Shell element models

Averaged component stresses at mid side nodes between elements at locations 0.5t and 1.5t from the intersection line are used. Stresses are extrapolated to the intersection line, and then the principal stresses are calculated. If the maximum absolute value of the principal stress is within 60 degrees of the normal to the intersection line, this stress is divided by the nominal stress to find the SCF. Otherwise, normal stress or minimum principal stress may be used.

For the S4 element model, it is not possible to directly read out stress components since the element does not have mid side nodes. The stress components are read out at the integration points and are extrapolated to the read out points by the use of the element shape functions. This is done with a Mathcad program made specifically for this purpose. The stresses obtained are non-averaged stresses since the integration point from a single element is used. For this case this is considered to be unproblematic since the detail is symmetric, and thus the averaged stresses is expected to have the same value as the non-averaged stresses.

5.2.2.2 Solid element models

For Joint 1, and as described in IIW [4] as an acceptable method, averaged principal stresses are read out at 0.5t and 1.5t from the intersection line. This is done for simplicity, but for the other joints a more comprehensive method has been used, as described in chapter 4. The principal stresses are then extrapolated to the hot spot location. Care must be taken in areas

where the state of stress is complex when using this method, as the direction of the principal stress may change. In the case of Joint 1, the stress direction does not change notably, and we can use this simplification without any issues.

For Model IV, where one element is used though the thickness of the plate, the surface centre element stress is used for extrapolation. This stress is non-averaged.

5.2.3 Joint 1 - Model I

This model uses S4 elements with a txt element mesh. Symmetrical boundary conditions are used. Principal and component stresses are read at integration points and extrapolated by the use of element shape functions to the read out points at 0.5t and 1.5t. The stresses are non-averaged.

5.2.3.1 Results

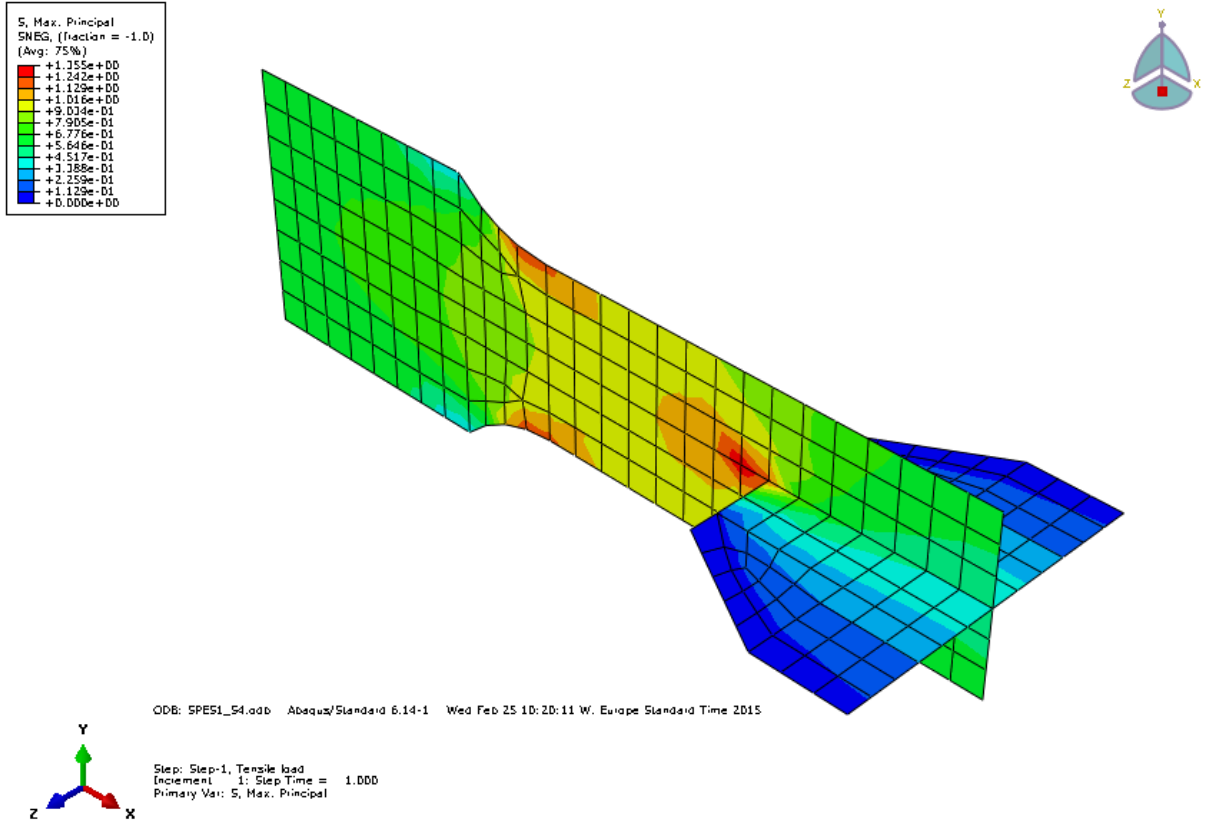


Figure 5-2: Plot of Joint 1 Model I, S4 elements, maximum principal stress contour

Joint 1 Model I	txt, non-averaged		
Read out points	1.5t	0.5t	HSS
Node number	Int. Pts.	Int. Pts.	33
Elements	129	132	
S11	1,149	1,543	1,74
S22	-0,063	-0,012	0,0135
S12	0,047	0,167	0,227
S1 (calculated)			1,769
S2 (calculated)			-0,016
S.eff			1,769
Target SCF			1,32
Error			25,40 %

Table 5-1: Joint 1 Model I results

5.2.3.2 Observations

Joint 1 Model I shows the highest error percentage of all the 5 different models. It overestimates the SCF by 25.4%. Direct read out and extrapolation of principal stresses compared to read out and extrapolation of component stresses show little difference in this case, only about 0.1% difference. Given that this is the only element used without quadratic formulation, it was expected that this model would show the greatest deviation from the target SCF.

5.2.4 Joint 1 – Model II

This model uses S8R elements with a txt element mesh. Symmetrical boundary conditions are used. Component stresses are read at mid-side nodes which are located at the read out points at 0.5t and 1.5t. The stresses are averaged.

5.2.4.1 Results

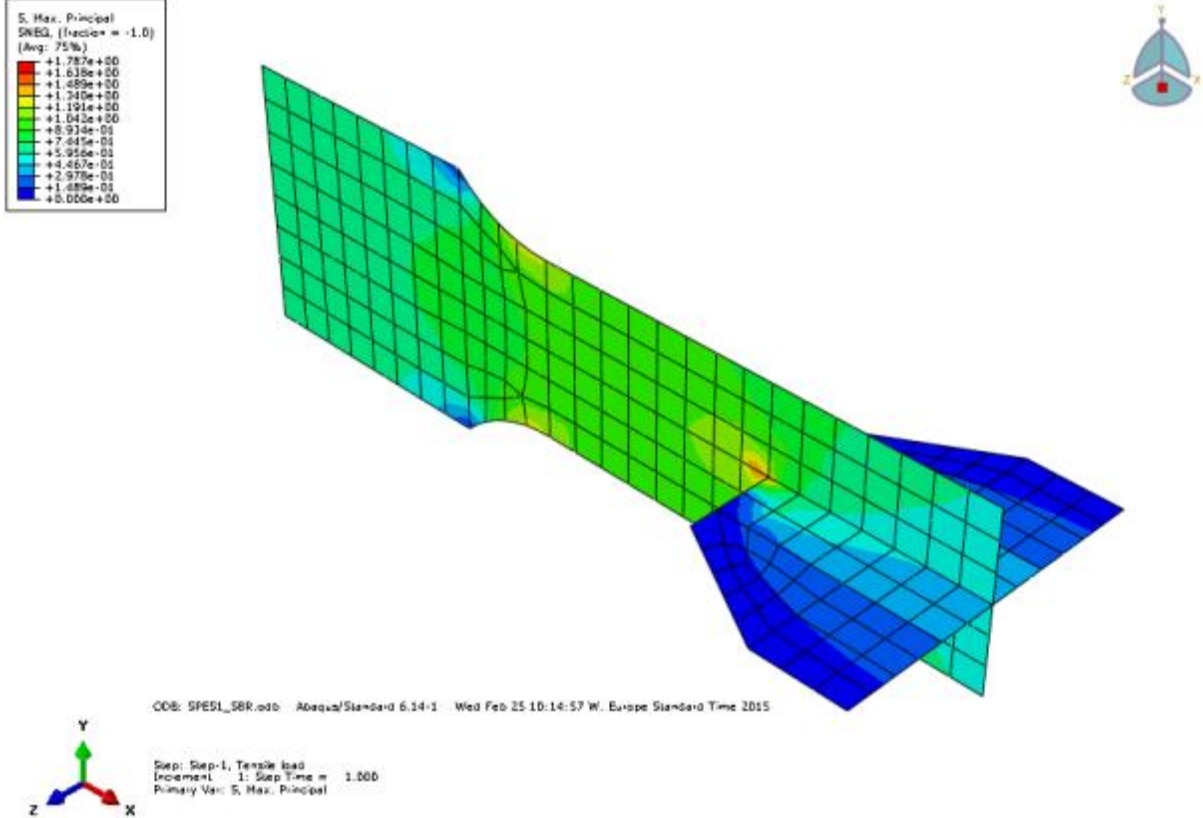


Figure 5-3: Plot of Joint 1 Model II, S8R elements, maximum principal stress contour

Joint 1 Model II	txt, averaged		
	1.5t	0.5t	HSS
Read out points	615	622	33
Node number	615	622	33
Elements	-	-	-
S11	1,145	1,465	1,626
S22	-0,093	-0,044	-0,020
S12	0	0	0
S1 (read out)	1,145	1,465	1,626
S2 (read out)	-0,093	-0,044	-0,020
S1 (calculated)			1,626
S2 (calculated)			-0,020
S.eff			1,626
Target SCF			1,32
Error %			18,80 %

Table 5-2: Joint 1 Model II results

5.2.4.2 Observations

The error percentage in this model is less than in Model I. The more accurate results are due to a quadratic element formulation. Results from direct read out of principal stresses, and principal stresses calculated from stress components, are equal.

5.2.5 Joint 1 – Model III

This model uses S8R5 elements with a txt element mesh. Symmetrical boundary conditions are used. Component stresses are read at mid-side nodes which are located at the read out points at 0.5t and 1.5t. The stresses are averaged.

5.2.5.1 Results

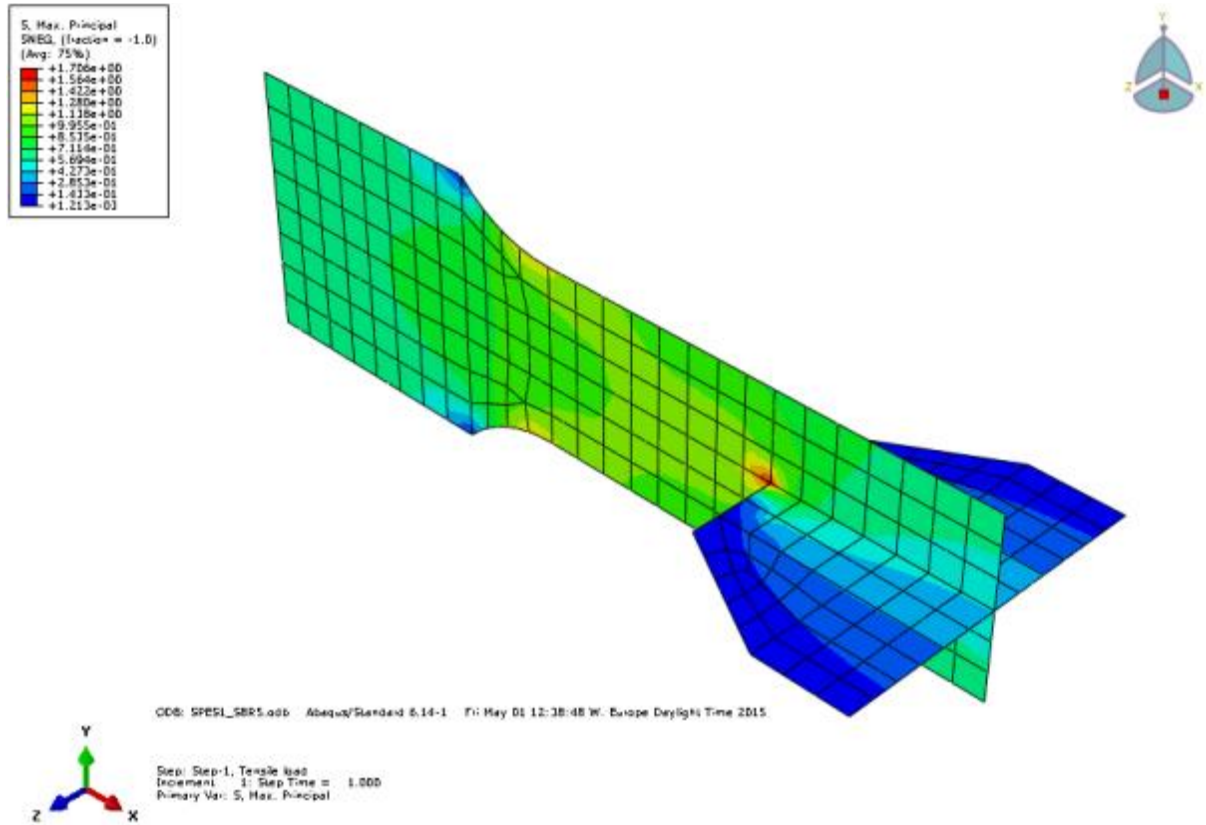


Figure 5-4: Plot of Joint 1 Model III, S8R5 elements, maximum principal stress contour

Joint 1 Model III	txt, averaged		
	1.5t	0.5t	HSS
Read out points	1.5t	0.5t	HSS
Node number	615	622	33
Elements	-	-	-
S11	1,132	1,408	1,546
S22	-0,069	-0,113	-0,134
S12	0	0	0
S1 (read out)	1,132	1,408	1,546
S2 (read out)	-0,069	-0,113	-0,134
S1 (calculated)			1,546
S2 (calculated)			-0,134
S.eff			1,546
Target SCF			1,32
Error %			14,59 %

Table 5-3: Joint 1 Model III results

5.2.5.2 Observations

The only difference between Model II and Model III is that Model III uses a thin shell element formulation, where each node has 5 d.o.f. instead of 6. The extra d.o.f. in Model II is used to account for transverse shear deformation. It is observed that with S8R5 elements we are closer to the experimental target SCF, with an error of 14.59%.

5.2.6 Joint 1 – Model IV

This model uses C3D20R elements with a txt element mesh, meaning one element through the thickness of the plate. Symmetrical boundary conditions are used. Component stresses are read at the element faces which are located at the read out points at 0.5t and 1.5t. The stresses are non-averaged.

5.2.6.1 Results

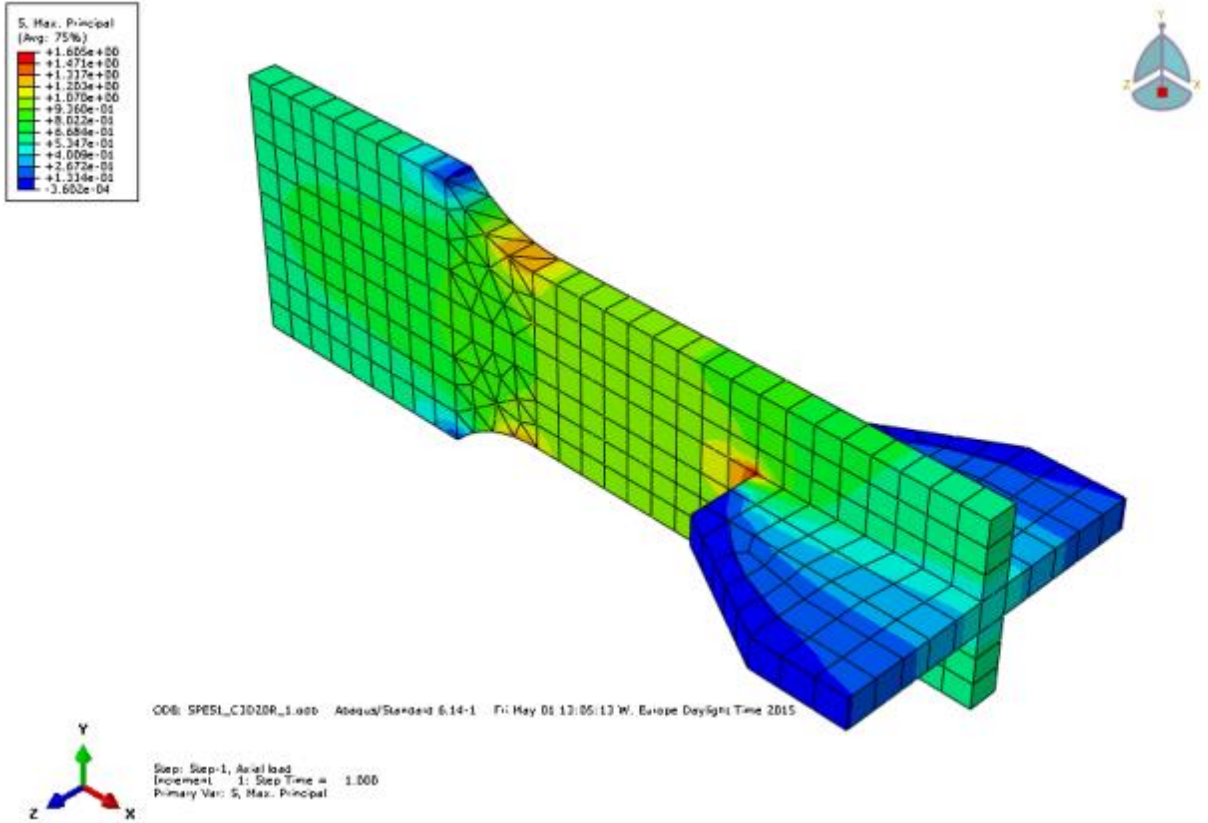


Figure 5-5: Plot of Joint 1 Model IV, C3D20R elements, 1 element through thickness, maximum principal stress contour

Joint 1 Model IV	txt, non-averaged		
Read out points	1.5t	0.5t	HSS
Element face	Face 4	Face 4	-
Elements	118	117	-
S11	1,108	1,306	1,405
S22	-0,074	-0,050	-0,038
S33	-0,018	0,221	0,340
S12	0,000	0,124	0,186
S13	0,000	0,000	0,000
S23	-0,004	0,016	0,026
S1 (read out)	1,108	1,306	1,405
S2 (read out)	-0,018	0,222	0,341
S3 (read out)	-0,075	0,051	0,114
S.eff			1,405
Target SCF			1,32
Error %			6,07 %

Table 5-4: Joint 1 Model IV results

5.2.6.2 Directionality of principal stresses

It is seen that the principal stresses change direction somewhat near the stress singularity. It is recommended that the principal stress direction is within 60 degrees of the normal to the intersection line [x]. When extrapolation is performed, the principal stress S1 and the stress normal to the intersection plane is the same. This means the effect of the change in stress direction is negligible for the purpose of calculating the SCF.

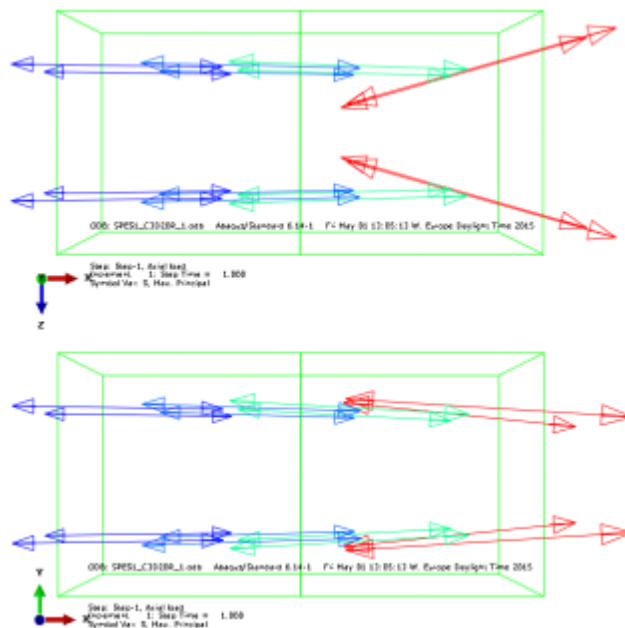


Figure 5-6: Top view and side view of principal stress direction on read out elements

5.2.6.3 Observations

Model IV is quite accurate in terms of estimating the target SCF, with an error of only 6.07%.

5.2.7 Joint 1 – Model V

This model uses C3D20R elements with a $0.25t \times 0.25t$ element mesh, meaning four elements through the thickness of the plate. Symmetrical boundary conditions are used. Component and principal stresses are read at the element corner nodes located on the surface at the read out points $0.5t$ and $1.5t$. The stresses are averaged.

5.2.7.1 Results

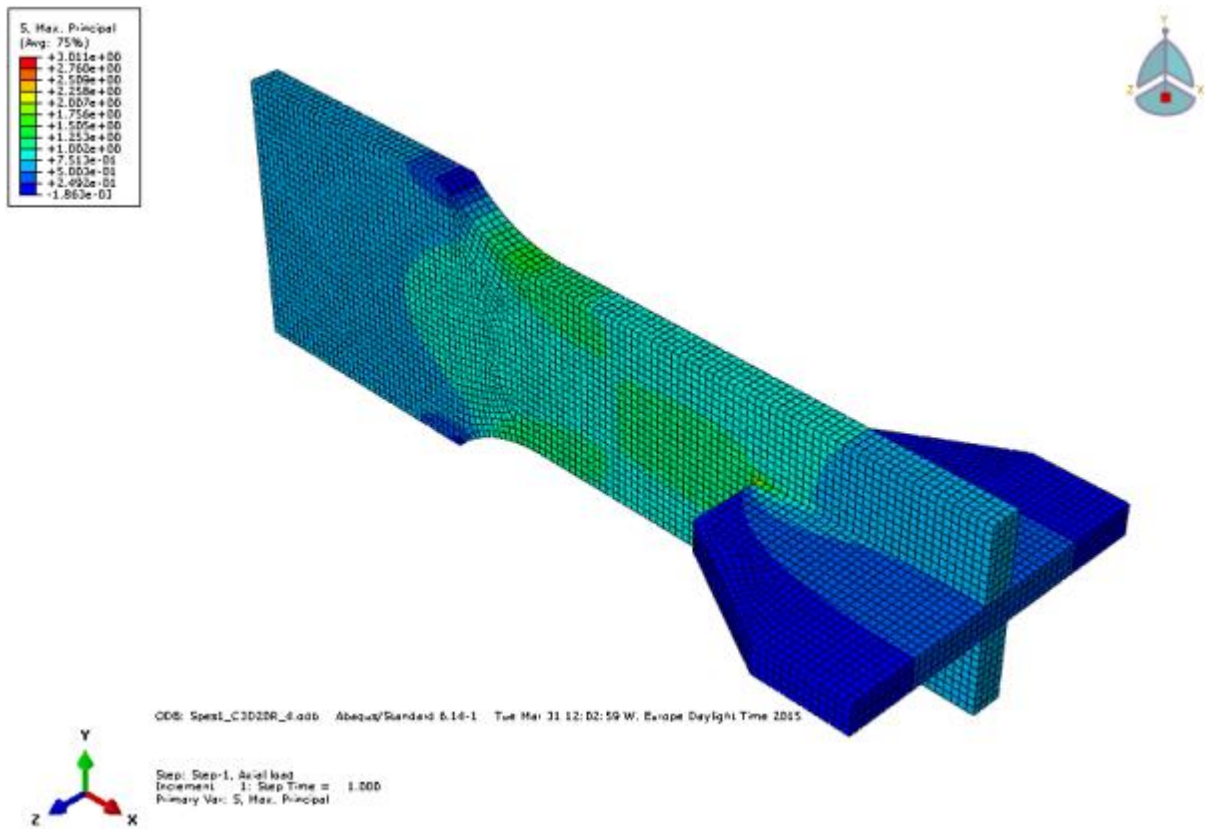


Figure 5-7: Plot of Joint 1 Model V, C3D20R elements, 4 elements through thickness, maximum principal stress contour

Joint 1 Model V	txt, averaged		
Read out points	1.5t	0.5t	HSS
Node number	35739	35913	15
Element	-	-	-
S11	1,112	1,211	1,261
S22	-0,076	-0,133	-0,162
S33	0,000	0,023	0,034
S12	0,000	0,000	0,000
S13	0,000	-0,006	-0,008
S23	0,000	0,000	0,000
S1 (read out)	1,112	1,211	1,261
S2 (read out)	0,000	0,023	0,034
S3 (read out)	-0,076	-0,133	-0,162
S.eff			1,261
Target SCF			1,32
Error %			-4,65 %

Table 5-5: Joint 1 model V results

5.2.7.2 Directionality of principal stresses

We observe that the max principal stress remains close to unidirectional until the very last element row in front of the singularity. This indicates that it is unproblematic to use read out of max principal stress as basis for SCF calculation.

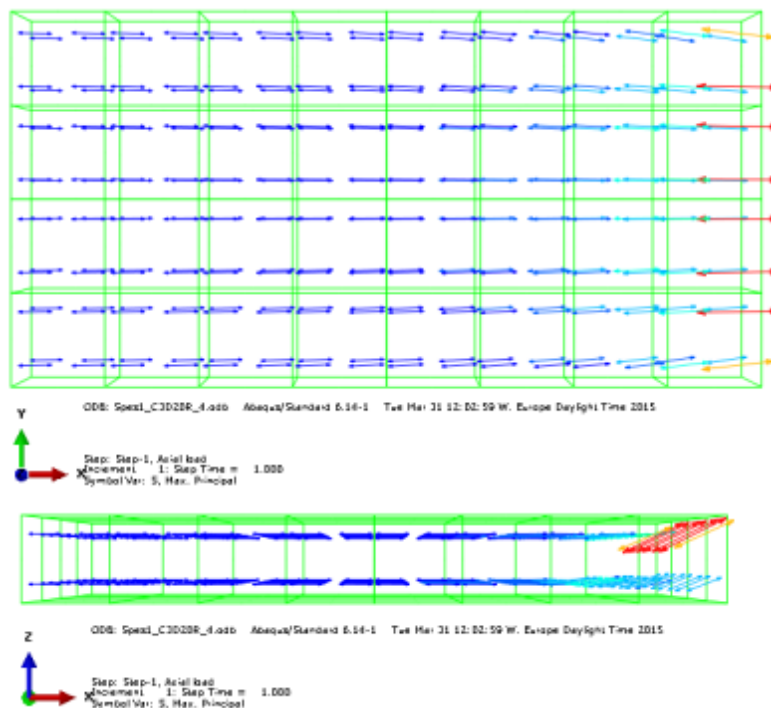


Figure 5-8: Top view and side view of principal stress direction on top layer of elements from intersection line to 2T from intersection line. Intersection line is on the right of the figure.

5.2.7.3 Observations

Model V under predicts the SCF 4.65% compared to the target SCF. Although it is the most accurate SCF obtained out of all the models, under predicting the SCF is not desirable since this will overestimate the calculated fatigue life of a structure.

Visually from the contour plots and symbol plots it can be seen that the influence of the singularity becomes more and more localized as higher order elements are used, as well as when the mesh is refined.

5.2.8 Result summary – Joint 1

Joint name	Element	Mesh	Averaging	Read out procedure	SCF	Error
Joint 1 model I	S4	txt	No	Integration points	1,769	25,40 %
Joint 1 model II	S8R	txt	Yes	Mid-side nodes	1,626	18,80 %
Joint 1 model III	S8R5	txt	Yes	Mid-side nodes	1,546	14,59 %
Joint 1 model IV	C3D20R	txt	No	Surface face centre	1,405	6,07 %
Joint 1 model V	C3D20R	0.25t x 0.25t	Yes	Element corner node	1,261	-4,65 %

Table 5-6: Joint 1 result summary

5.2.8.1 Notes

- DNVGL recommended methods are followed exactly with Model II and Model III.
- Model V is not described anywhere, but is done for testing purposes
- Results from Model IV should after DNVGL-RP-0005 be extrapolated from integration points. However since Abaqus has this functionality implemented in the software, it should be utilized to save work. Also DNVGL-RP-0005 encourages use of averaged nodal stresses, which is not used here since the stress is found at the centre of the surface of the node.
- DNVGL recommends using 8-node reduced integration shell elements, meaning it is not encouraged to use the S4 element we utilized in Model I.
- The most accurate result found in Model V. However the result from Model IV should be considered more reliable, since this does not underestimate the SCF.

5.3 Joint 2 – Simple T-joint

5.3.1 Introduction

It was selected to do an analysis on a simple tubular T-joint to further explore the differences in methodologies and element selection. The joint is of a geometry often found in flare towers or bridges on offshore structures. Efthymiou equations were also used to calculate the SCFs by use of parametric formulas. This serves as comparison for our analysis results. However the SCFs calculated by parametric formulas are not always exact, as shown in HSE “Stress concentration factors for simple tubular joints”. They are calibrated to have a good fit with FEM results or test results, but they are not perfect. Comparisons are made in reference [2] between measurements on steel specimens, acrylic specimens and predicted SCF according to different sets of parametric SCF equations. Based on joint type and load condition, there are different levels of under prediction or over prediction of the SCF by use of parametric formulas.

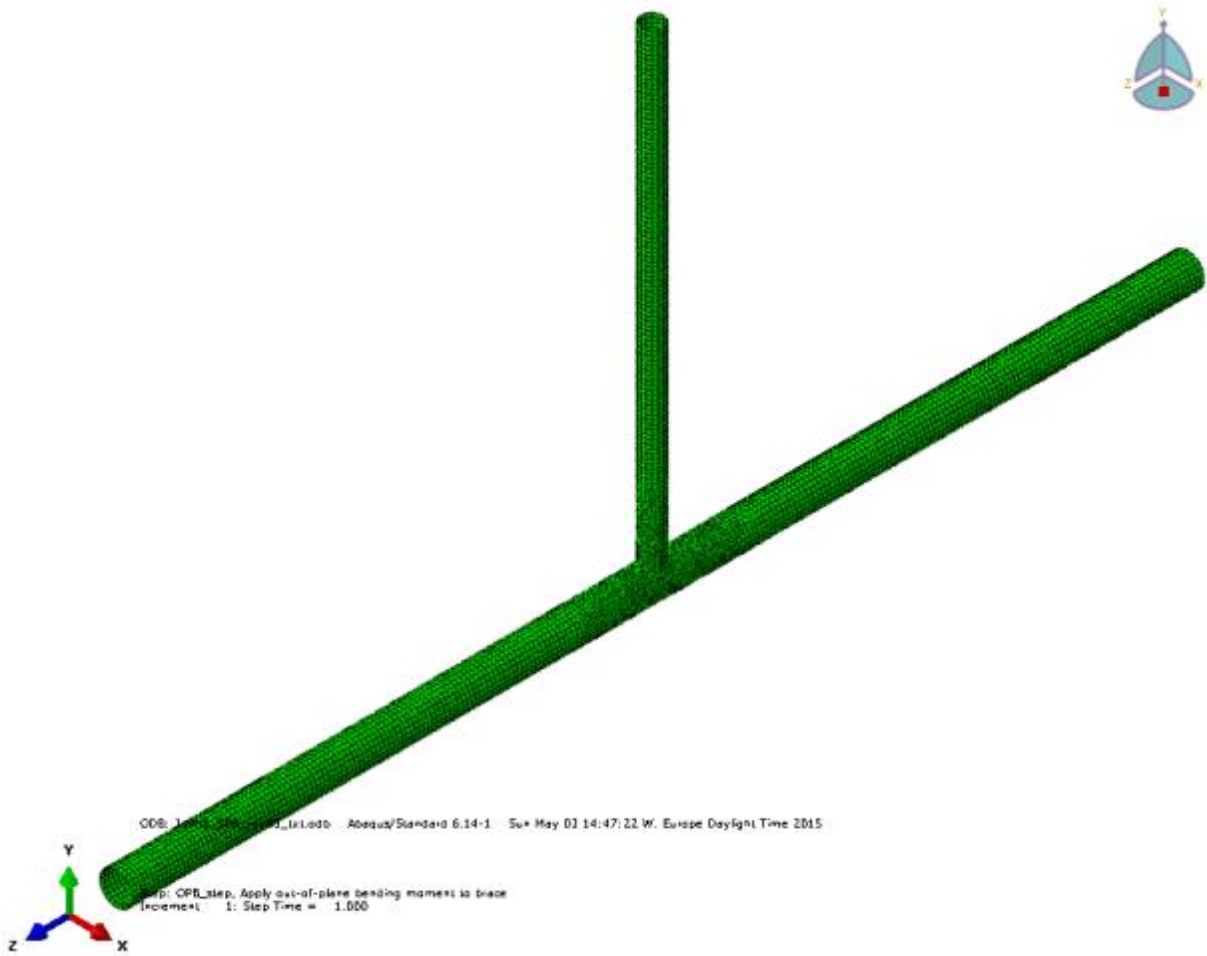


Figure 5-9: Joint 2 – Overview of geometry

5.3.2 General geometry

The model extends to the neighbouring joints. This is done to capture the effect of the bending moment on the crown of the chord.

	Chord	Brace
Length	10 m	4.5 m
Outer Diameter	323.9 mm	219.1 mm
Thickness	15.9 mm	12.7 mm

Table 5-7: Joint 2 geometry

The brace is connected at the midpoint of the chord, at 5m. Lengths are centre/centre to neighbouring joints. Chord ends are fixed for all models.

5.3.3 Comparison of chord lengths

To investigate the effect of the boundary conditions in the model a comparison of two different chord lengths has been performed. For the axial load case, it is expected that a full length chord will increase the SCF at the crown position due to the additional bending moment. Efthymiou and Durkin [7] define a long chord as a chord with $\alpha > 12$, which translates to $L > 6D$. In the comparison, a chord of length $6D$ is used.

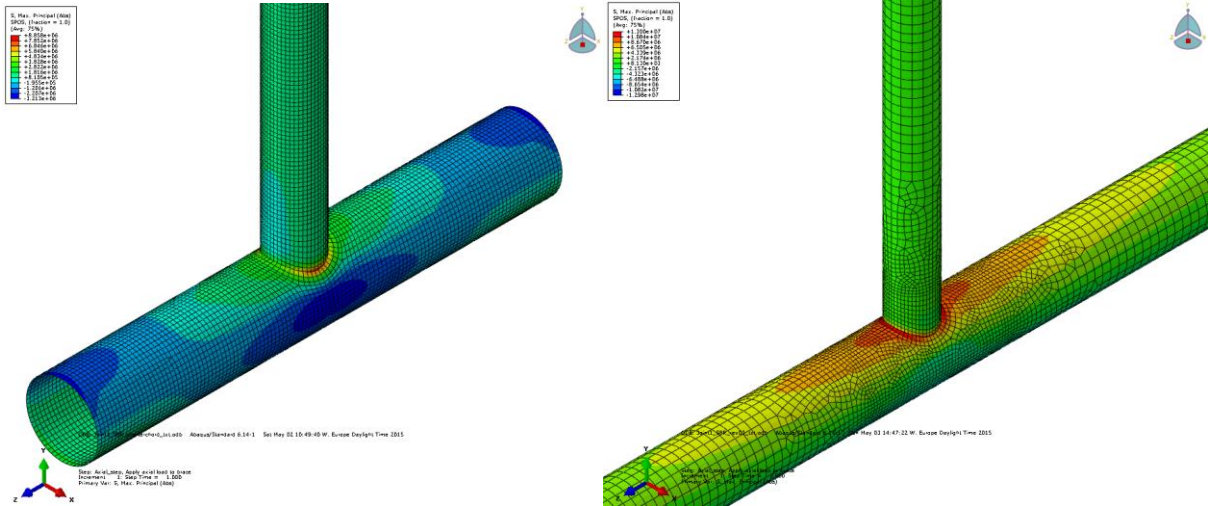


Figure 5-10: Comparison of maximum principal stress contour plots, axial load case, with a chord length of 2m (left) and a full chord length of 10m (right)

It is clear that the full extent of the model must be included to obtain realistic SCF values for the joint.

5.3.4 Efthymiou SCFs

Efthymiou SCFs have been calculated for the joint, by use of formulas found in section 2.6.3.

Load case	Position	SCF
Axial load	Chord crown	10.096
	Chord saddle	8.242
	Brace crown	5.172
	Brace saddle	7.012
In-plane bending	Chord crown	2.837
	Brace crown	2.506
Out-of-plane bending	Chord saddle	7.565
	Brace saddle	5.238

Table 5-8: Calculated SCF values for Joint 2

5.3.5 Evaluation of Efthymiou SCFs

Evaluation of different sets of parametric SCF formulas for simple tubular joints has been performed in [2]. An excerpt of this document is included here for simple T/Y-joints.

Table 1 T/Y-joints - Axial - Chord saddle - Efthymiou values						
Steel/Acrylic	No of Pts	Database		Pred SCF/Recorded SCF		
		Mean	%st dev of Eqn	% P/R < 0.8	% P/R < 1.0	% P/R > 1.5
Steel	28	1,07	10,6 %	0,0 %	28,6 %	0,0 %
Acrylic	57	1,19	23,8 %	0,0 %	12,3 %	8,8 %
Pooled	85	1,15	21,1 %	0,0 %	17,6 %	5,9 %
Table 2 T/Y-joints - Axial - Chord crown - Efthymiou values						
Steel/Acrylic	No of Pts	Database		Pred SCF/Recorded SCF		
		Mean	%st dev of Eqn	% P/R < 0.8	% P/R < 1.0	% P/R > 1.5
Steel	9	1,12	25,6 %	0,0 %	22,2 %	22,2 %
Acrylic	39	1,21	17,8 %	0,0 %	10,3 %	5,1 %
Pooled	48	1,19	19,5 %	0,0 %	12,5 %	8,3 %
Table 3 T/Y-joints - Axial - Brace saddle - Efthymiou values						
Steel/Acrylic	No of Pts	Database		Pred SCF/Recorded SCF		
		Mean	%st dev of Eqn	% P/R < 0.8	% P/R < 1.0	% P/R > 1.5
Steel	8	1,29	25,1 %	0,0 %	12,5 %	12,5 %
Acrylic	39	1,14	24,0 %	5,1 %	25,6 %	7,7 %
Pooled	47	1,17	24,6 %	4,3 %	23,4 %	8,5 %

Table 4 T/Y-joints - Axial - Brace crown - Efthymiou values						
Steel/Acrylic	No of Pts	Database		Pred SCF/Recorded SCF		
		Mean	%st dev of Equn	% P/R < 0.8	% P/R < 1.0	% P/R > 1.5
Steel	4	1,55	19,6 %	0,0 %	0,0 %	75,0 %
Acrylic	31	1,62	34,2 %	0,0 %	3,2 %	64,5 %
Pooled	35	1,61	32,7 %	0,0 %	2,9 %	65,7 %
Table 5 T/Y-joints - OPB - Chordside - Efthymiou values						
Steel/Acrylic	No of Pts	Database		Pred SCF/Recorded SCF		
		Mean	%st dev of Equn	% P/R < 0.8	% P/R < 1.0	% P/R > 1.5
Steel	18	1,1	13,4 %	0,0 %	22,2 %	0,0 %
Acrylic	55	1,11	15,5 %	0,0 %	20,0 %	1,8 %
Pooled	73	1,11	14,9 %	0,0 %	20,5 %	1,4 %
Table 6 T/Y-joints - OPB - Braceside - Efthymiou values						
Steel/Acrylic	No of Pts	Database		Pred SCF/Recorded SCF		
		Mean	%st dev of Equn	% P/R < 0.8	% P/R < 1.0	% P/R > 1.5
Steel	9	1,54	36,3 %	0,0 %	0,0 %	44,4 %
Acrylic	39	1,17	20,4 %	0,0 %	17,9 %	7,7 %
Pooled	48	1,24	27,8 %	0,0 %	14,6 %	14,6 %
Table 7 T/Y-joints - IPB - Chordside - Efthymiou values						
Steel/Acrylic	No of Pts	Database		Pred SCF/Recorded SCF		
		Mean	%st dev of Equn	% P/R < 0.8	% P/R < 1.0	% P/R > 1.5
Steel	21	1,09	16,7 %	4,8 %	28,6 %	0,0 %
Acrylic	60	1,17	13,0 %	0,0 %	10,0 %	0,0 %
Pooled	81	1,15	14,4 %	1,2 %	14,8 %	0,0 %
Table 8 T/Y-joints - IPB - Braceside - Efthymiou values						
Steel/Acrylic	No of Pts	Database		Pred SCF/Recorded SCF		
		Mean	%st dev of Equn	% P/R < 0.8	% P/R < 1.0	% P/R > 1.5
Steel	24	1,22	19,9 %	0,0 %	16,7 %	4,2 %
Acrylic	43	1,39	19,6 %	0,0 %	2,3 %	32,6 %
Pooled	67	1,33	21,2 %	0,0 %	7,5 %	22,4 %

Table 5-9: Excerpt from Ref [2], evaluation of Efthymiou equations against physical test database

As seen from these tables the Efthymiou equations in most cases provide a relatively accurate SCF prediction, but it varies between load cases and geometrical configurations. It is difficult to draw conclusions from this data. However it is possible on a general basis to see where Efthymiou equations are more likely to grossly over predict results. “Axial load – Brace crown” and “OPB – Braceside” are such load cases. It is also seen that it is quite rare that the calculated SCF from the equations is less than 80% of the measured SCF. This is quite reassuring, as such large under predictions can lead to large overestimations in the life expectancy of a structure.

It is seen that the parametric Efthymiou equations are not perfect and come with some uncertainties. The equations are made from curve fitting to FEM analysis results and have a certain validity range. They are convenient in that they quick to calculate, and are thoroughly reviewed [2, 3]. If a detailed model of the joint in question can be produced, this may yield more accurate results, depending on how accurate the equations are for the particular geometry in question. Keep in mind an analysis of a detailed solid model can both increase and decrease SCFs so it may or may not be helpful with regards to documenting a longer life for the structure.

5.3.6 Loading and boundary conditions

Loading has been applied to obtain a 1MPa nominal stress in the brace member for all load cases.

$$F_{axial} = \sigma_{1MPa} * A_{brace} = 8235 N$$

$$M_B = \frac{\sigma_{1MPa} * I_{brace}}{y} = 401.82 Nm$$

Boundary conditions are applied at the intersection centreline for the neighbouring joints. This is to obtain the correct SCFs in the axial load case. Brace length is modelled to the neighbouring joint as well, however this is less critical. Since the brace is loaded with a point load and moments by use of a coupling connection to the brace end surface, it is sufficient that the length of the brace is modelled so that the prevention of deformation at the brace end due to the coupling does not influence the joint SCF.

5.3.7 Methodology

Two different extrapolation schemes have been used for this joint. One which follow the guidelines given for tubular joints, and one which follow the guidelines given for other joints. This concerns the position of the stress read out points in relation to the weld toe or joint intersection, and it follows that the extrapolation formula must suit the read out point locations. Both methodologies are described in [1].

For Joint 2, all models have their direct stress components read out and extrapolated to the hot spot location. At the hot spot location the principal stress is calculated, as well as the “DNV formula” [1] for hot spot stress. Usually the maximum value of these 3 or 4 (depending on shell or solid element model) is taken as the hot spot stress, but it is also dependent on directionality of the stress.

For solid elements, the process of calculating the principal stresses from the stress components is quite time consuming. The component stresses are extrapolated to the hot spot location. Next the stress invariants must be calculated from component stresses and utilized to find the principal stress. However it was selected to follow this methodology for two reasons. Firstly it is considered the most correct way of extrapolating the stresses. Secondly the state of stress becomes increasingly complex near the weld intersection, meaning the direction of the principal stresses is changing over the extrapolation distance. This could cause errors in extrapolation, if stresses significantly different directions were used as basis for the extrapolation.

Extrapolation formulas for Joint 2 are as follows:

For stress read out points 0.5T and 1.5T

$$\sigma_{hs} = 1.5 * \sigma_{0.5} - 0.5 * \sigma_{1.5}$$

For stress read out points a and b at chord crown

$$\sigma_{hs} = 1.75 * \sigma_a - 0.75 * \sigma_b$$

For stress read out points a and b at chord saddle

$$\sigma_{hs} = 2.119 * \sigma_a - 1.119 * \sigma_b$$

For stress read out points a and b at brace crown and brace saddle

$$\sigma_{hs} = 1.444 * \sigma_a - 0.444 * \sigma_b$$

5.3.8 Joint 2 – Model overview

The following models have been made and analysed

Joint 2 model overview					
Model	Element type	Meshing	No. of models	Mesh size	Read out points
I	S8R Shell	Fine (adapted)	1	7.5 - 8.4mm	a and b (tubular)
II	S8R Shell	txt	2	12.7mm, 15.9mm	0.5T and 1.5T
III	S8R5 Thin shell	txt	2	12.7mm, 15.9mm	0.5T and 1.5T
IV	C3D20R Solid	txt	1	12.7mm, 15.9mm	0.5T and 1.5T
V	C3D20R Solid	Fine (adapted)	1	7.5 - 8.4mm	a and b (tubular)
VI	S8R Shell	txt	2	12.7mm, 15.9mm	0.5T and 1.5T

Table 5-10: Overview of the models created for Joint 2

5.3.9 Joint 2 – Stress distribution

For the purpose of visualizing the stress distributions plots of the absolute max principal stress values of Joint 2 for the different load cases are presented here. The plots presented are from model I, remaining stress contour plots and mesh variants can be found in Appendix A.

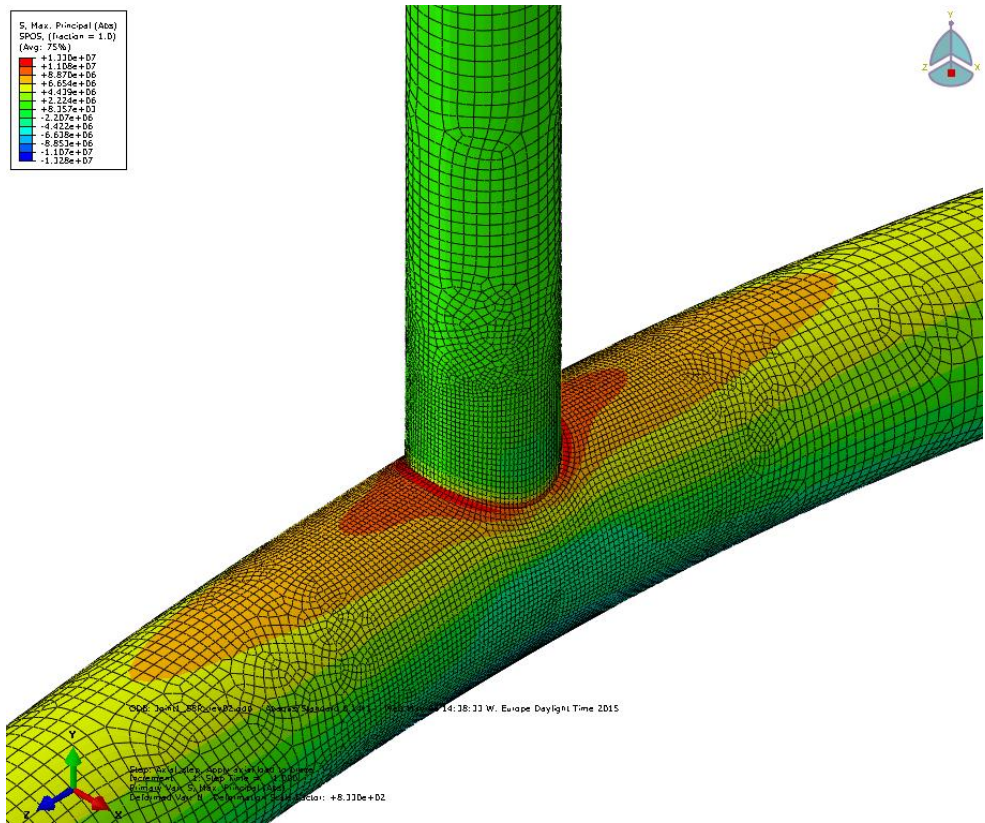


Figure 5-11: Joint 2 – Axial load – Abs. max principal stress contour

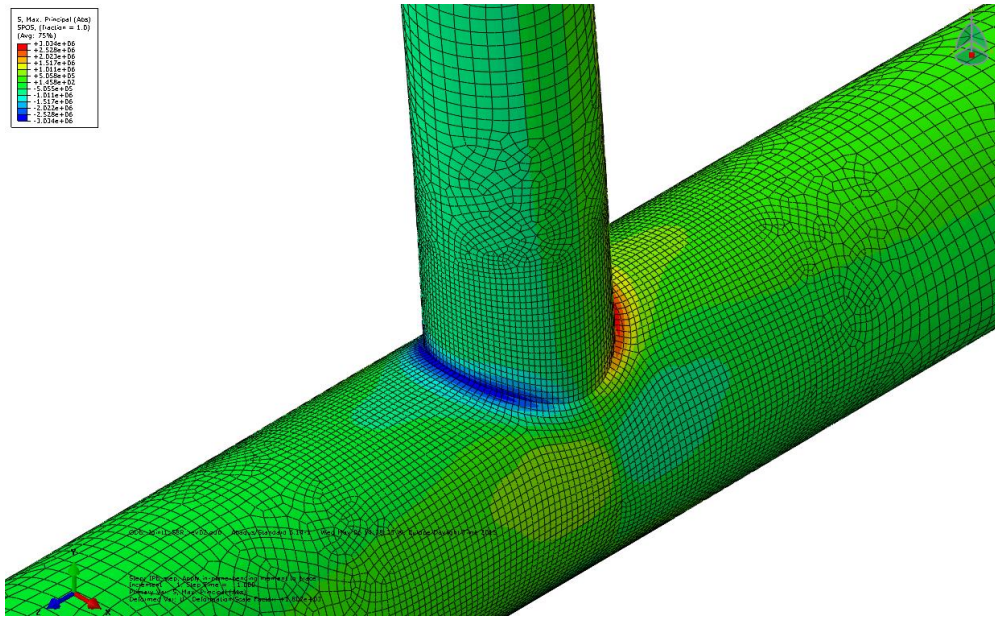


Figure 5-12: Joint 2 – IPB load – Abs. max principal stress contour

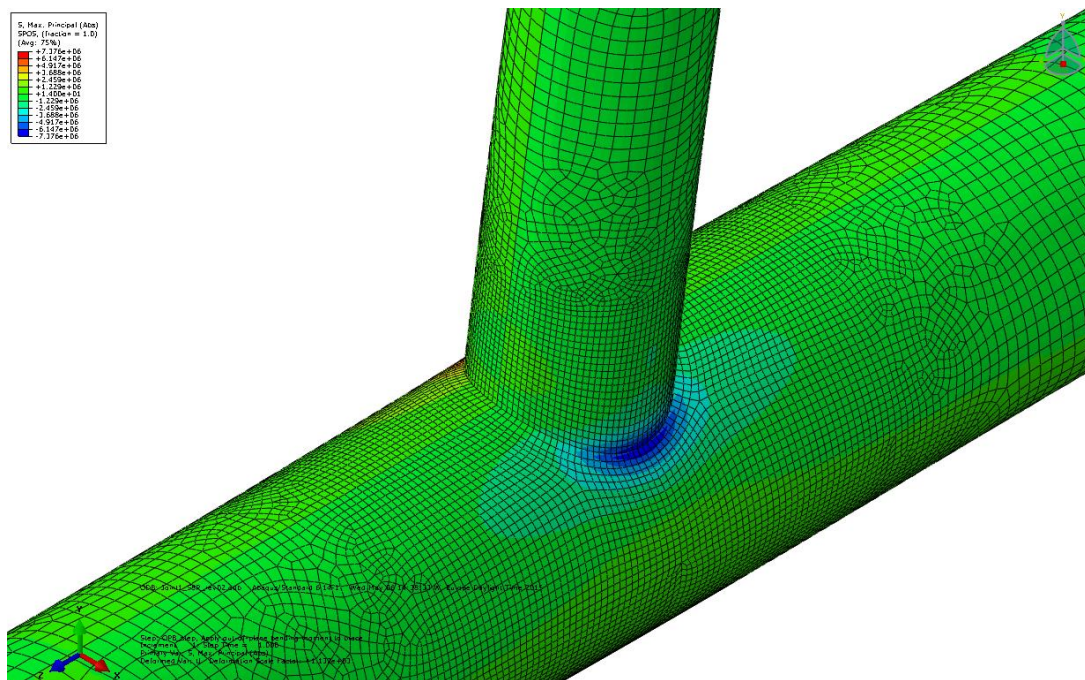


Figure 5-13: Joint 2 – OPB load – Abs. max principal stress contour

5.3.10 Joint 2 – Model I

This model uses S8R elements with a relatively fine element mesh, refined such that element corner nodes are located at stress read out locations. In practice the mesh is adapted to these read out positions, but general length and width of the elements range from 7.4mm to 8.4mm locally around the joint intersection. Away from the intersection the mesh transitions into a coarser mesh to reduce computational effort. Component stresses are read at the element corner nodes which are located at the read out points at a and b. The stresses are averaged. Component stresses are extrapolated to the hot spot, where principal stress is calculated from the stress components.

Only method A from [1] is calculated for model I, due to tubular joint stress read out points a and b being utilized.

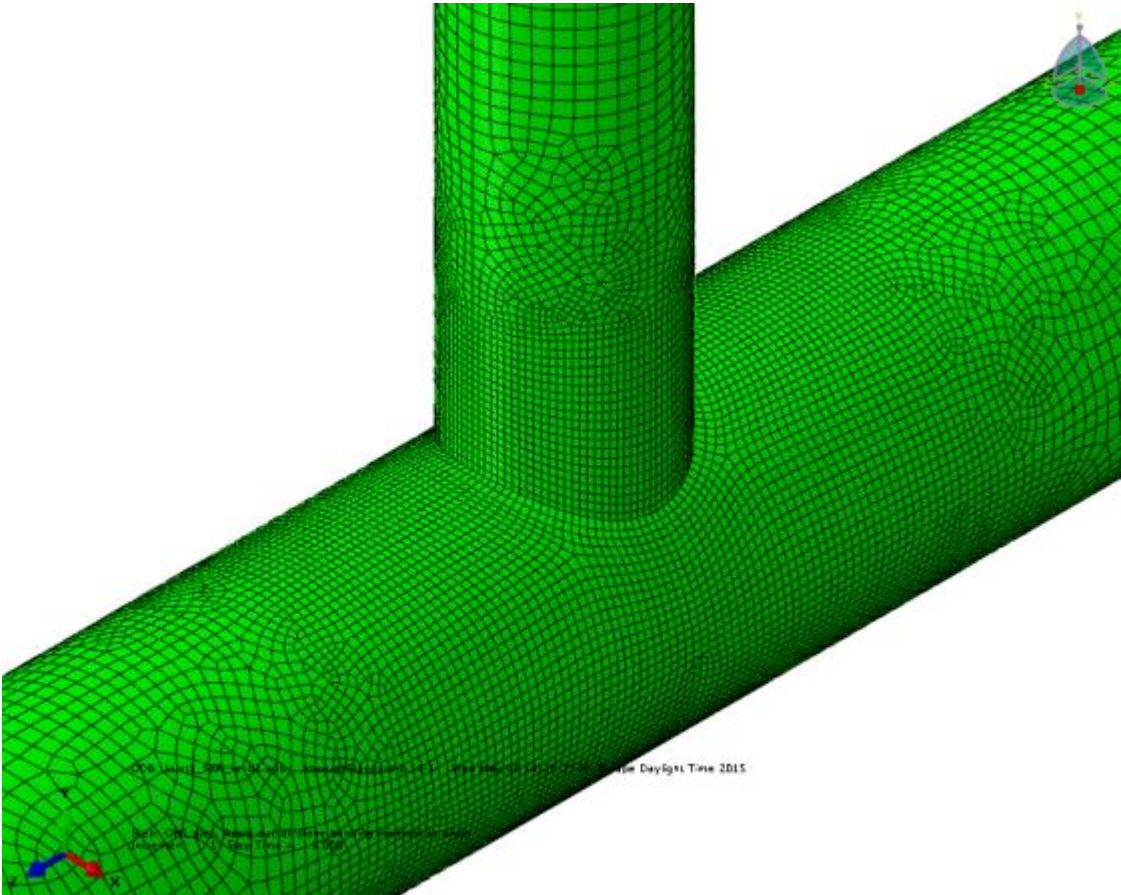


Figure 5-14: Plot of Joint 2 – Model I

5.3.10.1 Model I – Results

Detailed extraction spreadsheet can be found in Appendix B. This includes all stress components at read out positions and extrapolation procedure. Below are the SCF results in tabulated form.

Joint 2 Model I				
Load case	Position	Efthymiou SCF	Method A SCF	Method A / Efthymiou
Axial	Chord crown	10,096	12,432	1,23
	Brace crown	5,172	5,077	0,98
	Chord saddle	8,242	7,655	0,93
	Brace saddle	7,012	10,894	1,55
IPB	Chord crown	2,837	3,202	1,13
	Brace crown	2,506	2,375	0,95
OPB	Chord saddle	7,565	7,899	1,04
	Brace saddle	5,238	7,052	1,35

Table 5-11: Joint 2 Model I results

5.3.10.2 Model I – Observations

Two results can be observed to deviate significantly from the Efthymiou equations, and both results are from the brace saddle position. Both for the axial load case and for the OPB load case the calculated SCF from FEM analysis is significantly higher than the Efthymiou SCF. This is believed to be due to the absence of the weld geometry for the shell model. The weld geometry has the effect of distributing the stresses more evenly over a larger area of the cross section, but also adds additional stiffness locally around the weld. Depending on the geometry of the area of the weld, this may increase or decrease the SCF. As seen later for the solid models of Joint 2, the effect at the saddle position is a reduced SCF from including the weld.

5.3.11 Joint 2 – Model II

This model uses S8R elements with a txt mesh locally around the joint intersection. Read out points are on element mid side nodes, at 0.5t and 1.5t from the hot spot. Averaged stresses are evaluated. Component stresses are extrapolated to the hot spot, where principal stress is calculated from the stress components. Method A and B SCFs are calculated for this model and the results are compared to each other.

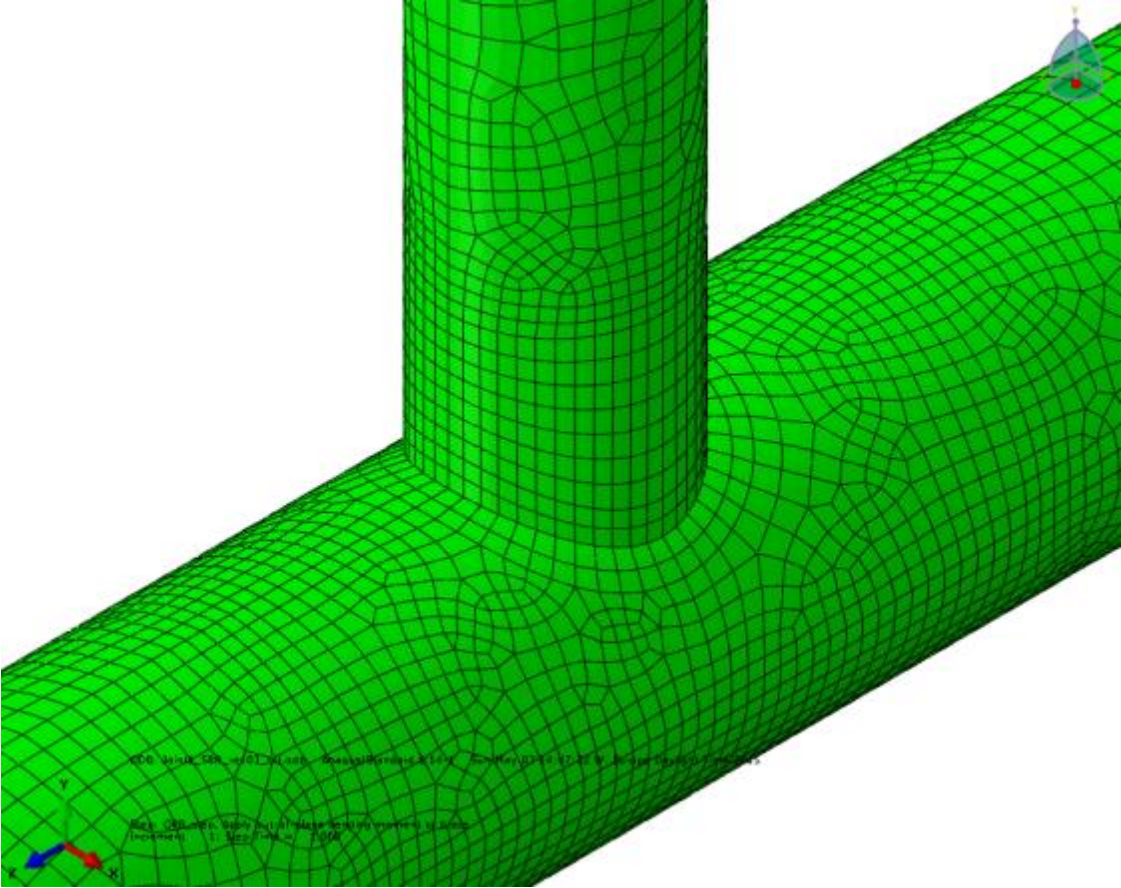


Figure 5-15: Plot of Joint 2 – Model II

5.3.11.1 Model II – Results

For Model II, there are 2 analyses performed with different mesh densities. One model is created for the brace and one for the chord, each with a txt mesh adapted to the thickness of the respective member.

Detailed extraction spreadsheet can be found in Appendix B. This includes all stress components at read out positions and extrapolation procedure. Below are the SCF results in tabulated form.

Joint 2 model II							
Load case	Position	Efthymiou SCF	Method A SCF	Method B SCF	Method A / Efthymiou	Method B / Efthymiou	Method A / Method B
Axial	Chord crown	10,096	12,401	13,229	1,23	1,31	0,94
	Brace crown	5,172	5,364	4,923	1,04	0,95	1,09
	Chord saddle	8,242	7,524	7,498	0,91	0,91	1,00
	Brace saddle	7,012	11,402	10,019	1,63	1,43	1,14
IPB	Chord crown	2,837	3,192	2,967	1,13	1,05	1,08
	Brace crown	2,506	2,533	2,327	1,01	0,93	1,09
OPB	Chord saddle	7,565	7,804	7,248	1,03	0,96	1,08
	Brace saddle	5,238	7,178	6,929	1,37	1,32	1,04

Table 5-12: SCF results for Joint 2 Model II according to [1]

5.3.11.2 Model II – Observations

All results are derived from average nodal values of component stresses at the appropriate read out point. Comparison of average and non-average stresses has been performed for this model, the differences are found to be negligible and are not presented here. This is likely due to the symmetric geometry of the model, and stresses are expected to have equal value at the centreline of symmetry regardless of which side of the centreline the stress values are extracted from. One thing to be alert of is that the stresses on neighbouring elements can have opposite values in some load cases. In those cases the average stresses can cancel each other out, and stresses can average to zero.

The results following the methodology for welded joints other than tubular joints produce similar results as for Model I, where tubular methodology was followed. The largest difference is found for the brace saddle position, where the SCF increases further when the stress read out points are closer together. This is expected in an area with a high stress gradient. It is also shown by the fact that the method B SCF is significantly lower than the method A SCF. Since method B applies a flat slope of 1.12 to the SCF regardless of the local stress gradient, a lower SCF is obtained in regions with steep stress gradients.

5.3.12 Joint 2 – Model III

This model uses S8R5 elements with a txt mesh locally around the joint intersection. Read out points are on element mid side nodes, at 0.5t and 1.5t from the hot spot. Average stresses are evaluated. Component stresses are extrapolated to the intersection line, where principal stress is calculated from the stress components.

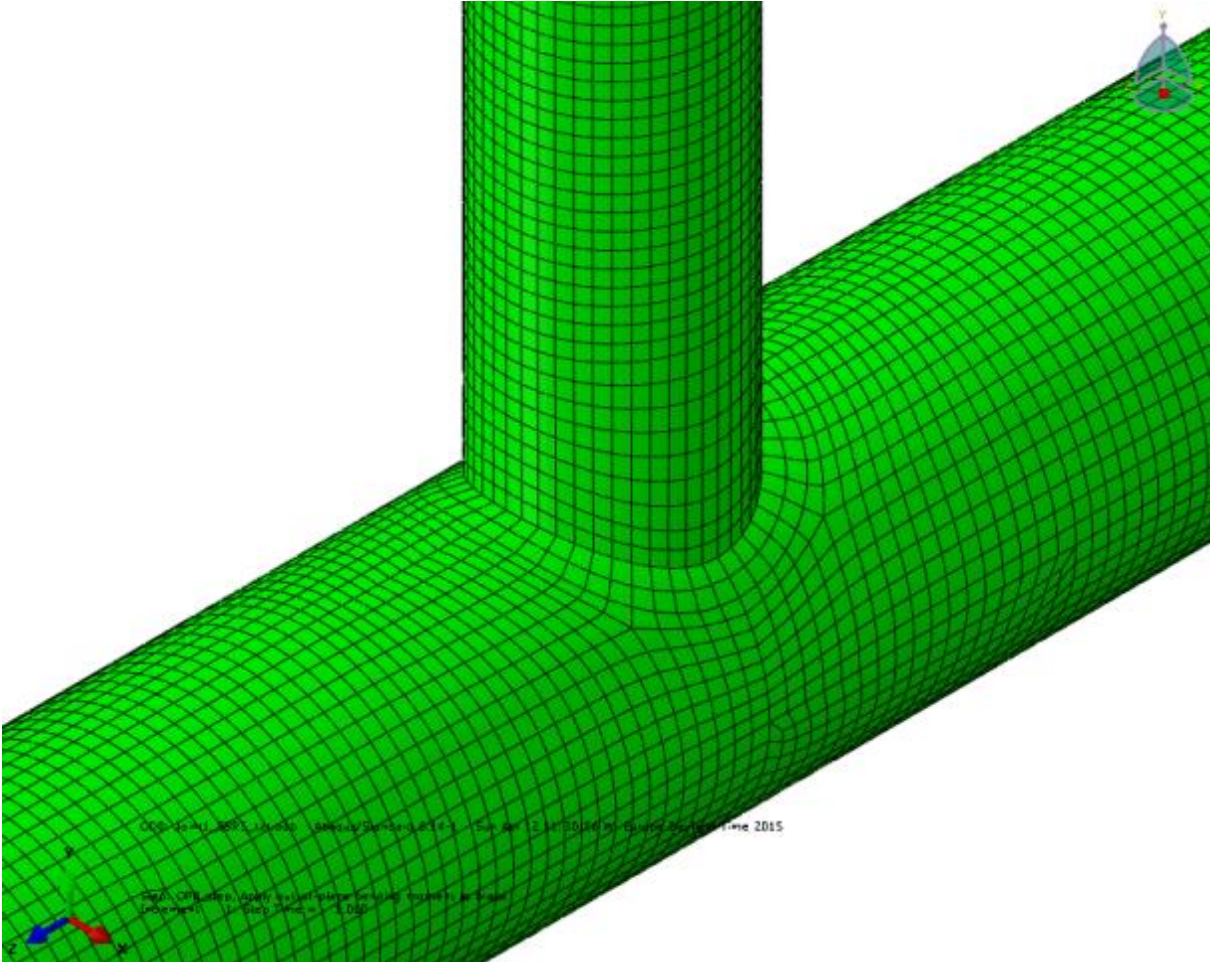


Figure 5-16: Plot of Joint 2 – Model III

5.3.12.1 Model III – Results

For Model III, there are 2 models with different mesh densities. For stress contours and mesh structure refer to Appendix A. For detailed stress extrapolation spreadsheets refer to Appendix B.

Joint 2 model III							
Load case	Position	Efthymiou SCF	Method A SCF	Method B SCF	Method A / Efthymiou	Method B / Efthymiou	Method A / Method B
Axial	Chord crown	10,096	12,409	13,236	1,23	1,31	0,94
	Brace crown	5,172	5,273	4,868	1,02	0,94	1,08
	Chord saddle	8,242	7,609	7,399	0,92	0,90	1,03
	Brace saddle	7,012	11,523	10,101	1,64	1,44	1,14
IPB	Chord crown	2,837	3,201	2,975	1,13	1,05	1,08
	Brace crown	2,506	2,539	2,331	1,01	0,93	1,09
OPB	Chord saddle	7,565	7,897	7,309	1,04	0,97	1,08
	Brace saddle	5,238	7,238	6,982	1,38	1,33	1,04

Table 5-13: SCF results for Joint 2 Model III

5.3.12.2 Model III – Observations

It is most natural to compare the results from Model III with the results from Model II. This is due to that they both use 8-noded elements with read out points at the same locations. Model II uses S8R elements, which have a thick shell formulation including the transverse shear contribution, while Model III with S8R5 is a thin shell formulation which does not include this.

There are no noteworthy differences in the results between the two models. This implies the transverse shear stiffness is not very high, and the geometry can be described as thin shell.

5.3.13 Joint 2 – Model IV

This model uses C3D20R elements with a txt mesh. Weld geometry is included in the model. The weld toe length is taken as 0.5x brace thickness, which is approximately 6.5mm. Element mid side nodes are located at 0.5t and 1.5t on both chord and brace. The elements on the chord conform well to txt element grid, where chord thickness is 15.9mm. Elements on the brace side are slightly wider than the 12.7mm brace thickness as they share their width with the chord side elements, however the element length along the normal to the intersection line is equal to brace thickness.

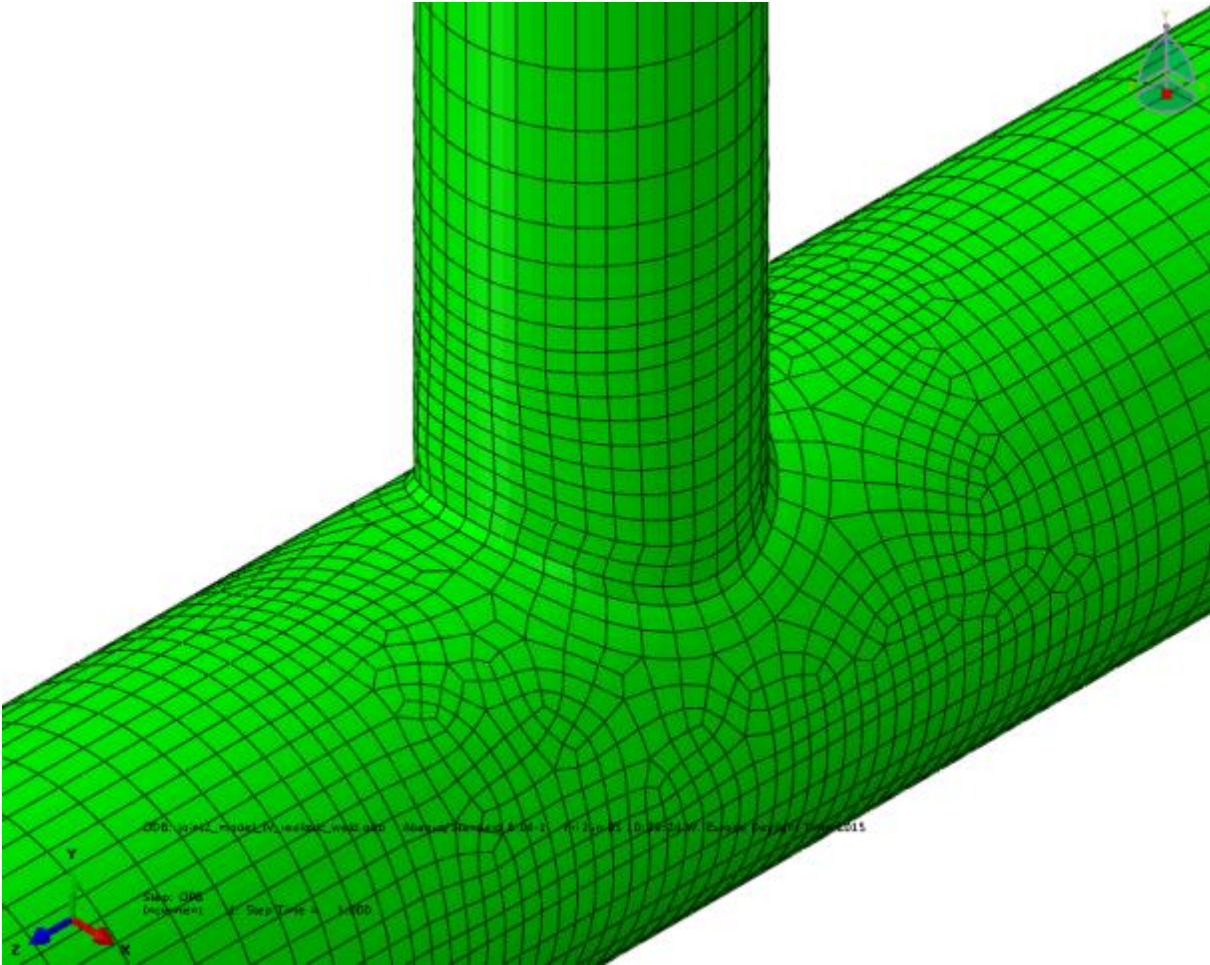


Figure 5-17: Plot of Joint 2 – Model IV

5.3.13.1 Mesh

The meshing around the weld intersection took careful consideration when constructing a txt mesh. The “weld element” includes the brace wall thickness and uses the same E-modulus as the rest of the model. Below are a few plots showing the mesh arrangement near the weld. More plots can be found in Appendix A.

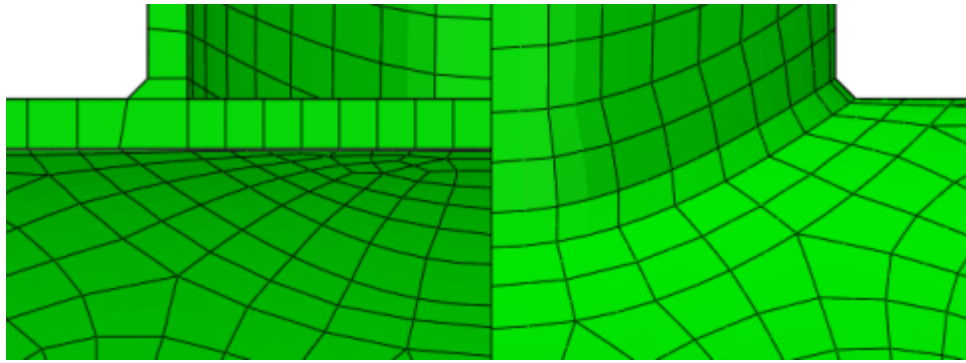


Figure 5-18: Model IV mesh layout with cross section at crown, viewed from side

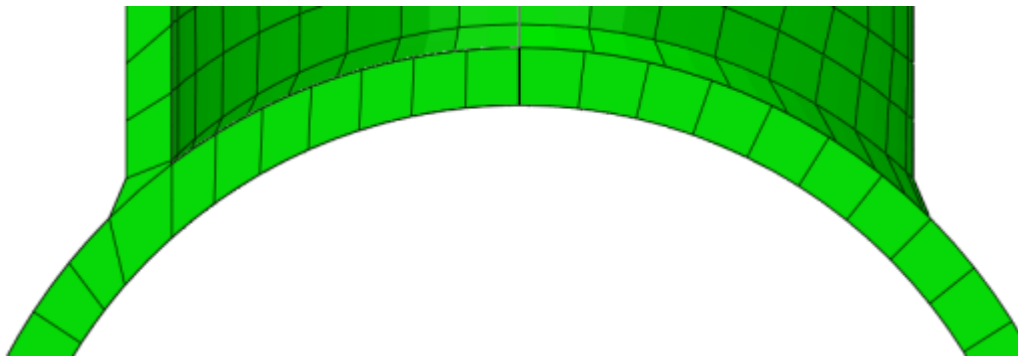


Figure 5-19: Model IV mesh layout with cross section at saddle, viewed from chord end

5.3.13.2 Results

Joint 2 Model IV							
Load case	Position	Efthymiou SCF	Method A SCF	Method B SCF	Method A / Efthymiou	Method B / Efthymiou	Method A / Method B
Axial	Chord crown	10,096	13,785	14,410	1,37	1,43	0,96
	Brace crown	8,242	4,096	3,548	0,50	0,43	1,15
	Chord saddle	5,172	5,846	6,012	1,13	1,16	0,97
	Brace saddle	7,012	7,629	5,754	1,09	0,82	1,33
IPB	Chord crown	3,877	1,991	1,874	0,51	0,48	1,06
	Brace crown	2,872	1,659	1,553	0,58	0,54	1,07
OPB	Chord saddle	11,858	4,922	4,559	0,42	0,38	1,08
	Brace saddle	7,191	4,325	3,896	0,60	0,54	1,11

Table 5-14: SCF results for Joint 2 Model IV

For Model IV both averaged and non-averaged results have been evaluated. The results presented in the table above are based on averaged stresses, as there were negligible differences between the two. Two methods of extrapolation were tested for this model. One was direct read out and extrapolation of principal stresses, the other was read out and extrapolation of component stresses with calculation of principal stress at the hot spot. The results from the latter method are presented here, as some errors occurred when utilizing the

first method. The errors can be attributed to change of directionality of principal stresses from one read out point to the other.

5.3.13.3 Observations

The SCF for the IPB and OPB load cases are significantly lower for the solid model than for the shell models. This is most likely due to the inclusion of the weld in the model, which should particularly have an impact on the bending cases. The stresses around the weld due to bending will be better distributed to the surrounding material. From [1] chapter 4.2, regarding SCFs for tubular joints, it is stated “More reliable results are obtained by including the weld in the model. This implies the use of three-dimensional elements.”

On the other hand, HSE tables show little tendency for SCFs to be overestimated by a large amount for these load cases. This contradiction is somewhat troublesome for drawing conclusions of which set of SCFs are more accurate.

5.3.14 Joint 2 – Model V

This model uses C3D20R elements with a relatively fine mesh. Weld geometry is included in the model. The weld toe length is taken to be 0.5x brace thickness, approximately 6.5mm. Stress read out points are according to tubular joint methodology at points a and b. The mesh is adapted so that element corner nodes are located at the stress read out points. Element size is around 7-9mm locally around the joint intersection. The chord and brace has 2 elements through thickness. Component stresses are extrapolated to the weld toe hot spot where the principal stresses are calculated.

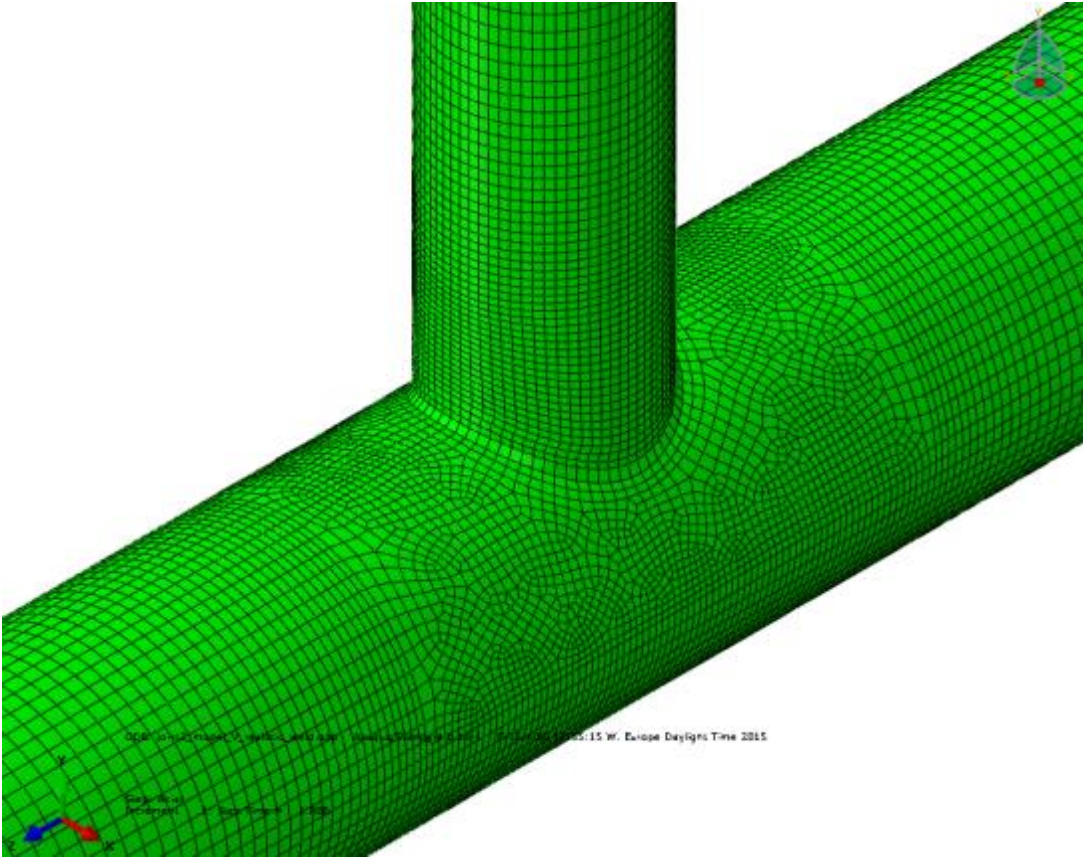


Figure 5-20: Plot of Joint 2 – Model V

5.3.14.1 Mesh

The mesh at the weld is mostly generated automatically, but partitioning has been performed to ensure the stress read out points are located in the correct position. Following are some figures of the mesh at the joint intersection.

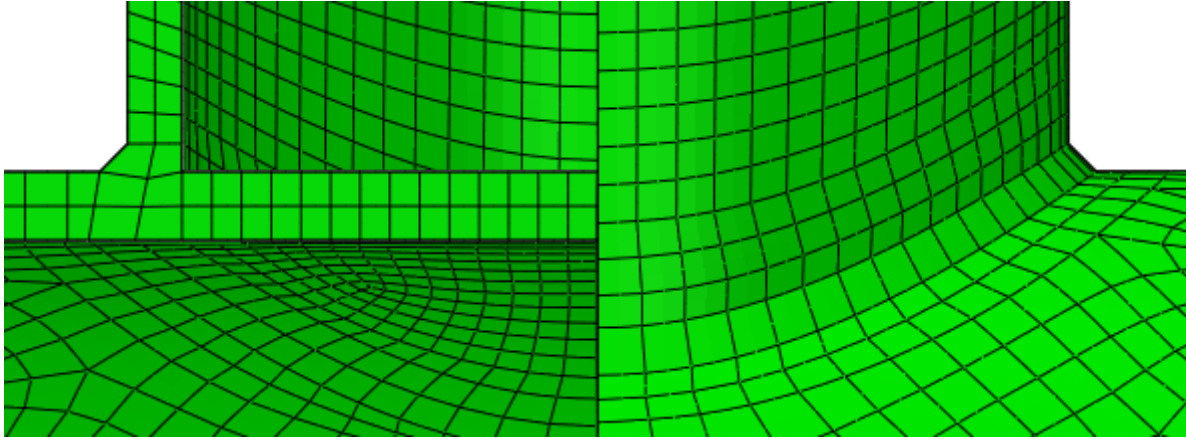


Figure 5-21: Model V mesh layout with cross section at crown, viewed from side

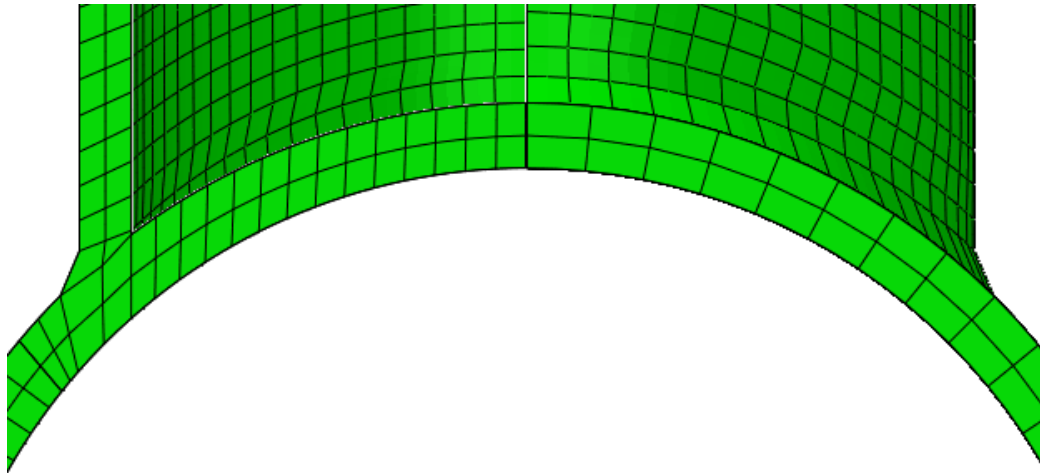


Figure 5-22: Model V mesh layout with cross section at saddle, viewed from chord end

5.3.14.2 Results

Joint 2 model V				
Load case	Position	Efthymiou SCF	Method A SCF	Method A / Efthymiou
Axial	Chord crown	10,096	13,224	1,31
	Brace crown	5,172	3,622	0,70
	Chord saddle	8,242	6,508	0,79
	Brace saddle	7,012	9,249	1,32
IPB	Chord crown	2,837	2,382	0,84
	Brace crown	2,506	1,728	0,69
OPB	Chord saddle	7,565	6,011	0,79
	Brace saddle	5,238	5,327	1,02

Table 5-15: SCF results for Joint 2 Model V

5.3.14.3 Observations

There are some difference in the results from Model IV and V. This is explained by the differences in stress read out locations, as well as change in mesh density. The slope for the extrapolation depends on the distance between the stress read out points, and due to the non-linear stress distribution in front of the weld toe results will be different depending on the read out point locations. For the brace, the stress read out locations are further from each other than for Model IV. For the chord the stress read out locations are closer to each other. This is especially significant in areas where the stress gradient is steep and it will directly impact the SCF value.

In most cases Model IV has the most accurate results, relative to the Efthymiou SCFs, but not without exceptions. The OPB brace saddle SCF closer to the Efthymiou value for Model V.

5.3.15 Comparison of results

Following are some visual representation of the results obtained in chapter 5.3.

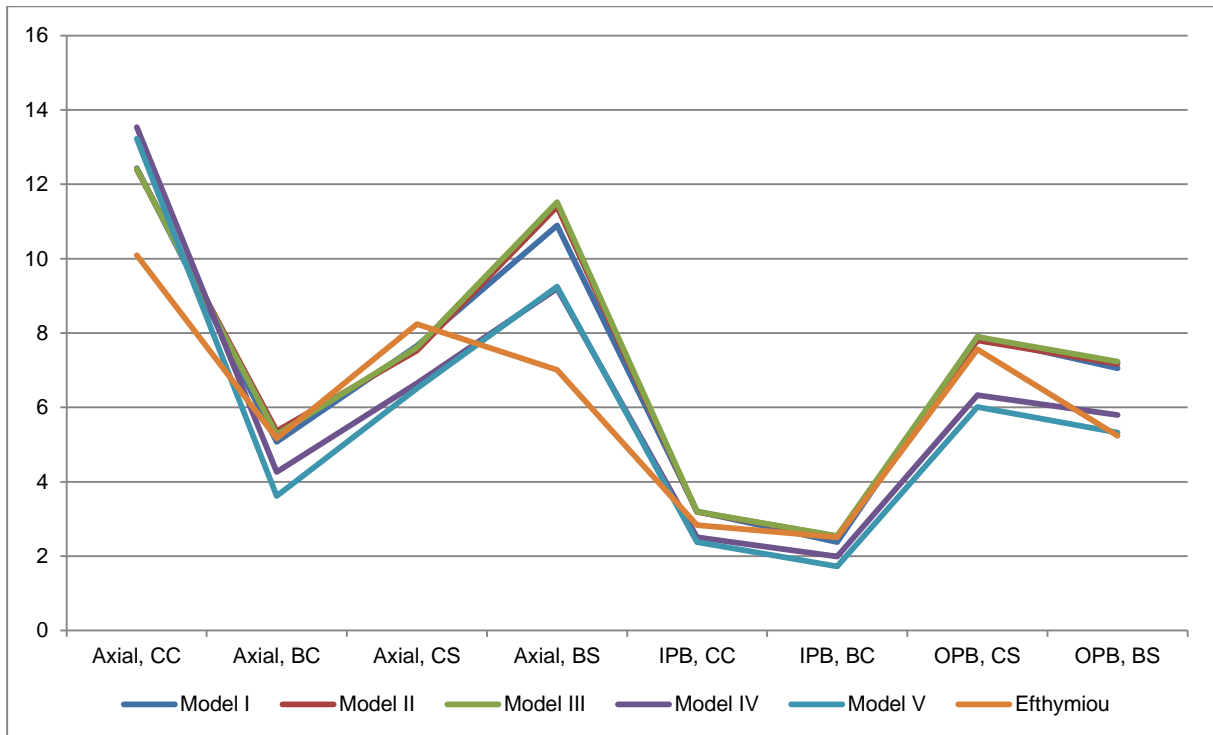


Figure 5-23: Model SCFs vs Efthymiou SCFs

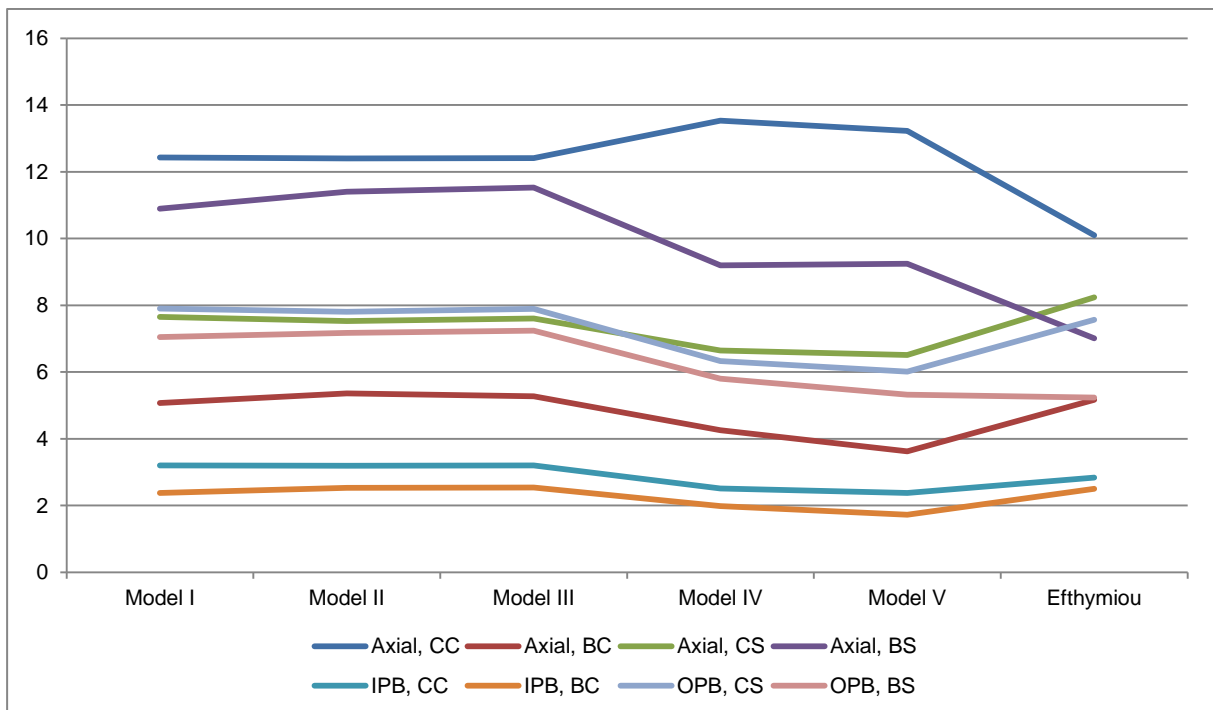


Figure 5-24: SCFs according to load case and position

The axial chord crown SCF is generally the largest SCF. It is seen to have higher values for the solid models than the shell models, which could be due to the additional stiffness the weld geometry represents. The Efthymiou SCF for the chord crown in the axial load case is seen to always be lower than the SCF obtained through FEM analysis. This means use of FEM analysis to obtain SCFs could be problematic due to that the axial load case is often the dominant load in this type of joints.

Other noticeable deviations from the Efthymiou SCF are found at the brace saddle position, for both relevant load cases. The second highest SCF according to the FEM analyses is again found for the axial load case, for the brace saddle. This indicates that for this particular joint geometry, a detailed FEM analysis will in most cases yield a lower expected lifetime for the joint.

5.3.16 Sources of errors

From the results obtained through FEM analyses it appears the most significant error is the absence of weld geometry in the shell models. This reduces the local stiffness at the joint intersection. It also neglects the more smooth transition of stresses between the brace and the chord. The stresses are distributed over a greater area when the weld is included.

The results are also highly mesh sensitive. Significant work has been put into making the mesh of acceptable quality. Most of the time spend on each analysis consist of creating a good model with a quality mesh.

The global loss of stiffness due to the absence of the weld for the shell models is also considered. This is compared by measuring the displacement at the brace end for each load case for the shell models and comparing with the displacements of the solid models which are expected to have correct stiffness. The greatest difference in displacement is found to be about 0.7%.

The averaging of stresses is also something to consider. Averaging of stresses is not necessarily the most accurate stress value for that particular point. In a few cases the stresses found at the read out points with averaging of stresses active were close to zero, when logically they should not be. This appeared to happen when positive and negative stresses on bordering elements cancelled each other out. The calculated SCF when this happened stood out because of the many comparisons that were available, but it is something that could be missed when calculating SCFs for joints where no comparisons are available. However, in

general, it was found that averaging of stresses made very little difference. For Joint 2, 2 shell models and 1 solid models had both averaged and non-averaged SCFs calculated. The difference found was negligible. For further work it was selected to only use averaged stresses. This is also in compliance with the DNVGL recommended practice [1].

5.4 Joint 3 and 4 – Case study – Tubular T-joint

5.4.1 Introduction

A simple tubular T-joint where the chord and brace has equal diameter, or parameter $\beta = 1$, produces a quite high SCF in the axial load case when using Efthymiou equations. There are also practical issues related to welding to take into account. The purpose of the case study is to investigate if a stiffened tubular joint may produce a lower SCF than a simple tubular T-joint. The joint geometry selected for the stiffened tubular joint was made to be easy to fabricate so the cost difference between the two joints would not differ excessively.

There are also other reasons to investigate this. Due to the complexity of welding the simple tubular T-joint, fabrication could possibly be more difficult, even though there are less parts involved than for the stiffened tubular joint. Depending on welding procedure the saddle position also may have less welding material than what is assumed in structural calculations of the joint.

When uncertainties regarding the physical geometry arise in the engineering phase, for instance if the resulting weld geometry is unknown, it may be useful to choose a design where the engineer has more control over the joint geometry. For instance inserting gusset plates to distribute stresses to a greater area, while taking care that the plate has a suitable stiffness. This is often seen in ship design.

Other times the location of a joint can dictate that a simple tubular joint is not suitable. This could for instance be the case when designing a connection point to the main structure for a vertical flare tower, where plated connections are required for horizontal force transfer.

In this section the two solutions are compared for joint geometry typical for a connection of a vertical flare tower to a platform. Shell models of both cases are compared with each other and Efthymiou equations. Analysis by use of solid elements is also performed, where the weld geometry is included.

The simple tubular T-joint is referred to as Joint 3, while the stiffened tubular T-joint is referred to as Joint 4.

5.4.2 General geometry

Selected members for the analysis are 18" tubulars of Schedule 60. This is from standard pipe size charts and translates to a OD of 457.2mm and a thickness of 19.05mm. The chord and

the brace have the same dimensions. Neighbouring joints are assumed 5m to each side of the joint centre, which yields a chord length of 10m.

The stiffener arrangement of joint 4 is a rectangular box welded to the chord, with a top plate which connects to the brace. The steel for the top plate has to be specified as Z-grade steel, due to the orientation of the load on this plate. The Z-grade steel plate has a thickness of 30mm in all analyses performed. For the stiffeners, 3 different thicknesses has been analysed to find the best distribution of stresses over the stiffener arrangement. 20mm, 16mm and 12mm stiffener plates have been considered.

The reason for experimenting with different stiffener thicknesses is that a very stiff stiffener detail connected to the softer tubular chord can produce high stress concentration factors. The stresses should be distributed in a balanced manner over the material of the joint for better fatigue performance. Also the load profile for the joint is also important in this consideration, and should be taken into account. This means if axial load from the brace is the dominant load, the axial SCFs are the most important for the calculated fatigue life of the joint, and a design which has lower axial SCFs should be aimed for.

Tubular members, 18" Schedule 60	
Steel grade	S355
Outside diameter	457.2mm
Thickness	19.05mm

Z-grade plate	
Steel grade	S355
Length x Width	497.2mm
Thickness	30mm

Stiffener plates	
Steel grade	S355
Thickness	20mm, 16mm, 12mm

Table 5-16: Section properties Joints 3 and 4

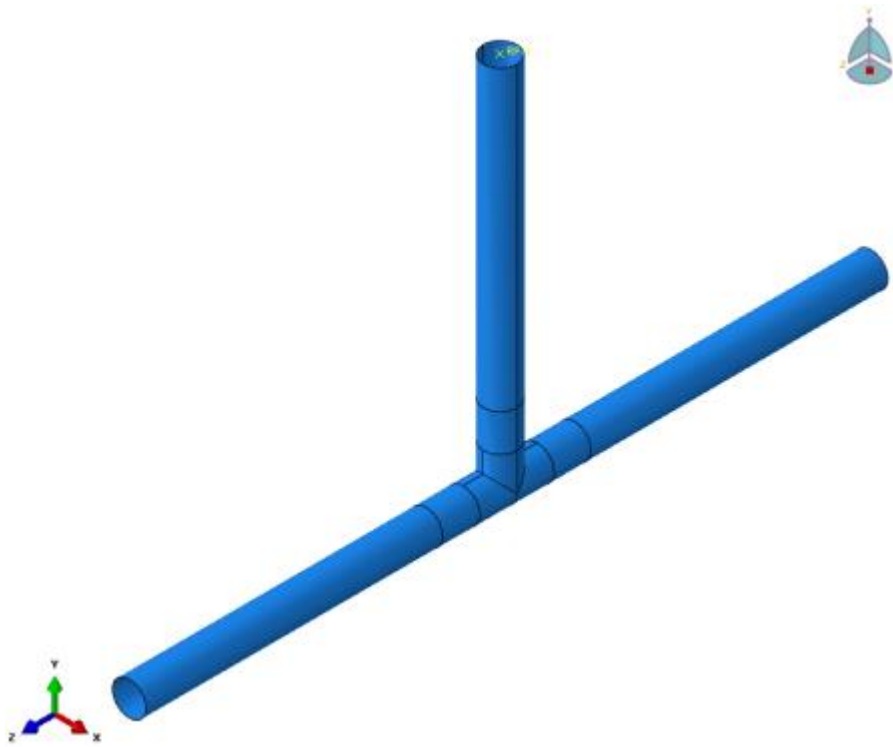


Figure 5-25: Joint 3 geometry overview

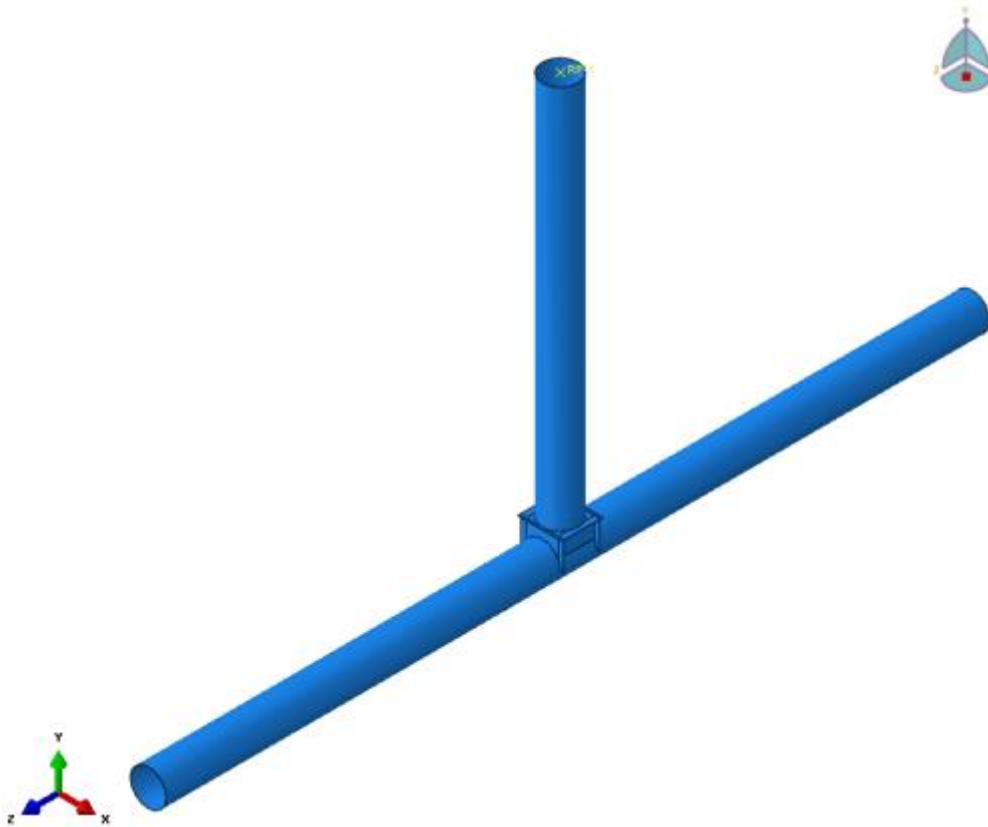


Figure 5-26: Joint 4 geometry overview

5.4.3 Efthymiou SCFs Joint 3

Efthymiou SCFs are calculated for Joint 3 for comparison against FEM results.

Load case	Position	SCF
Axial load	Chord crown	13.299
	Brace crown	5.547
	Chord saddle	5.026
	Brace saddle	3.699
In-plane bending	Chord crown	3.211
	Brace crown	2.440
Out-of-plane bending	Chord saddle	7.800
	Brace saddle	4.133

Table 5-17: Efthymiou SCFs for Joint 3

5.4.4 Loads and boundary conditions

Loading has been applied to obtain a 1MPa nominal stress in the brace member for all load cases.

$$F_{axial} = \sigma_{1MPa} * A_{brace} = 26222.1 N$$

$$M_B = \frac{\sigma_{1MPa} * I_{brace}}{y} = 2757.8 Nm$$

The joints are loaded through the end of the brace. Fixed boundary conditions are applied at each end of the chord.

5.4.5 Assembly

Joint 4 Model IV is a solid model that put together from 6 different part instances in the Abaqus assembly module. 3 of the parts are from solid elements and are as follows: brace local to the joint intersection including the top plate, the stiffeners including the weld toe, and the chord local to the joint intersection. These parts have been sectioned so that boundary areas are easily selected and can be coupled with the connecting parts by use of tie constraints.

The remaining 3 parts are made from shell elements. These elements are the 2 sections of chord connected to the solid chord part that is local to the joint intersection, and the 1 section

of brace that is connected to the solid brace part local to the joint intersection. The connection between shell and solid elements are made with the constraint shell-to-solid coupling.

5.4.6 Methodology

Extrapolation for Joint 3 and 4 is performed with the general method from [1], by using stress read out points at 0.5t and 1.5t. All meshes are adapted to txt mesh density. For extrapolating to the hot spot from the read out points the following equation is applied.

$$\sigma_{HS} = 1.5 * \sigma_{0.5T} - 0.5 * \sigma_{1.5T}$$

All stress components are extrapolated to the hot spot, and the principal stress is calculated from the components at the hot spot location. This is true also for the solid element model, see chapter 4.9 for a description of the process.

5.4.7 Joint 3 and 4 – Model overview

Joint 3 and 4 model overview						
Joint	Model	Element type	Meshing	No. of models	Stiffeners	Mesh sizes
3	I	S8R Shell	txt	1	N/A	19.1mm
4	I	S8R Shell	txt	3	20mm	19.1mm, 20mm, 30mm
4	II	S8R Shell	txt	3	16mm	16mm, 19.1mm, 30mm
4	III	S8R Shell	txt	3	12mm	12mm, 19.1mm, 30mm
4	IV	C3D20R Solid	txt	1	20mm	19.1mm, 20mm, 30mm

Table 5-18: Overview of the models created for Joint 3 and 4

5.4.8 Stress distribution and screening

Screening is performed to investigate which areas of Joint 4 are subject to stress concentrations. By having this information the mesh can be adapted to have the required quality and density in these areas. Stress distributions are also shown for Joint 3 to visualize the locations of the stress concentration factors. The stress distributions shown are absolute max principal stress contours.

5.4.8.1 Joint 3 – Stress distribution

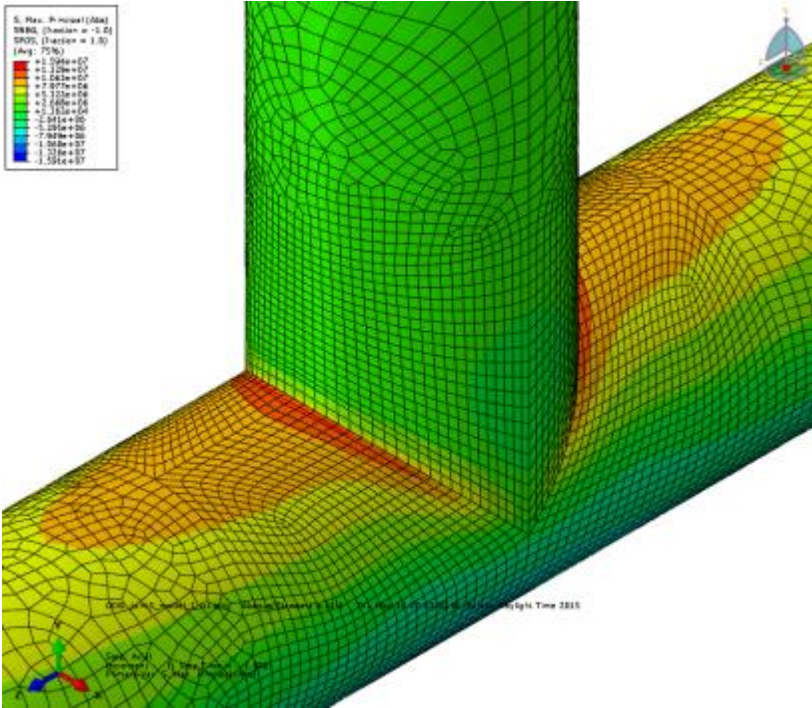


Figure 5-27: Joint 3 – Axial load – Abs. max principal stress contour

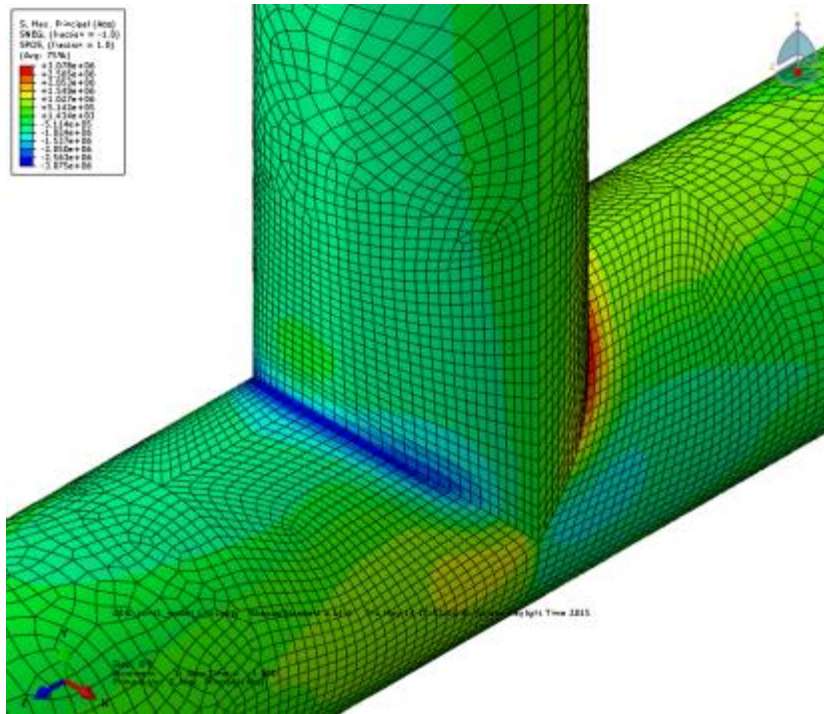


Figure 5-28: Joint 3 – IPB load – Abs. max principal stress contour

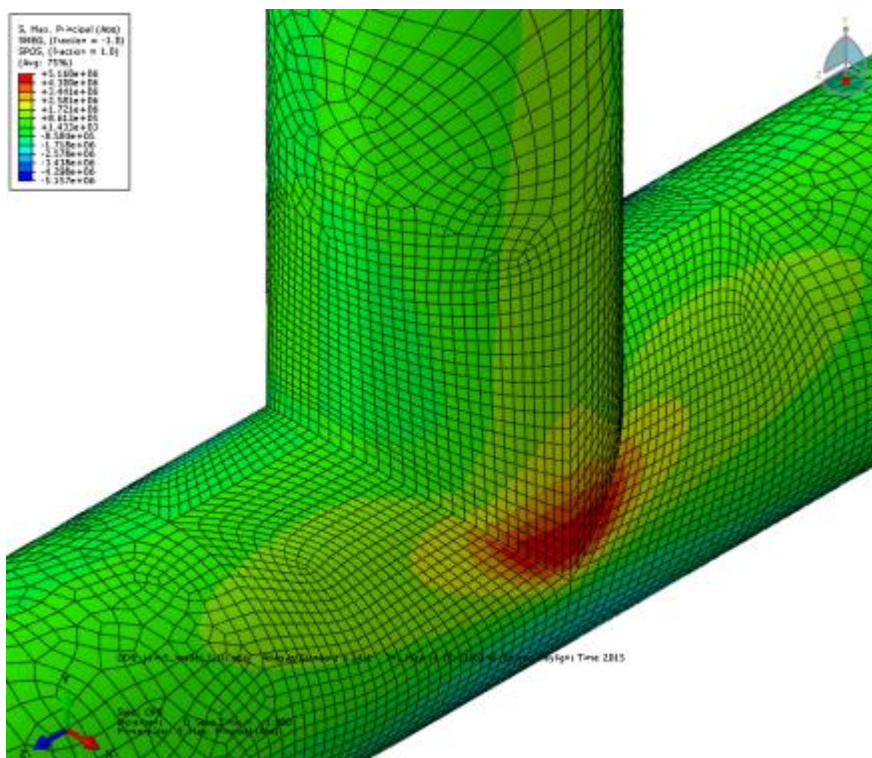


Figure 5-29: Joint 3 – OPB load – Abs. max principal stress contour

5.4.8.2 Joint 4 – Stress distribution and screening

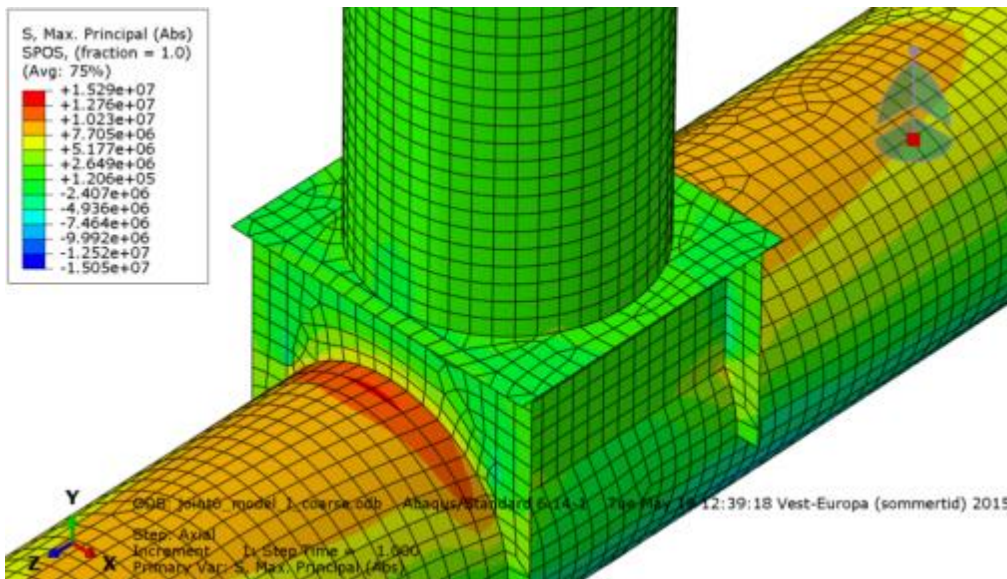


Figure 5-30: Joint 4 – Axial load – Abs. max principal stress contour

Shown in the figure above is the axial load case. For a 20mm stiffener plate it is clear that the maximum SCF in this load case is located on the chord. The SCF for the stiffener plate adjacent to the chord is also calculated for the varying thicknesses of stiffener plates used.

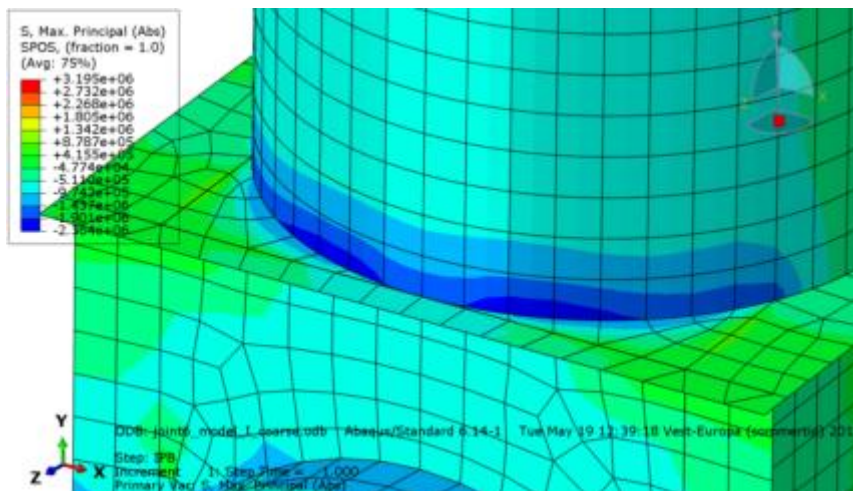


Figure 5-31: Joint 4 – IPB load – Abs. max principal stress contour

For the IPB load case shown above, the maximum hot spot stress could be located at four different positions. The brace, the top plate connected to the brace, the chord and the stiffener plate adjacent to the chord have possible hot spots. Making an acceptable quality mesh for the plate is challenging due to the location of the hot spot and the other stiffener plates which connects to the 30mm plate. Modelling the joint with more parts and connecting them with tie

constraints may simplify the meshing process, but could induce problems regarding the reliability of the results near the constraints. Method B from [1] is used to determine the SCF on the top plate.

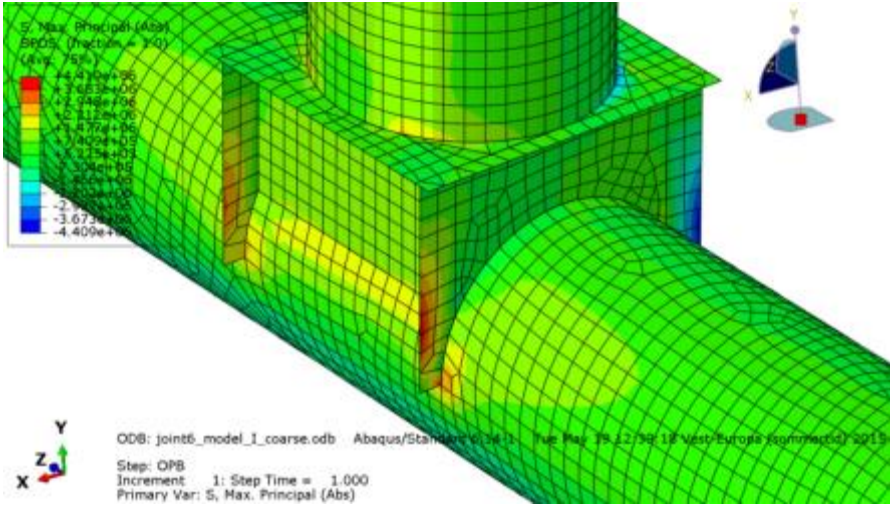


Figure 5-32: Joint 4 – OPB load – Abs. max principal stress contour

The figure above shows the OPB load case, where the hot spots are located on the chord where the circumferential stiffener plates connect, on the circumferential stiffener plates towards the chord and on the brace.

A summary of required models for the different load cases is found in the table below. For the top plate in in-plane bending, extrapolation according to Method B from [1] is used.

Load case	Mesh densities used at the various stress read out locations [mm]					
	Chord crown	Chord saddle	Stiffener crown	Stiffener edge	Top plate	Brace
Axial	19		12, 16, 20			
IPB	19		12, 16, 20		30	19
OPB	19			12, 16, 20		19

Table 5-19: Summary of Joint 4 mesh densities for different load cases

5.4.9 Joint 3 – Model I

Joint 3 Model I is a simple tubular T-joint with chord and brace members with equal diameters and thickness. Mesh is txt near the joint intersection and element used is S8R, thick-shell element.

The geometry of the joint is somewhat simplified when modelled with shell elements. A significant length of the material at the saddle would have to be cut away to enable a full penetration weld. This weld would not extend as far down as the brace saddle in the shell elements FEM model do, so there is a difference between the physical geometry of the joint and the FEM model. It could be possible to account for this by including this in a solid model, but with the double curvature and highly complex geometry of the weld it would require advanced modelling skills and exact measurements of the physical joint to accomplish. It was therefore selected to only perform a shell analysis of Joint 3.

Detailed plots of the solid model geometry, mesh and stress contours can be found in Appendix A. Extrapolation spreadsheets can be found in Appendix B.

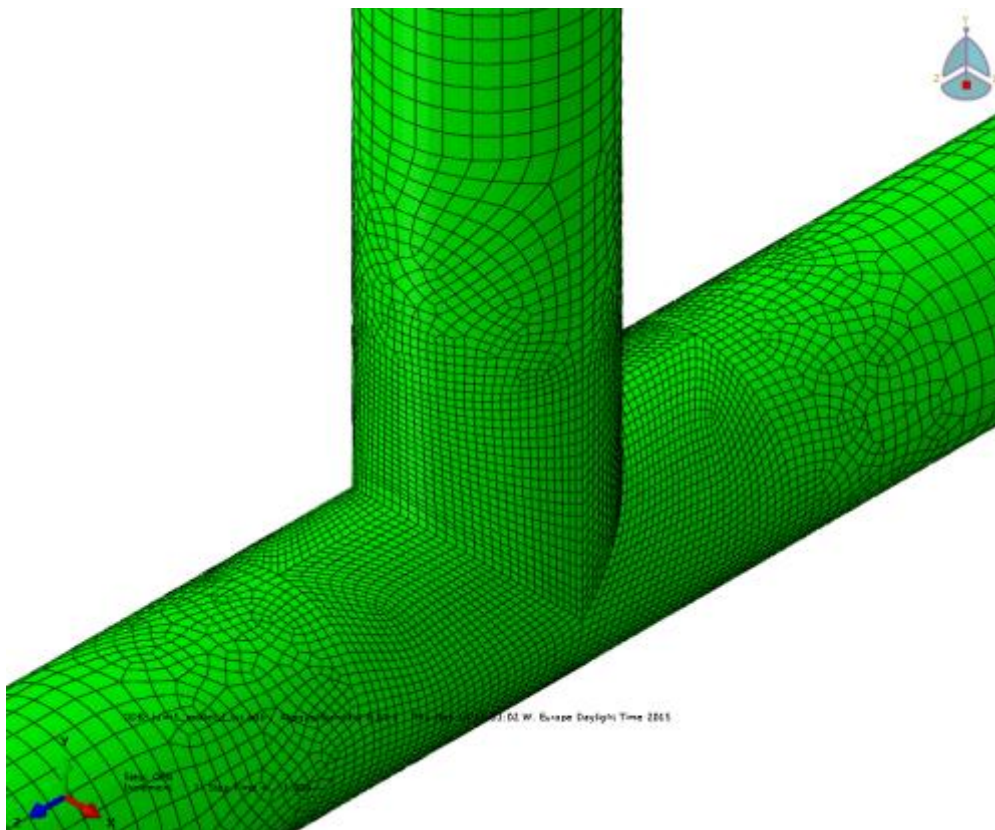


Figure 5-33: Plot of Joint 3 – Model I

5.4.9.1 Results

The final SCF results are tabulated in the table below. Component stresses are extrapolated from 0.5t and 1.5t distance from the intersection line to the hot spot, where the principal stress is calculated. Stresses are averaged. Detailed stress contour plots and mesh arrangement can be found in Appendix A, and the extrapolation spreadsheets can be found in Appendix B.

Joint 3 model I							
Load case	Position	Efthymiou SCF	Method A SCF	Method B SCF	Method A / Efthymiou	Method B / Efthymiou	Method A / Method B
Axial	Chord crown	13,299	14,303	15,129	1,08	1,14	0,95
	Brace crown	5,547	4,597	4,472	0,83	0,81	1,03
	Chord saddle	5,026	5,205	5,450	1,04	1,08	0,96
	Brace saddle	3,699	5,558	5,715	1,50	1,54	0,97
IPB	Chord crown	3,221	3,382	3,260	1,05	1,01	1,04
	Brace crown	2,44	1,802	1,666	0,74	0,68	1,08
OPB	Chord saddle	7,8	5,507	5,569	0,71	0,71	0,99
	Brace saddle	4,133	5,400	5,779	1,31	1,40	0,93

Table 5-20: Summary of SCFs for Joint 3 model I

5.4.9.2 Observations

From the results we observe that both method A and method B from [1] yield consistent results. The SCF for the brace saddle under axial load is predicted to be 50% higher than what the Efthymiou equations calculate. Also the SCF for the brace crown under IPB as well as the chord saddle subjected to OPB are predicted to be around 30% lower than what the Efthymiou equations report.

There are several possible causes of this discrepancy. Firstly, being that the chord and the brace are of equal diameter, the joint is an outlier when it comes to the validity of the Efthymiou equations. It lies on the upper boundary, meaning $\beta = 1$, for the ratio of brace to chord diameter. This also involves a geometry when the saddle position of the brace has a sharp 90° angle shape.

There is a database referenced in table B1.1 and B1.2 in [2] that has data that can be used as a direct comparison. It includes steel T-joint test sample of the same diameter as Joint 4 and $\beta = 1$. The experimentally measured SCF listed in the tables B1.1 and B1.2 [2] are much closer to the FEM analysis SCFs than the Efthymiou SCFs, so this adds credibility to the FEM results.

5.4.10 Joint 4 – Model I to III

3 shell element models are created for Joint 4. This is to investigate the effect of varying stiffener plate thickness. The objective of this is to obtain the most favourable stress distribution for the joint, to reduce the largest SCF and extend the expected lifetime of the joint.

Each shell element model has 3 different plate thicknesses, so 3 differently partitioned models with corresponding required mesh densities must be created. The nodes of the elements are then positioned for direct stress read out. This is done to conform to recommended practice [1] and avoid manually extrapolation of stresses internally over the elements.

Each model has 3 different load cases analysed, axial load, IPB and OPB. Coarse mesh screening is performed to determine hot spot stress locations.

The SCF of each of the 3 shell models are compared to the SCF of Joint 3 to evaluate the fatigue performance of the stiffening arrangement compared to the simple T-joint.

Detailed plots of the solid model geometry, mesh and stress contours can be found in Appendix A. Extrapolation spreadsheets can be found in Appendix B.

5.4.10.1 Results

Joint 4 Model I - 20mm stiffener plates				
Load case	Position	Method A SCF	Method B SCF	Method A / Method B
Axial	Chord crown	16,974	17,579	0,97
	Stiffener, chord crown position	9,245	8,686	1,06
IPB	Chord crown	1,773	1,793	0,99
	Brace	2,316	2,254	1,03
	Top plate, adjacent to brace		1,294	
OPB	Chord saddle, adjacent to circumferential stiffener	5,500	4,571	1,20
	Stiffener edge, adjacent to chord saddle position	5,862	4,402	1,33
	Brace	2,613	2,509	1,04

Table 5-21: Joint 4 Model I – SCF results

Joint 4 Model II - 16mm stiffener plates				
Load case	Position	Method A SCF	Method B SCF	Method A / Method B
Axial	Chord crown	15,362	16,097	0,95
	Stiffener, chord crown position	9,672	9,411	1,03
IPB	Chord crown	1,853	1,861	1,00
	Brace	2,425	2,361	1,03
	Top plate, adjacent to brace		1,392	
OPB	Chord saddle, adjacent to circumferential stiffener	4,953	4,093	1,21
	Stiffener edge, adjacent to chord saddle position	6,511	4,870	1,34
	Brace	2,618	2,518	1,04

Table 5-22: Joint 4 Model II – SCF results

Joint 4 model III - 12mm stiffener plates				
Load case	Position	Method A SCF	Method B SCF	Method A / Method B
Axial	Chord crown	13,915	14,782	0,94
	Stiffener, chord crown position	9,081	9,147	0,99
IPB	Chord crown	1,997	1,986	1,01
	Brace	2,528	2,460	1,03
	Top plate, adjacent to brace	-	1,530	N/A
OPB	Chord saddle, adjacent to circumferential stiffener	4,249	3,475	1,22
	Stiffener edge, adjacent to chord saddle position	9,003	7,005	1,29
	Brace	2,636	2,540	1,04

Table 5-23: Joint 4 Model III – SCF results

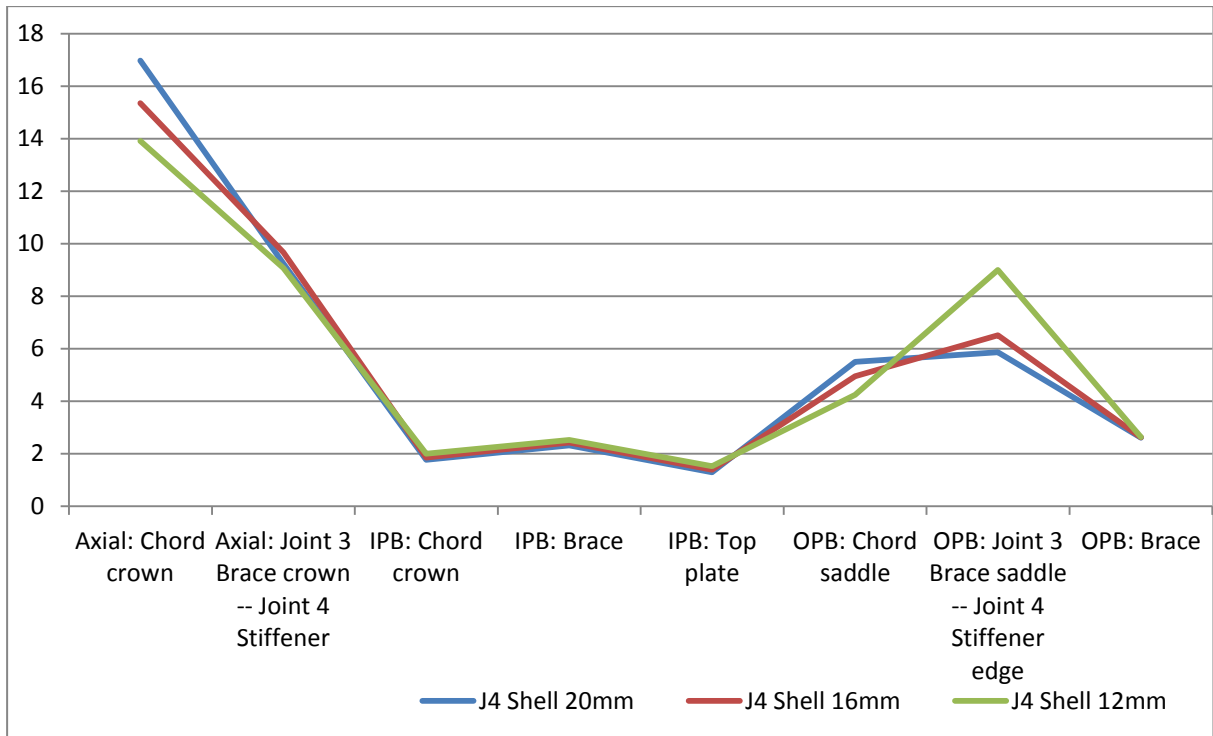


Figure 5-34: Variation in SCFs based on stiffener plate thickness

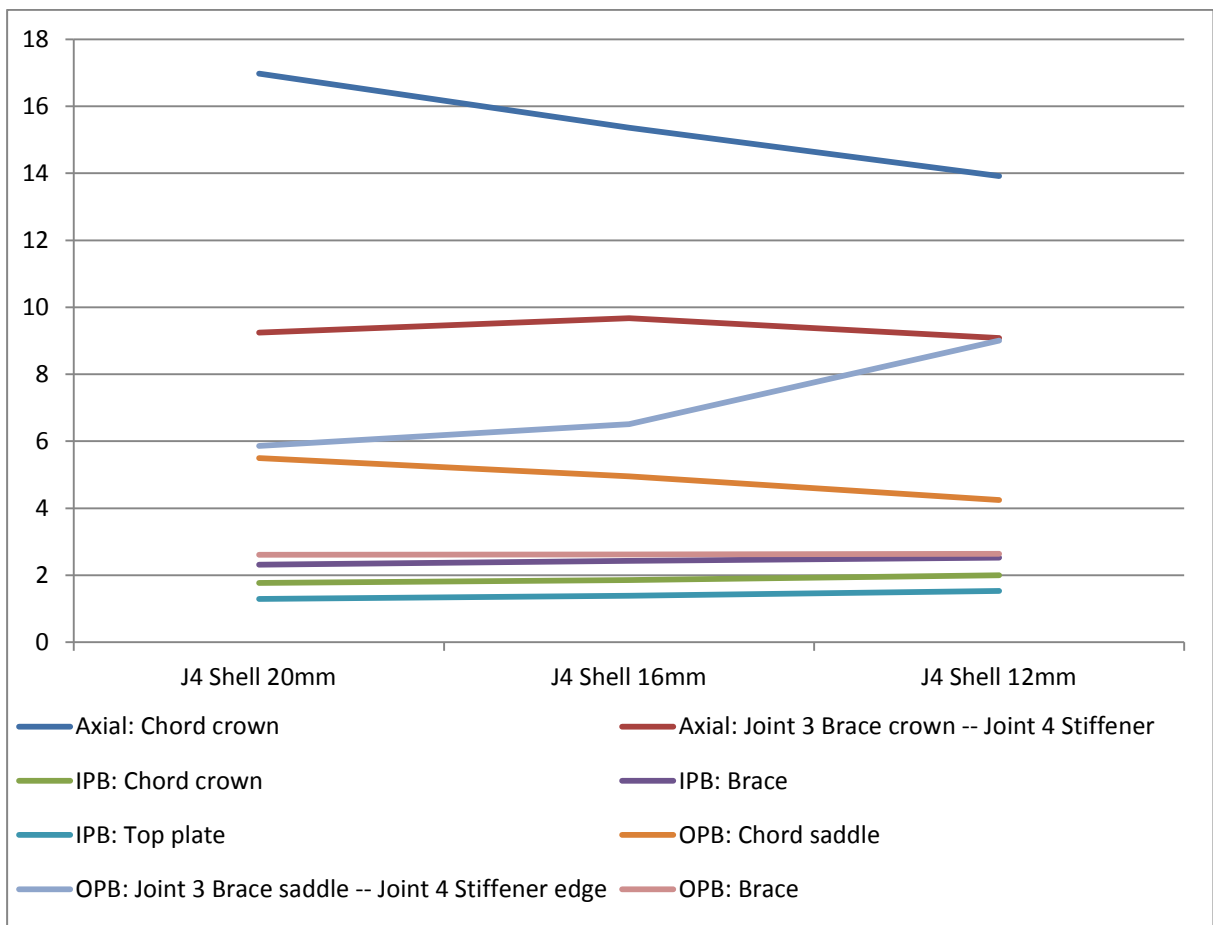


Figure 5-35: Change in SCF for different locations depending on stiffener plate thickness

5.4.10.2 Observations

From the results obtained from the shell models it is seen that certain SCFs can to some degree be controlled by use of different stiffener plate thicknesses. This is most prominent for the axial chord crown SCF and the OPB stiffener plate edge SCF. Depending on the load profile for the joint it is possible to select the best design for the specific application.

Comparing to Joint 3 SCFs, even though the locations of the hot spots are obviously different, some observations can be made. The axial SCF is quite similar for the two joints, especially when the stiffener plate thickness is taken as 12mm. However for the thicker stiffener plates the chord crown SCF increases, which is undesirable. Generally all IPB and SCFs for Joint 3 are higher than for Joint 4. For the OPB load case, the performance is similar between Joint 3 and 4 when the stiffener plate thickness is 20mm. However when stiffener thickness decreases, resulting stiffener edge SCF increases and Joint 3 will perform better.

Shell element model analysis of different Joint 4 geometries indicate that the simple tubular T-joint, Joint 3, will perform better in all load conditions but in-plane bending.

5.4.11 Joint 4 – Model IV

Joint 4 Model IV is a solid model of the stiffened tubular joint. Only the 20mm stiffener plate version has been analysed by this method. The model has been constructed by assembling 6 different parts in the Abaqus assembly module. This is done by using shell-to-solid couplings and tie constraints. To reduce computational effort, the chords and brace away from the joint intersection has been modelled with S8R shell elements.

The mesh is adapted so that txt mesh is obtained on the different parts with different thicknesses. Stress read outs are sampled at 0.5t and 1.5t away from the hot spot, and extrapolated to the hot spot. Individual stress components are extrapolated, and the principal stresses are calculated at the hot spot location. The weld toe length at the brace position is taken as 0.5x brace thickness, which is approximately 9.5mm. The weld toe length around the stiffeners is taken as 0.5x stiffener thickness, which is 10mm.

The resulting SCFs are compared to the results from models I to III, as well as Joint 3 SCFs. Direct comparison is only possible against Joint 4 Model I, as the same stiffener plate thickness is used in models I and IV.

Detailed plots of the solid model geometry, mesh and stress contours can be found in Appendix A. Extrapolation spreadsheets can be found in Appendix B.

5.4.11.1 Results

In the table below the SCFs calculated for Joint 4 Model IV are presented. They are compared graphically against Joint 4 Model I, which has equal stiffener plate thickness.

Joint 4 Model IV				
Load case	Position	Method A SCF	Method B SCF	Method A / Method B
Axial	Chord crown	16,990	17,422	0,98
	Stiffener, chord crown position	9,471	8,638	1,10
IPB	Chord crown	1,489	1,511	0,99
	Brace	1,960	1,912	1,03
	Top plate, adjacent to brace	0,597	0,424	1,41
OPB	Chord saddle, adjacent to circumferential stiffener	3,373	2,849	1,18
	Stiffener edge, adjacent to chord saddle position	2,458	1,817	1,35
	Brace	1,888	1,888	1,00

Table 5-24: Joint 4 Model IV – SCF results

5.4.11.2 Observations

It is observed that the significant SCF differences appear in the IPB and OPB load cases. The axial SCFs are virtually identical, with discrepancy of less than 2.5%. The IPB top plate SCF is significantly higher in the shell model than in the solid model. One possible cause is that the geometry of the joint above and below the top plate intersects. This is a known limitation of shell element models, as the path of forces through the top plate is unrealistic if the plates over and under the top plate intersect. A very sharp transition of forces takes place, with no load distributing effect through the top plate thickness. To obtain a realistic behaviour of this type of joint a solid model is required.

Other probable reasons for improved performance for the solid model are the effects of including the weld geometry. Local stiffness is increased, but stresses transition more smoothly and to a greater area.

5.4.12 Comparison of results

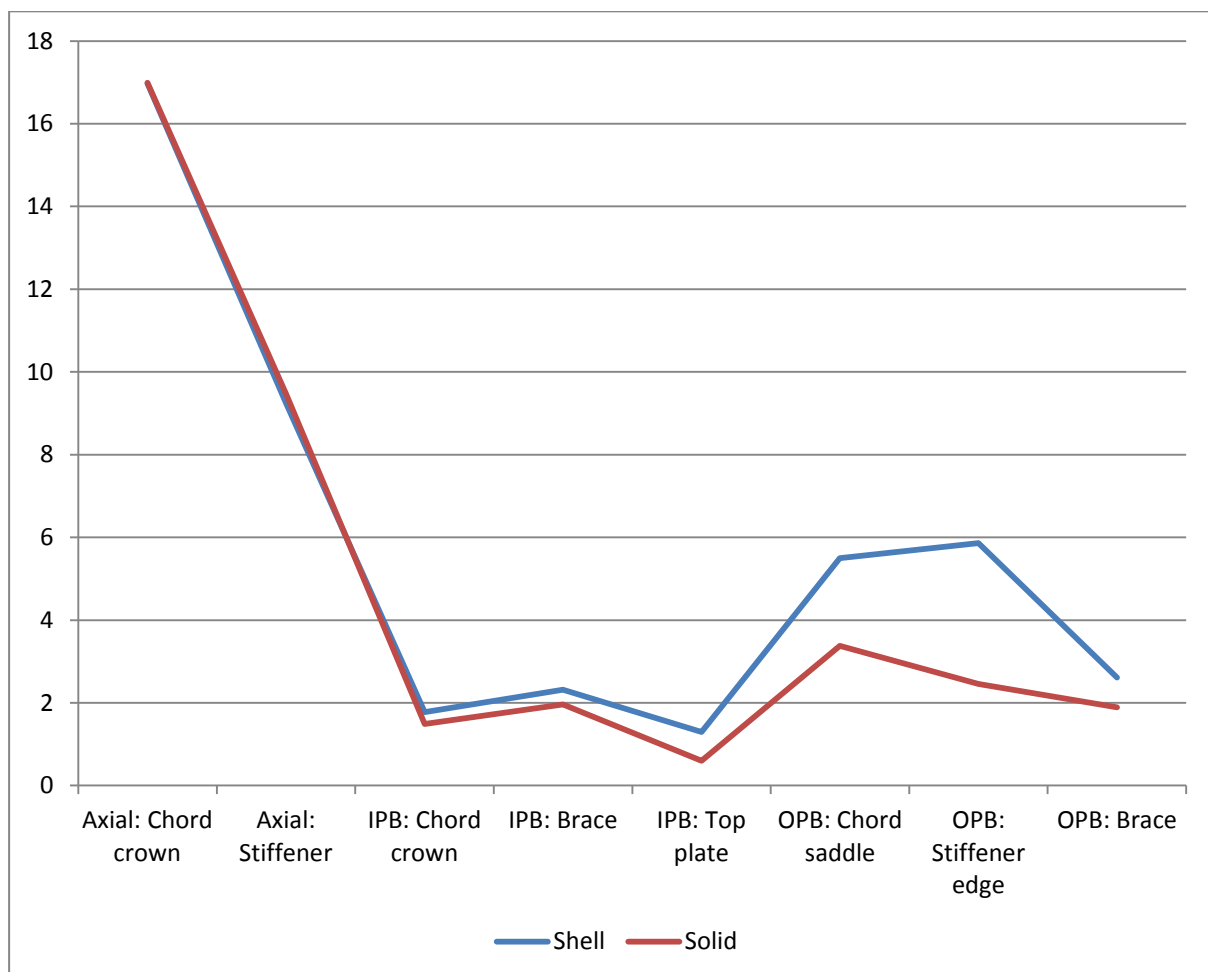


Figure 5-36: Joint 4 Model I compared to Joint 4 Model IV

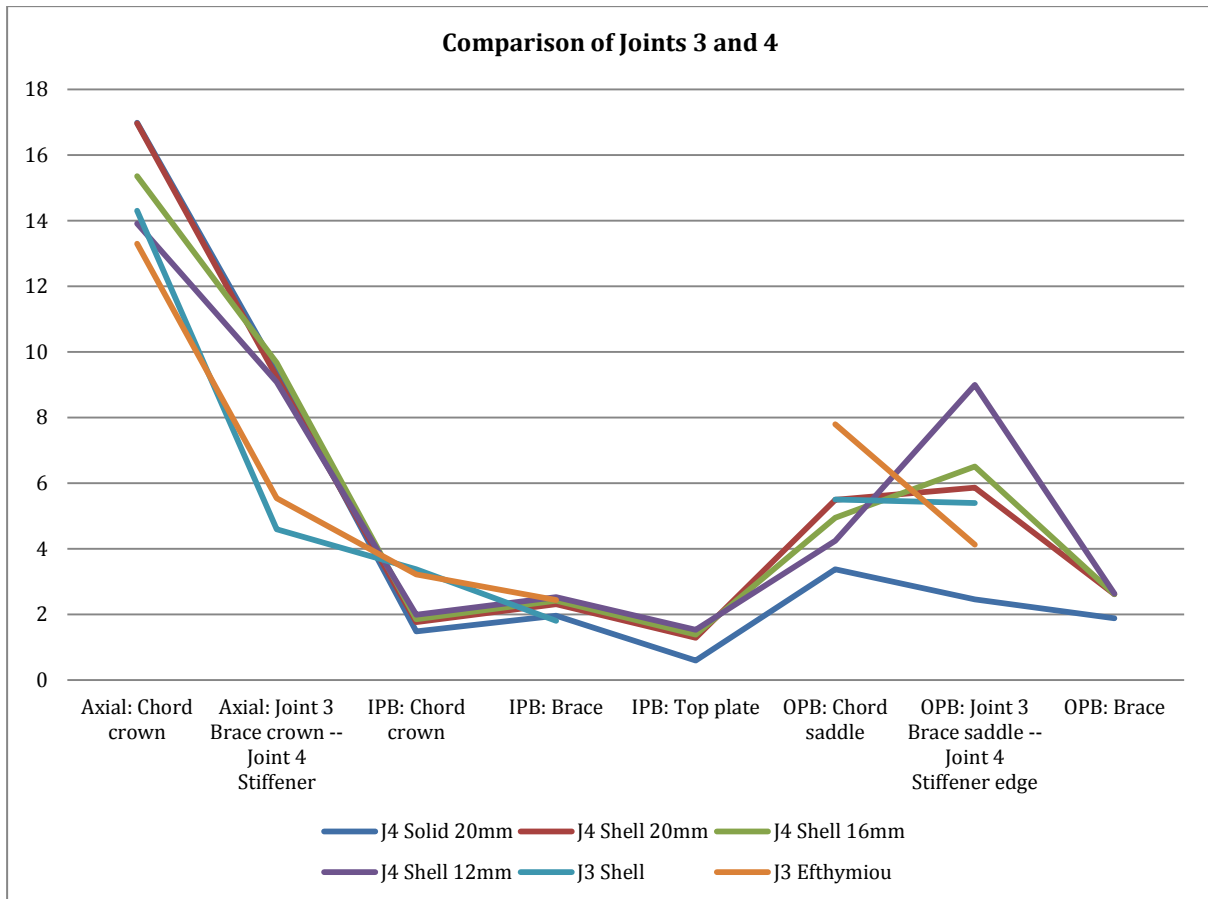


Figure 5-37: Comparison of Joint 3 and 4 results

From the results of the case study we can draw some conclusions. Overall there is little benefit in using the stiffener arrangement proposed. However, analysis with solid elements including weld geometry show improved performance in both in-plane bending and out-of-plane bending. If more alternative stiffener thicknesses were explored with solid element modelling a better overall solution may have been found. Unfortunately the inclusion of the weld geometry had little effect for the highest SCF, namely the axial chord crown SCF.

When it comes to design improvement of the stiffened tubular joint, the areas that need improvement can be identified by the size of the SCFs. It is clear that the transition between the stiffener and the chord needs to be optimized to improve fatigue performance. Internal stiffeners, a smoother transition between stiffener and chord or a local thickness increase of the chord are possible choices for further investigation.

If from the global analysis it is clear that in-plane bending or out-of-plane bending are the dominant loads, the stiffener arrangement can be considered. If axial load dominates, the simple tubular joint performs better.

5.5 Joint 5 and 6 – Case study – Tubular K-joint

5.5.1 Introduction

To expand on the case study of equal diameter and thickness of a tubular T-joint, a study is performed on equal diameter and thickness of a tubular KT-joint. Again, for the case of the KT-joint, practical issues related to welding complicate the fabrication of the joint. Obtaining the exact 3D joint geometry including the weld can be difficult in the design phase of a structure. A simpler shell model can be created, but this does not take into account exactly how the weld connects the members of the joint.

The joint geometry investigated here is not very common, but can for instance appear near connection nodes of a flare tower against the main structure. At these connection points forces may be large, and brace members may be required to be large as well. In such cases the geometry near the connection to the main structure may also dictate that a plate stiffened tubular joint is required, for instance if the flare tower is vertical as opposed to angled outwards from the structure.

It is also interesting to see if the performance of the plate stiffened tubular joint can rival the performance of a simple tubular KT-joint, calculated from parametric equations or from FEM analysis as per [1].

5.5.2 General geometry

Selected members for the KT-joint are of equal dimensions as the members used in Joint 3 and 4. The dimensions of the members are typical for the lower part of a flare tower structure. Neighbouring joints are again modelled as 5m to each side of the joint centre, yielding a chord length of 10m.

The stiffener arrangement is redesigned to suit the diagonal braces coming in at a 45 degree angle. This is done by adding a diagonal top plate, the brace extending normally from the plane of the plate. The top plates have to be specified as Z-grade steel, meaning it will have good capacity for load normal to the plane of the plate. This top plate is taken to be 30mm thick in all models created for Joint 6. The stiffener plates are also kept at a constant thickness of 16mm for all analysis performed on Joint 6. In screening this has been found to be a balanced thickness in terms of stress distribution over the joint.

The joint is symmetric about the centre, so only SCFs near a single diagonal brace and centre brace and needs to be found.

Diagonal brace is referred to as Brace A, while the central brace is referred to as Brace B.

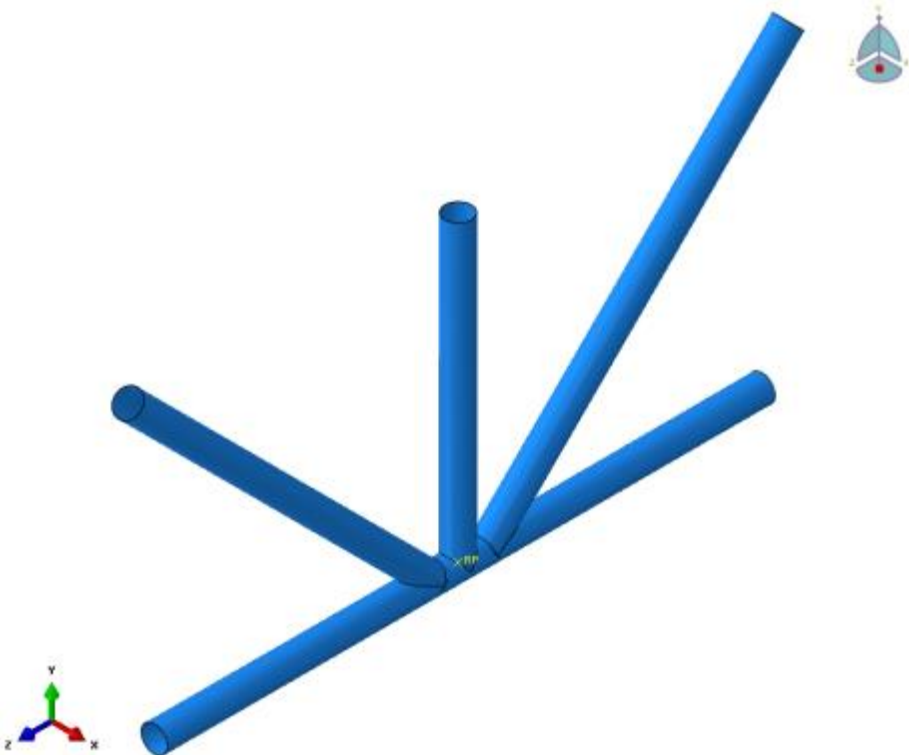


Figure 5-38: Joint 5 geometry overview



Figure 5-39: Joint 6 geometry overview

5.5.3 Efthymiou SCFs joint 5

Efthymiou SCFs are calculated for Joint 5 for comparison against FEM results.

Load case	Position	SCF
Axial load	Chord crown, near Brace A	10.974
	Brace A crown	5.547
	Chord saddle, near Brace A	2.886
	Brace A saddle	2.395
	Chord crown, near Brace B	13.299
	Brace B crown	5.547
	Chord saddle, near Brace B	2.886
	Brace B saddle	3.699
In-plane bending	Chord crown, near Brace A	2.520
	Brace A crown	2.677
	Chord crown, near Brace B	3.211
	Brace B crown	2.440
Out-of-plane bending	Chord saddle, near Brace A	3.771
	Brace A saddle	1.998
	Chord saddle, near Brace B	6.265
	Brace B saddle	3.320

Table 5-25: Efthymiou SCFs for Joint 6

It is worth noting that several of the Efthymiou SCFs for Brace B are identical to the Efthymiou SCFs for the simple tubular T-joint Joint 3.

5.5.4 Loads and boundary conditions

Loading has been applied to obtain a 1MPa nominal stress in the brace member for all load cases.

$$F_{axial} = \sigma_{1MPa} * A_{brace} = 26222.1 N$$

$$M_B = \frac{\sigma_{1MPa} * I_{brace}}{y} = 2757.8 Nm$$

The joints are loaded through the end of the brace. Fixed boundary conditions are applied at each end of the chord.

5.5.5 Special load cases

In joint types where more than one brace is involved, i.e. in K, KT and X-joints the relative magnitude and direction of the nominal brace-end loads and moments has a significant influence on SCFs. Generally this leads to 9 required load cases.

- 1. Balanced axial load
- 2. One-brace-only loaded with axial load
- 3. Unbalanced axial load

and similarly for in-plane bending and out-of-plane bending [1, 7, 13]

The parametric Efthymiou equations include these effects by applying influence functions. The derivation of the influence functions is based on superposition of linear elastic stress fields.

For a KT-joint two axial load cases are covered by Efthymiou equations. Balanced axial load and one brace only loaded axially. For IPB loading, the direction of the moments does not have any significant effect on the SCFs. The influence of the moment on one brace on another can be considered as zero. For OPB in KT-joints two load cases should be analysed. Unbalanced OPB on all three braces and each brace loaded independently. The SCFs for the unbalanced load case are considerably higher than those found from independently loaded braces, especially when gaps are small or overlaps are present. For independently loaded braces, the stiffening effect from unloaded braces is substantial [13].

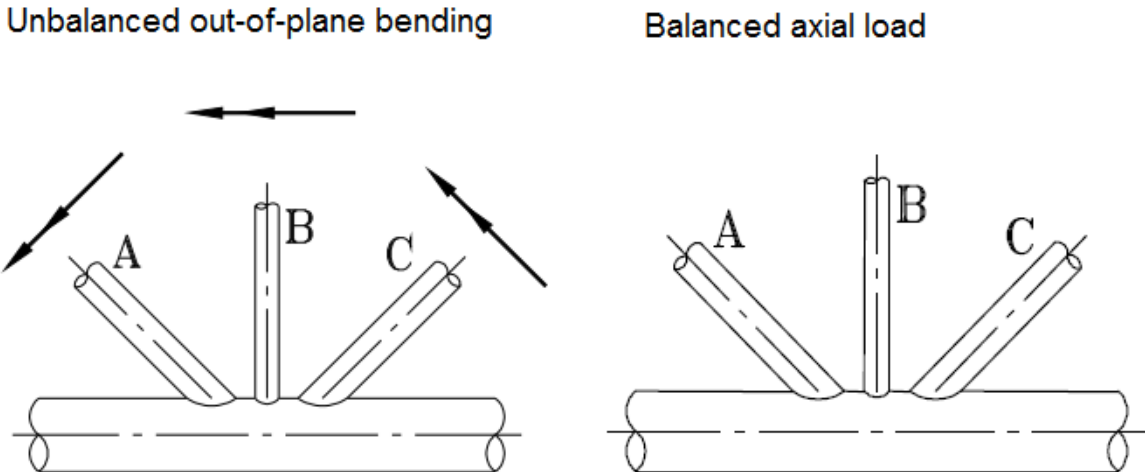


Figure 5-40: Unbalanced out-of-plane bending and balanced axial load [1]

5.5.6 Assembly

Joint 6 Model II is a solid model, which is put together in Abaqus assembly module from independently modelled parts. The regions local to the joint are modelled with solid parts, while the regions away from the joint are modelled as shell elements. Solid parts of the model include the brace local to the joint, the 30mm top plate including welds against the chord, the 16mm stiffener plates and the chord local to the joint. Shell parts of the model are the braces away from the joint and the chord away from the joint.

The solid parts are partitioned so that neighbouring areas can be selected and coupled with the connected parts by tie constraints. The shell parts are connected to the solid parts by shell-to-solid couplings. Each part is meshed individually to suit the txt mesh scheme for read out and extrapolation of stresses.

5.5.7 Methodology

Extrapolation for Joint 5 and 6 is performed with the general method from [1], by using stress read out points at 0.5t and 1.5t. All meshes are adapted to txt mesh density. For extrapolating to the hot spot from the read out points the following equation is applied.

$$\sigma_{HS} = 1.5 * \sigma_{0.5T} - 0.5 * \sigma_{1.5T}$$

All stress components are extrapolated to the hot spot, and the principal stress is calculated from the components at the hot spot location. This is true also for the solid element model, see chapter 5.3.6 for a description of the process.

5.5.8 Joint 5 and 6 – Model overview

Joint 5 and 6 model overview					
Joint	Model	Element type	Meshing	No. of models	Mesh sizes
5	I	S8R Shell	txt	2	19.1mm
6	I	S8R Shell	txt	3	16mm, 19.1mm, 30mm
6	II	C3D20R Solid	txt	1	16mm, 19.1mm, 30mm

Table 5-26: Overview of models created for Joint 5 and 6

It was selected to make 2 models for Joint 5. One to adapt the mesh at the crown position to a txt pattern, and one to adapt the mesh at the saddle position to txt.

For Joint 6 Model I, 3 models were created, each one with a mesh density to suit either the chord/brace, the stiffeners or the top plate. Joint 6 Model II is a solid model assembled from individually meshed parts, so only one properly partitioned model was required to extract hot spot stresses.

5.5.9 Stress distribution and screening

Joint 5 Model I is a simple tubular KT-joint with chord and brace members with equal diameters and thickness. Mesh is txt near the joint intersection and element used is S8R, thick-shell element.

5.5.9.1 Joint 5 – Stress distribution

Following are plots of the abs. max principal stress distribution for the 3 different load cases. These indicate the physical location of the stress concentrations.

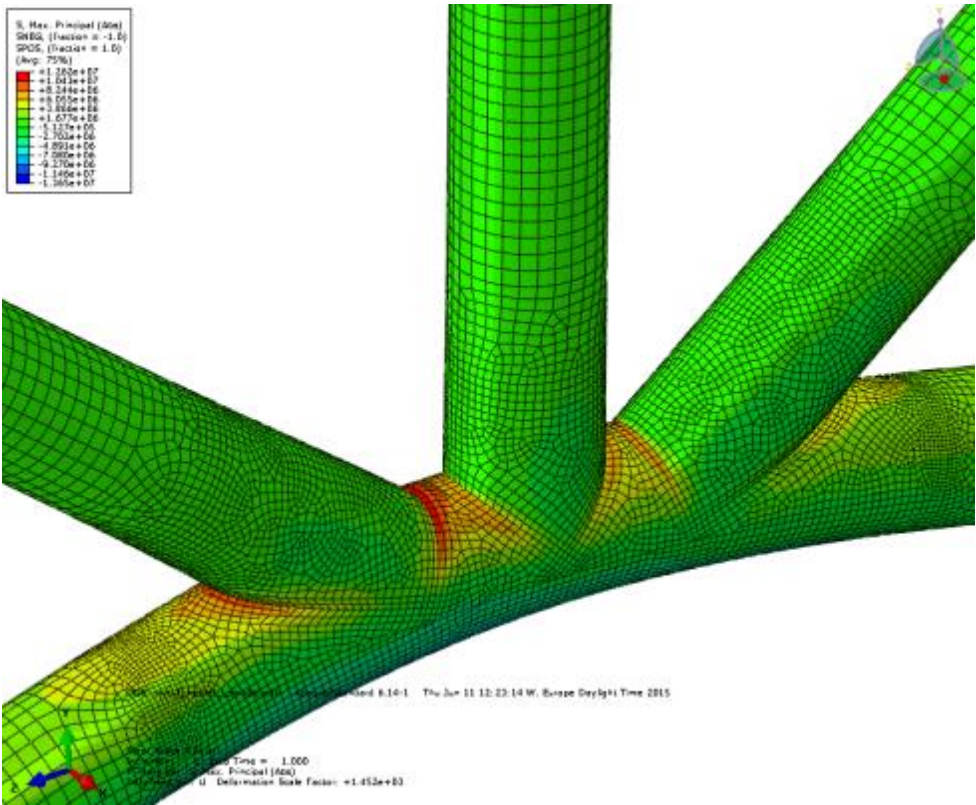


Figure 5-41: Joint 5 – Brace A Axial load – Abs. max principal stress contour

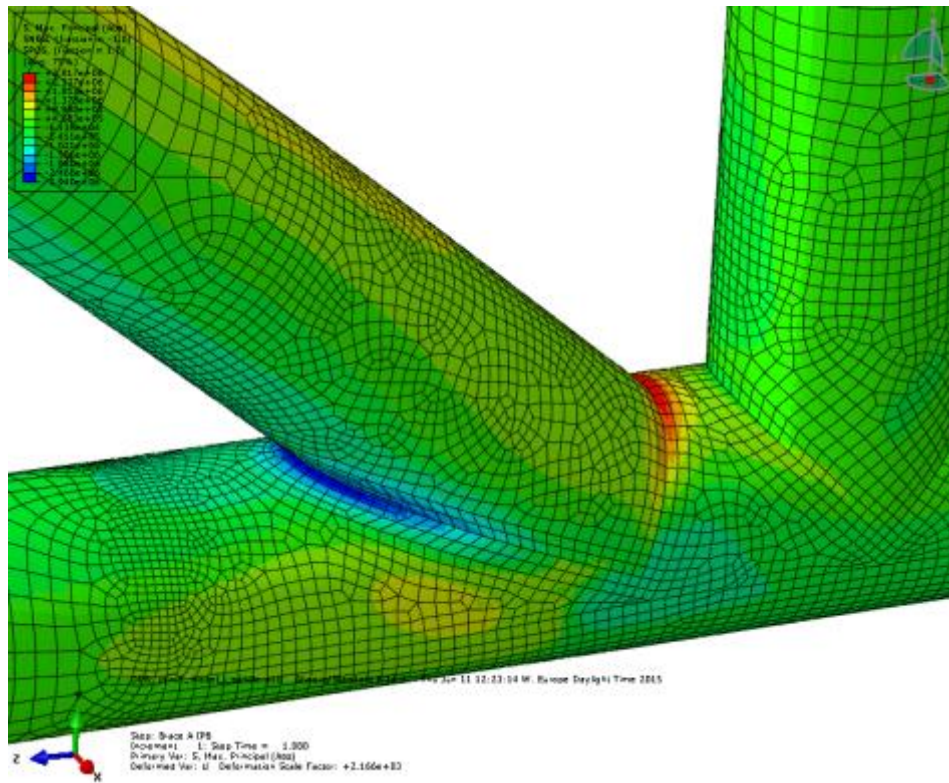


Figure 5-42: Joint 5 – Brace A IPB load – Abs. max principal stress contour

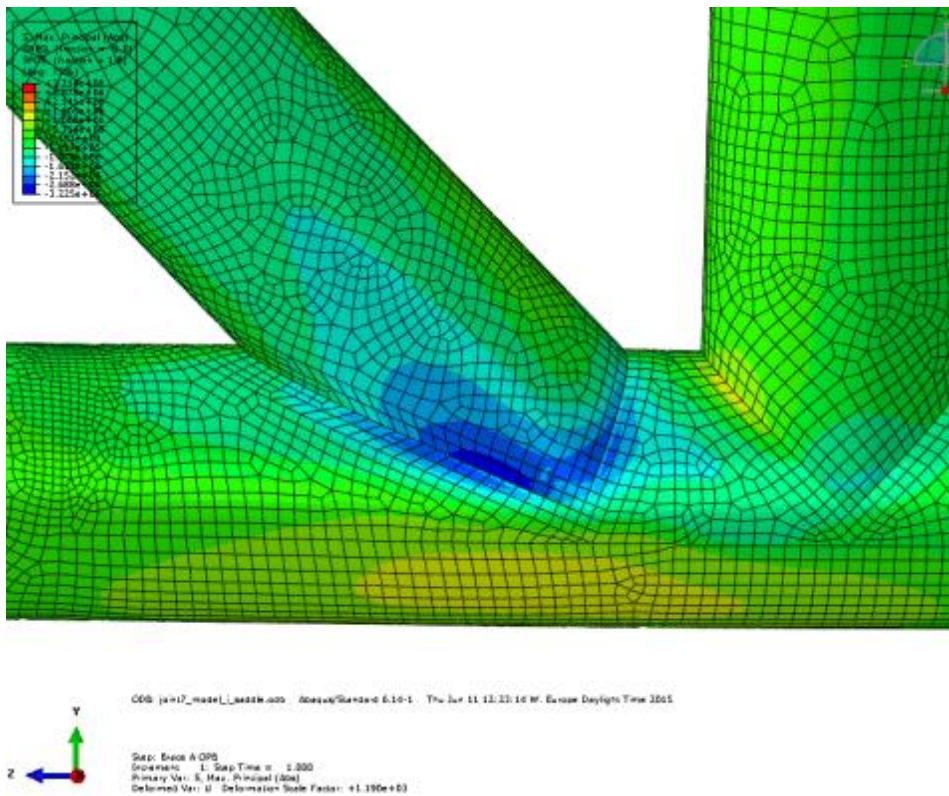


Figure 5-43: Joint 5 – Brace A OPB load – Abs. max principal stress contour

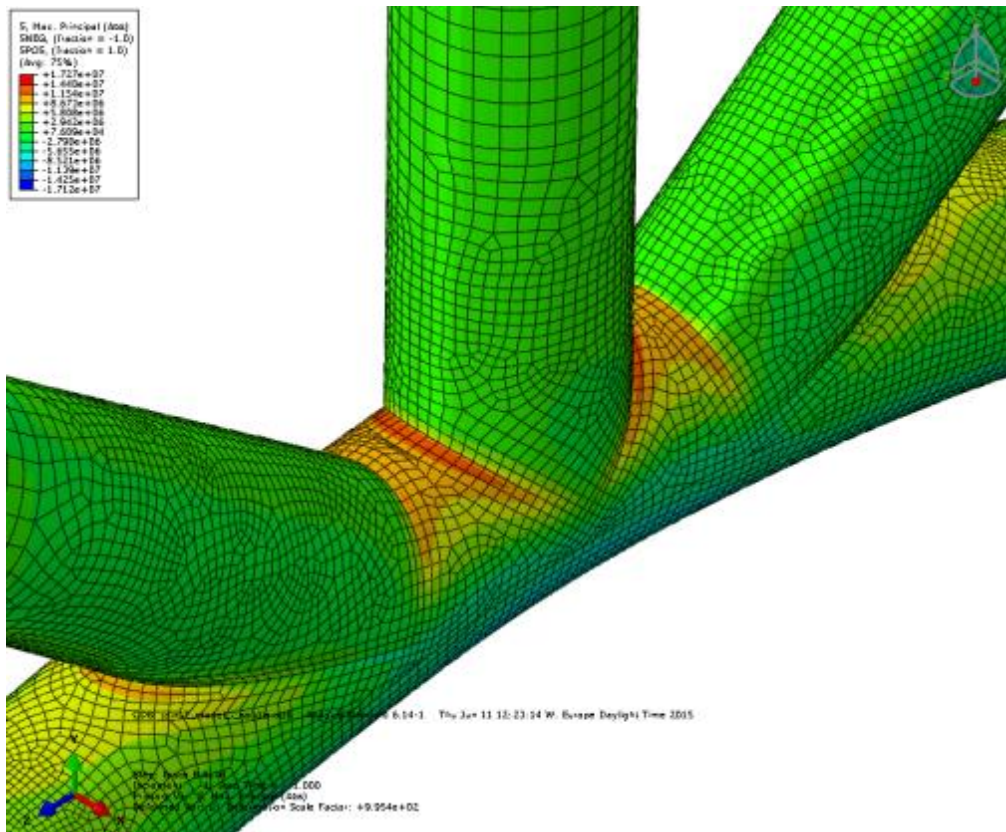


Figure 5-44: Joint 5 – Brace B Axial load – Abs. max principal stress contour

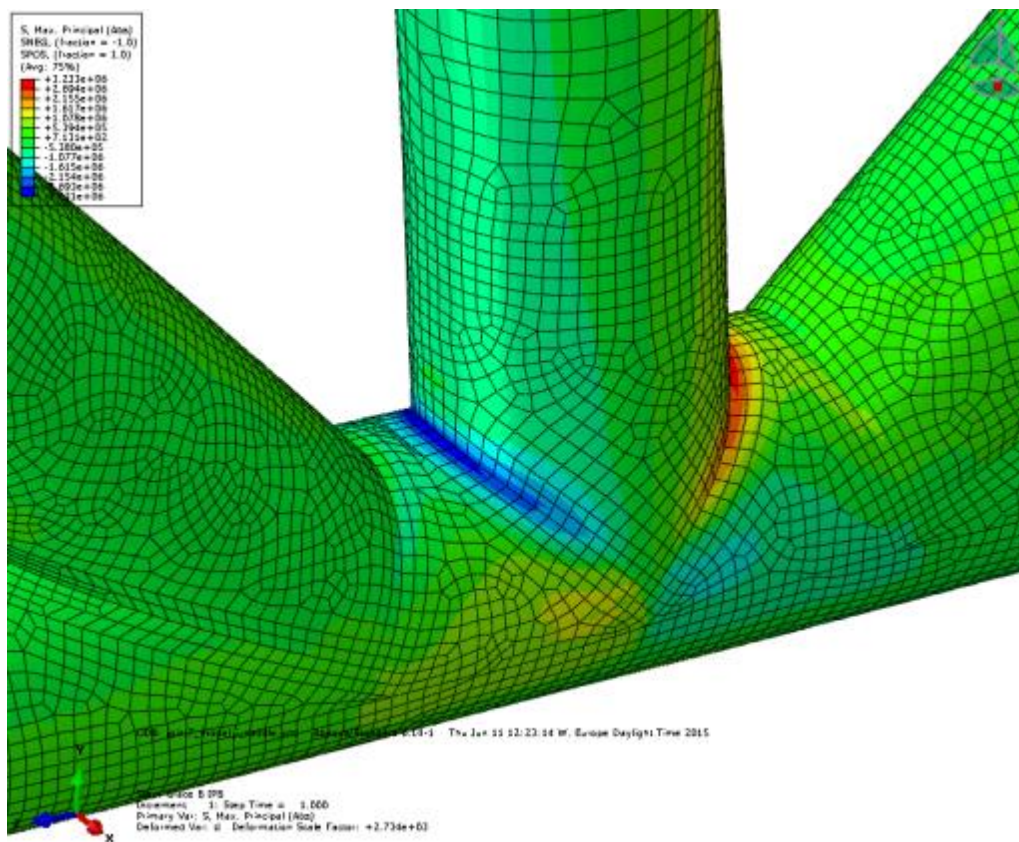


Figure 5-45: Joint 5 – Brace B IPB load – Abs. max principal stress contour

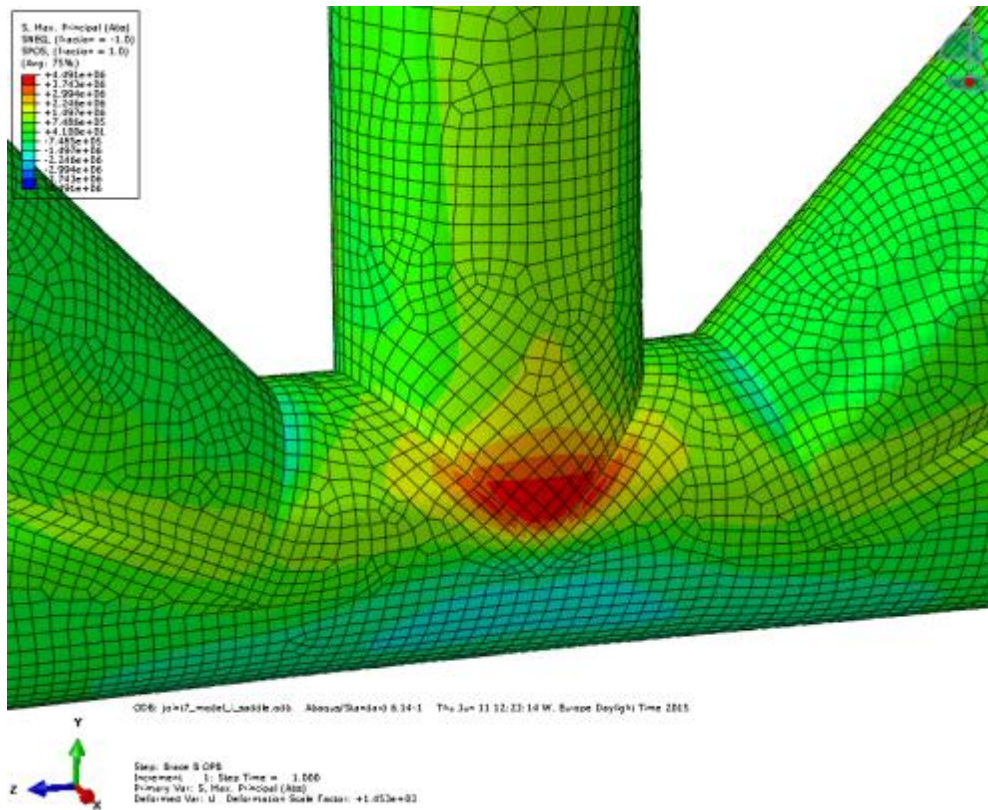


Figure 5-46: Joint 5 – Brace B OPB load – Abs. max principal stress contour

5.5.9.2 Joint 6 – Stress distribution and screening

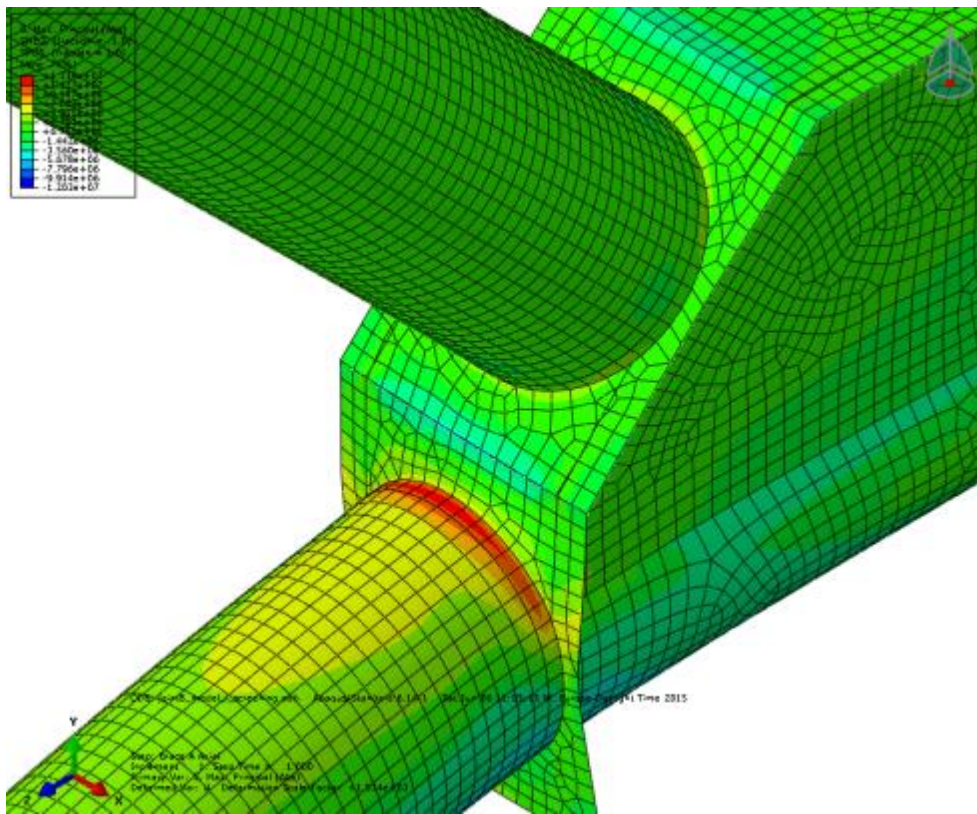


Figure 5-47: Joint 6 – Brace A Axial load – Abs. max principal stress contour

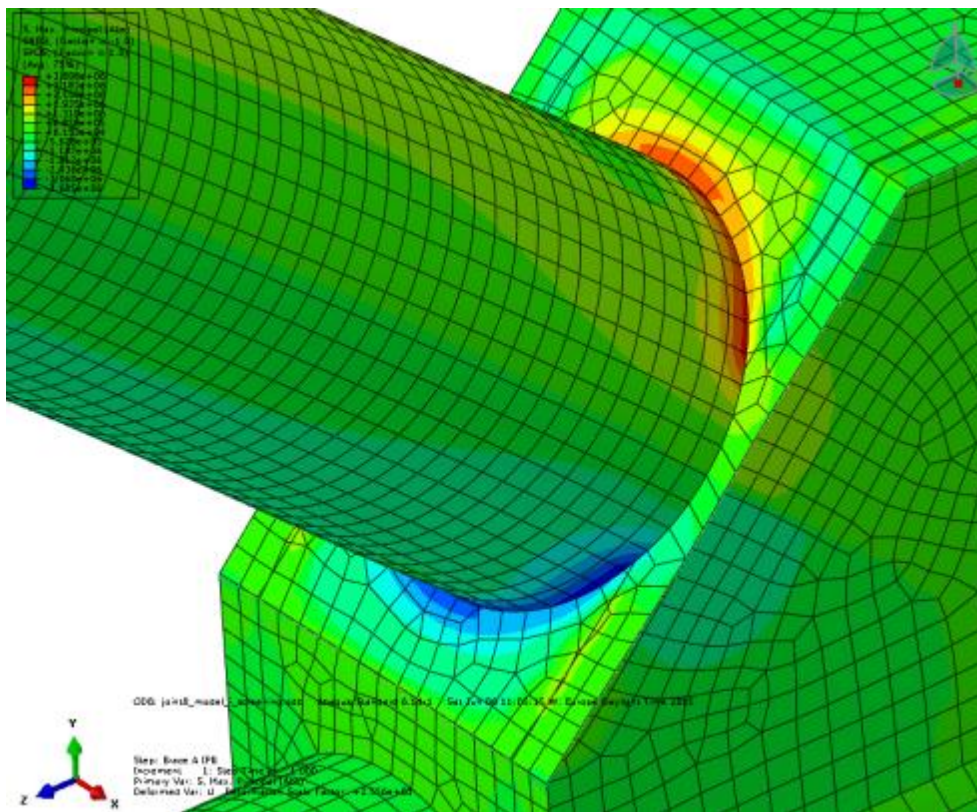


Figure 5-48: Joint 6 – Brace A IPB load – Abs. max principal stress contour

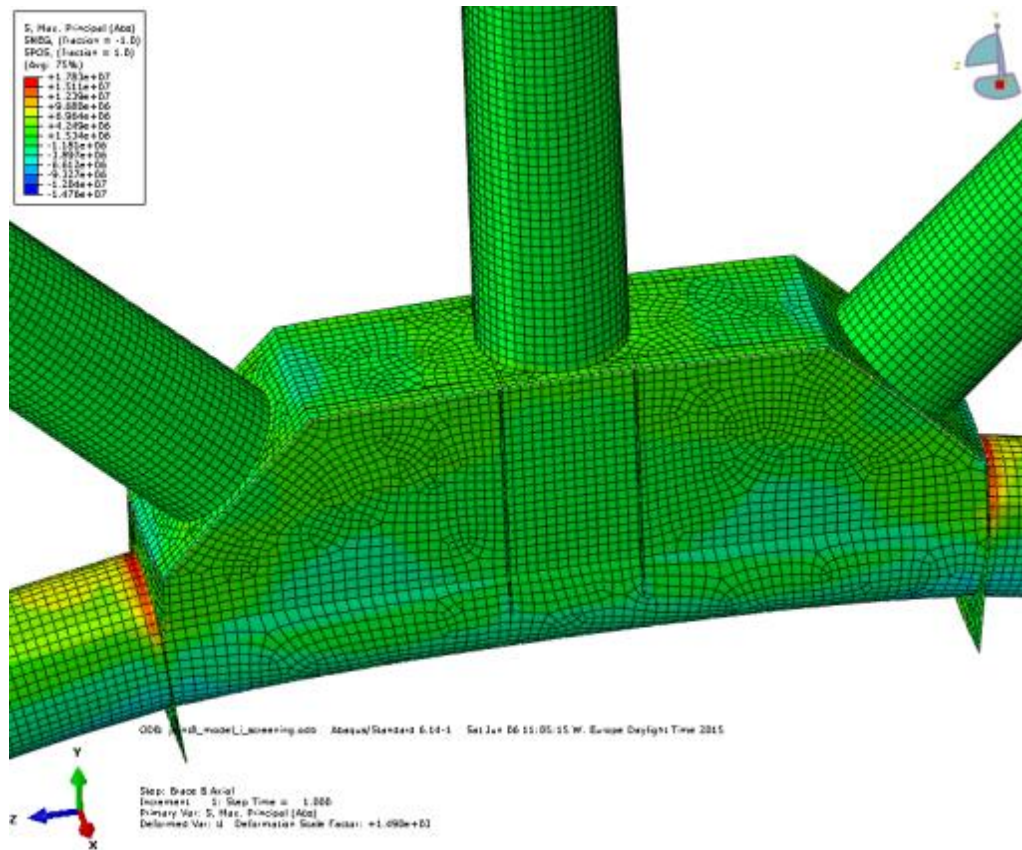


Figure 5-51: Joint 6 – Brace B Axial load – Abs. max principal stress contour

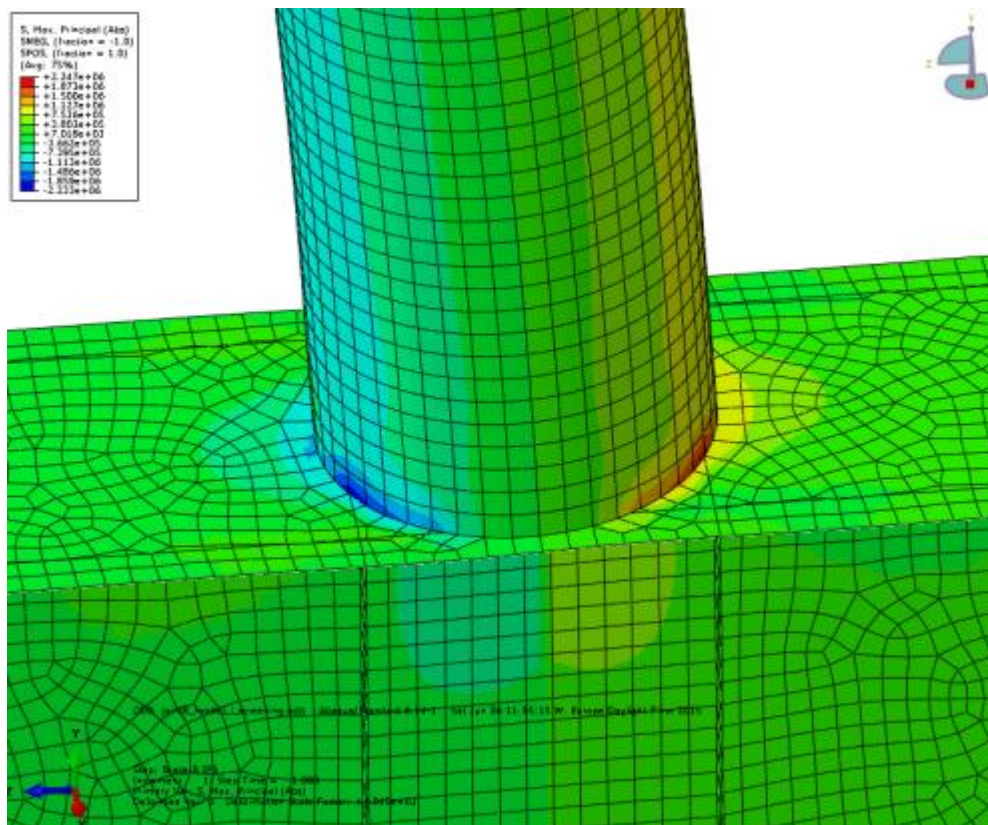


Figure 5-52: Joint 6 – Brace B IPB load – Abs. max principal stress contour

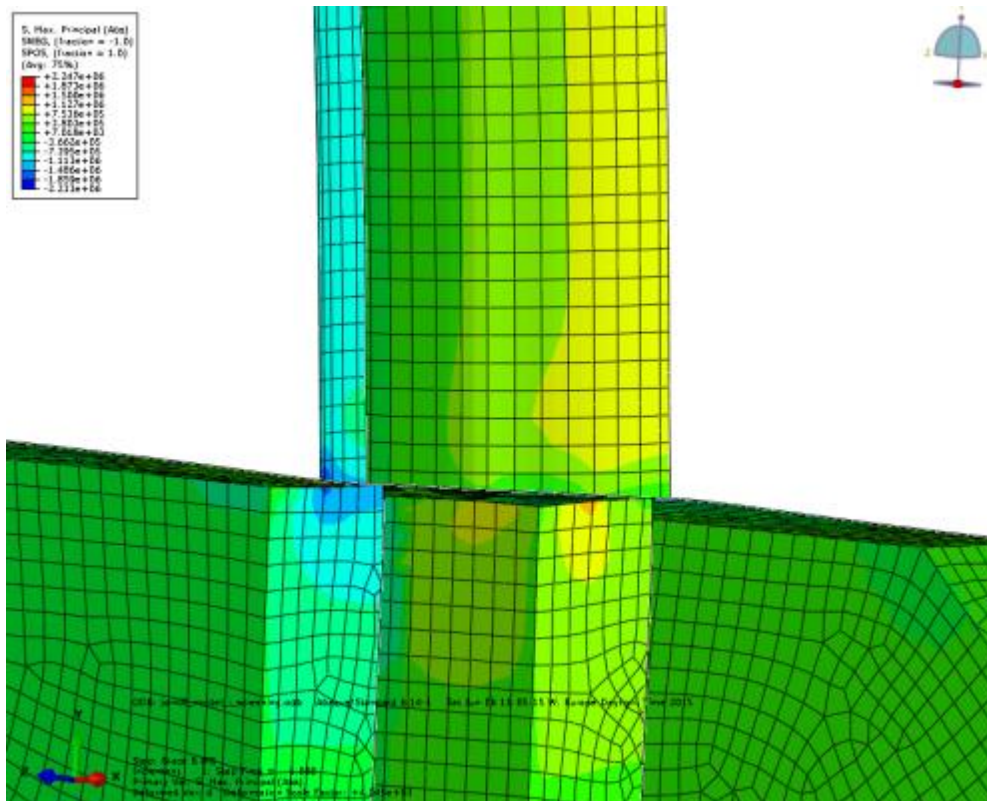


Figure 5-53: Joint 6 – Brace B IPB load – Abs. max principal stress contour

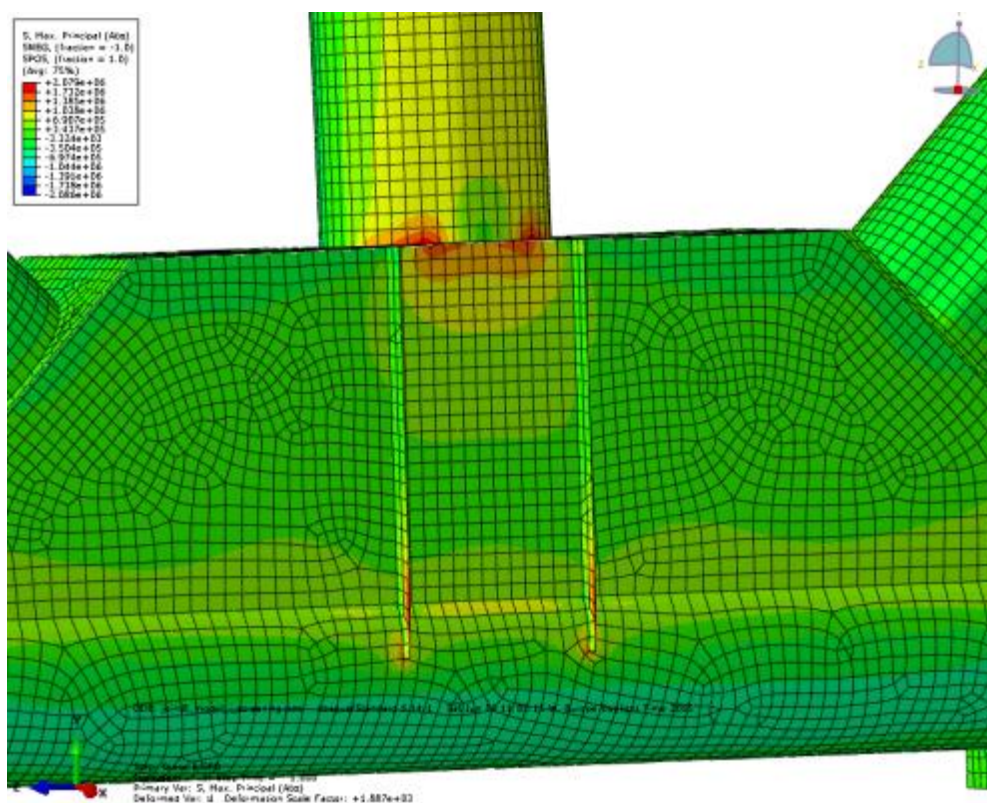


Figure 5-54: Joint 6 – Brace B OPB load – Abs. max principal stress contour

5.5.10 Joint 5 – Model I

Joint 5 Model I is a simple tubular KT-joint with chord and brace members with equal diameters and thickness. Mesh is txt near the joint intersection and element used is S8R, thick-shell element.

The shell element model is an idealized model of the physical joint. In reality the geometry of the weld near the saddle position is different, due to the cut-out performed to be able to weld here. The geometry is highly complex and would be difficult to model exactly with solid elements. It was therefore selected to perform only a shell model analysis of Joint 5.

5.5.10.1 Results

The final SCF results are tabulated in the table below. Component stresses are extrapolated from 0.5t and 1.5t distance from the intersection line to the hot spot, where the principal stress is calculated. Stresses are averaged. A and B refers to diagonal brace and central brace respectively. Because of symmetry, both diagonal braces will have the same sets of SCFs for all load cases.

Load case	Position	Efthymiou SCF	Method A SCF	Method B SCF	Method A/ Efthymiou	Method B / Efthymiou	Method A / Method B
Axial	Chord crown, A	10,974	13,437	13,786	1,22	1,26	0,97
	Brace crown, A	5,547	6,456	5,886	1,16	1,06	1,10
	Chord saddle, A	2,886	2,602	2,826	0,90	0,98	0,92
	Brace saddle, A	2,395	6,286	6,141	2,62	2,56	1,02
IPB	Chord crown, A	2,52	3,384	3,239	1,34	1,29	1,04
	Brace crown, A	2,677	2,061	1,958	0,77	0,73	1,05
OPB	Chord saddle, A	3,771	3,238	3,068	0,86	0,81	1,06
	Brace saddle, A	1,998	3,236	3,384	1,62	1,69	0,96

Load case	Position	Efthymiou SCF	Method A SCF	Method B SCF	Method A/ Efthymiou	Method B / Efthymiou	Method A / Method B
Axial	Chord crown, B	13,299	15,097	15,864	1,14	1,19	0,95
	Brace crown, B	5,547	4,974	4,830	0,90	0,87	1,03
	Chord saddle, B	2,886	2,596	3,150	0,90	1,09	0,82
	Brace saddle, B	3,699	2,956	2,237	0,80	0,60	1,32
IPB	Chord crown, B	3,211	4,189	3,952	1,30	1,23	1,06
	Brace crown, B	2,44	2,325	2,157	0,95	0,88	1,08
OPB	Chord saddle, B	6,265	4,718	4,563	0,75	0,73	1,03
	Brace saddle, B	3,32	4,734	5,030	1,43	1,52	0,94

Table 5-27: SCF results for Joint 5

5.5.10.2 Observations

The results from the axial load cases by use of extrapolation method A generally show good correlation with Efthymiou SCFs, with one notable exception. Brace A saddle position has been calculated to have a much higher SCF than what the Efthymiou equations show.

Because of the special case of $\beta = 1$, the end of the brace has a sharp corner. Around this area we can observe a quite fluctuating stress field. The brace surface goes from a compressive surface stress at the corner position, to tension stress over a distance of less than 100mm. From the FEM analysis results it was selected to extrapolate the highest stresses found on the side of the chord. This was not strictly at the saddle position, but at an intermediate position between the saddle and the crown. Instead of reading the stresses at a fixed position, the choice was made to sample the stresses at the point which had the highest stress occurrence.

The same issue is encountered for the OPB case for both Brace A and Brace B. It was chosen to sample the stresses from the regions near the saddle with the highest stress values. The read out points chosen can be found in Appendix B in combination with the Abaqus input files.

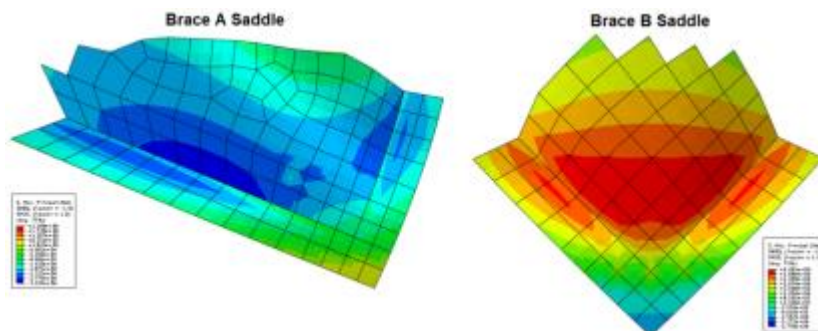


Figure 5-55: Brace A and B saddle positions - Abs. max principal stress contour - OPB load cases

5.5.11 Joint 6 – Model I

Joint 6 Model I is a shell model of a KT-joint where a stiffener arrangement has been modelled. The intent is to investigate the effects the stiffener arrangement has on the SCFs compared to an unstiffened KT-joint. The chord and brace are of equal dimensions as for Joint 5, and the boundary conditions and load are applied equally as well. This enables some comparison of the two solutions.

The choice of the stiffener design was made to try to obtain a fabrication friendly solution, and also one that can be readily checked by FEM analysis.

From the coarse mesh screening the required stress read out position were visualized, and the mesh was adapted to suit these locations.

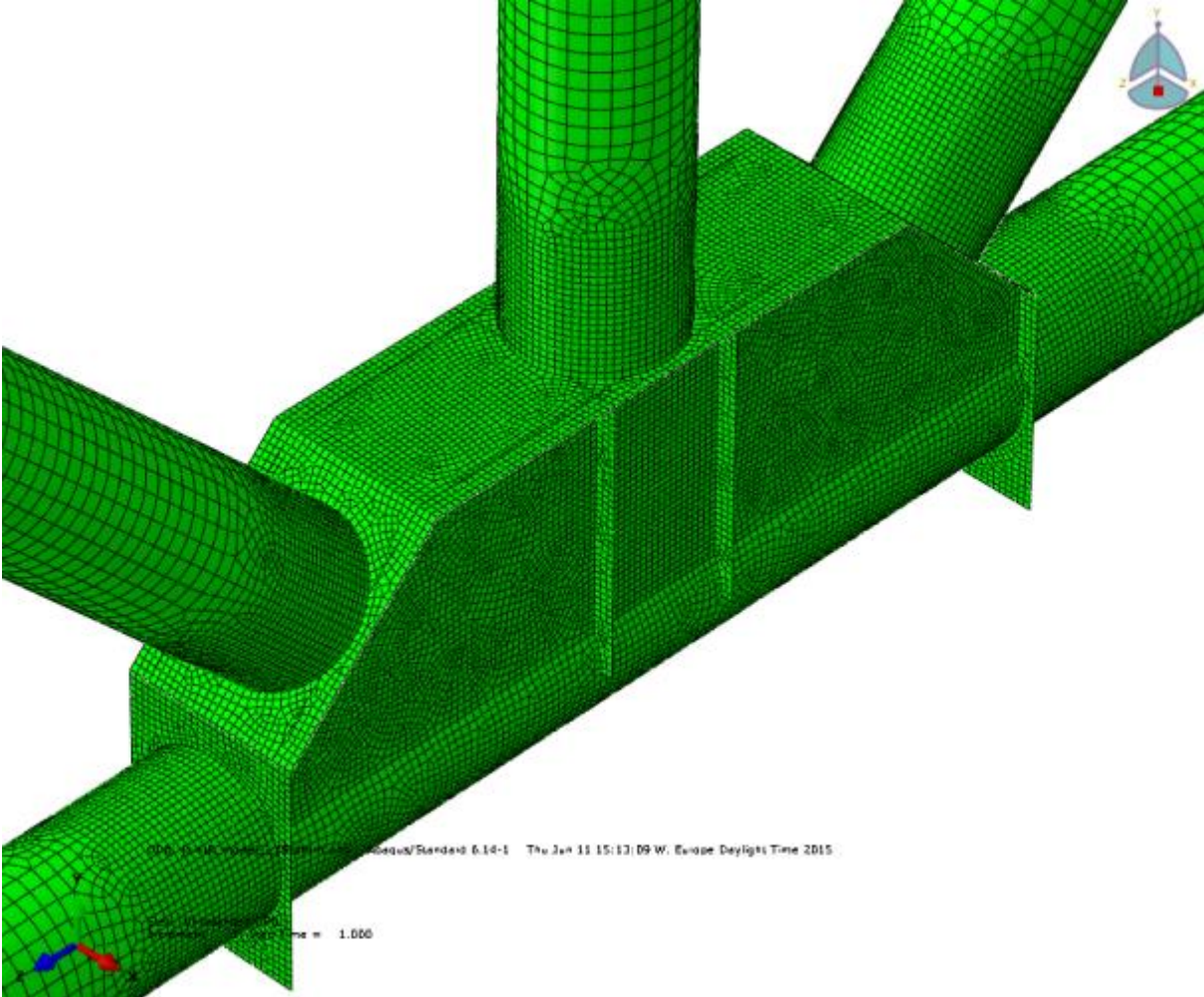


Figure 5-56: Plot of Joint 6 – Model I

5.5.11.1 Results

Load case	Position	Method A SCF	Method B SCF	Method A / Method B
Axial	Chord crown	16,266	16,195	1,00
	Brace A, above stiffeners	5,052	4,780	1,06
	Top plate, adjacent to brace A	2,049	1,700	1,21
	Top plate, chord crown	6,005	4,918	1,22
IPB	Brace A, above stiffeners	3,616	3,574	1,01
	Top plate, adjacent to brace A	3,375	2,978	1,13
	Longitudinal stiffener, below brace intersection	2,715	2,794	0,97
OPB	Brace A, above stiffeners	3,261	3,046	1,07
	Top plate, adjacent to brace A	1,641	1,253	1,31
	Longitudinal stiffener, below brace intersection	2,158	2,212	0,98

Load case	Position	Method A SCF	Method B SCF	Method A / Method B
Axial	Chord crown	21,956	21,690	1,01
	Brace B, above stiffeners	3,636	3,386	1,07
	Top plate, adjacent to brace B	3,451	3,550	0,97
	Top plate, chord crown	8,675	7,318	1,19
IPB	Brace B, above stiffeners	2,199	2,169	1,01
	Top plate, adjacent to brace B	1,294	1,231	1,05
	Longitudinal stiffener, below brace intersection	1,738	1,779	0,98
OPB	Brace B, above stiffeners	2,044	2,039	1,00
	Top plate, adjacent to brace B	1,134	0,761	1,49
	Longitudinal stiffener, below brace intersection	1,427	1,453	0,98

Table 5-28: SCF results for Joint 6 – Model I

5.5.11.2 Observations

A very high SCF is observed at the chord crown position for the Joint 6 Brace B Axial load case, 45% higher than for the same point for Joint 5, the simple KT-joint. Joint 6 consistently shows higher SCFs than Joint 5, except when subjected to out-of-plane bending. In-plane bending SCFs are of similar magnitude for the two joints.

5.5.12 Joint 6 – Model II

Joint 6 Model II is a stiffened KT-joint modelled with C3D20R solid elements. The model also uses S8R elements further away from the joint intersection to reduce computational effort. The geometry of the model is the same as for Model I, with the exception of the inclusion of the weld toe. The weld toe length of the weld is taken as half the thickness of the members which has the weld groove cut out.

The mesh is adapted to a txt mesh at the stress read out points, and stresses are sampled at 0.5t and 1.5t.

Detailed plots of the solid model geometry, mesh and stress contours can be found in Appendix A. Extrapolation spreadsheets can be found in Appendix B.

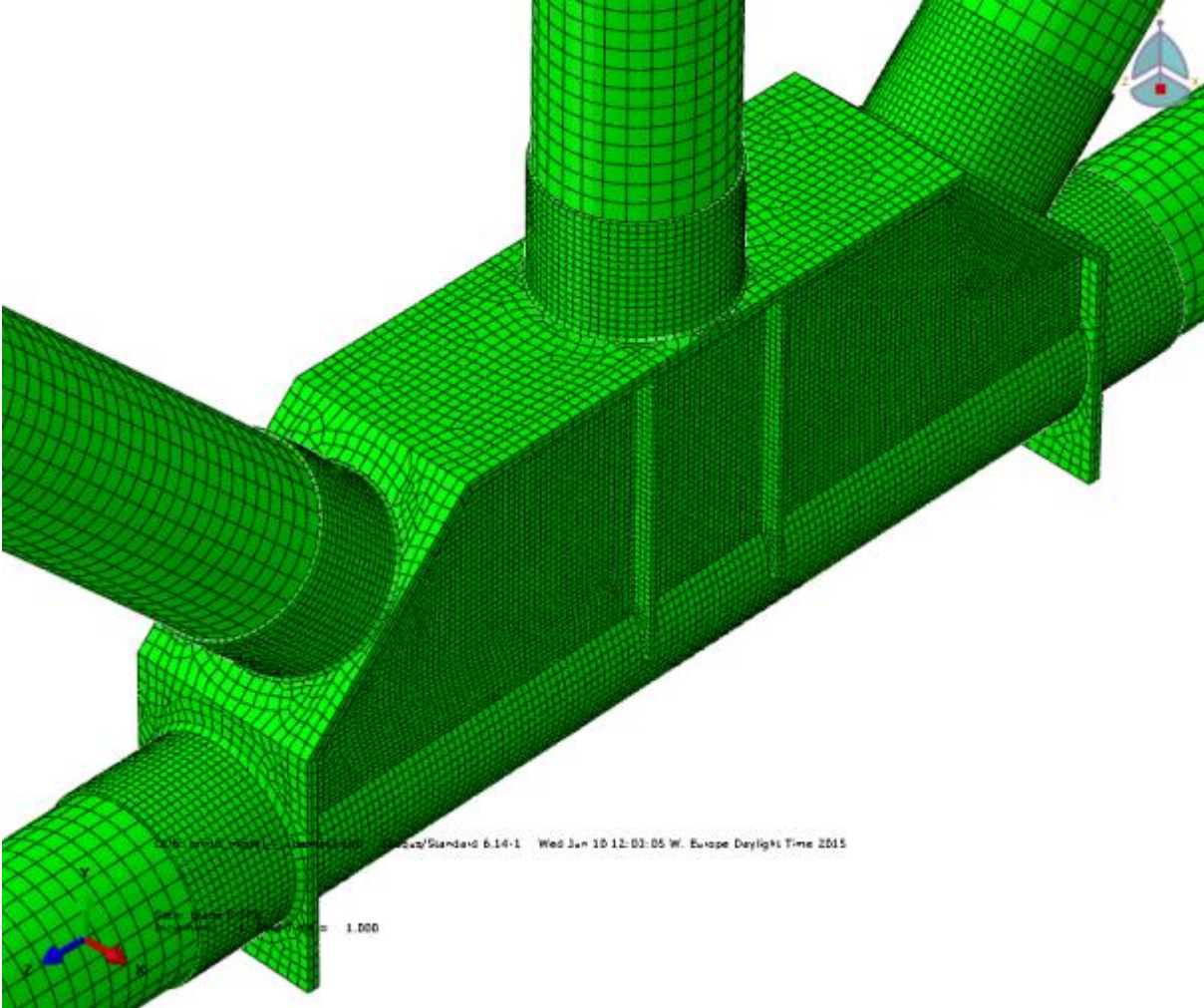


Figure 5-57: Plot of Joint 6 – Model II

5.5.12.1 Results

Load case	Position	Method A SCF	Method B SCF	Method A / Method B
Axial	Chord crown	15,276	14,972	1,02
	Brace A, above stiffeners	4,450	4,164	1,07
	Top plate, adjacent to brace A	3,612	2,766	1,31
	Top plate, chord crown	5,873	4,236	1,39
IPB	Brace A, above stiffeners	3,431	3,330	1,03
	Top plate, adjacent to brace A	2,823	2,367	1,19
	Longitudinal stiffener, below brace intersection	2,626	2,632	1,00
OPB	Brace A, above stiffeners	2,348	2,293	1,02
	Top plate, adjacent to brace A	0,667	0,561	1,19
	Longitudinal stiffener, below brace intersection	1,664	1,724	0,97

Load case	Position	Method A SCF	Method B SCF	Method A / Method B
Axial	Chord crown	20,394	19,843	1,03
	Brace B, above stiffeners	3,445	3,087	1,12
	Top plate, adjacent to brace B	3,363	3,474	0,97
	Top plate, chord crown	8,769	6,623	1,32
IPB	Brace B, above stiffeners	1,955	1,925	1,02
	Top plate, adjacent to brace B	1,037	0,996	1,04
	Longitudinal stiffener, below brace intersection	1,359	1,427	0,95
OPB	Brace B, above stiffeners	1,868	1,869	1,00
	Top plate, adjacent to brace B	0,385	0,356	1,08
	Longitudinal stiffener, below brace intersection	1,568	1,619	0,97

Table 5-29: SCF results for Joint 6 – Model II

5.5.12.2 Observations

It is difficult to draw clear conclusions for Joint 6 Model II. In comparison with the shell model of Joint 6, slightly better performance is seen for the IPB and OPB cases for both braces. For the axial load case the opposite is seen. Here the SCF at the chord crown is higher for the solid model, which is consistent with the results from analysis of the other joints investigated.

It can be observed that the SCFs for the top plate near Brace B are negligible for the IPB and OPB cases, with a SCF around 1 or lower. A fairly large difference between shell and solid results is found for the SCF for the top plate for both braces in the OPB load case. This can be attributed to the weakness of shell elements when connecting plate elements through a perpendicular plate.

5.5.13 Comparison of results

Joint 5 and 6 obviously do not share geometry, or exact hot spot locations. However some similarities can be drawn between the two and comparison can be made between some of the hot spot SCFs. Below is a table displaying what SCFs are compared to each other, and graphs that visualize results for easier comparison.

Joint 6 position	Joint 5 position
Chord crown	Chord crown
Brace, above stiffeners	Brace Crown
Z-steel plate, adjacent to brace	Chord saddle
Z-steel plate, chord crown	Brace saddle
Brace, above stiffeners	Brace crown
Z-steel plate, adjacent to brace	Chord crown
Longitudinal stiffener, below brace intersection	
Brace, above stiffeners	Brace saddle
Z-steel plate, adjacent to brace	Chord saddle
Longitudinal stiffener, below brace intersection	

Table 5-30: Overview of comparisons made between Joint 5 and 6

As seen from the table, the results are not in all instances directly comparable.

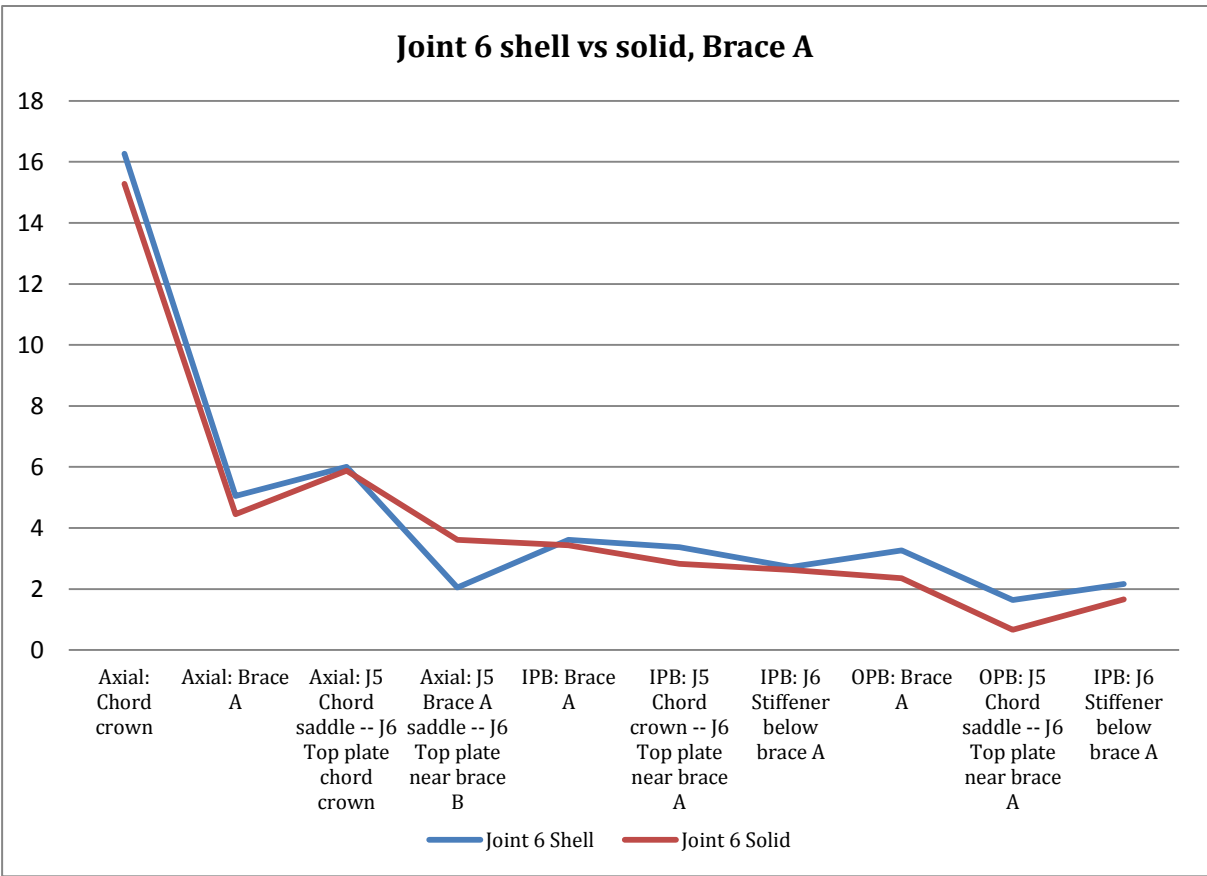


Figure 5-58: Comparison of shell and solid SCFs for Joint 6 near diagonal Brace A

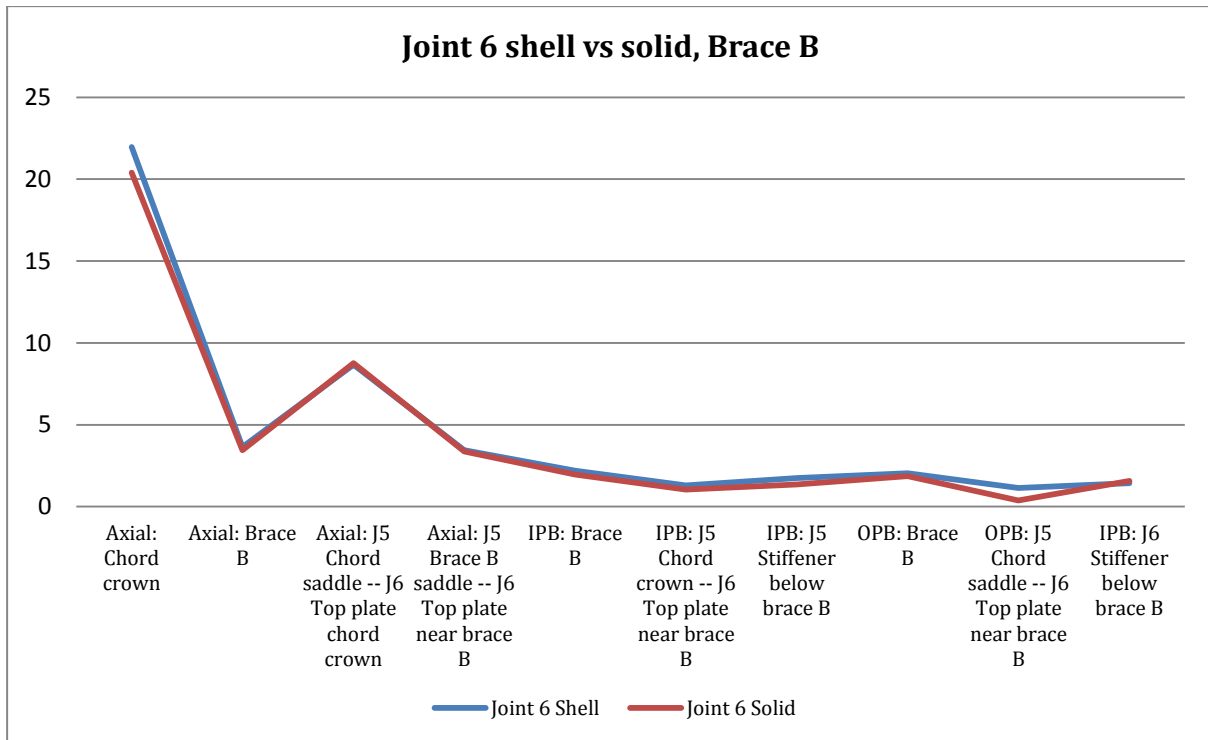


Figure 5-59: Comparison of shell and solid SCFs for Joint 6 near centre Brace B

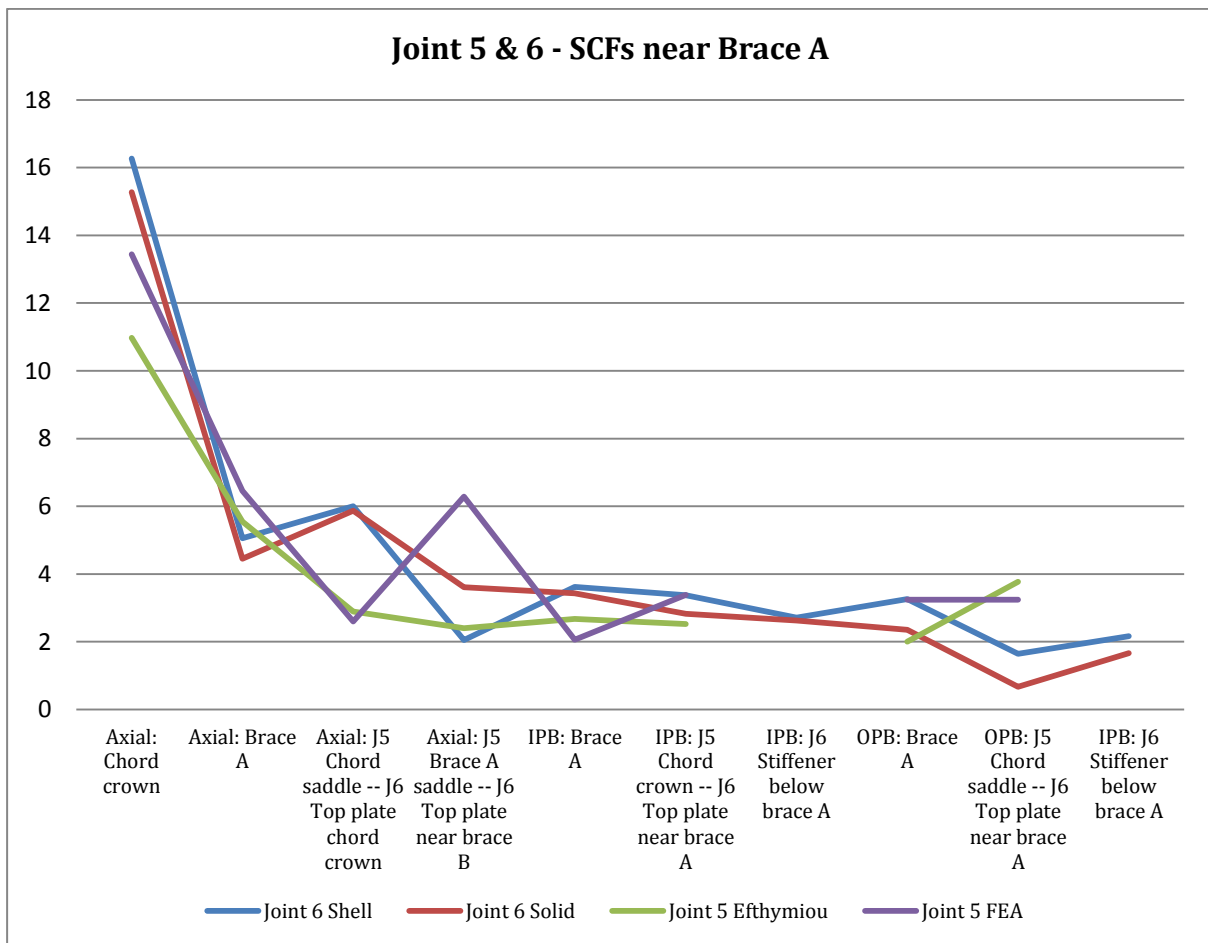


Figure 5-60: Comparison of Joint 5 and 6 SCFs near diagonal Brace A

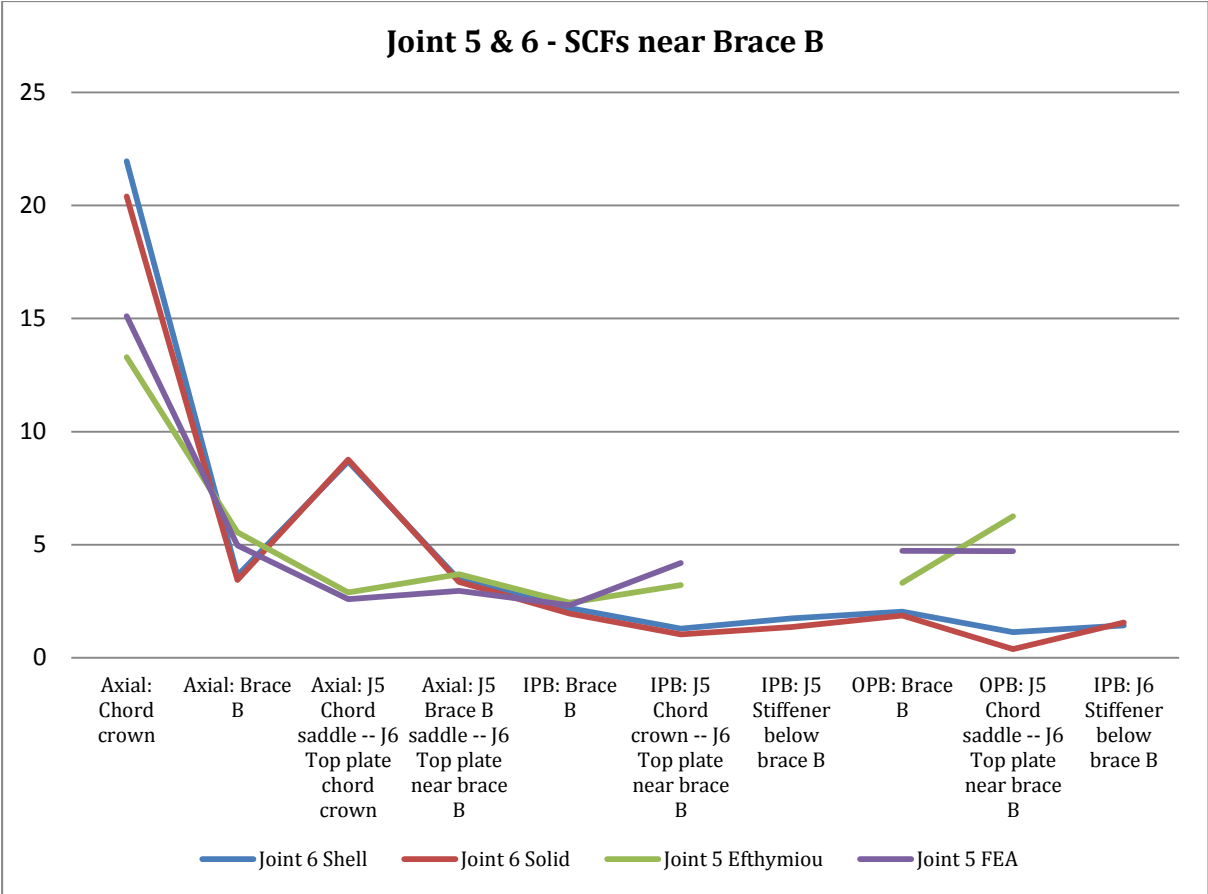


Figure 5-61: Comparison of Joint 5 and 6 SCFs near centre Brace B

6 Discussion

6.1 Efthymiou equations

Performance of the Efthymiou parametric SCF equations have been a much debated topic during the work on this thesis. [2] show that the parametric equations have some tendency to over or underestimate SCFs in comparison with measurements taken from physical samples, with a bias to the conservative side. Also the method used for developing the equations brings uncertainties into the picture. The FEM analysis dataset the equations are based on is not continuous, but a finite set of geometries within a certain validity range. Since curve fitting is performed to develop the parametric equations, results from the dataset that do not fit the curve get smoothed with the rest of the results, which may be of significance when parameters are bordering the validity range of the equations if the dataset is limited. In the case of $\beta = 1$, as investigated in this thesis, the geometry at the saddle position has a sharp corner. This complicates the read out of stresses in this area, and is connected to some uncertainty as the stress read out positions for the Efthymiou FEM analyses are not known. In general the performance of the equations is fairly good, and they rarely underestimate the SCF according to [2]. They should be utilized, but if fatigue calculations show high utilization, or with parameters being outside or bordering the validity range of the equations, it may be considered to perform FEM analyses as an alternative option to reduce uncertainties.

A discrepancy between the Efthymiou axial chord crown SCFs and the FEM established axial chord crown SCFs is observed. This is general for models analysed in the thesis, and the cause for this is not clear. Boundary conditions assumed for the Efthymiou equations are fixed chord ends, this is also the case for the FEM analysis models.

6.2 FEM analysis results

For the simple tubular Joint 2, the inclusion of the weld geometry in the solid models yielded lower SCF values for all load cases and positions, except for the axial load case at chord crown position where the SCF increased. Incidentally this is the highest SCF from all load cases and positions, so this is an important result for a fatigue analysis of the joint.

For the case studies investigated the stiffened tubular joints perform differently than the simple joints fatigue wise. A general observation in the axial load cases is that the stiffened tubular joint performance is poor, and the axial SCFs are higher than for the corresponding simple tubular joints. For in-plane bending the stiffened Joint 4 performed better than the simple Joint 3. Joint 5 and Joint 6 performed similarly for in-plane bending. For out-of-plane bending stiffened Joints 4 and 6 show decreased SCFs when performing solid element analyses, and performed best of all models for this load case. The out-of-plane bending case was the only load case which the stiffened tubular joints consistently showed better performance.

The KT-joints 5 and 6 are joints with multiple braces, and needs additional load cases analysed. Balanced axial load and unbalanced out-of-plane bending are the two load relevant load cases. Since Joint 6 performed well in out of plane bending, it would be interesting to see its performance under unbalanced out-of-plane bending compared to Joint 5. However these analysis have not been performed in this thesis, but is possible future work.

6.3 Solid versus shell models

Concerning SCF results from solid model versus results from shell models, SCFs in most load cases and positions are lower with the solid model. This can be attributed to the weld increasing the area the load is distributed over. However, as seen for all joints investigated, the SCF axial load case at chord crown position increases. This is typical when a stiff part connects to a softer part, in this case the brace that transfers loads axially to the chord absorbing loads as plate bending at the crown position. Including the weld at the crown position increases the stiffness of the stiffest part further. Also for all joints investigated, the axial load chord crown SCF is the highest SCF. Although a higher SCF not typically what is desired, results cannot be chosen at will. The better and more detailed model may pick up on unexpected phenomena which should be taken into account.

6.4 Design improvements of joints

The design of the stiffened tubular joints could improve in various ways. The most convenient way is to increase local thickness of the chord, or use ring stiffened joints. These well-known solutions have been extensively studied in the past, and are not in the scope of this thesis.

6.5 Methodology for derivation of hot spot stress

Most of the work performed has been checked with both Method A and Method B from [1]. Both methods have strengths and weaknesses. Method A is referred to in IIW [4] as a relatively coarse mesh, with its txt mesh density. However the method is very practically oriented in that it is relatively easy to make a good txt mesh, and it reduces computational effort in comparison with a finer mesh. Stress is read at two points and linearized, and as such takes into account the local stress gradient near the hot spot.

The downside to this is that the stress read out point furthest away from the hot spot needs to be readily available for stress read out. Depending on geometry the point could be obstructed by other plates, the geometry could be too cramped in the area to produce a decent quality mesh or the plate could simply not extend far enough that the 1.5t position exists. In cases like this Method B may be able to provide a SCF. The weakness of Method B is that it applies a constant slope of 1.12 to the stress read out, so it can underestimate the SCF significantly when the stress gradient is steep. Significant overestimates are rare however. Examples of this are seen when comparing results from the different joints.

It is seen from results that the SCF calculated with use of Method B rarely is more than 10% higher than SCFs calculated by Method A. However there are seen numerous examples in this thesis of the method B SCF being more than 10% lower than the method A SCF. In Joint 4 and 6 this was quite often the case in areas where the geometry was congested. Several accounts of Method B estimating a SCF only 65-80% of the Method A SCF were seen.

Choosing between method A and method B should be based on some experience with both methods, their strengths and weaknesses. A shell model in conjunction with method B is the simplest and fastest approach, but risks underestimating SCFs in areas with steep stress gradients. A shell model with method A requires a bit more control over the mesh, increased manual work with extrapolation, but can pick up on higher SCFs in areas with steeper stress gradients. One should take into consideration the limitations of shell elements. Analysis with a solid model means the workload is higher in terms of modelling, meshing, extrapolating and computational effort. However if a solid model is modelled correctly and meshed in a good manner it should perform well in nearly every case, without the caveats of the shell elements. The choice between methodologies comes down to joint geometry, time available and competence of the analyst.

7 Conclusion

Analysis of Joint 2, a simple tubular T-joint, displays good correlation between the different FEM analysis methods performed. The solid models have lower SCFs for all load cases and positions except for the axial load case at chord crown, where they are seen to be about 6-9% higher.

The case study comparing the unstiffened tubular T-joint with $\beta = 1$, and the stiffened tubular T-joint with $\beta = 1$, Joints 3 and 4 respectively, show the following results. A higher stiffener plate thickness increases chord crown SCF under axial load, as well as the chord saddle SCF in out-of-plane bending but reduces the SCF on the stiffener itself for out-of-plane bending. For an equal stiffener plate thickness of 20mm, the solid FEM model yielded lower SCFs for all load cases, except chord crown position for axial loading where SCFs are identical. Comparing the simple and the stiffened joints in the case study, better overall performance is seen for the simple tubular joint. The Efthymiou SCFs and the FEM results for Joint 3 correspond well.

The case study comparing the unstiffened tubular KT-joint with $\beta = 1$, and the stiffened tubular KT-joint with $\beta = 1$, Joints 5 and 6 respectively, show the following results. There are some differences for Joint 6 depending on if a shell or solid model is used. The solid model is seen to yield overall lower SCFs both the diagonal brace and the central brace. When comparing with Joint 5, the equivalent simple tubular joint, Joint 5 has better performance when subjected to axial loads, while Joint 6 has better performance for out-of-plane bending. This is seen to be the case for both the diagonal and the central brace. Efthymiou equations correspond well with FEM results for Joint 5, except for the Brace A saddle subjected to axial load, where FEM analysis estimates 160% higher SCF. This result is somewhat uncertain as the stress read outs are taken some distance away from the saddle, at the point of the highest stress concentration for the load case.

The stiffened tubular joints analysed in this thesis show better performance for out-of-plane bending, but significantly worse performance for axial loading, compared to the simple tubular joint equivalents.

Analysis with solid models including weld geometry compared to shell models with no weld geometry yields slightly *different* results. Based on the findings in the work performed herein it is not possible to generalize any specific load case or position, but for a majority of cases solid model analysis yield lower SCFs. This does necessarily imply better overall fatigue performance as this is dependent on which SCF is dominant.

Compared to SCFs calculated by Efthymiou parametric equations, SCFs for the axial load case at chord crown position are seen to be higher. Other SCFs show better correlation with the Efthymiou equations.

8 References

- [1] DNVGL-RP-0005, "RP-C203: Fatigue design of offshore steel structures," ed, 2014.
- [2] HSE, "Stress Concentration Factors for Simple Tubular Joints," OTH 354, 1997.
- [3] ISO 19902, "Petroleum and natural gas industries - Fixed steel offshore structures," ed, 2007.
- [4] IIW and A. F. Hobbacher, "Recommendations for Fatigue Design of Welded Joints and Components (update)," Paris, France, IIW doc. IIW-1823-07 (XIII-2151r4-07/XV-845r4-07), 2008.
- [5] ABS, "Fatigue Assessment of Offshore Structures," ed, 2003.
- [6] API RP 2A-LRFD, "Recommended Practice for Planning, Designing and Constructing Fixed Offshore Platforms - Load and Resistance Factor Design," ed, 1993.
- [7] M. Efthymiou and S. Durkin, "Stress Concentrations in T/Y and gap/overlap K-joints," in *The Fourth International Conference on Behaviour of Offshore Structures (BOSS'85)*, Delft, The Netherlands, 1985, pp. 429-440.
- [8] E. Niemi, W. Fricke, and S. J. Maddox, *Fatigue Analysis of Welded Components: Designer's Guide to the Structural Hot-Spot Stress Approach*: Woodhead Publishing, 2006.
- [9] Dassault Systèmes Simulia Corp. (2014). *Abaqus Analysis User's Guide*.
- [10] R. D. Cook, D. S. Malkus, M. E. Plesha, and R. J. Witt, *Concepts and Applications of Finite Element Analysis*, Fourth ed.: John Wiley & Sons. Inc., 2002.
- [11] NORSOK N-004, "Design of steel structures," 2013.
- [12] A. C. Wordsworth and G. P. Smedley, "Stress concentration factors at unstiffened tubular joints," in *European Offshore Steels Research Seminar*, 1978.
- [13] M. Efthymiou, "Development of SCF Formulae and Generalised Influence Functions for use in Fatigue Analysis," in *Conference on recent developments in tubular joints technology*, Surrey, The United Kingdom, 1988.
- [14] Wikiversity. (2015, 15.03.2015). *Principal stresses*. Available: https://en.wikiversity.org/wiki/Principal_stresses

Appendix A – Stress contours

A.1 Joint 1

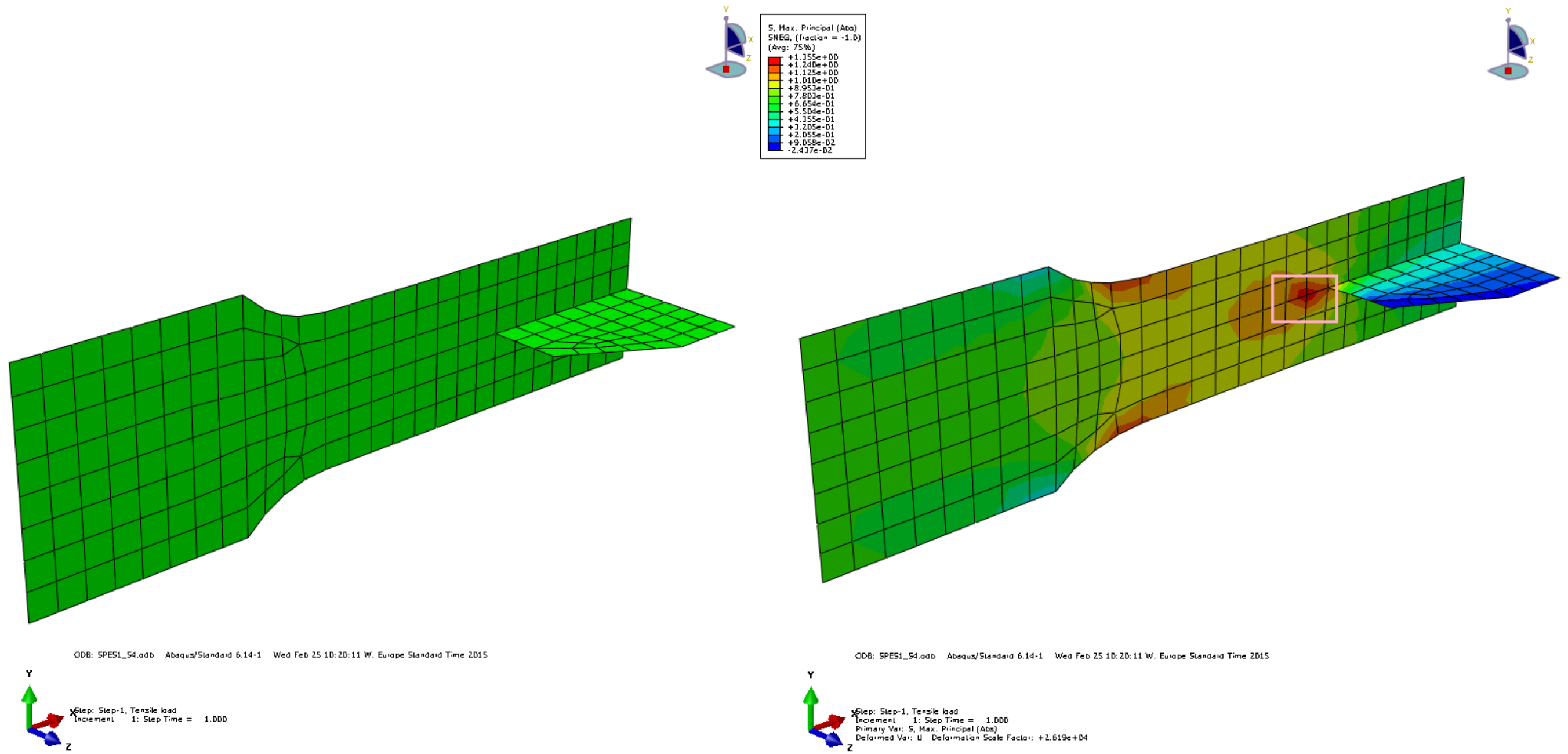


Figure A-1-1: Joint 1 Model I (S4) Left: Mesh, Right: Abs. max principal stress countour and stress read out region

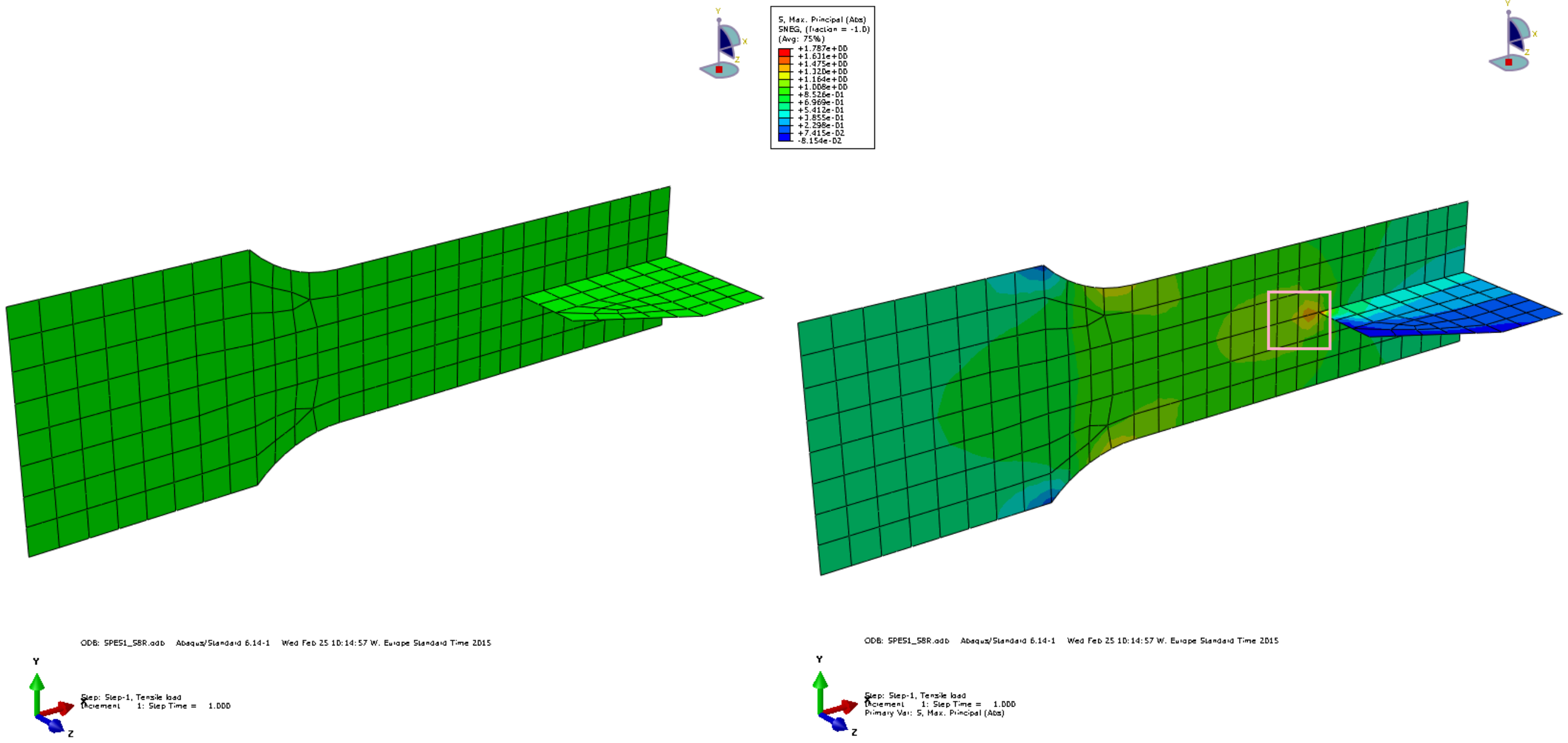


Figure A-1-2: Joint 1 Model II (S8R) Left: Mesh, Right: Abs. max principal stress countour and stress read out region

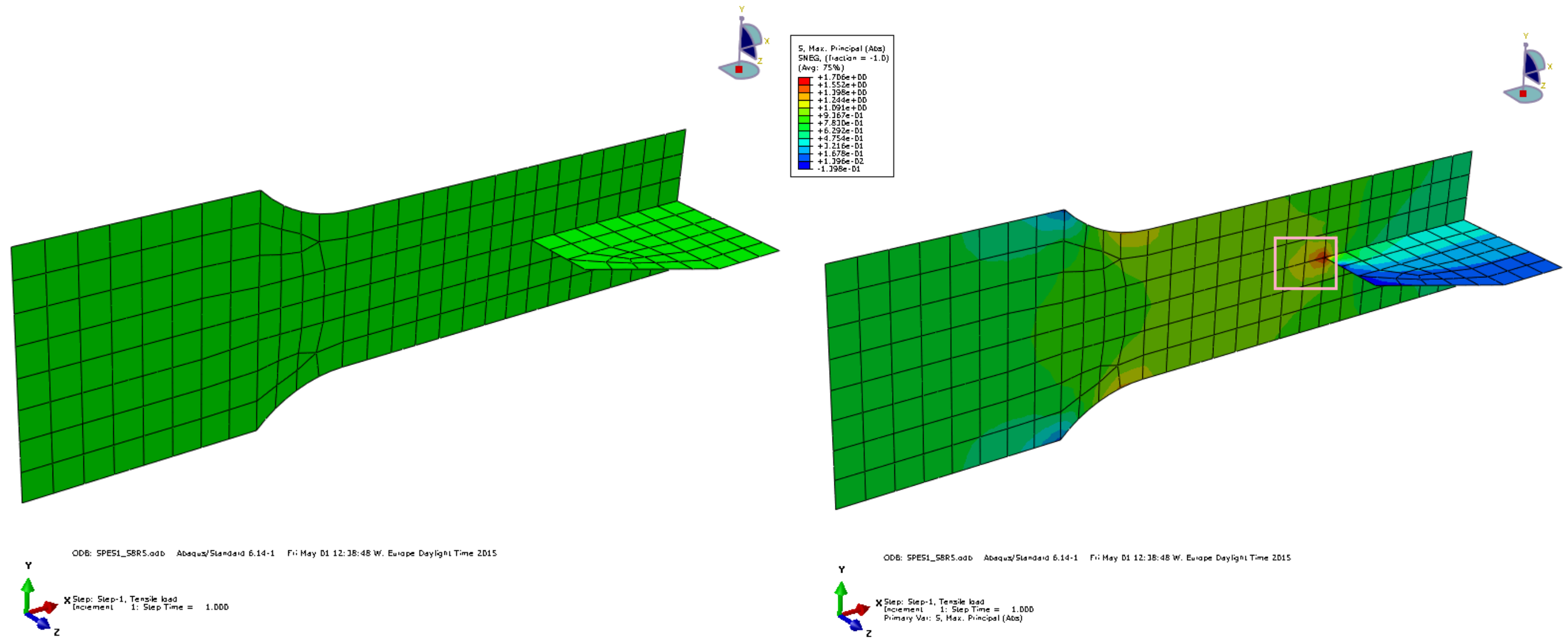


Figure A-1-3: Joint 1 Model III (S8R5) Left: Mesh, Right: Abs. max principal stress contour and stress read out region

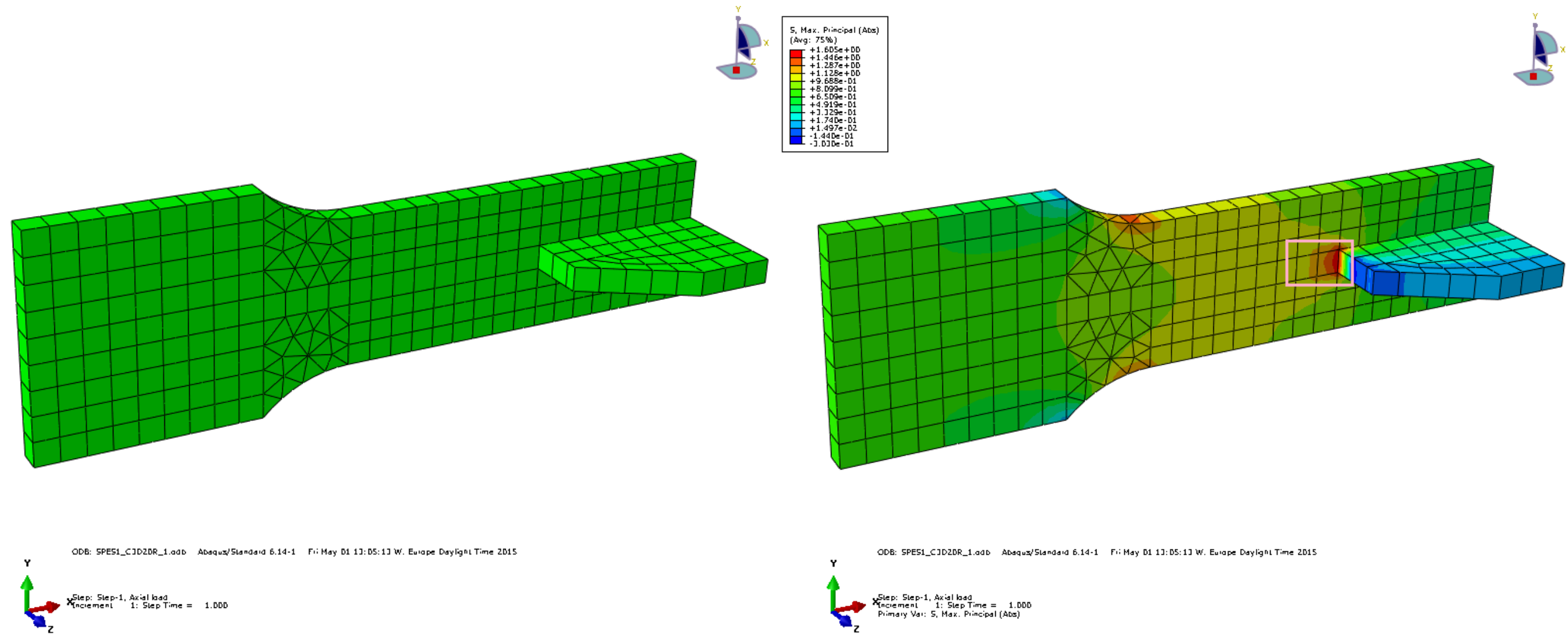


Figure A-1-4: Joint 1 Model IV (C3D20R – 1 element through thickness) Left: Mesh, Right: Abs. max principal stress contour and stress read out region

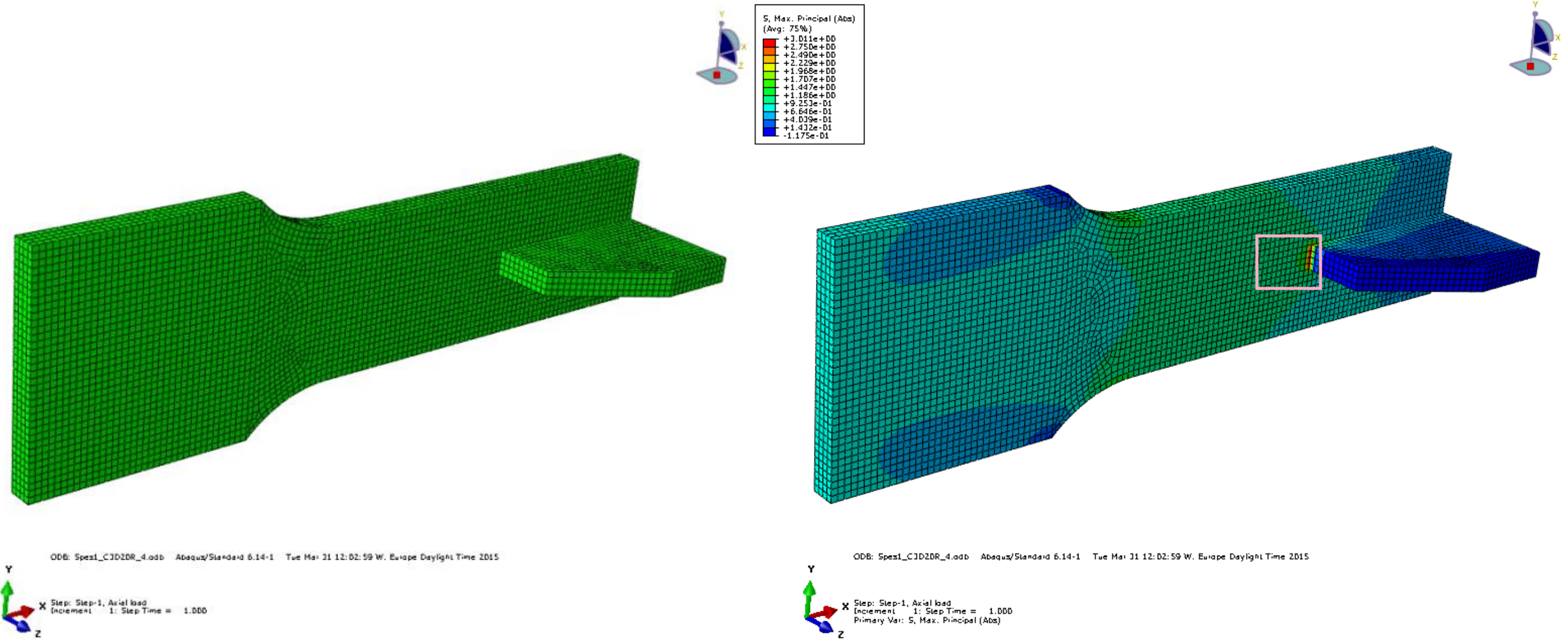


Figure A-1-5: Joint 1 Model V (C3D20R – 4 elements through thickness) Left: Mesh, Right: Abs. max principal stress contour and stress read out region

A.2 Joint 2

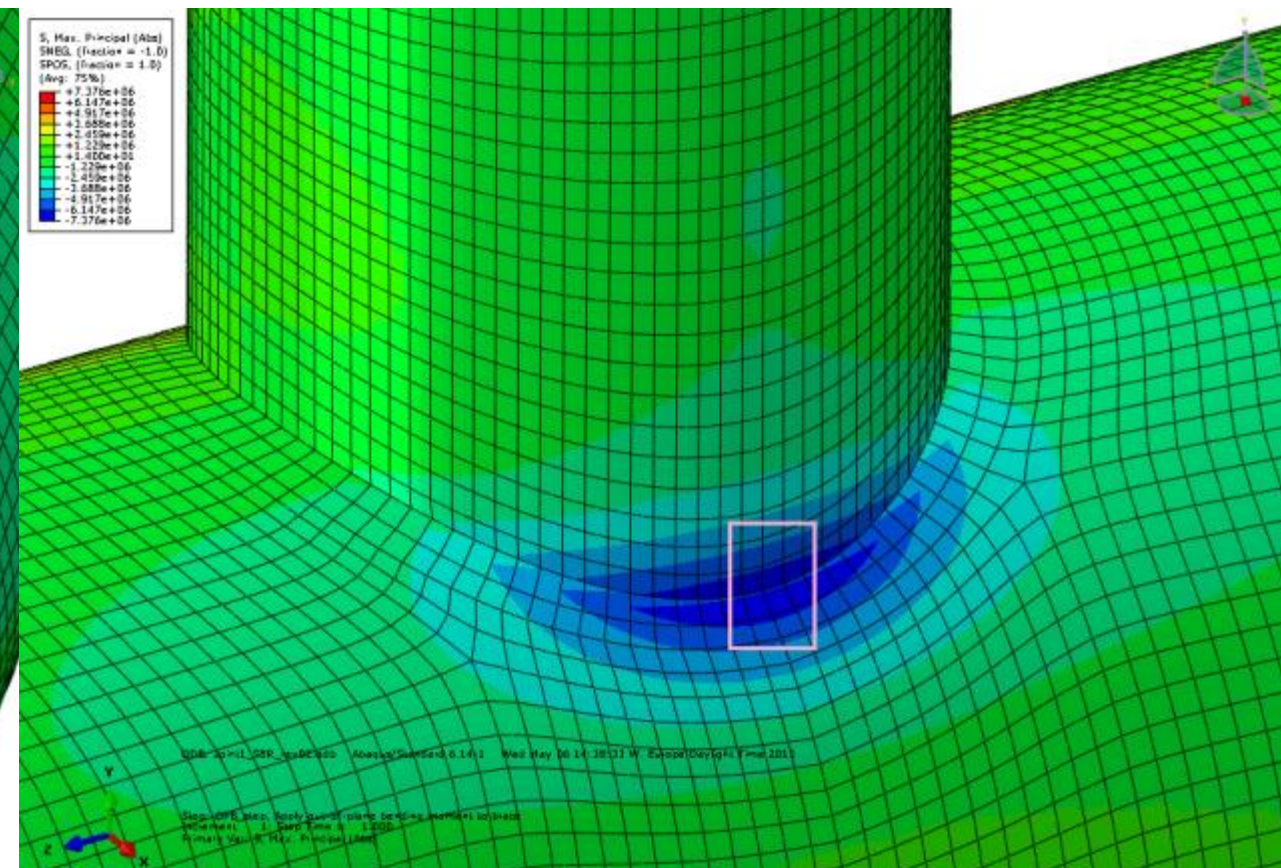
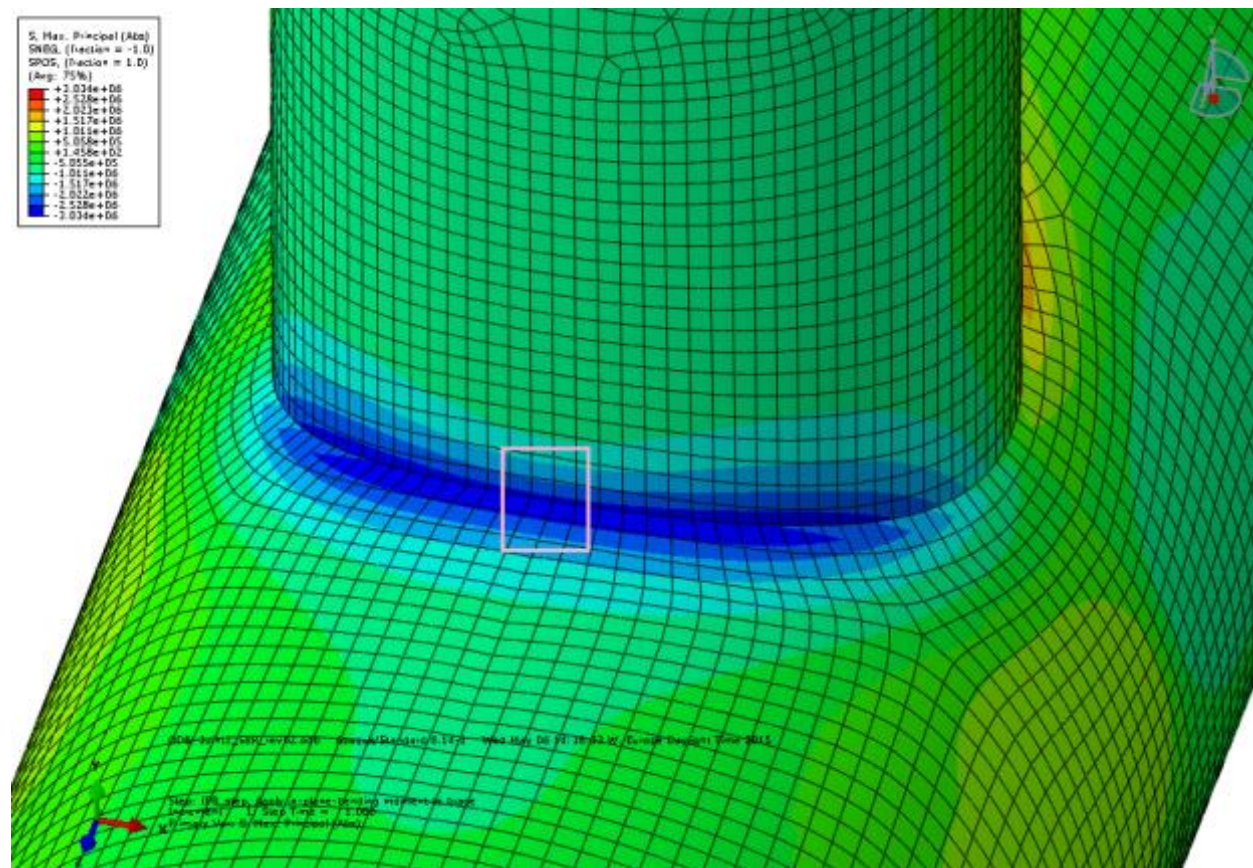
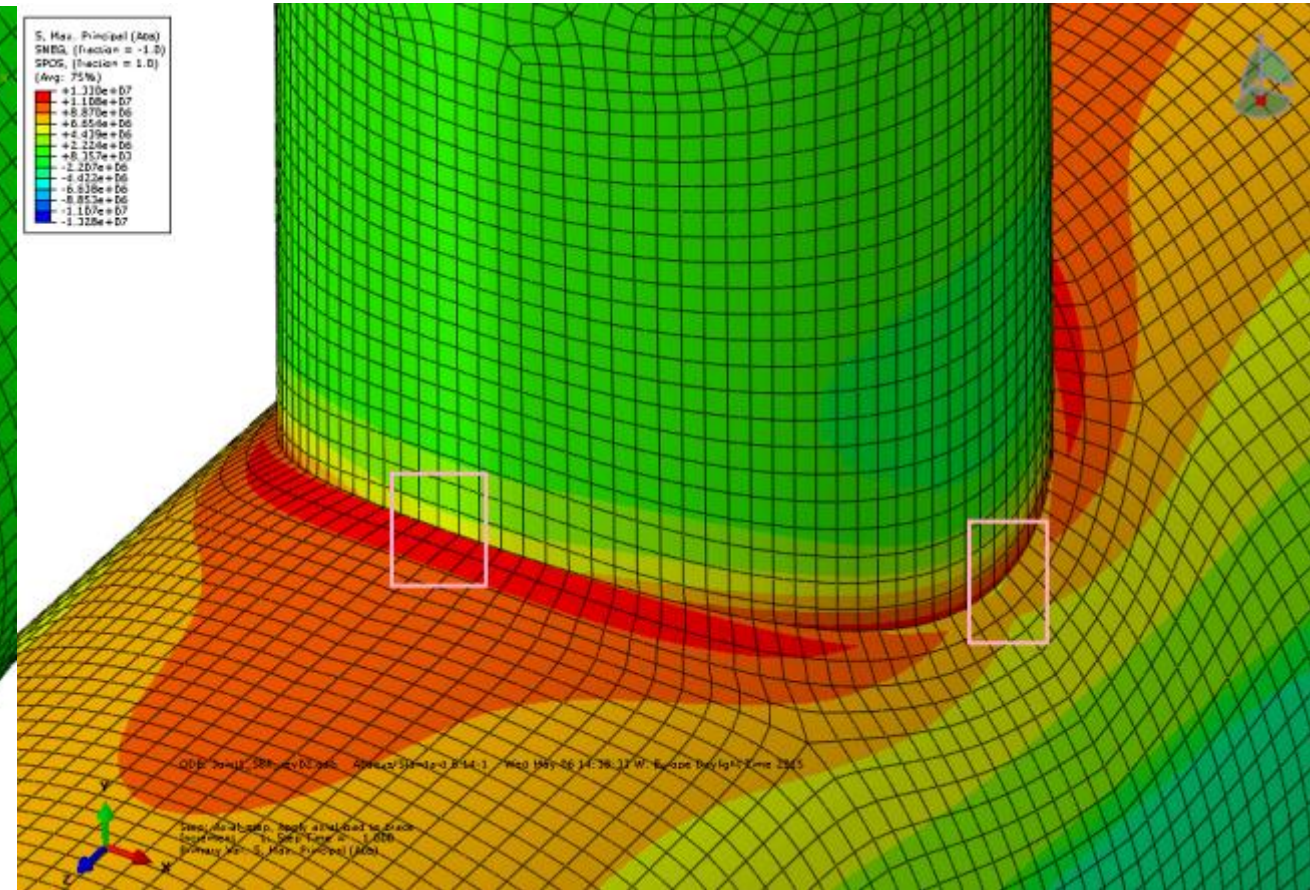
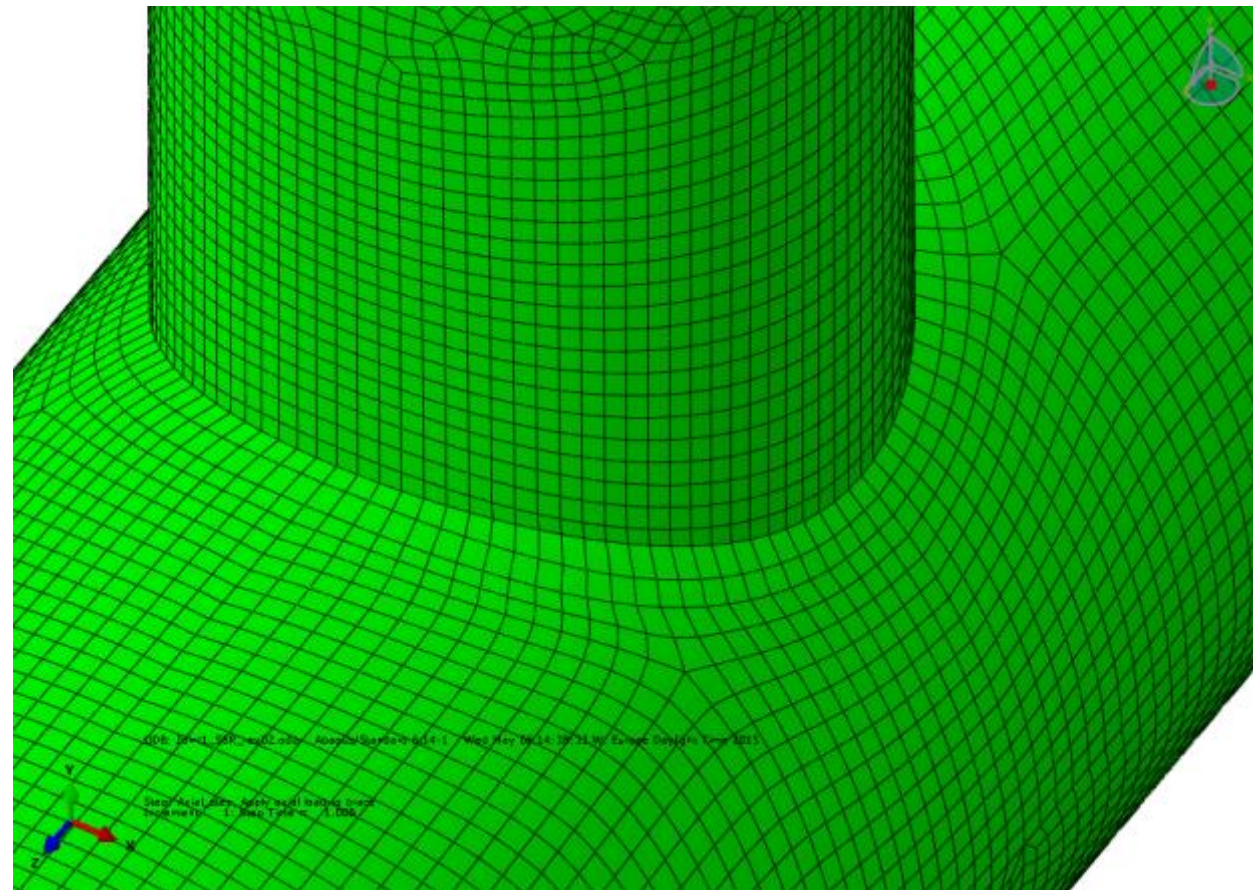


Figure A-2-1: Joint 2 Model I (S8R, relatively fine mesh)

Upper left: Mesh

Lower left: Abs. max principal stress countour and stress read out region for IPB load case

Upper right: Abs. max principal stress countour and stress read out region for Axial load case

Lower right: Abs. max principal stress countour and stress read out region for OPB load case

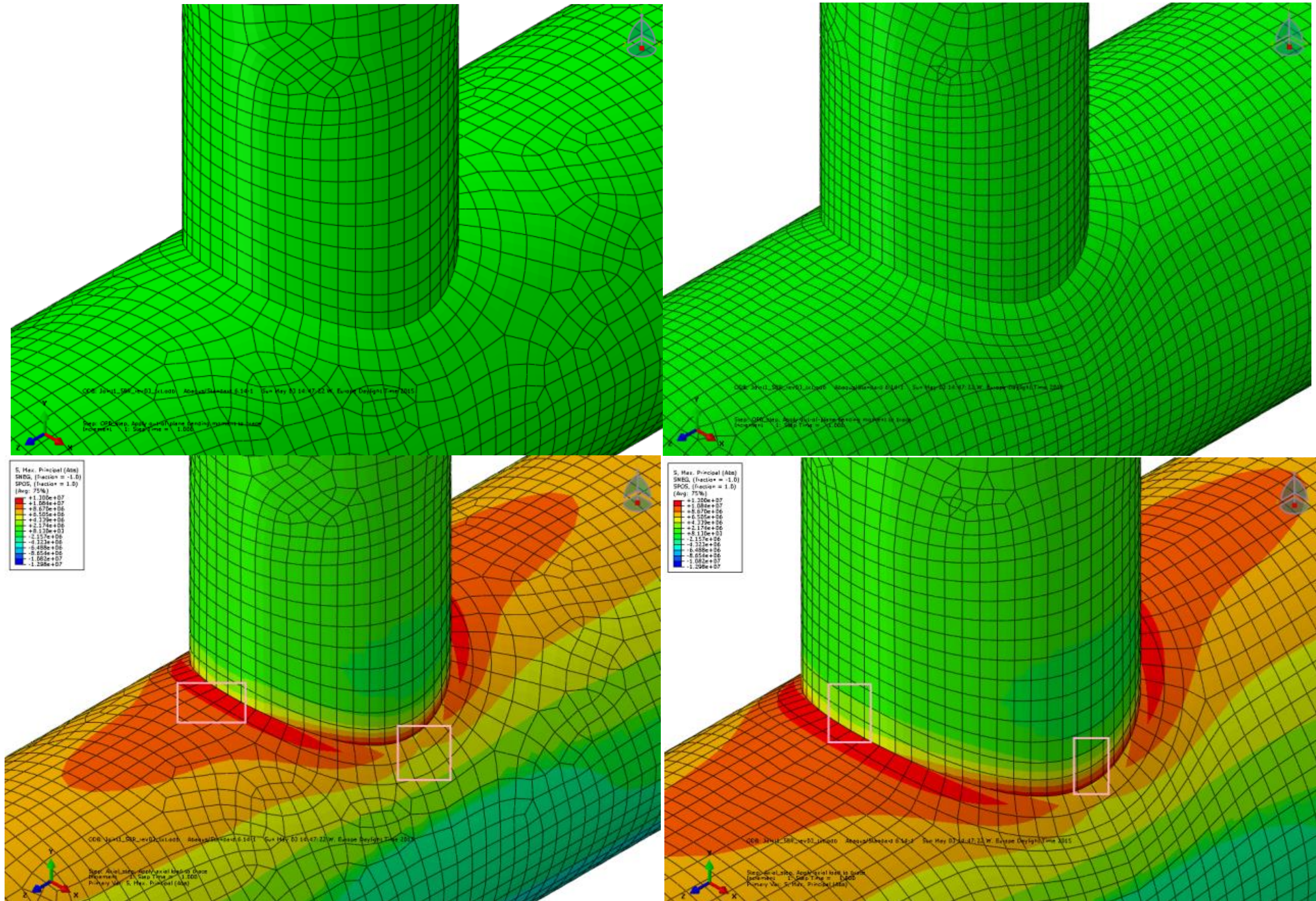


Figure A-2-2: Joint 2 Model II (S8R, 2 meshes of t x t)

Upper left: Mesh adapted to chord thickness

Upper right: Mesh adapted to brace thickness

Lower left: Abs. max principal stress contour and stress read out region for axial load case, chord side

Lower right: Abs. max principal stress contour and stress read out region for axial load case, brace side

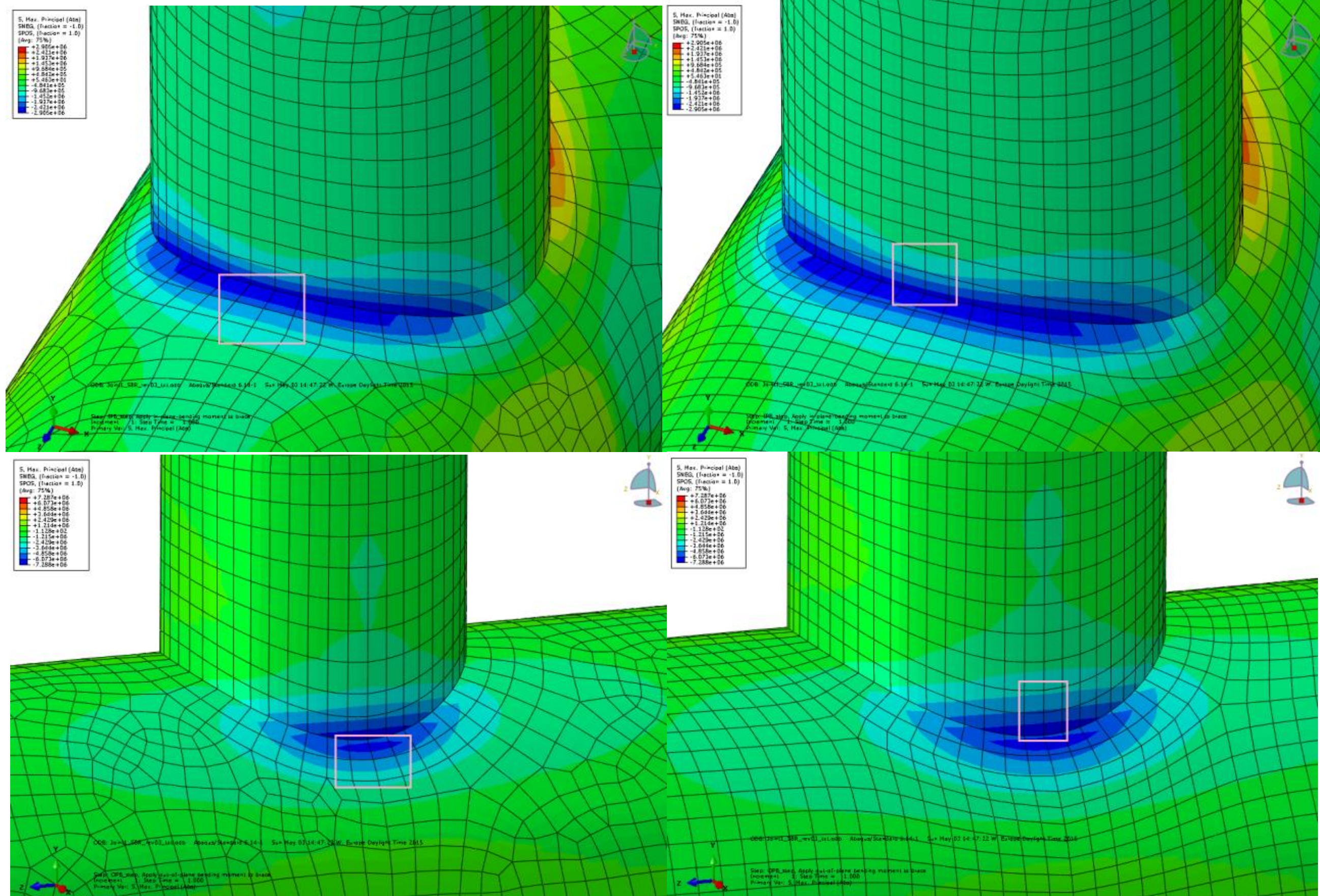


Figure A-2-3: Joint 2 Model II (S8R, 2 meshes of t x t)

Upper left: Abs. max principal stress countour and stress read out region for IPB load case, chord side
Lower left: Abs. max principal stress countour and stress read out region for OPB load case, chord side

Upper right: Abs. max principal stress countour and stress read out region for IPB load case, brace side
Lower right: Abs. max principal stress countour and stress read out region for OPB load case, brace side

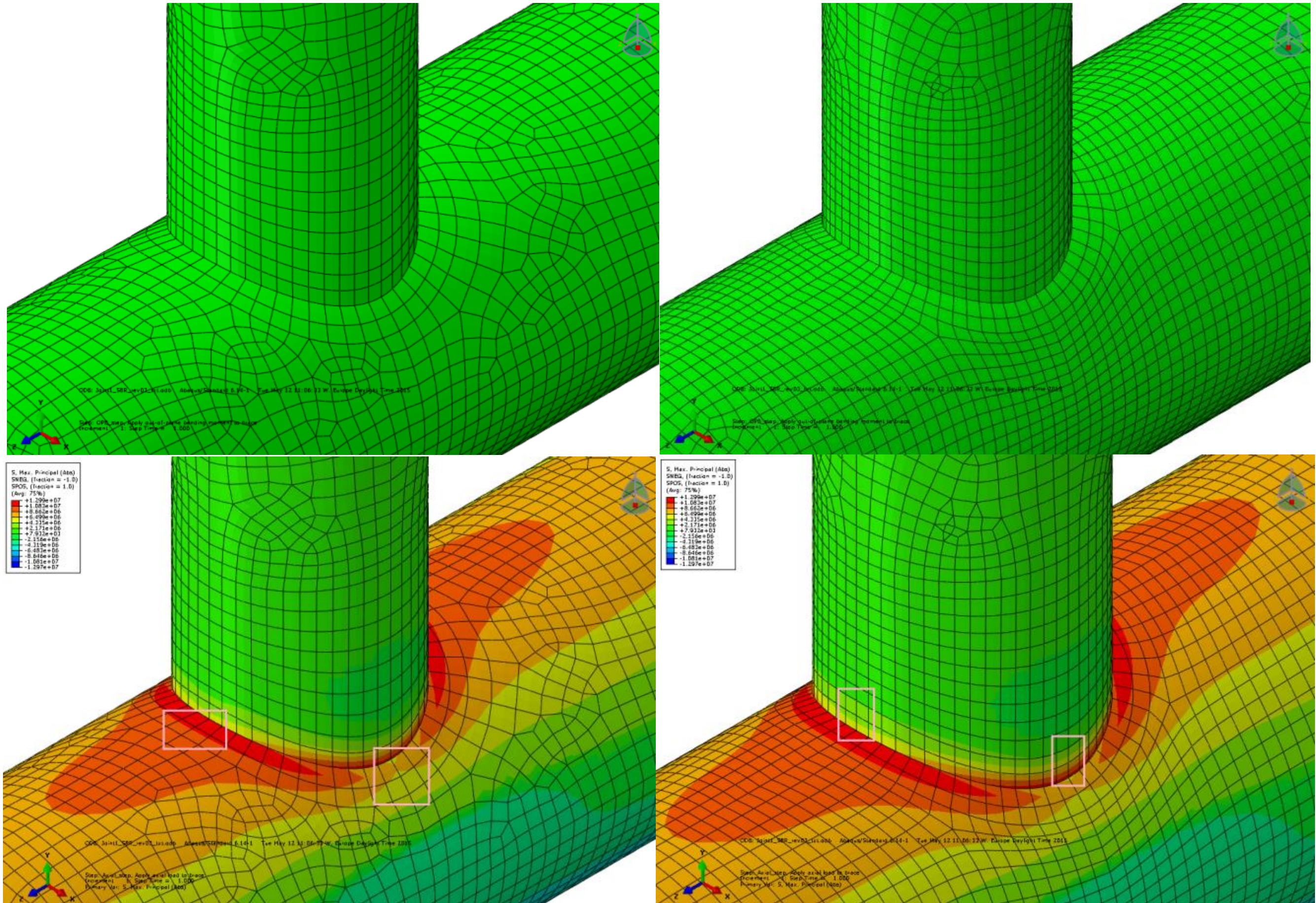


Figure A-2-4: Joint 2 Model III (S8R5, 2 meshes of t x t)

Upper left: Mesh adapted to chord thickness

Upper right: Mesh adapted to brace thickness

Lower left: Abs. max principal stress countour and stress read out region for axial load case, chord side

Lower right: Abs. max principal stress countour and stress read out region for axial load case, brace side

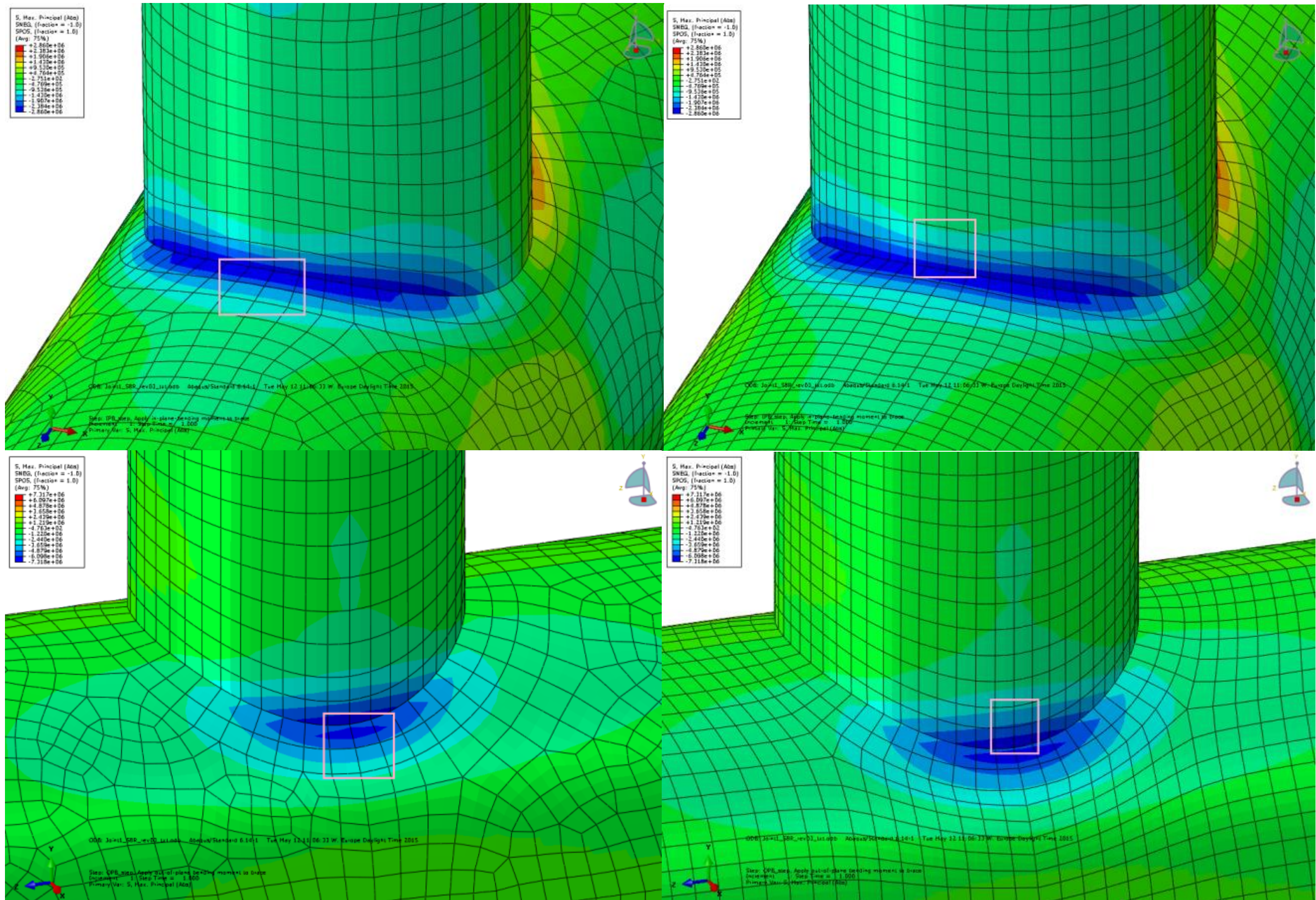


Figure A-2-5: Joint 2 Model III (S8R5, 2 meshes of t x t)

Upper left: Abs. max principal stress countour and stress read out region for IPB load case, chord side
 Lower left: Abs. max principal stress countour and stress read out region for OPB load case, chord side

Upper right: Abs. max principal stress countour and stress read out region for IPB load case, brace side
 Lower right: Abs. max principal stress countour and stress read out region for OPB load case, brace side

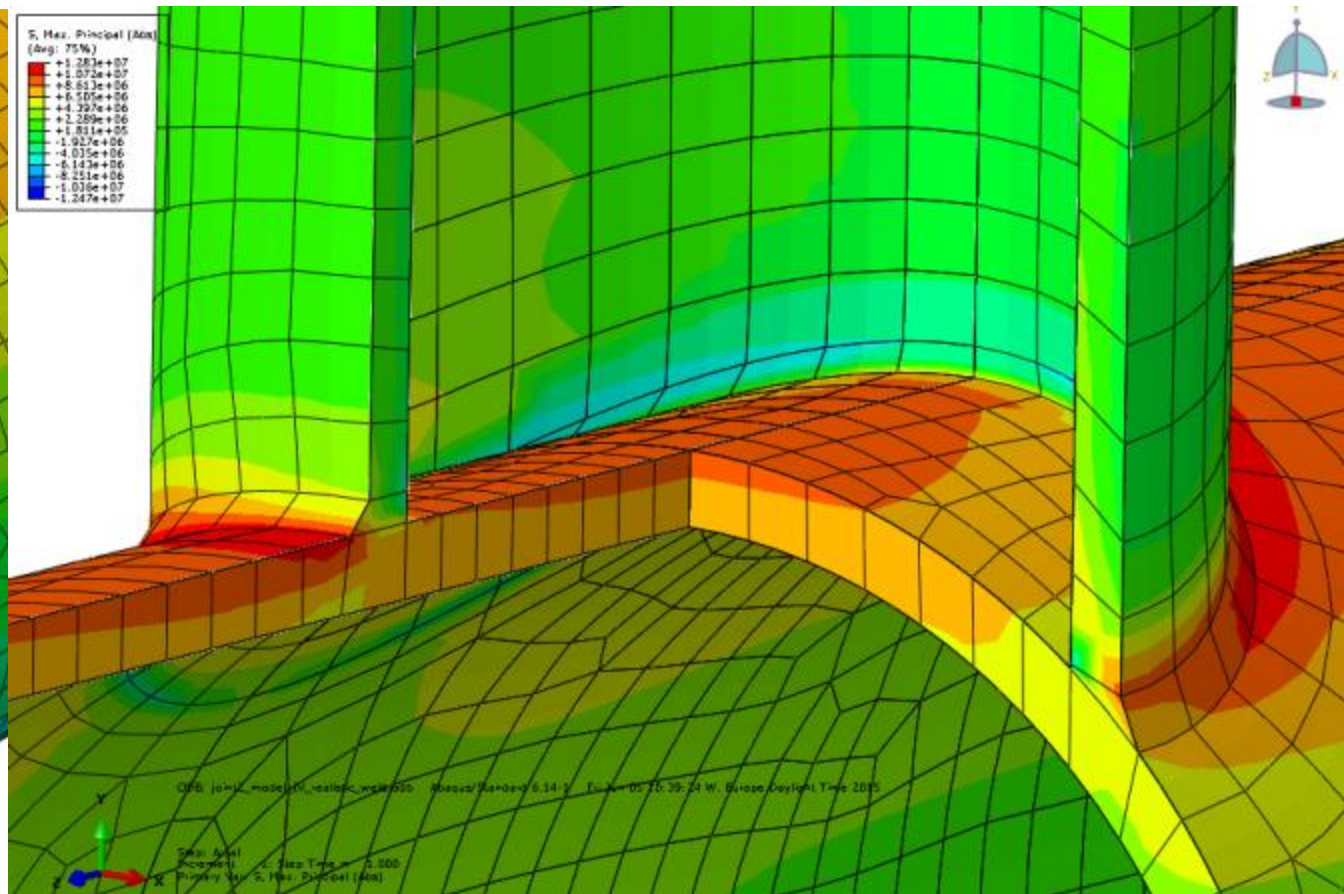
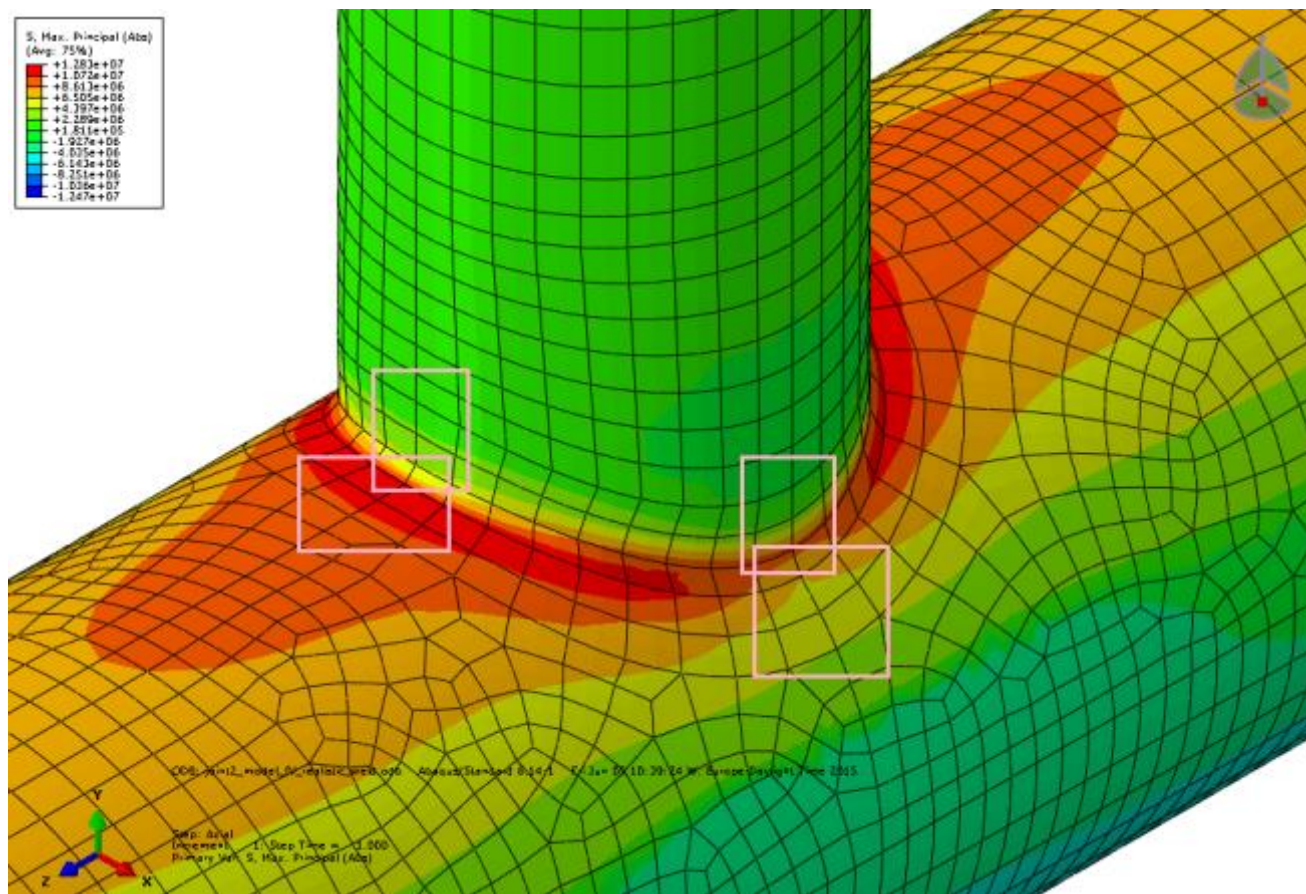
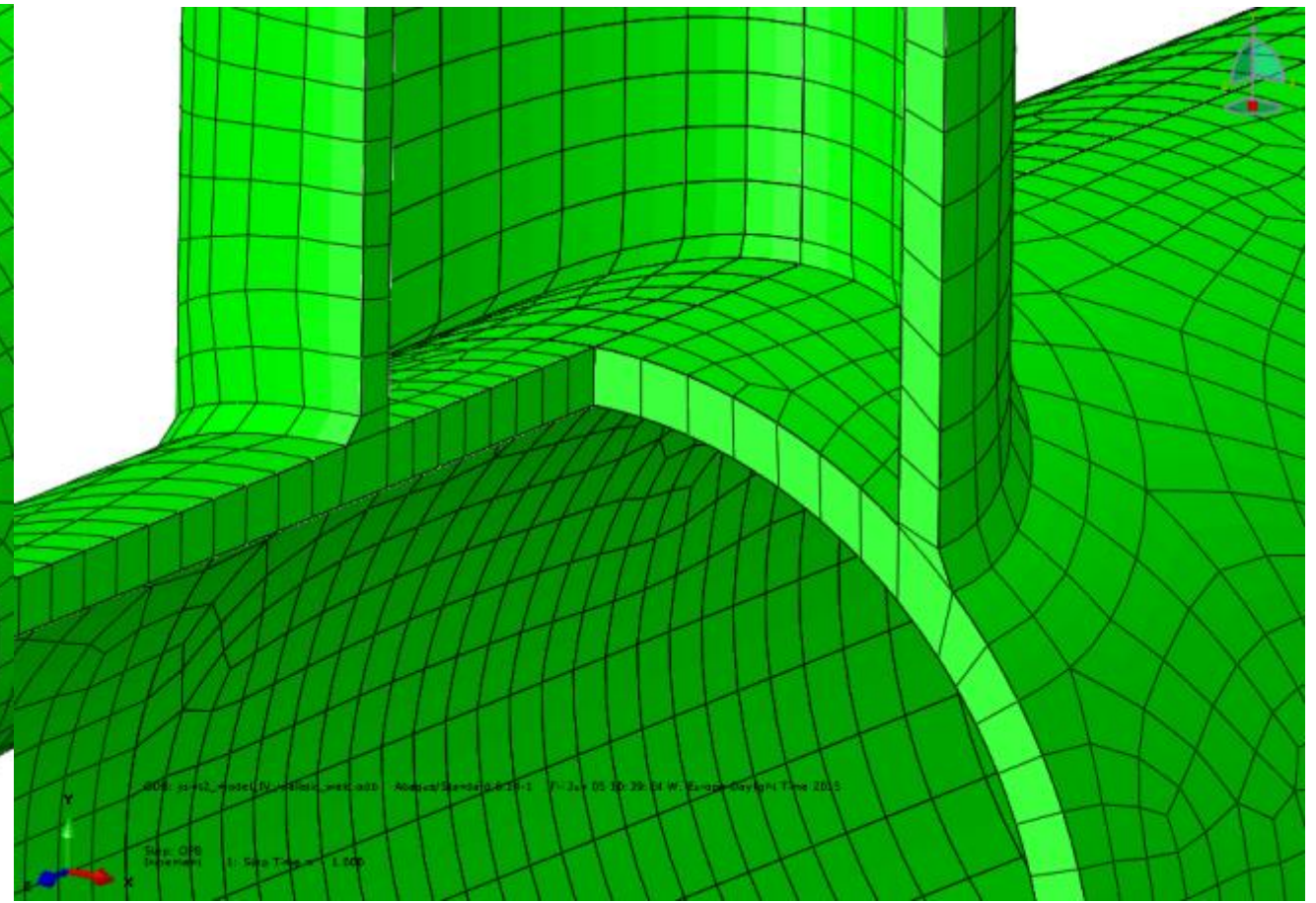
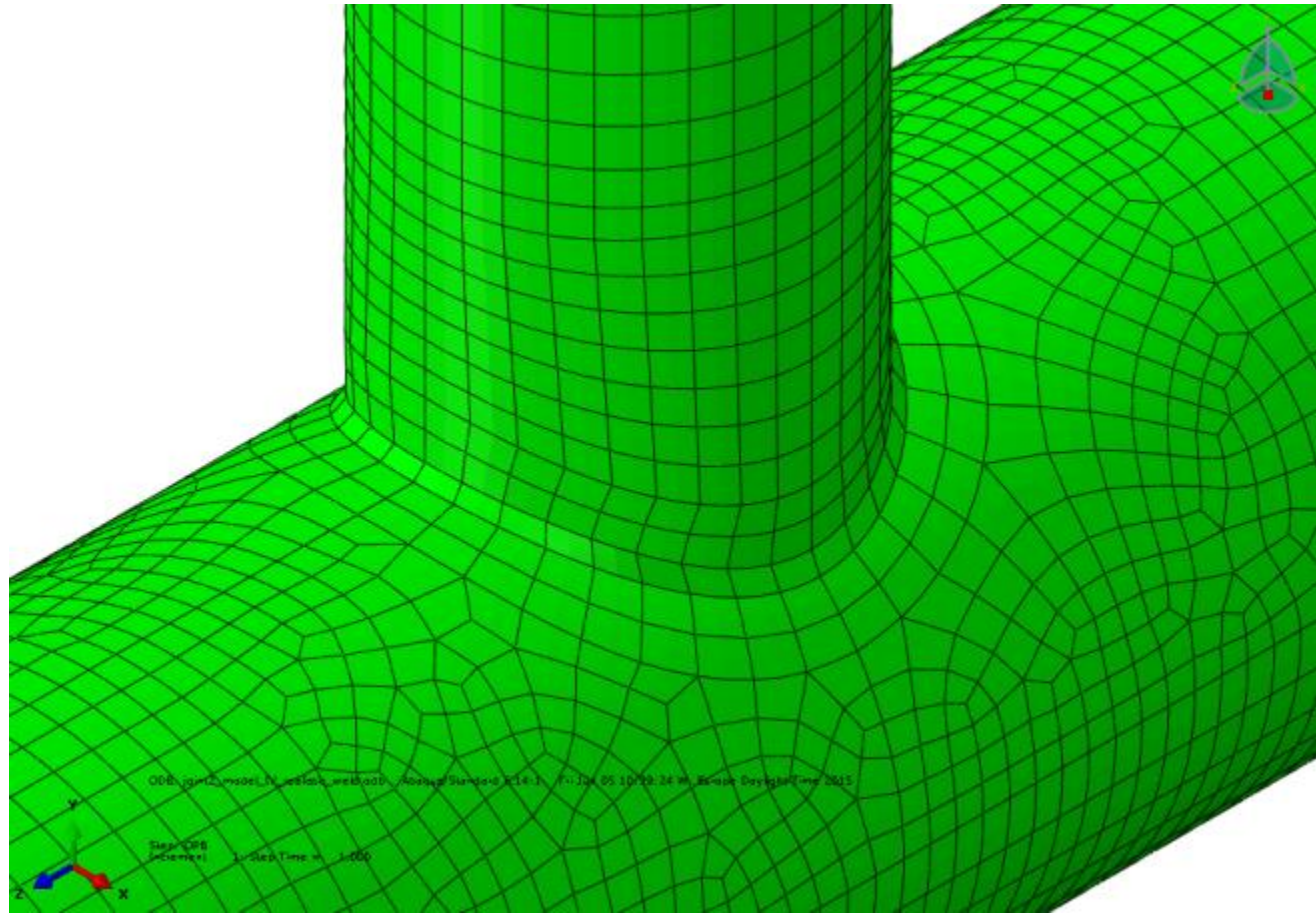


Figure A-2-6: Joint 2 Model IV (C3D20R, t x t mesh)

Upper left: Mesh

Lower left: Abs. max principal stress countour and stress read out region for axial load case

Upper right: Mesh cross section

Lower right: Abs. max principal stress countour with cut out for axial load case

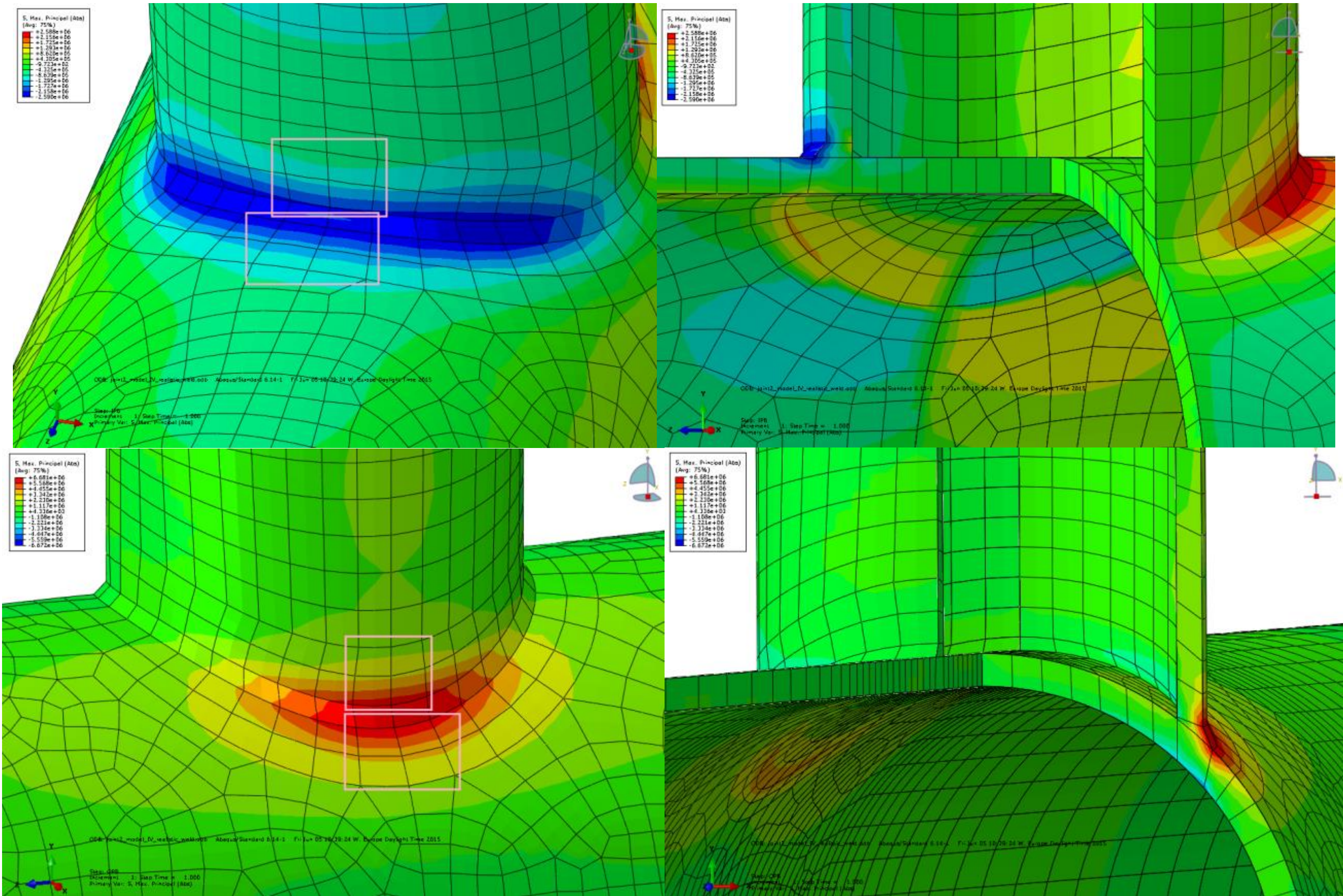


Figure A-2-7: Joint 2 Model IV (C3D20R, t x t mesh)

Lower left: Abs. max principal stress countour and stress read out region for IPB load case
 Lower left: Abs. max principal stress countour and stress read out region for OPB load case

Lower right: Abs. max principal stress countour with cut out for IPB load case
 Lower right: Abs. max principal stress countour with cut out for OPB load case

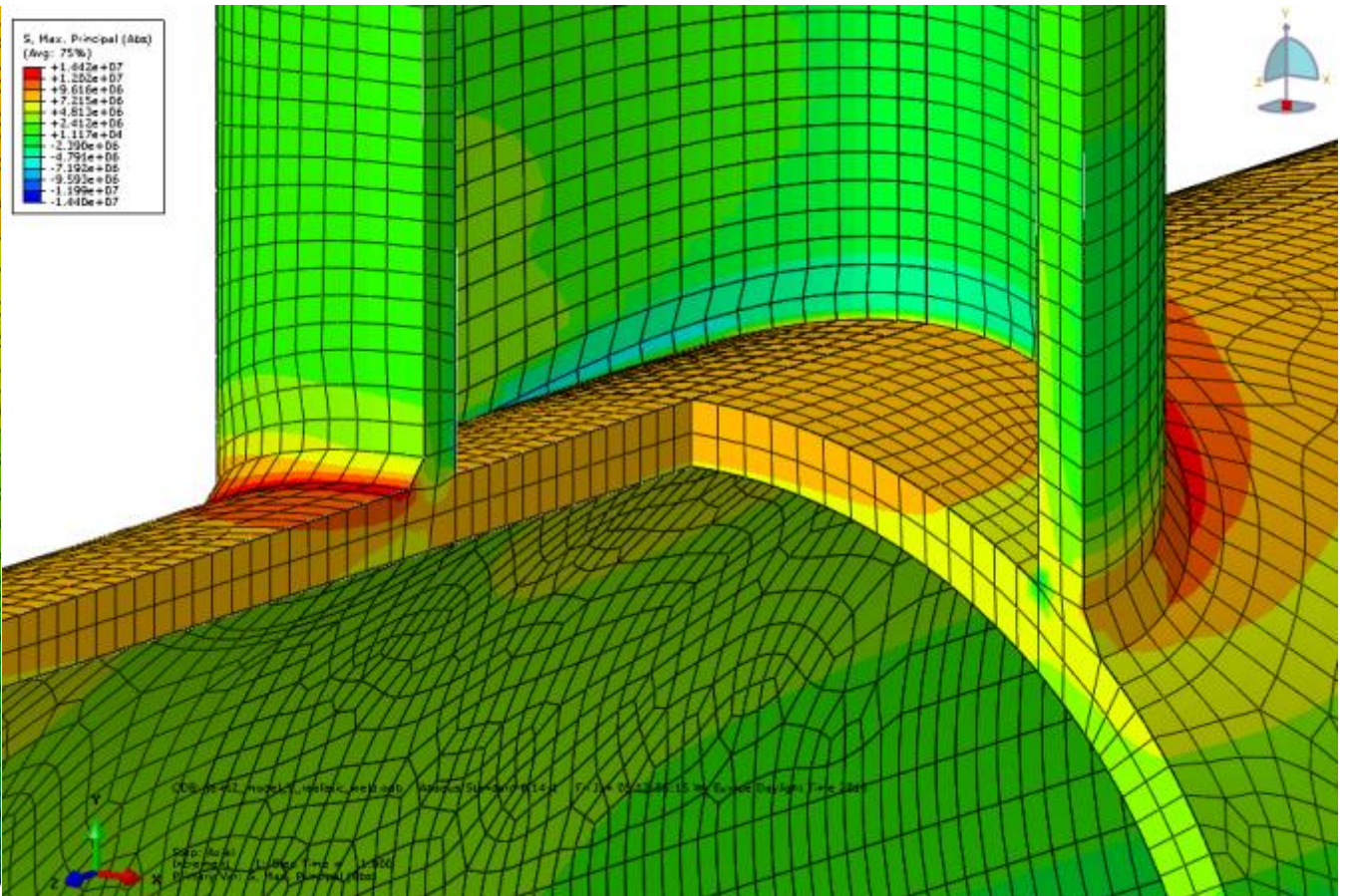
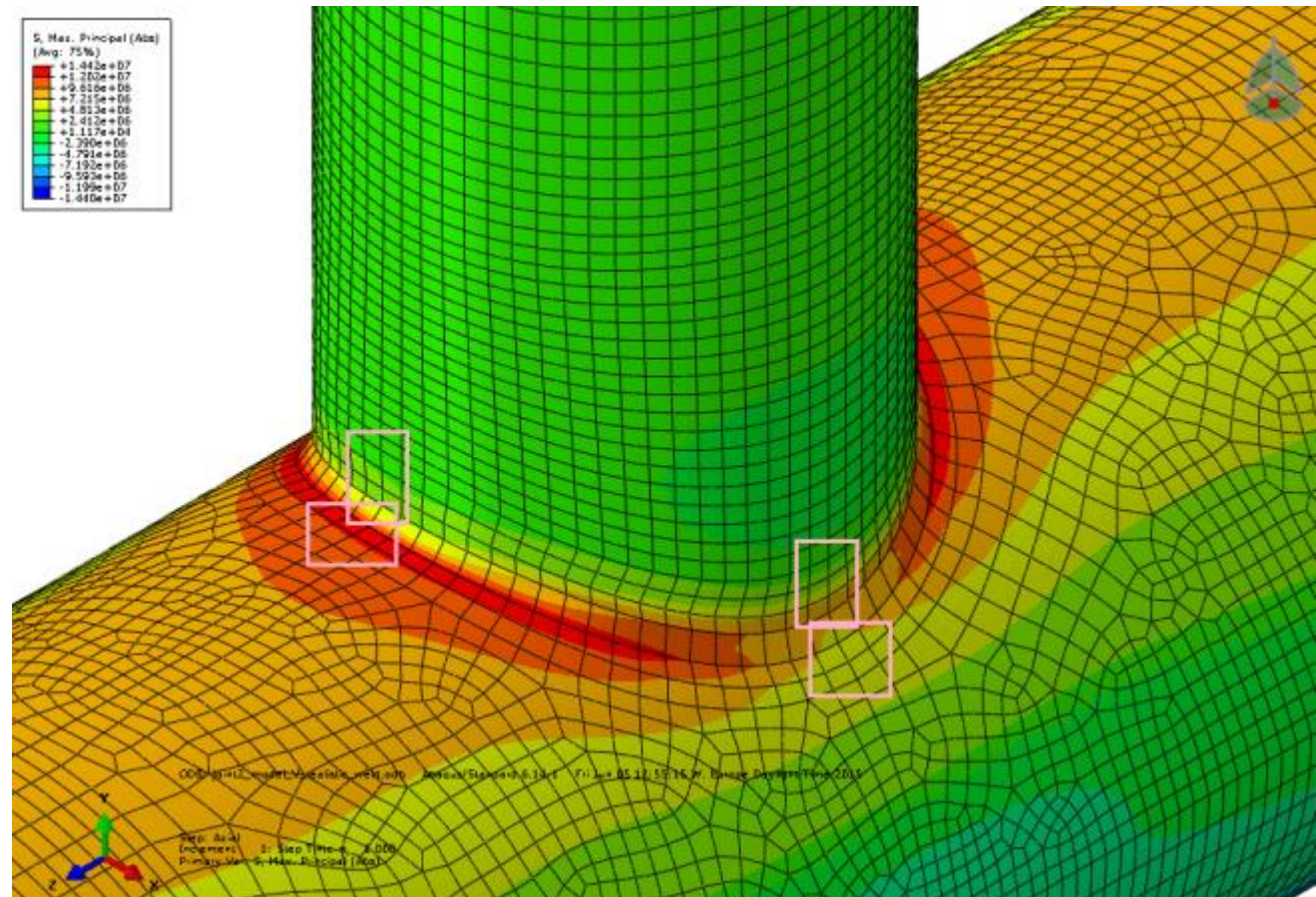
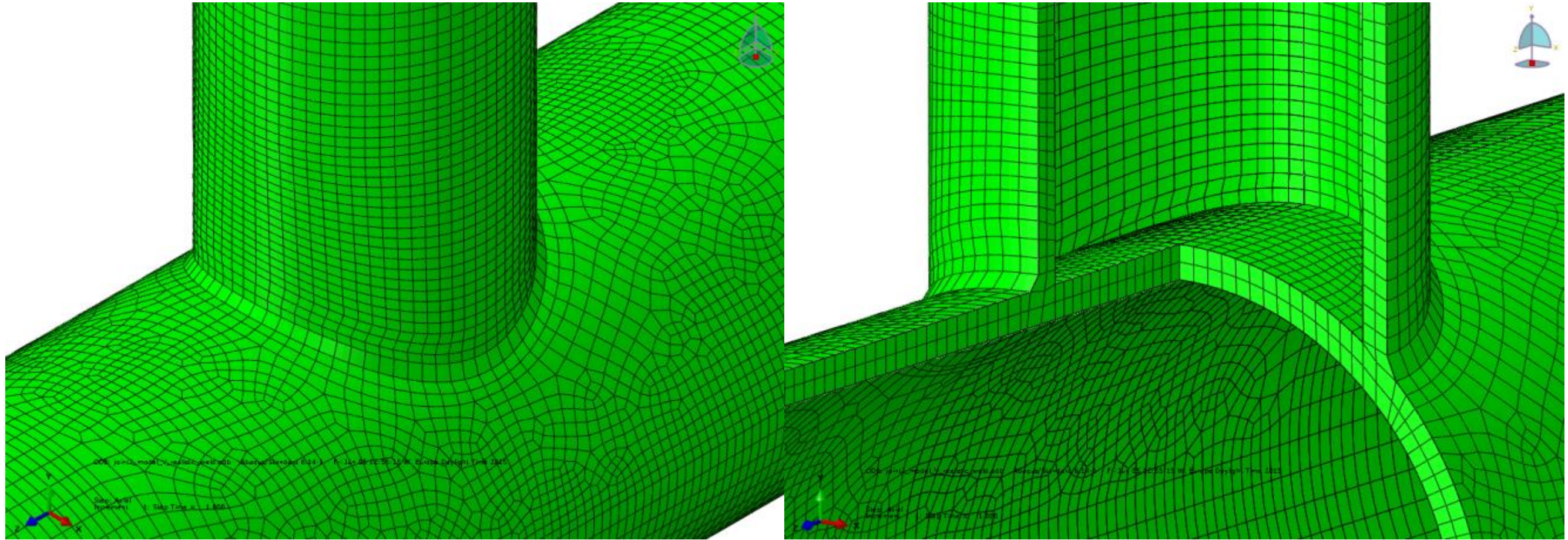


Figure A-2-8: Joint 2 Model V (C3D20R, relatively fine mesh)

Upper left: Mesh
 Lower left: Abs. max principal stress countour and stress read out region for axial load case

Upper right: Mesh cross section
 Lower right: Abs. max principal stress countour with cut out for axial load case

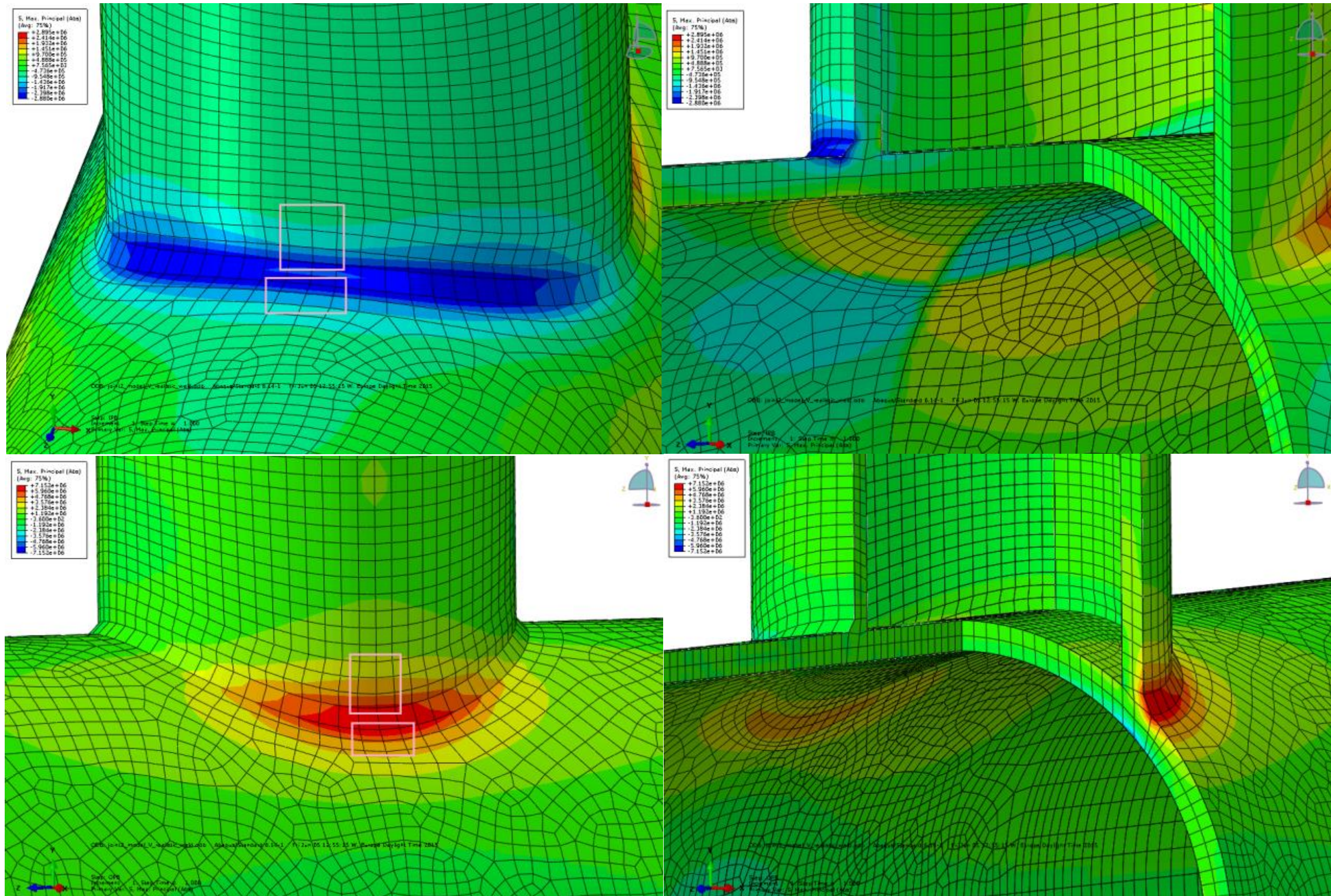


Figure A-2-9: Joint 2 Model V (C3D20R, relatively fine mesh)

Lower left: Abs. max principal stress countour and stress read out region for IPB load case
 Lower left: Abs. max principal stress countour and stress read out region for OPB load case

Lower right: Abs. max principal stress countour with cut out for IPB load case
 Lower right: Abs. max principal stress countour with cut out for OPB load case

A.3 Joint 3

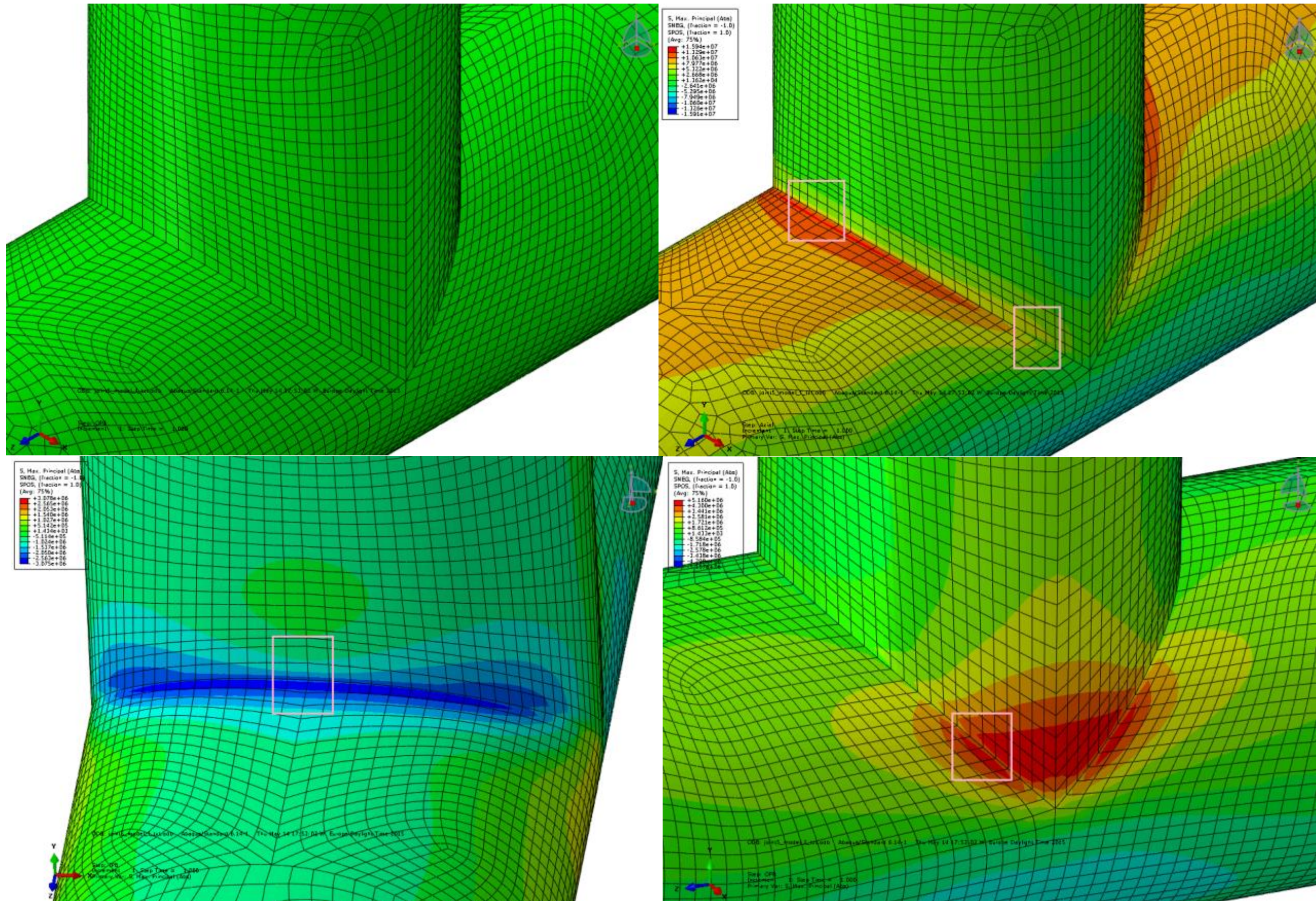


Figure A-3-1: Joint 3 Model I (S8R, t x t)

Upper left: Mesh

Lower left: Abs. max principal stress countour and stress read out region for IPB load case

Upper right: Abs. max principal stress countour and stress read out region for Axial load case

Lower right: Abs. max principal stress countour and stress read out region for OPB load case

A.4 Joint 4

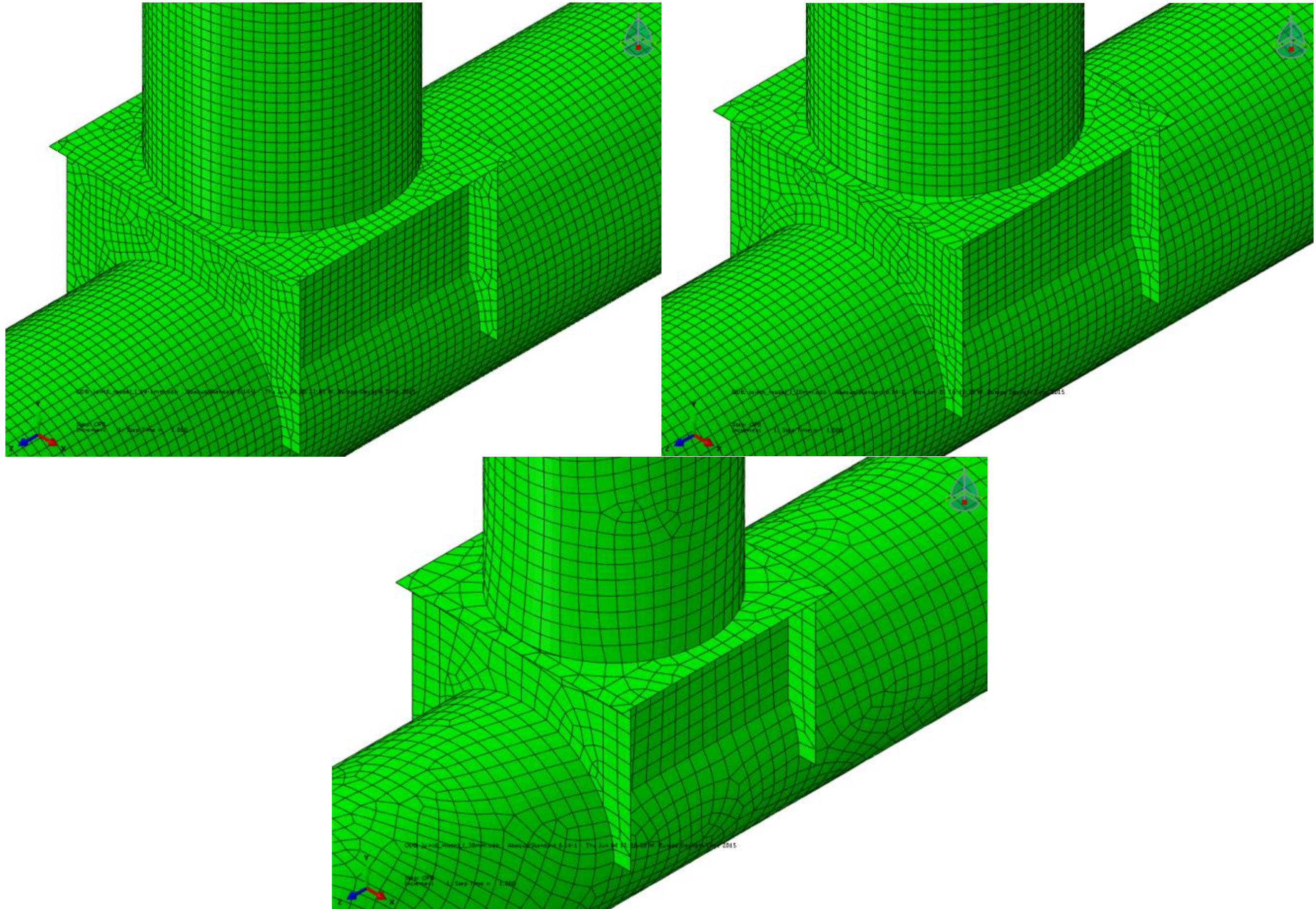


Figure A-4-1: Joint 4 Model I (S8R, t x t, 19.1mm chord/brace, 20mm stiffeners, 30mm top plate)

Upper left: Mesh 19.1mm density
 Lower: Mesh 30mm density

Upper right: Mesh 20mm density

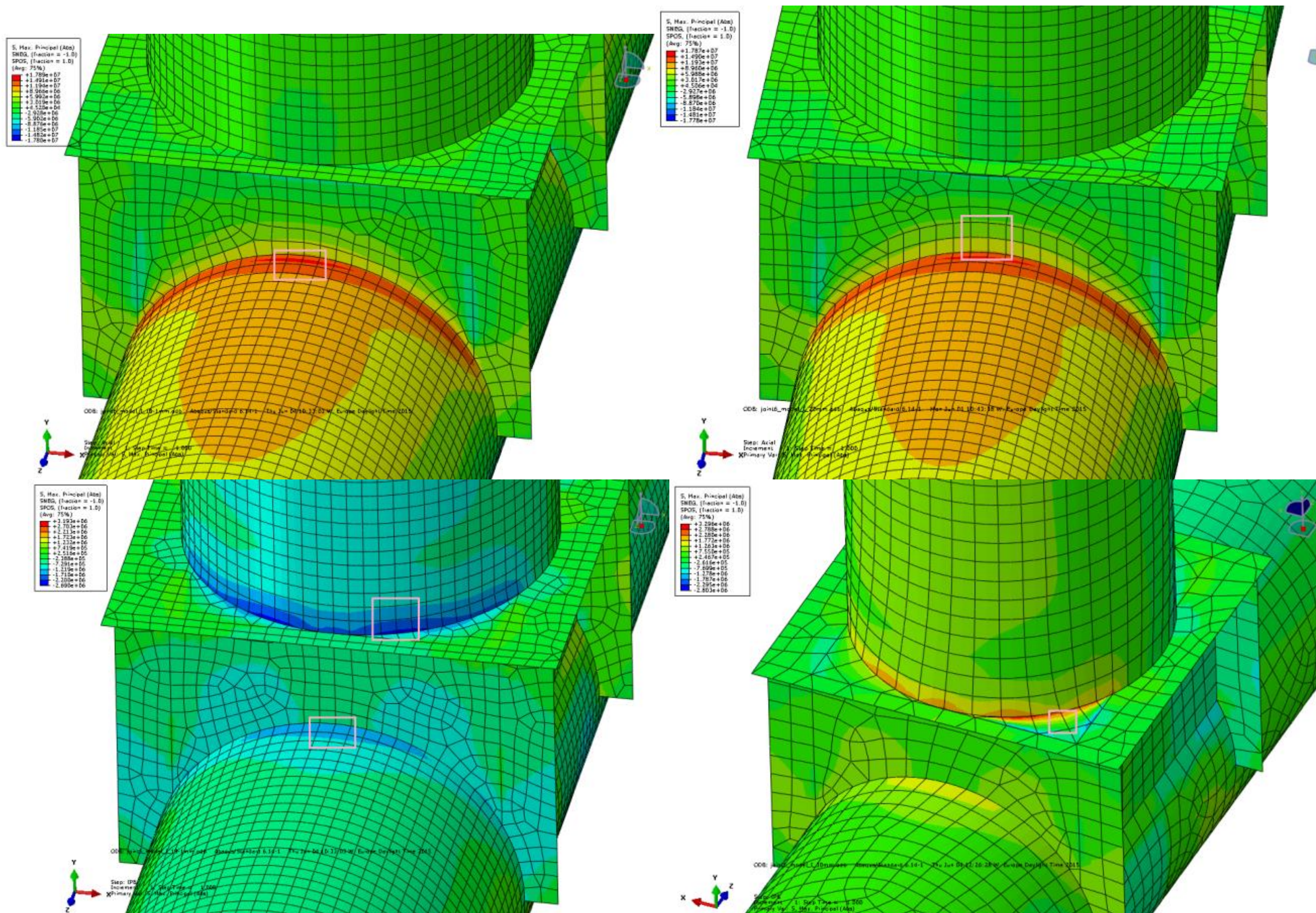


Figure A-4-2: Joint 4 Model I (S8R, t x t, 19.1mm chord/brace, 20mm stiffeners, 30mm top plate)

Upper left: Abs. max principal stress countour and stress read out region for axial load case, 19.1mm mesh
Lower left: Abs. max principal stress countour and stress read out region for IPB load case, 19.1mm mesh

Upper right: Abs. max principal stress countour and stress read out region for axial load case, 20mm mesh
Lower right: Abs. max principal stress countour and stress read out region for IPB load case, 30mm mesh

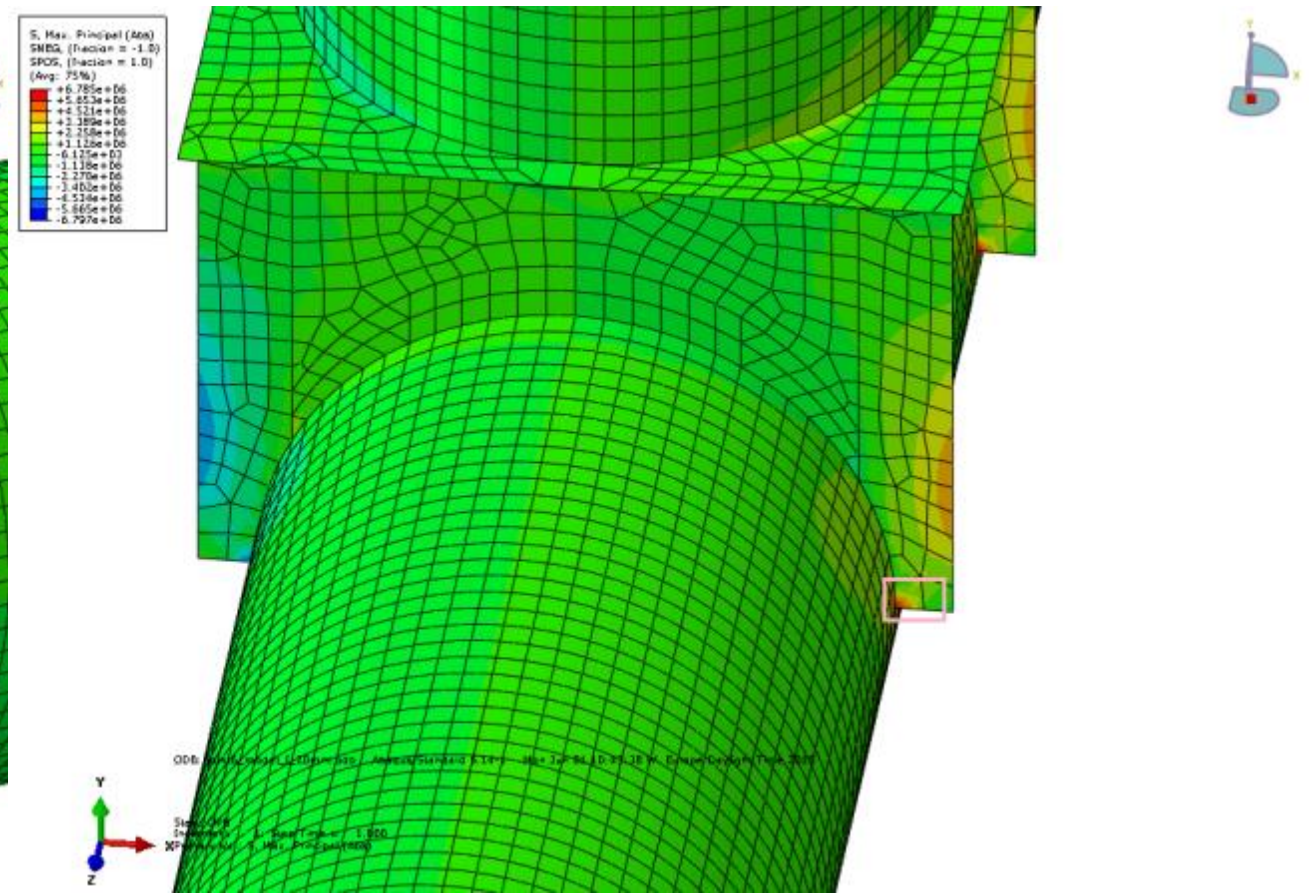
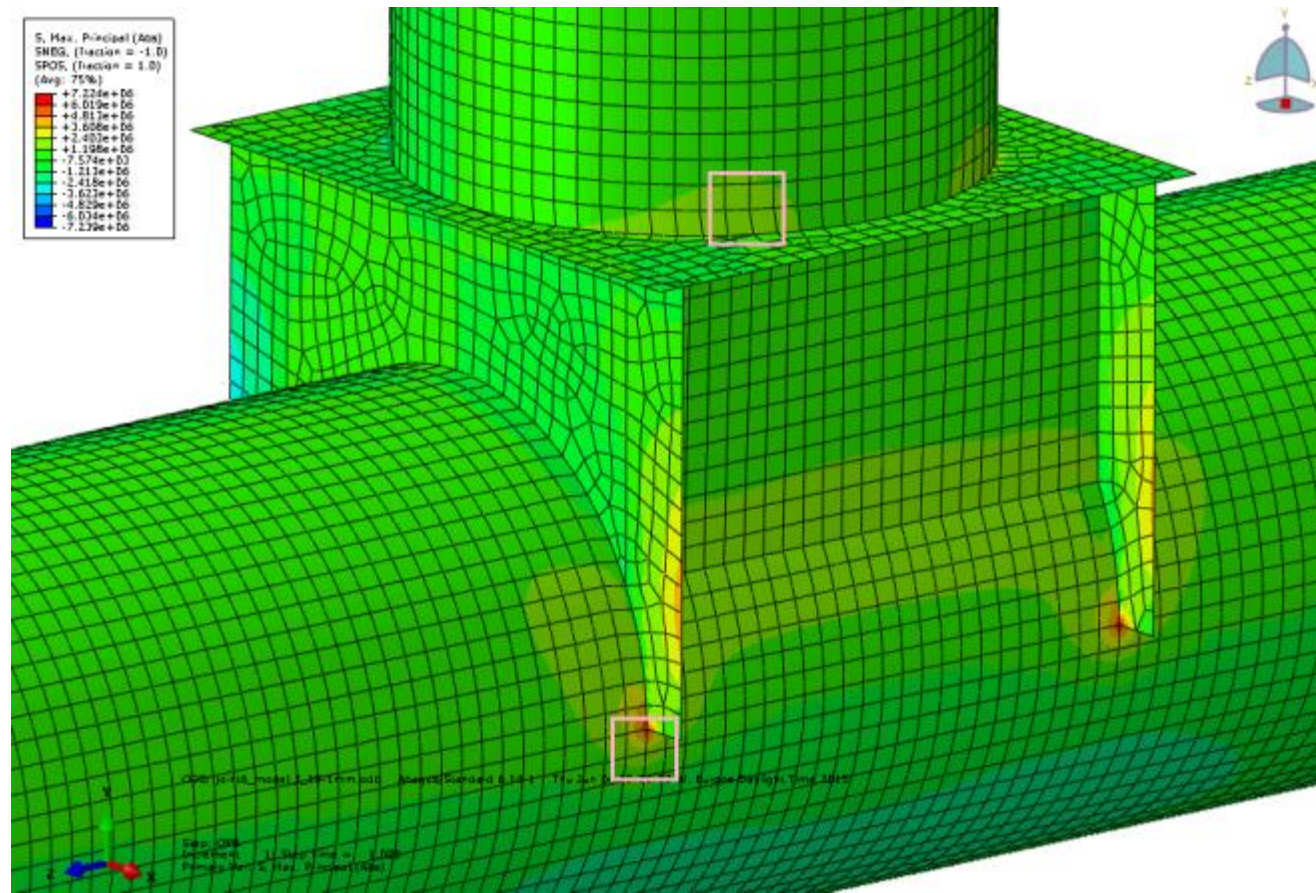


Figure A-4-3: Joint 4 Model I (S8R, t x t, 19.1mm chord/brace, 20mm stiffeners, 30mm top plate)

Upper left: Abs. max principal stress contour and stress read out region for OPB load case, 19.1mm mesh

Upper right: Abs. max principal stress contour and stress read out region for OPB load case, 20mm mesh

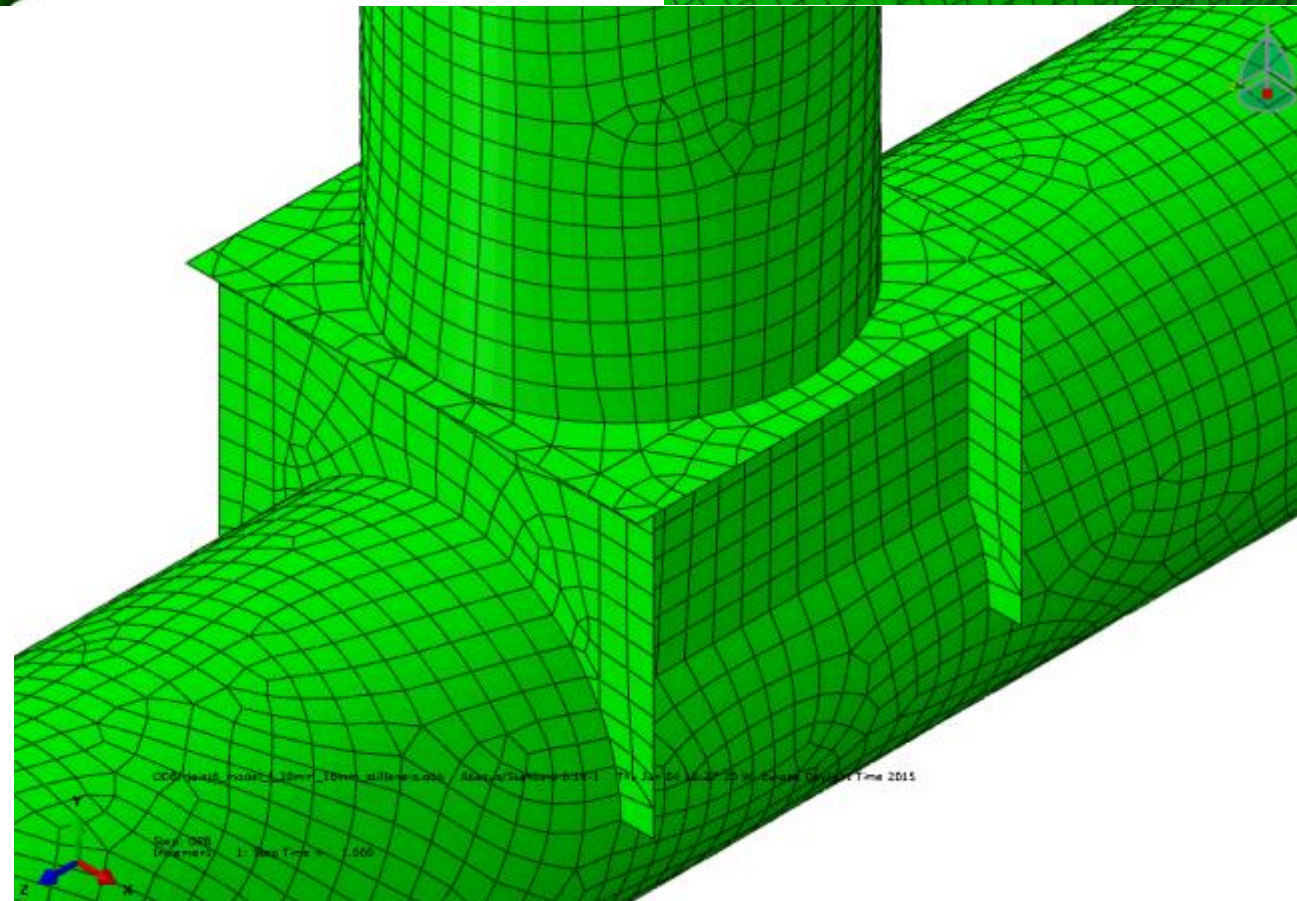
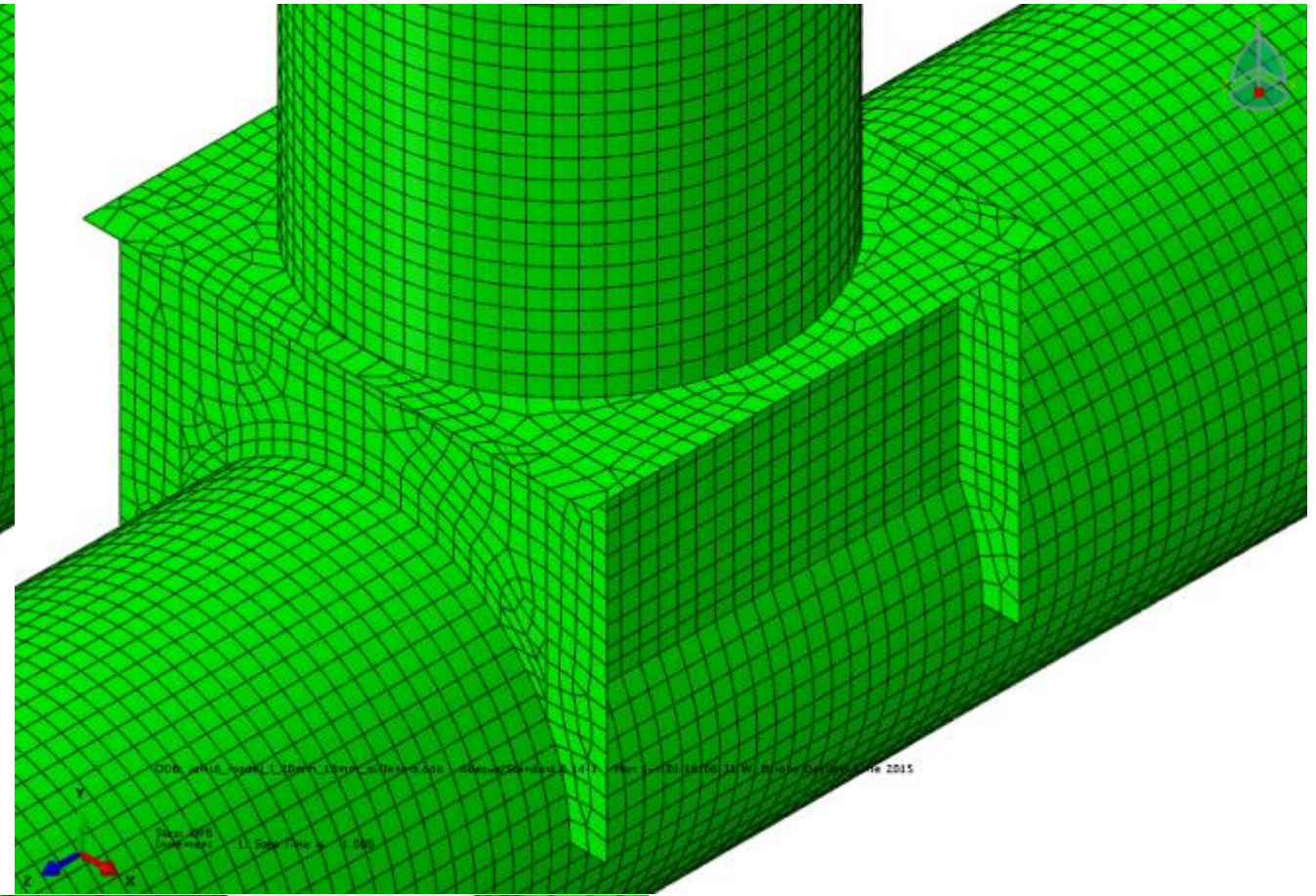
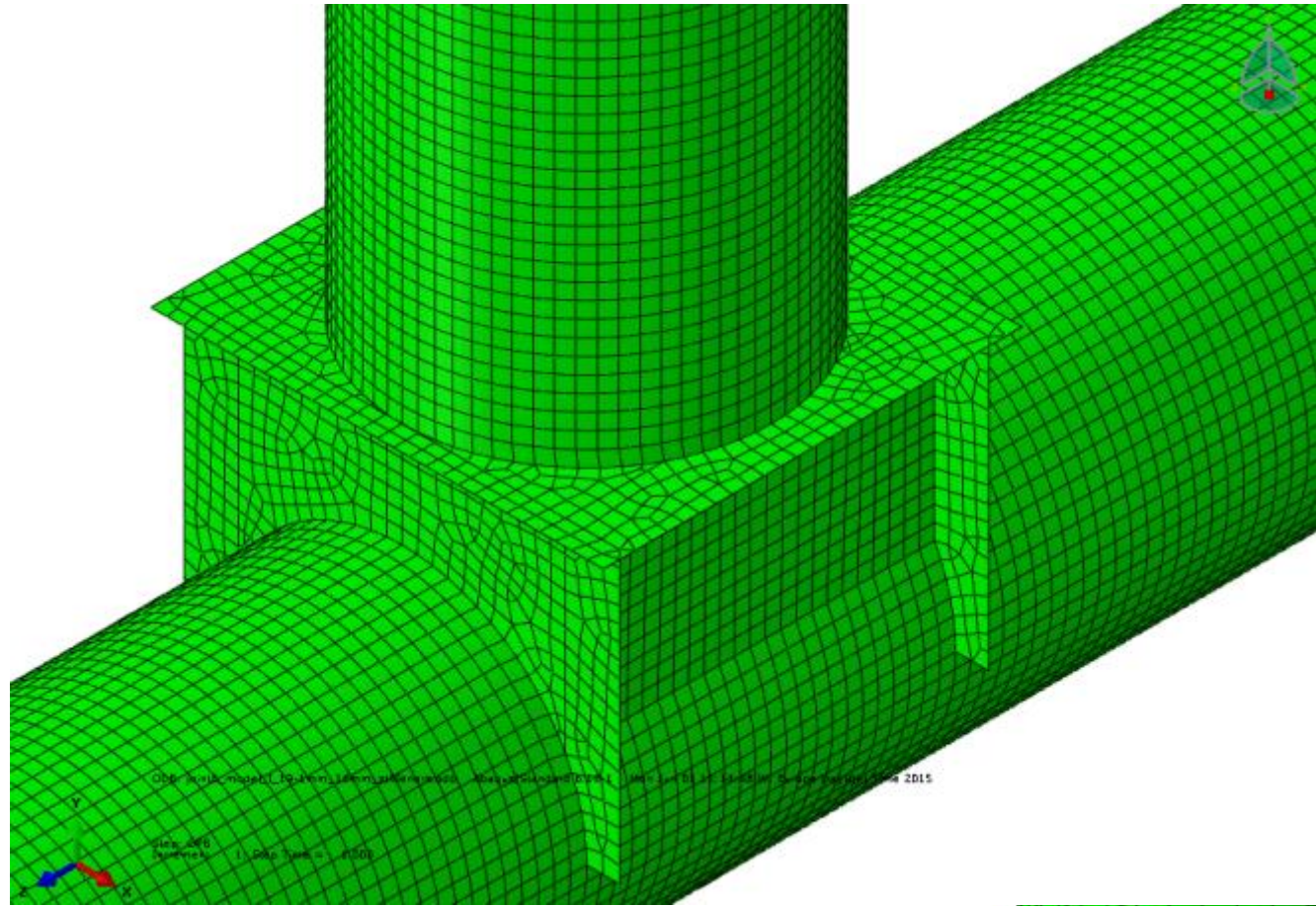


Figure A-4-4: Joint 4 Model II (S8R, t x t, 19.1mm chord/brace, 16mm stiffeners, 30mm top plate)
Upper left: Mesh 19.1mm density Upper right: Mesh 16mm density
Lower: Mesh 30mm density

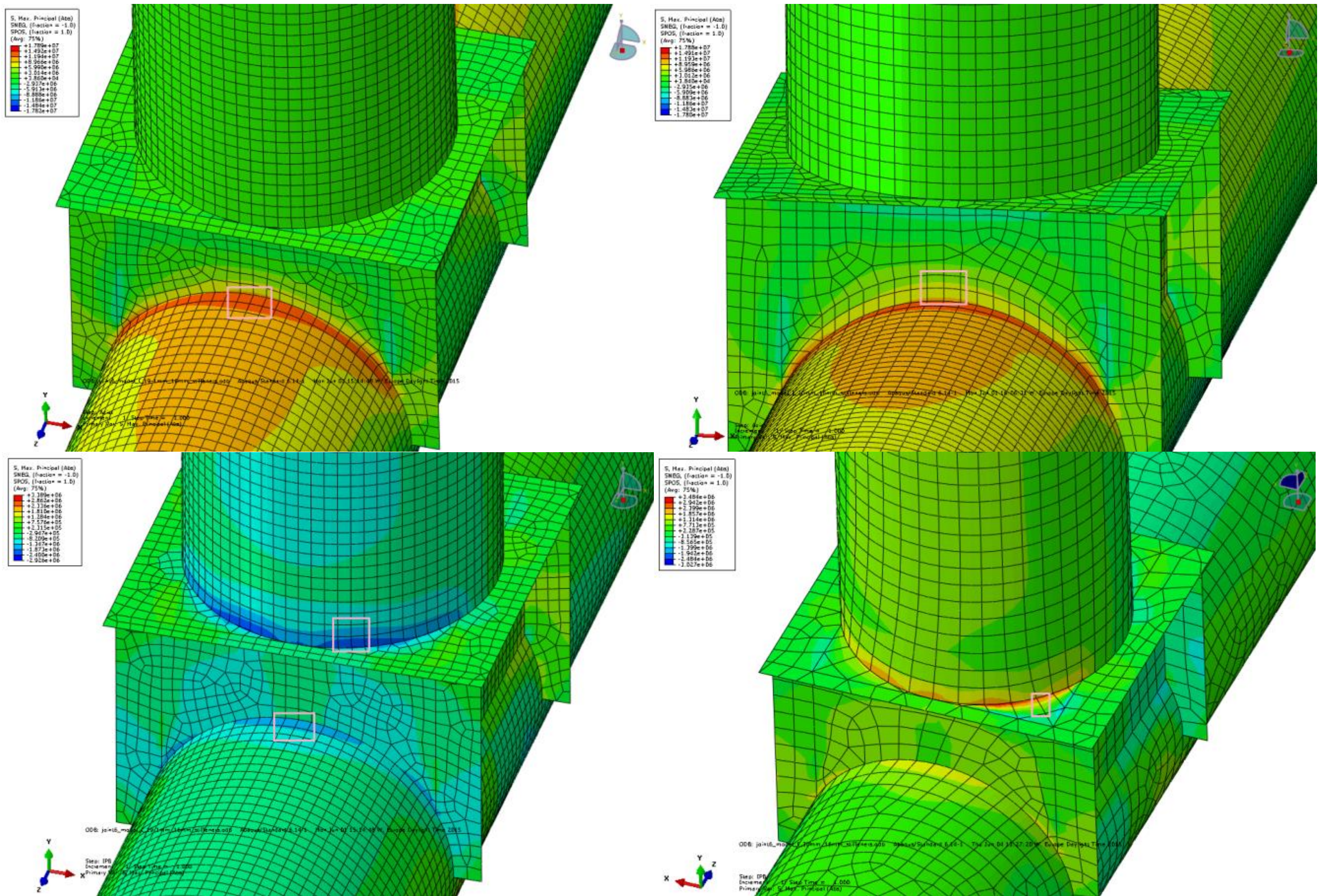


Figure A-4-5: Joint 4 Model II (S8R, t x t, 19.1mm chord/brace, 16mm stiffeners, 30mm top plate)

Upper left: Abs. max principal stress countour and stress read out region for axial load case, 19.1mm mesh
 Lower left: Abs. max principal stress countour and stress read out region for IPB load case, 19.1mm mesh

Upper right: Abs. max principal stress countour and stress read out region for axial load case, 16mm mesh
 Lower right: Abs. max principal stress countour and stress read out region for IPB load case, 30mm mesh

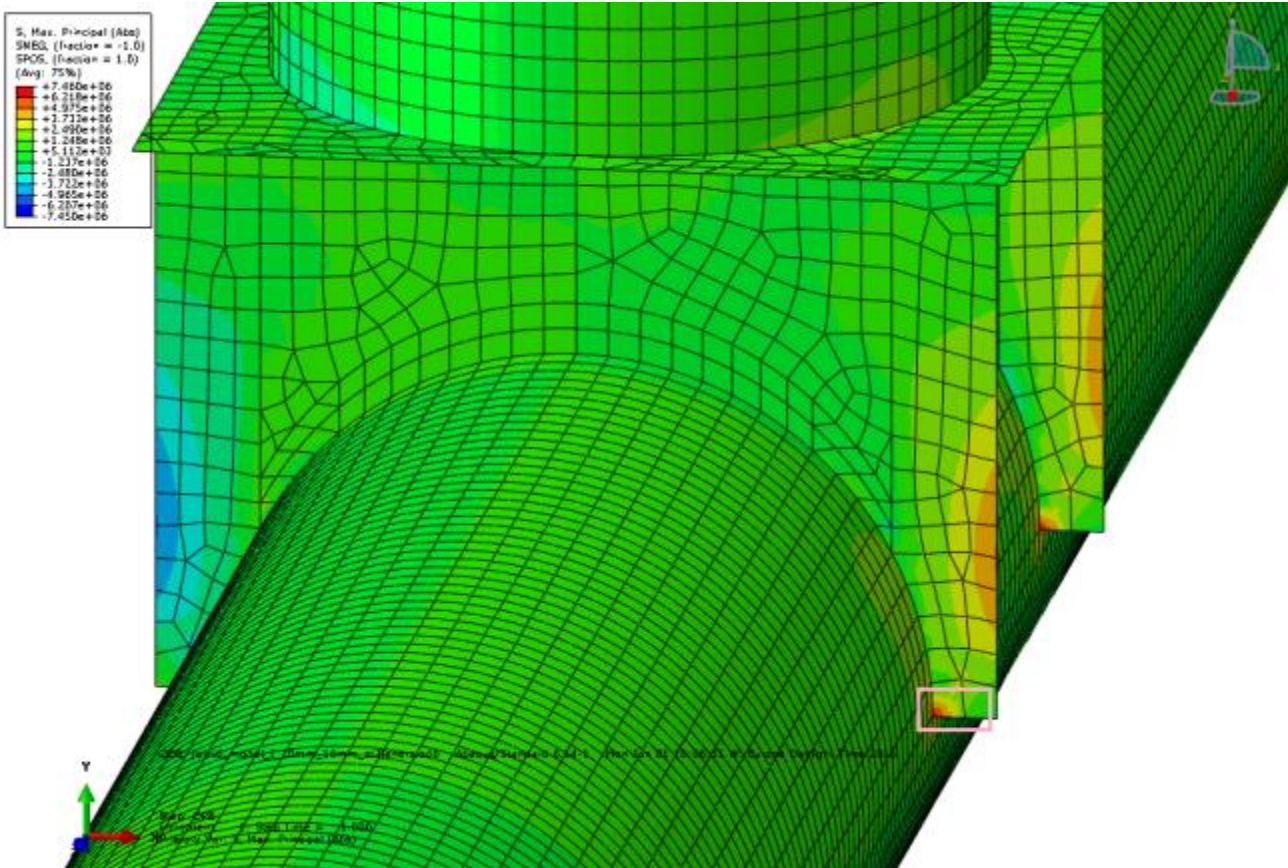
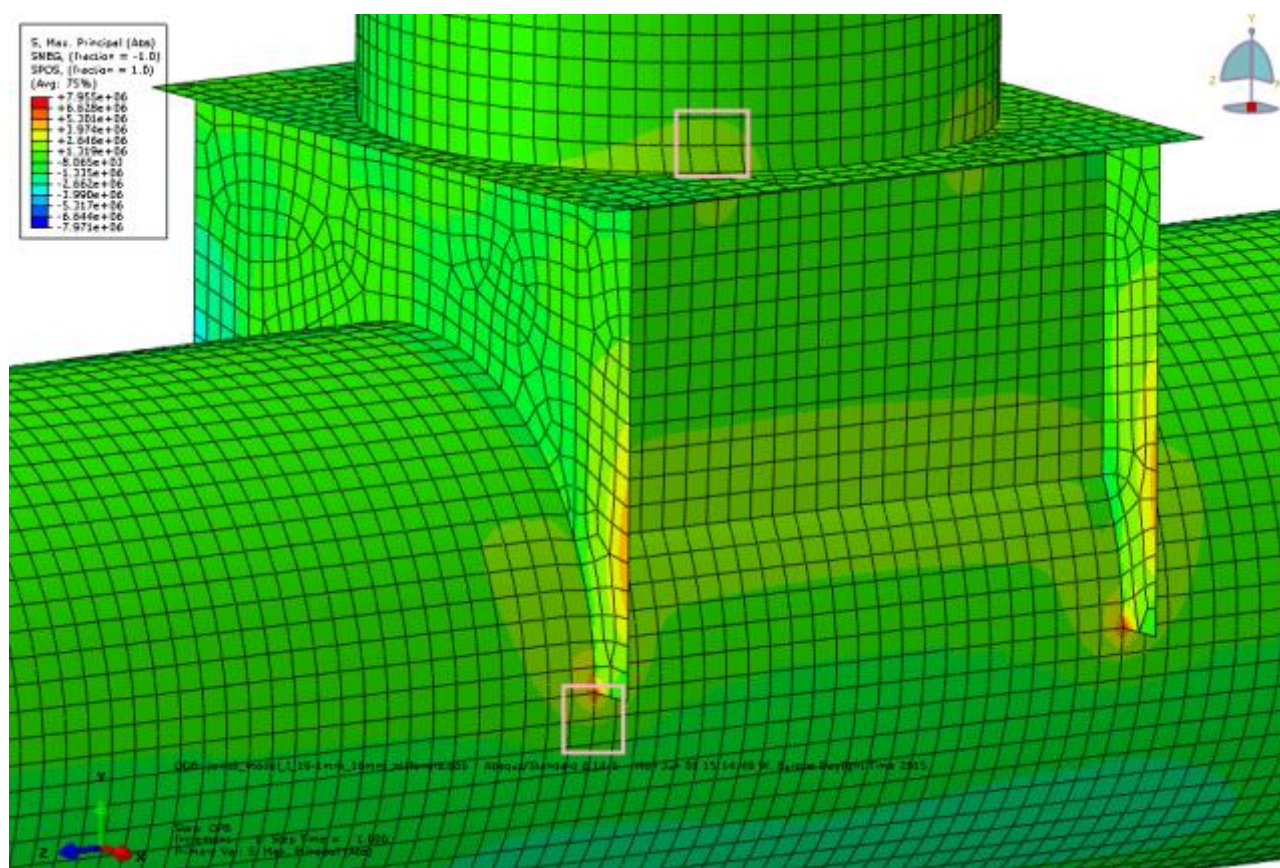


Figure A-4-6: Joint 4 Model II (S8R, t x t, 19.1mm chord/brace, 16mm stiffeners, 30mm top plate)

Upper left: Abs. max principal stress countour and stress read out region for OPB load case, 19.1mm mesh

Upper right: Abs. max principal stress countour and stress read out region for OPB load case, 16mm mesh

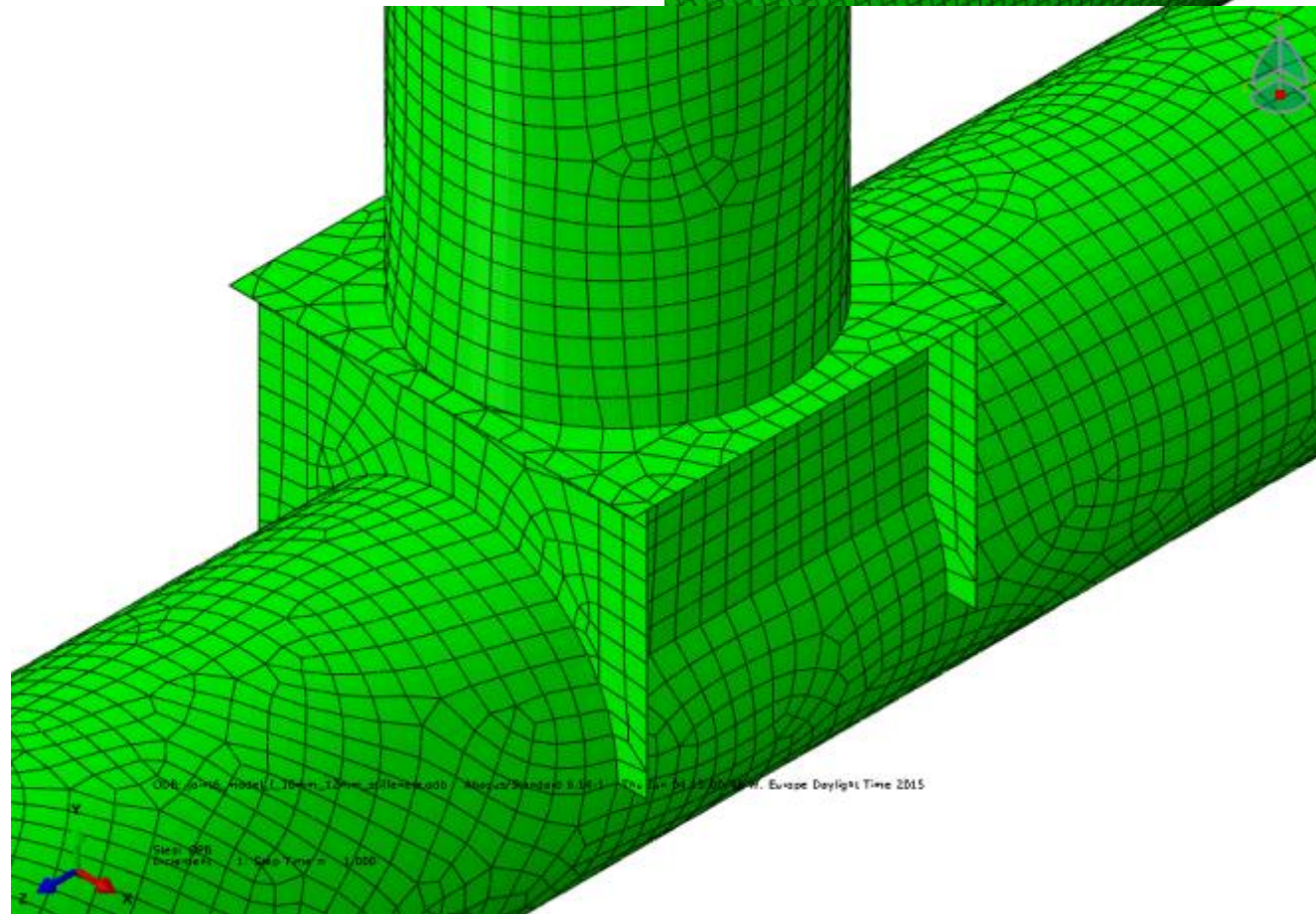
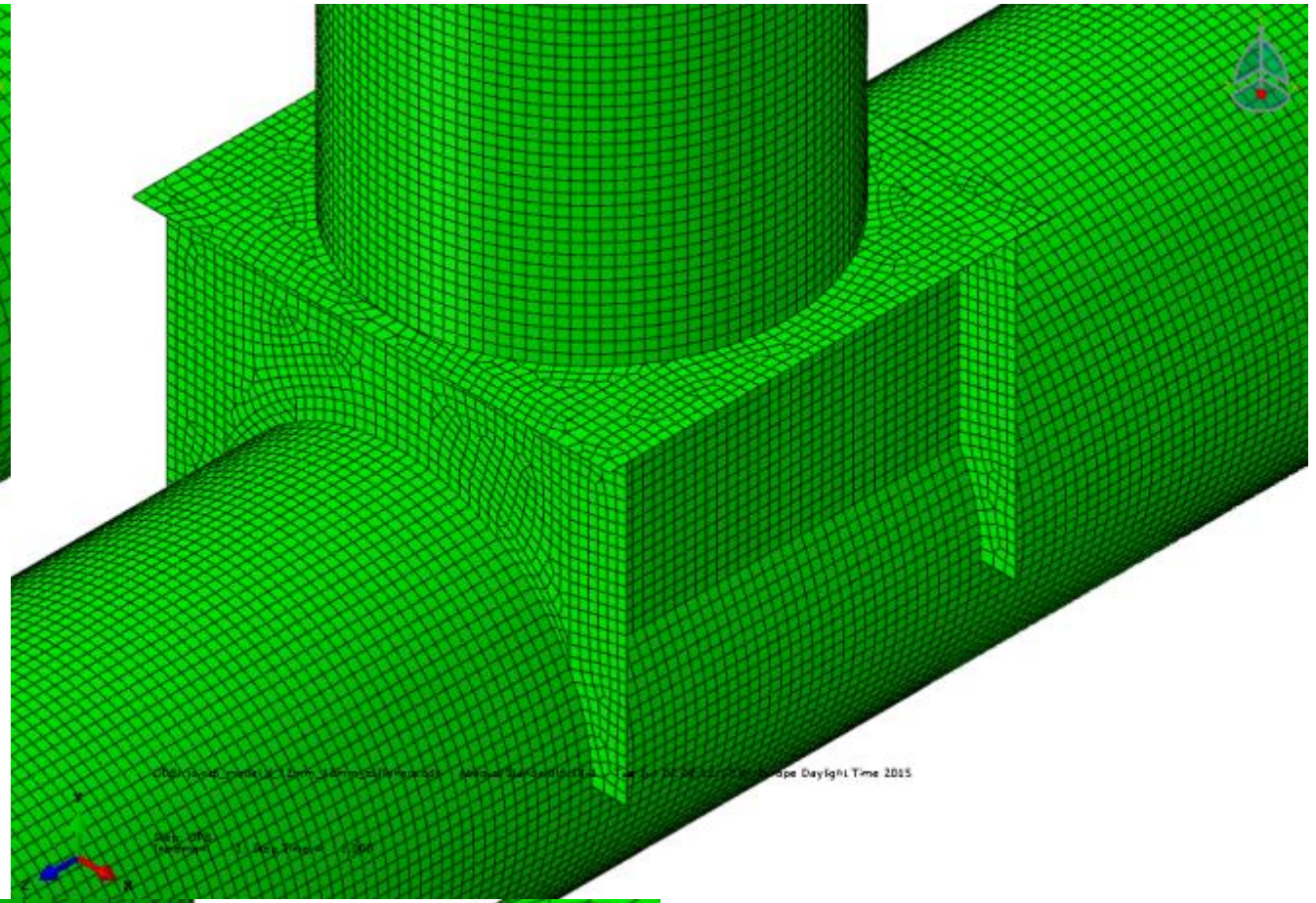
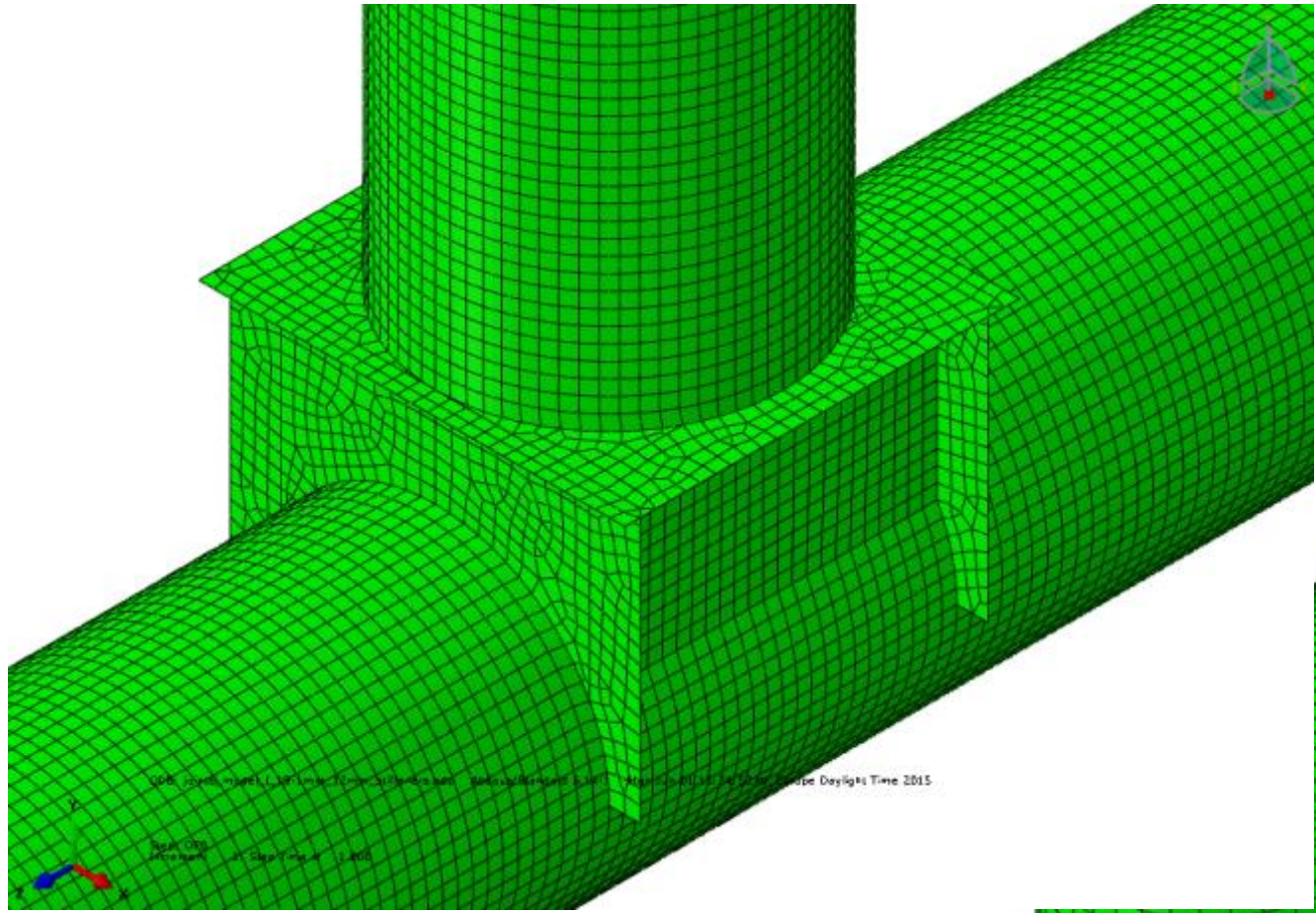


Figure A-4-7: Joint 4 Model III (S8R, t x t, 19.1mm chord/brace, 12mm stiffeners, 30mm top plate)
Upper left: Mesh 19.1mm density Lower: Mesh 30mm density Upper right: Mesh 12mm density

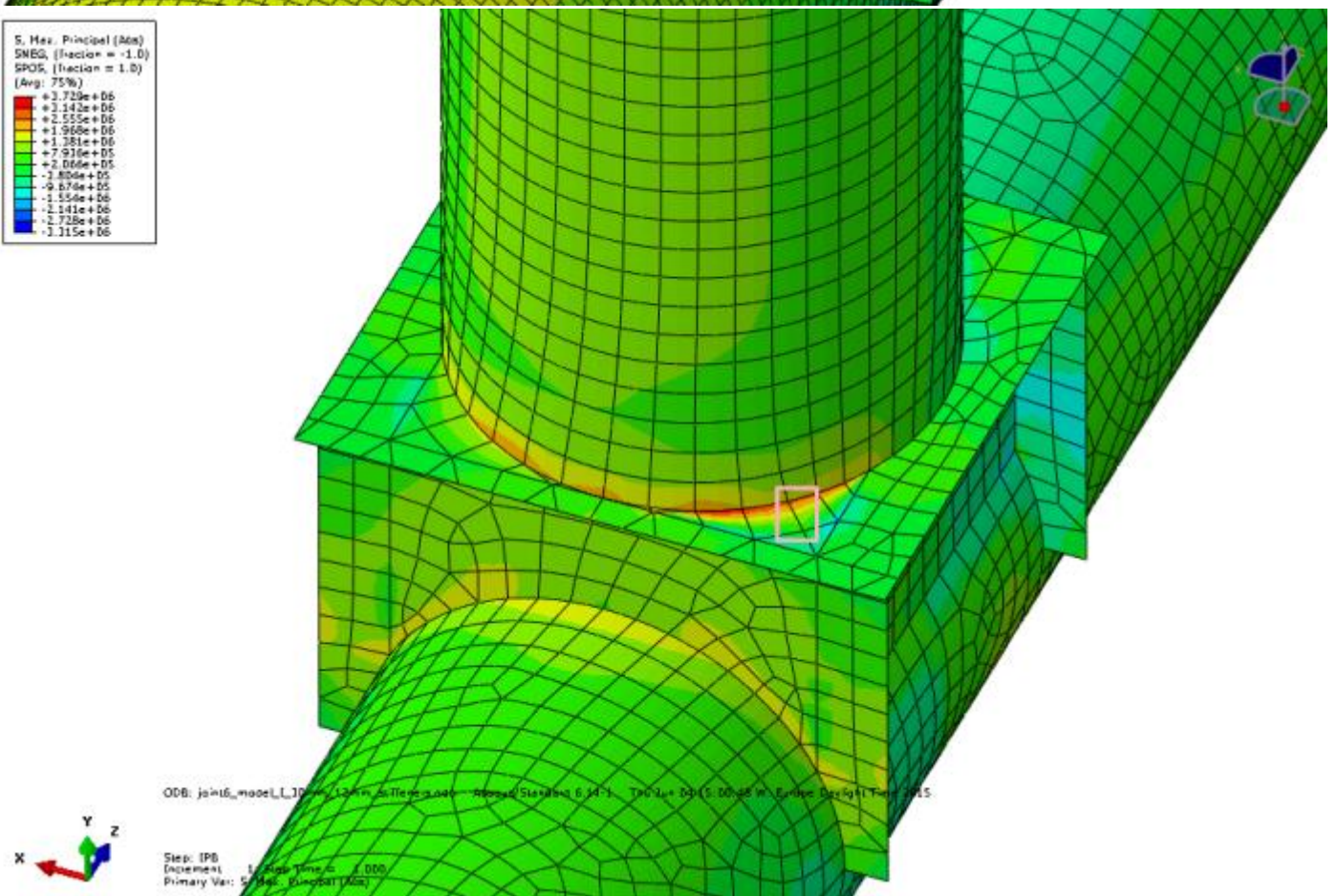
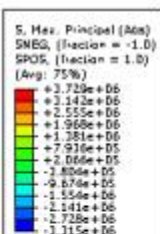
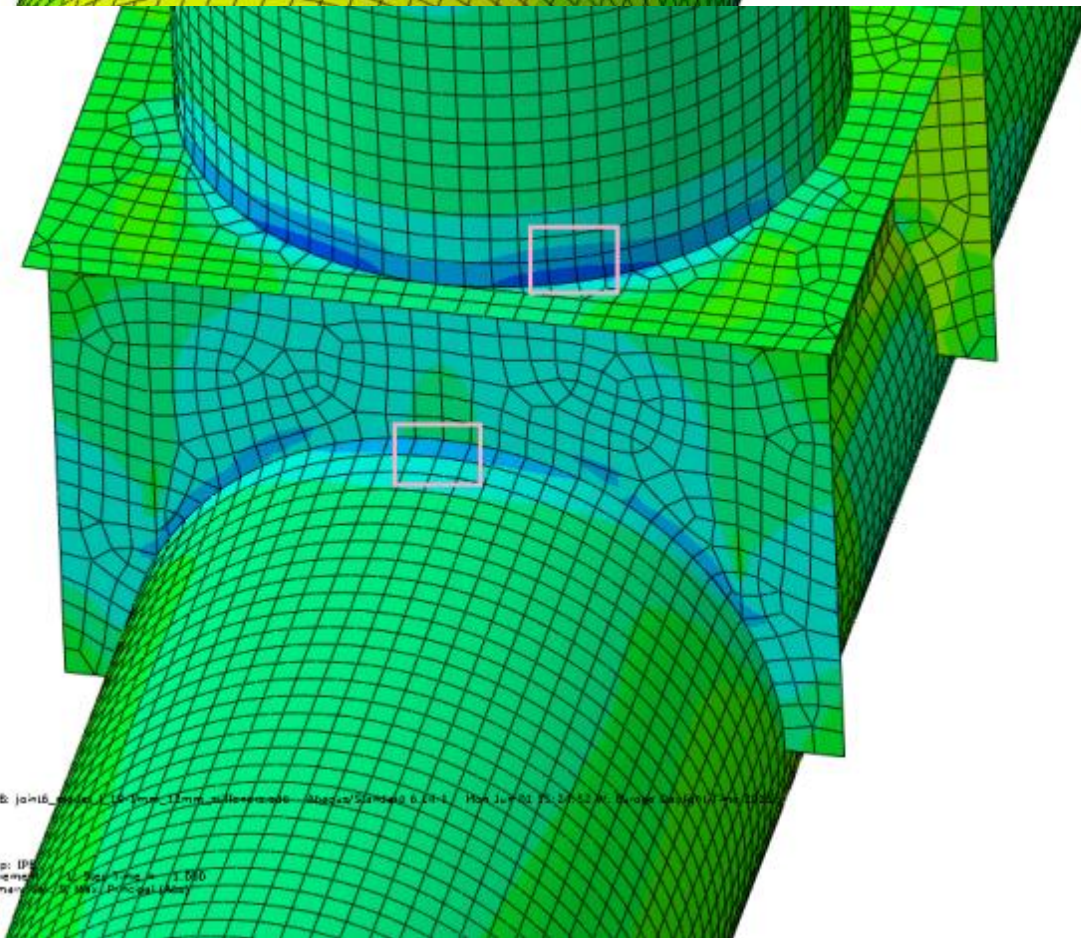
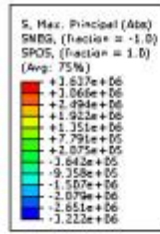
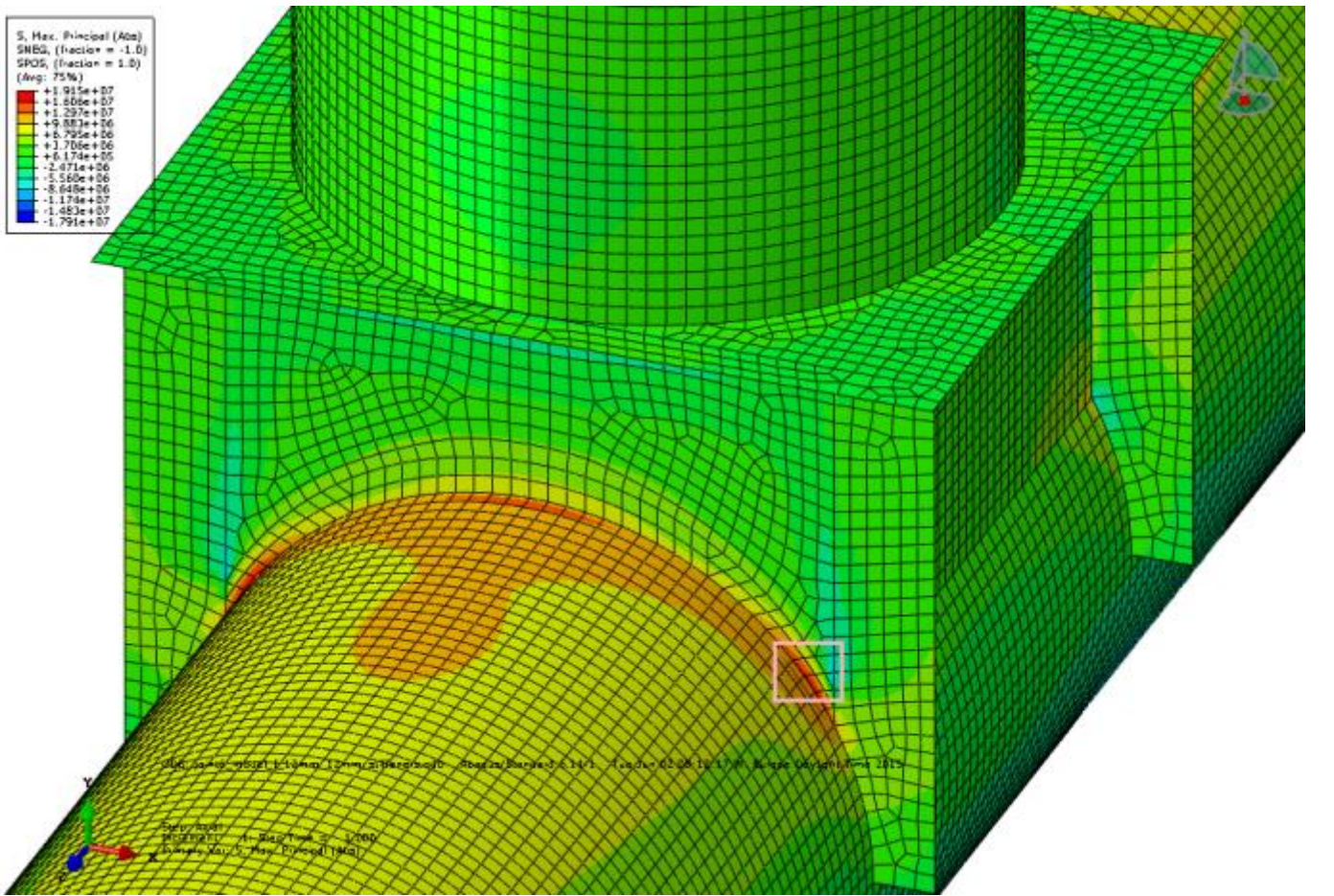
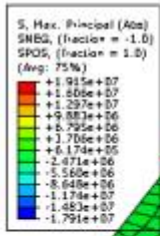
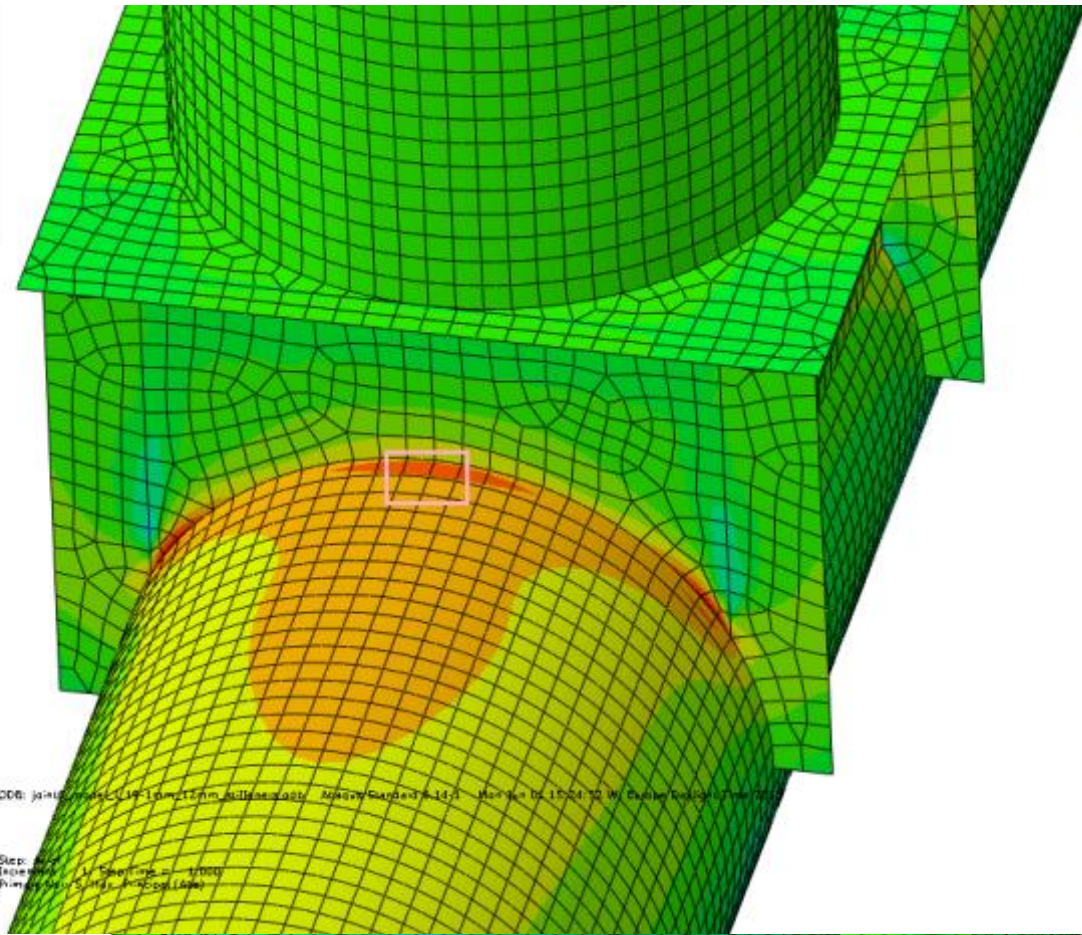
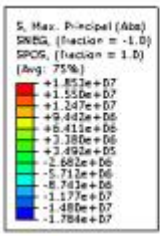


Figure A-4-8: Joint 4 Model III (S8R, t x t, 19.1mm chord/brace, 12mm stiffeners, 30mm top plate)

Upper left: Abs. max principal stress countour and stress read out region for axial load case, 19.1mm mesh
Lower left: Abs. max principal stress countour and stress read out region for IPB load case, 19.1mm mesh

Upper right: Abs. max principal stress countour and stress read out region for axial load case, 12mm mesh
Lower right: Abs. max principal stress countour and stress read out region for IPB load case, 30mm mesh

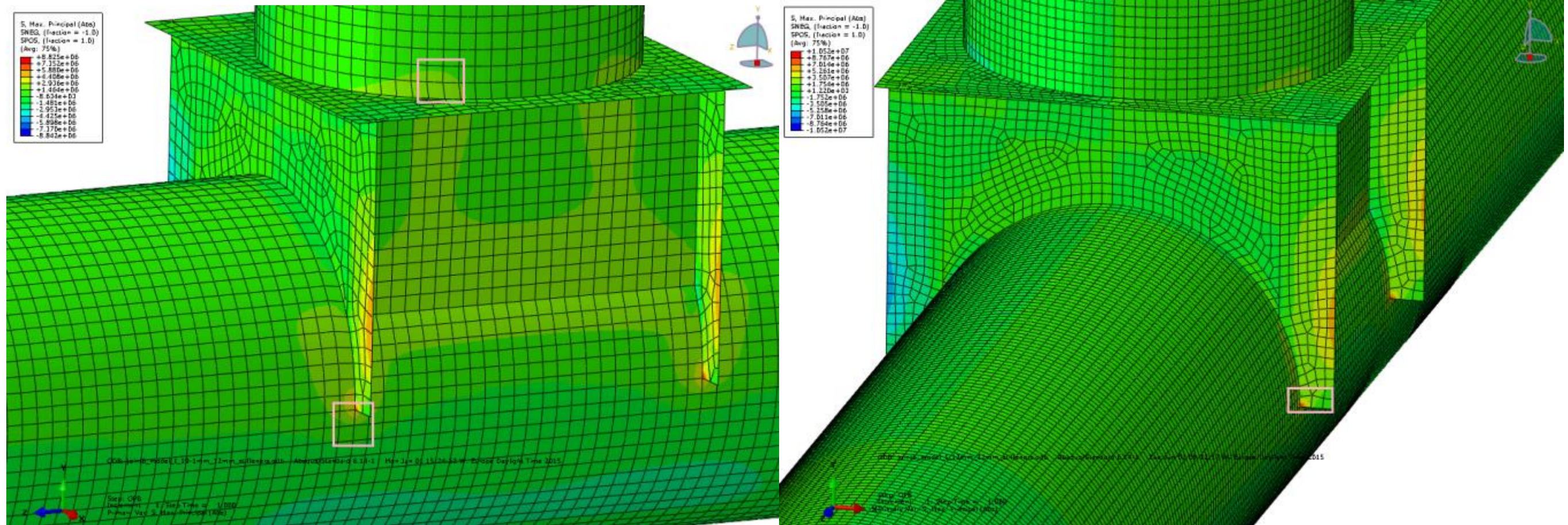
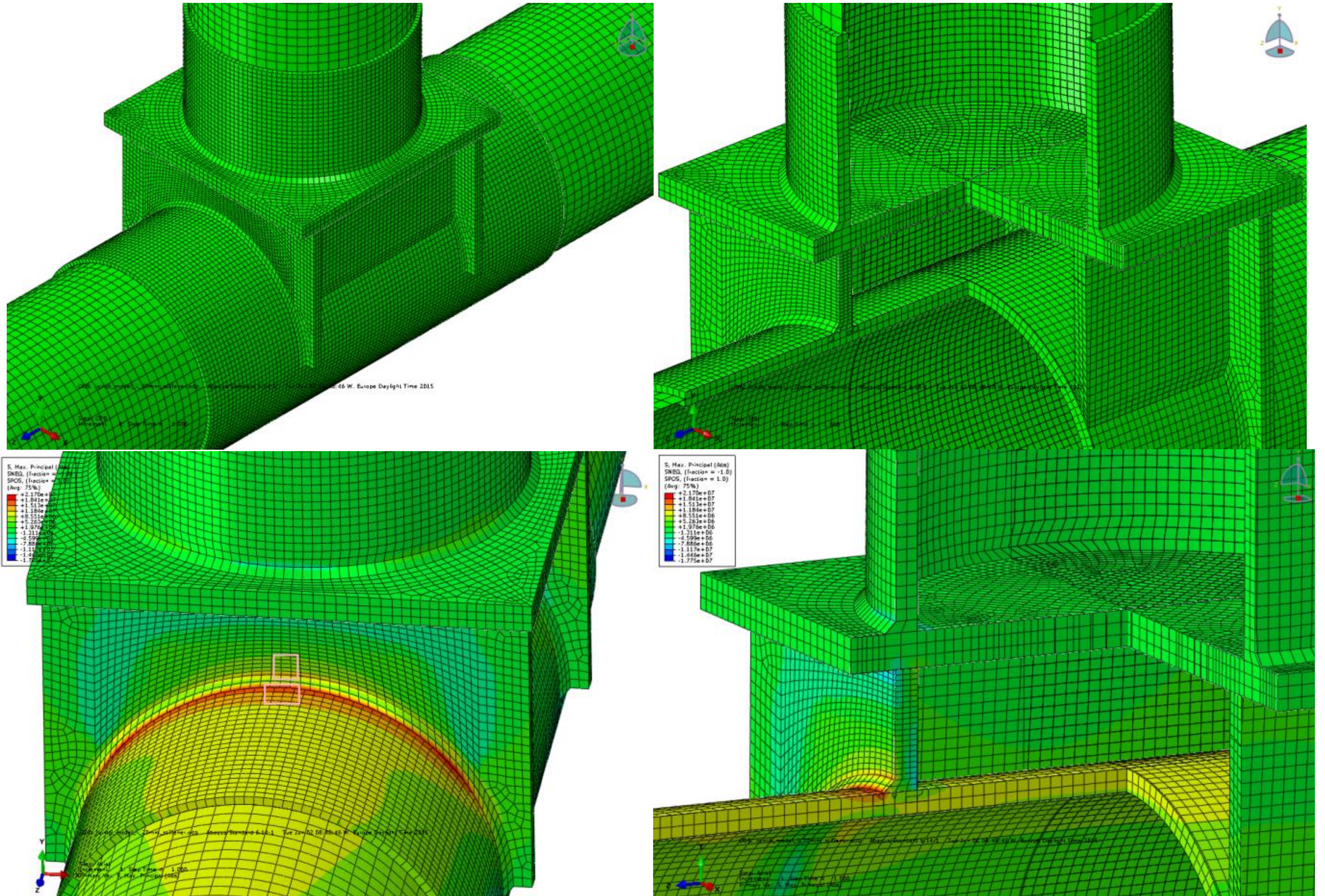


Figure A-4-9: Joint 4 Model III (S8R, t x t, 19.1mm chord/brace, 12mm stiffeners, 30mm top plate)

Upper left: Abs. max principal stress countour and stress read out region for OPB load case, 19.1mm mesh

Upper right: Abs. max principal stress countour and stress read out region for OPB load case, 12mm mesh

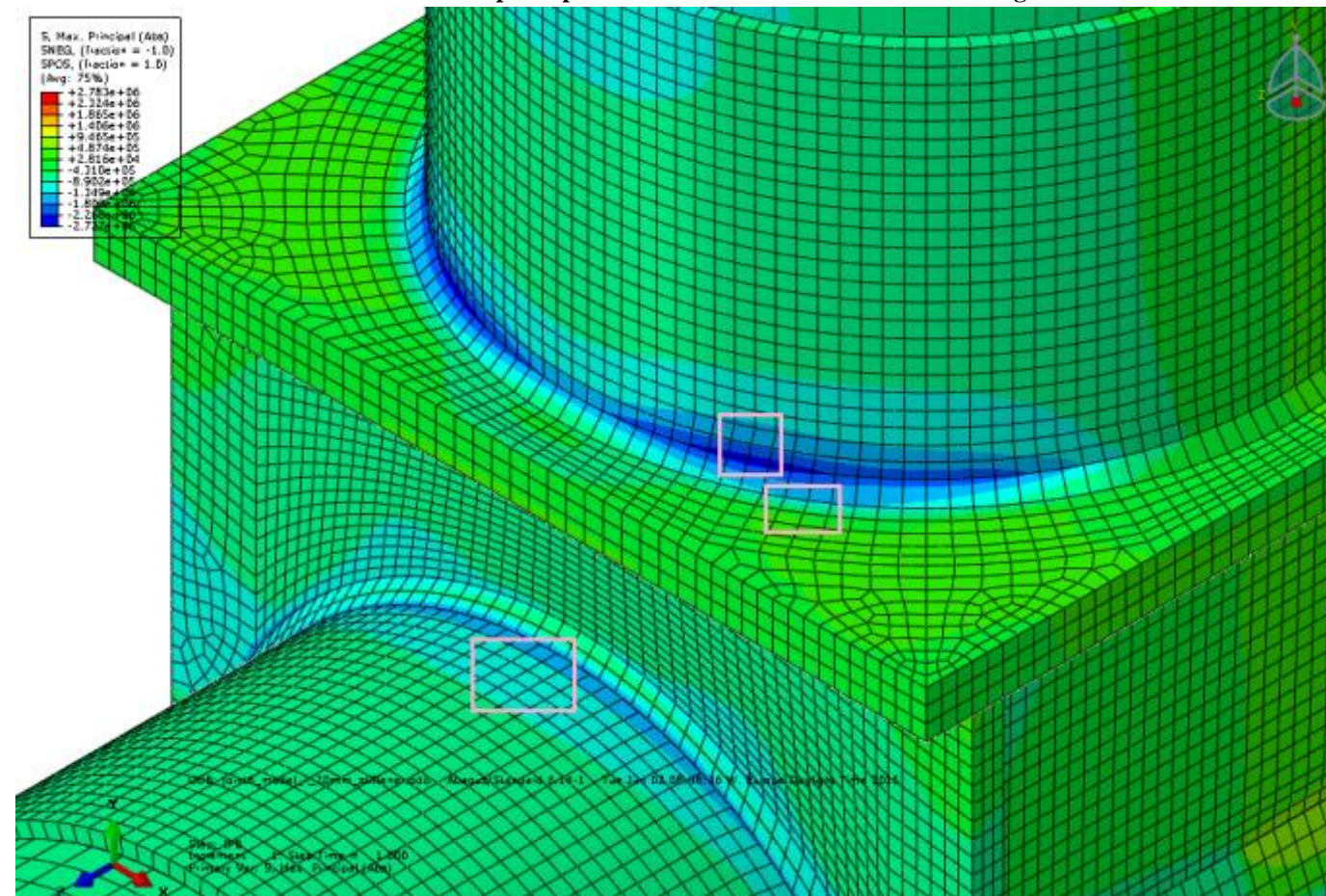


Upper left: Mesh

Figure A-4-10: Joint 2 Model IV (C3D20R, relatively fine mesh)

Upper right: Mesh cross section

Lower left: Abs. max principal stress countour and stress read out region for axial load case



Lower right: Abs. max principal stress countour with cut out for axial load case

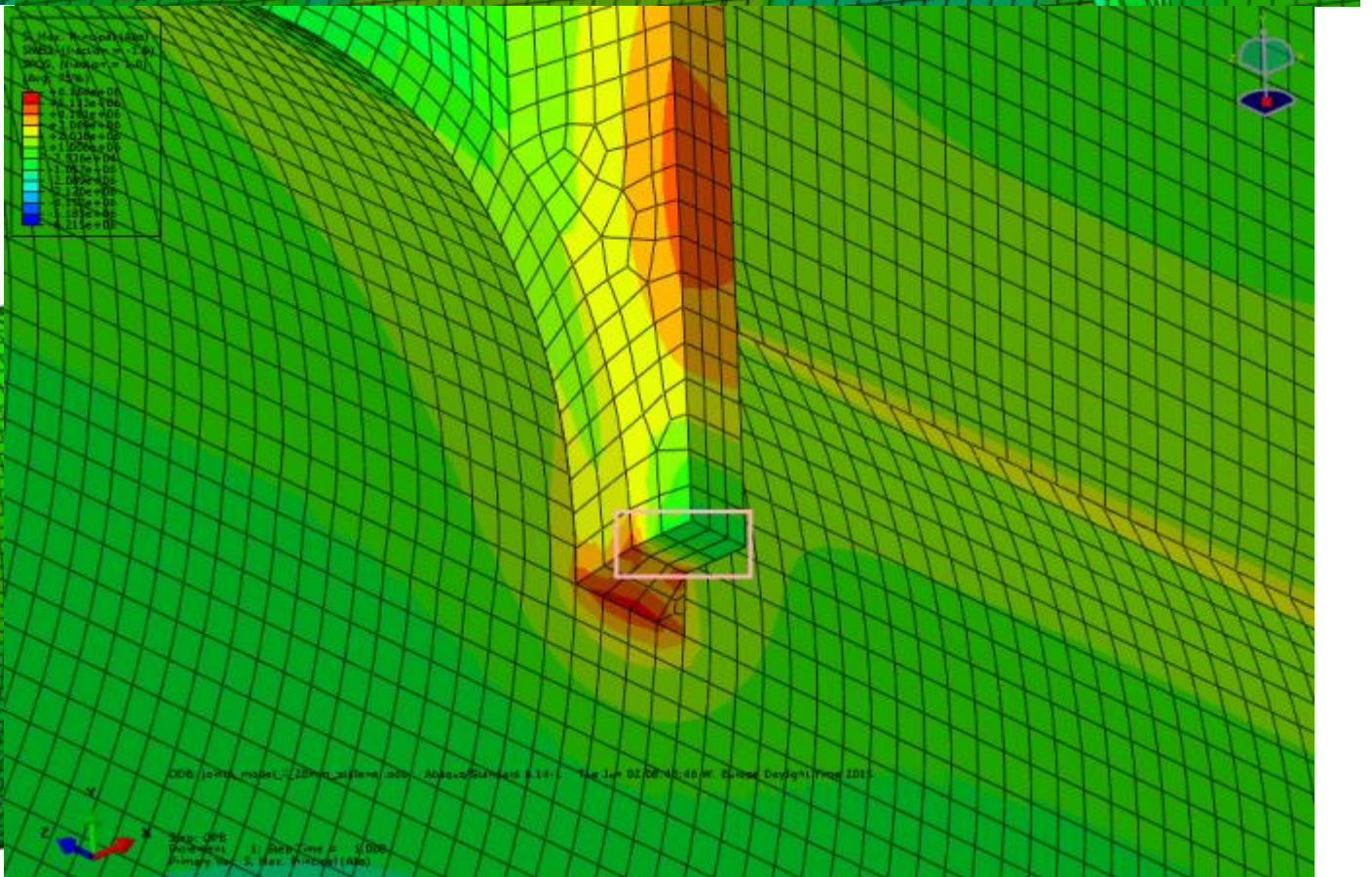
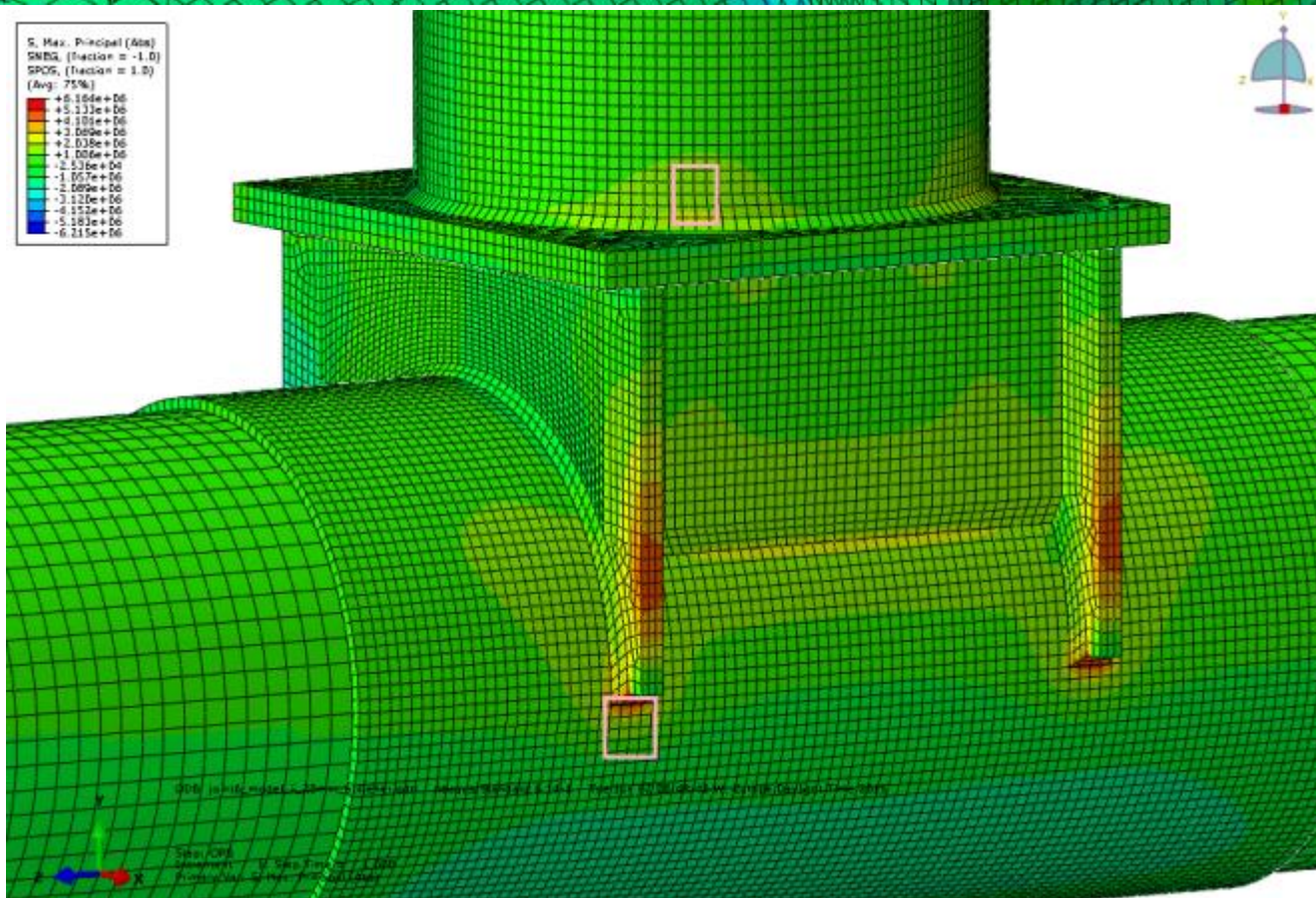
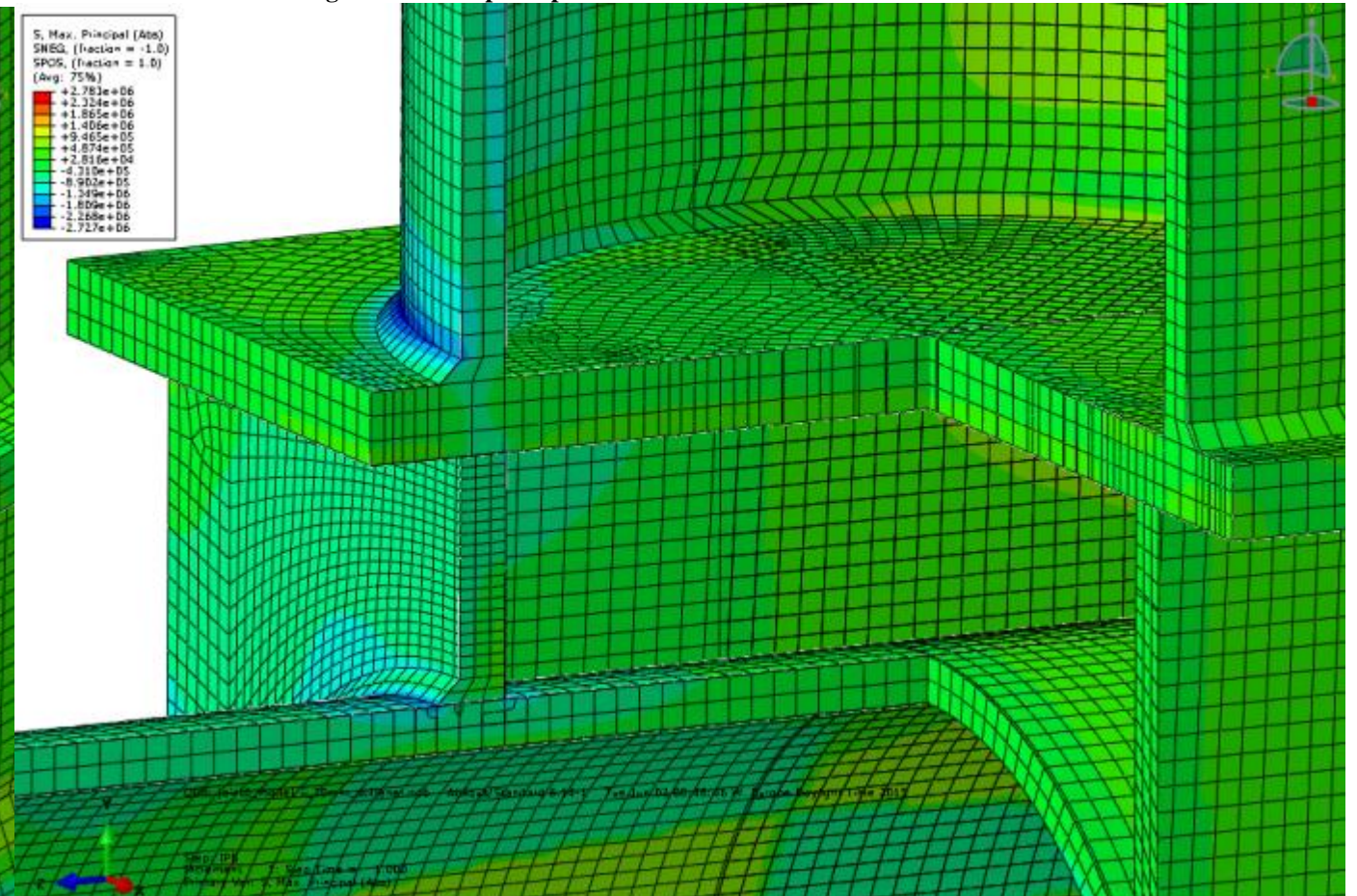


Figure A-4-11: Joint 2 Model IV (C3D20R, relatively fine mesh)

Lower left: Abs. max principal stress countour and stress read out region for IPB load case
Lower left: Abs. max principal stress countour and stress read out region for OPB load case

Lower right: Abs. max principal stress countour with cut out for IPB load case
Lower right: Abs. max principal stress countour and stress read out region for OPB load case

A.5 Joint 5

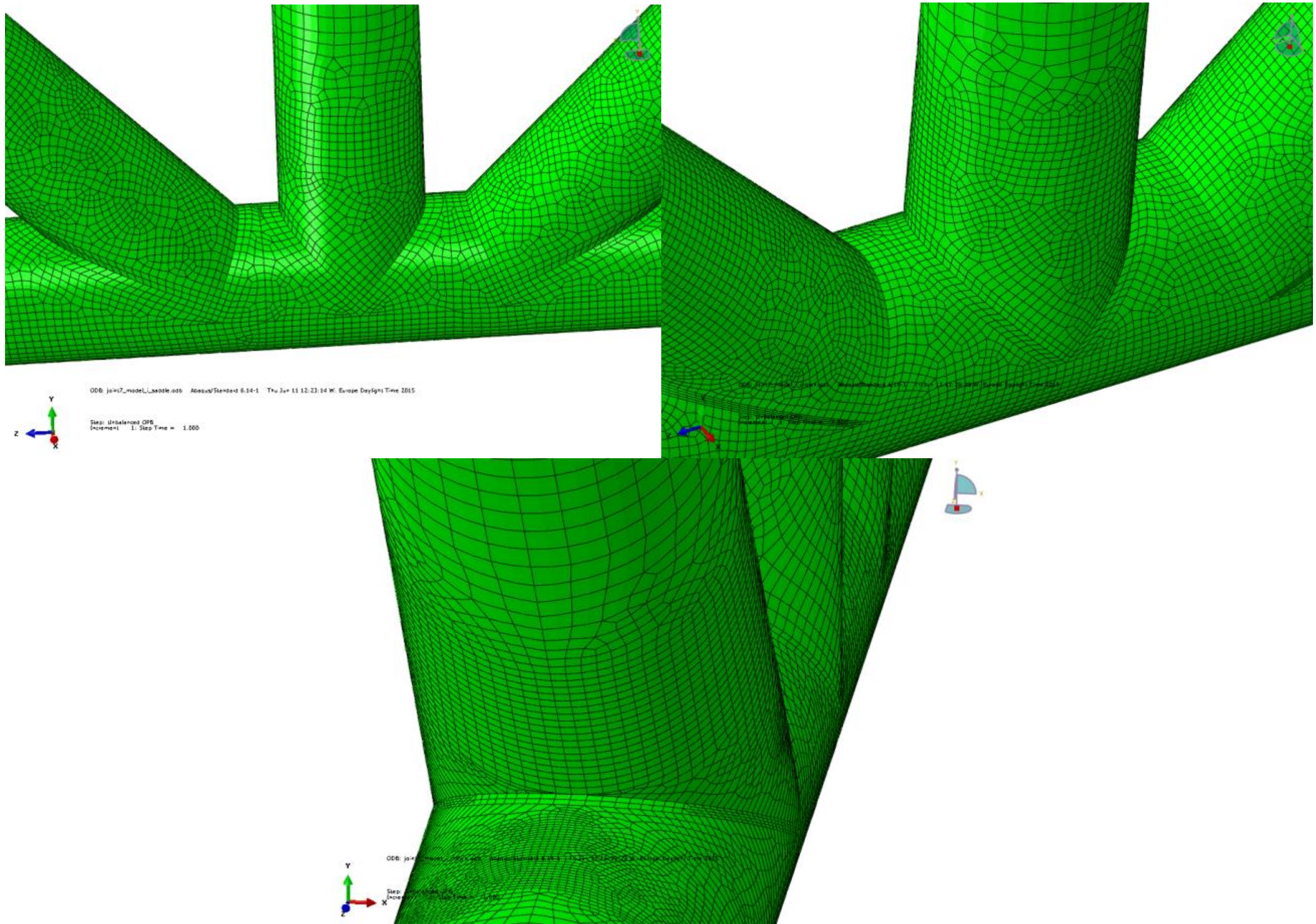


Figure A-5-1: Joint 5 Model I (S8R, t x t, 2 models where mesh is adapted to either saddle or crown position)

Upper left: Mesh adapted to saddle position

Lower: Mesh adapted to crown position, behind diagonal brace

Upper right: Mesh adapted to crown position

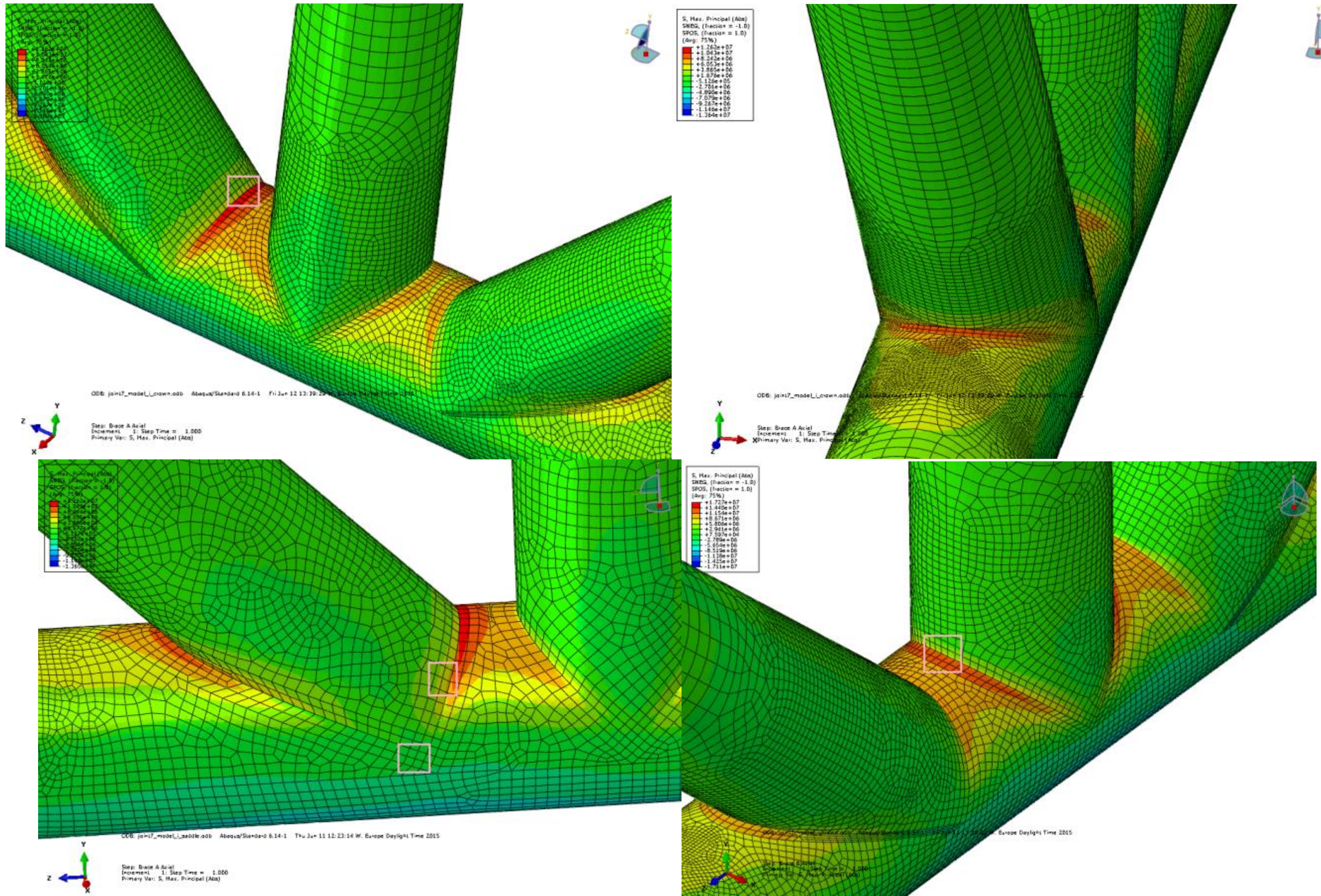


Figure A-5-2: Joint 5 Model I (S8R, t x t, 2 models where mesh is adapted to either saddle or crown position)

Upper left: Abs. max principal stress contour and stress read out region for diagonal brace axial load case, crown
 Lower left: Abs. max principal stress contour and stress read out region for diagonal brace axial load case, saddle

Upper right: Abs. max principal stress contour for diagonal brace axial load case, crown
 Lower right: Abs. max principal stress contour and stress read out region for central brace axial load case, crown

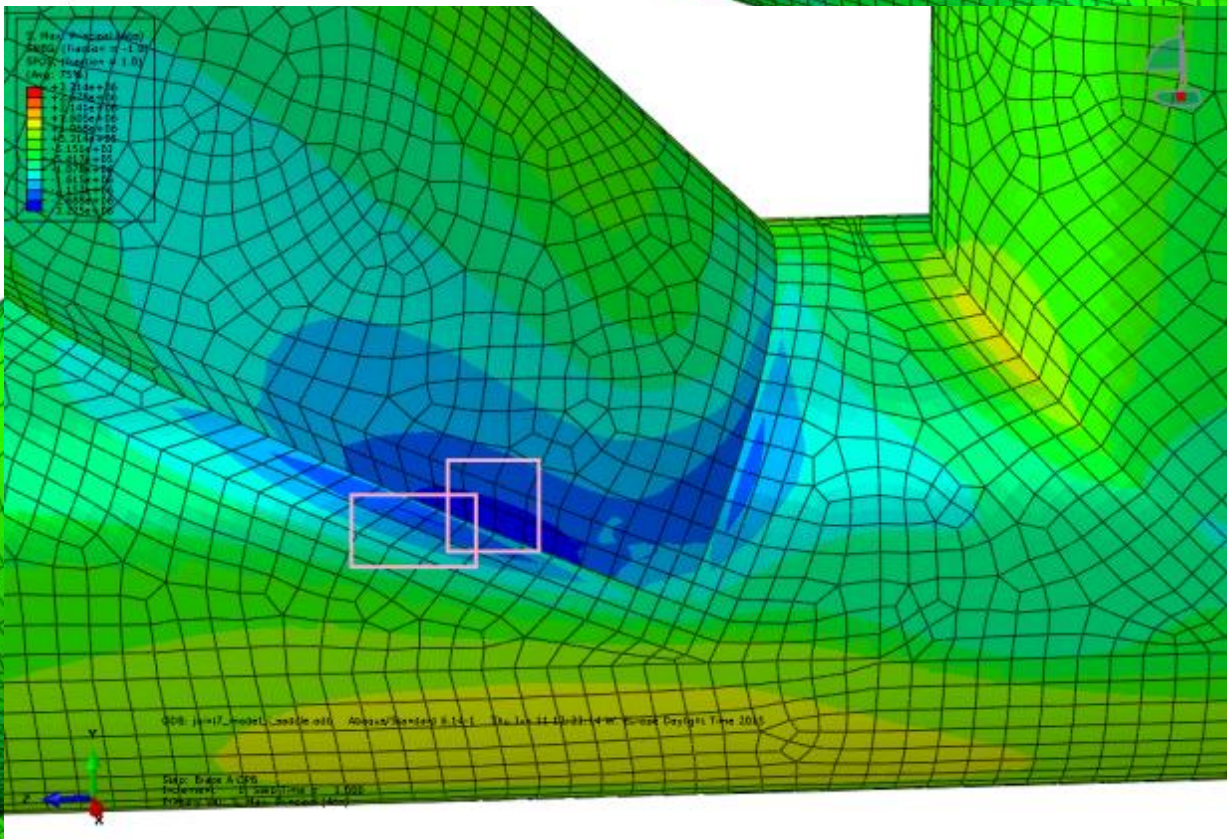
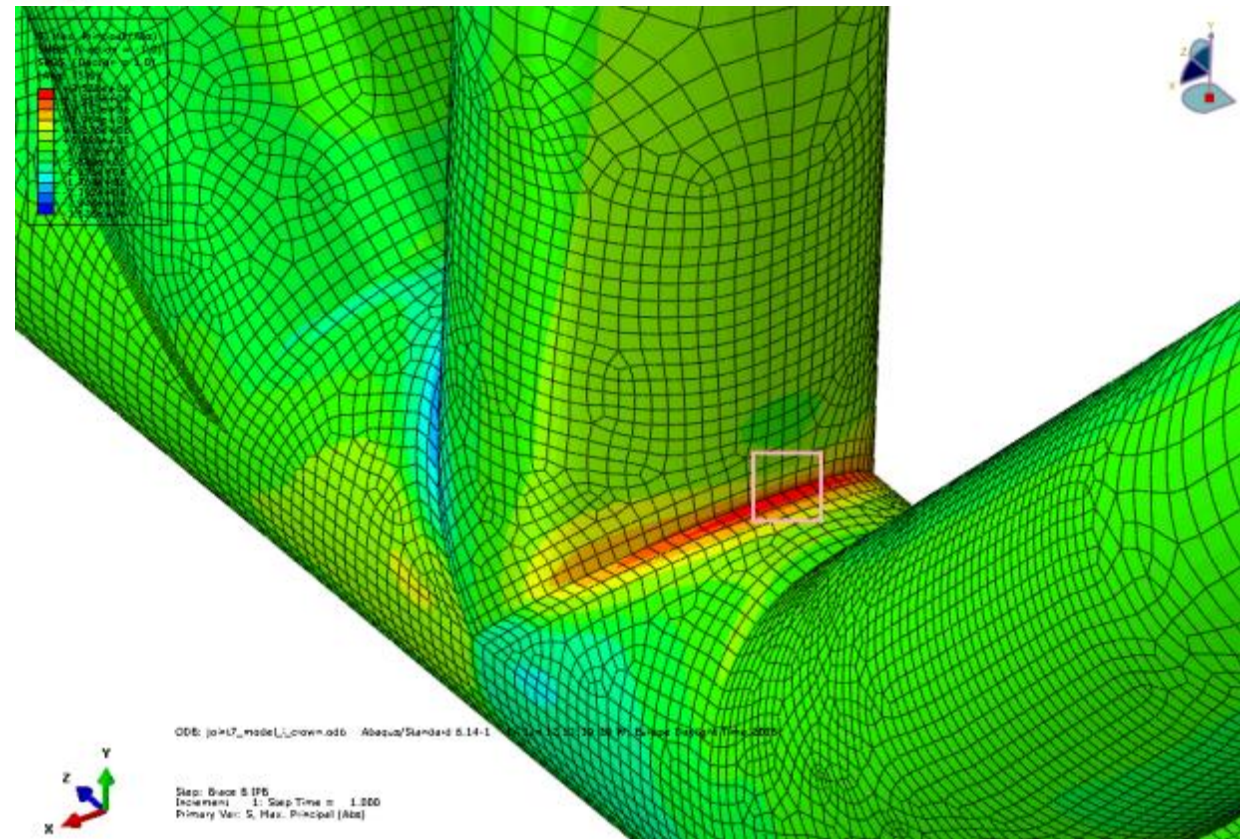
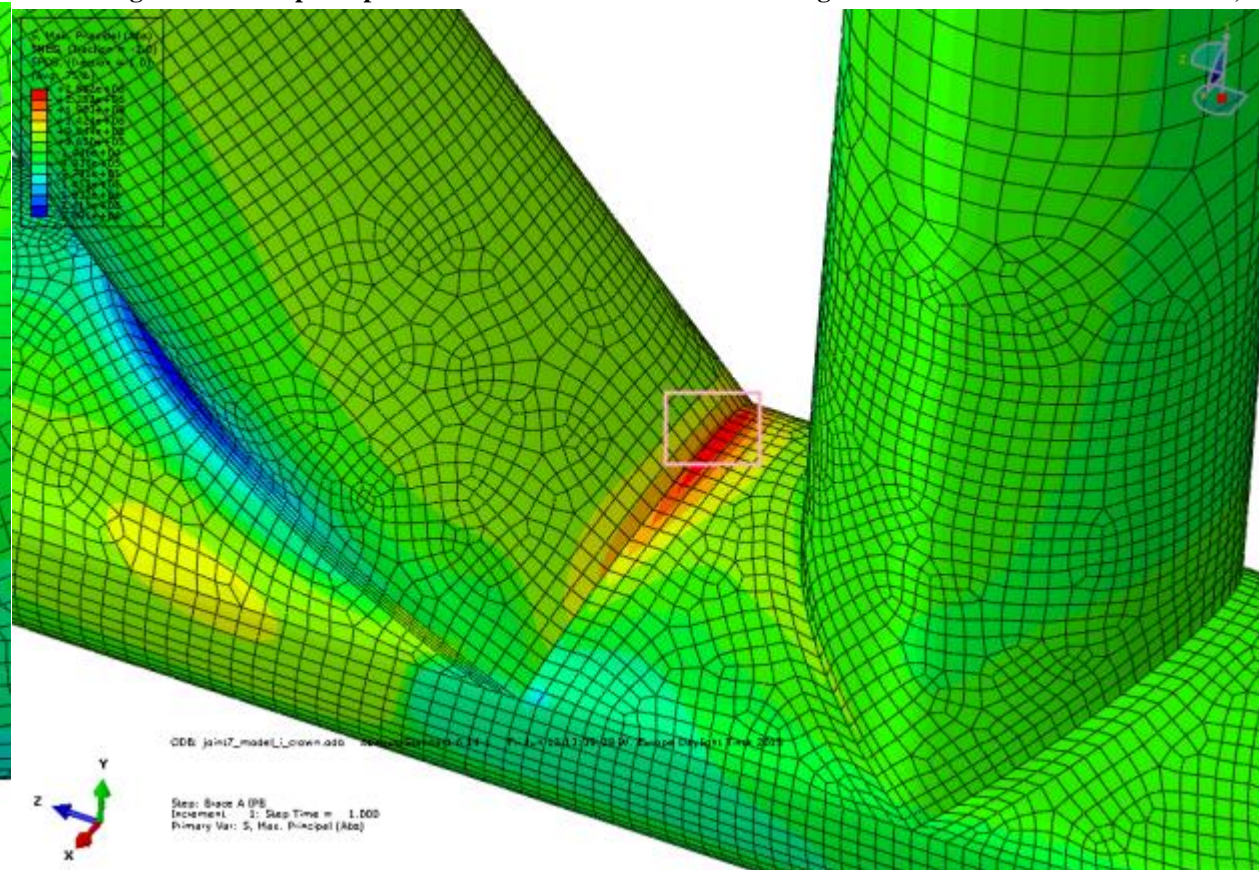
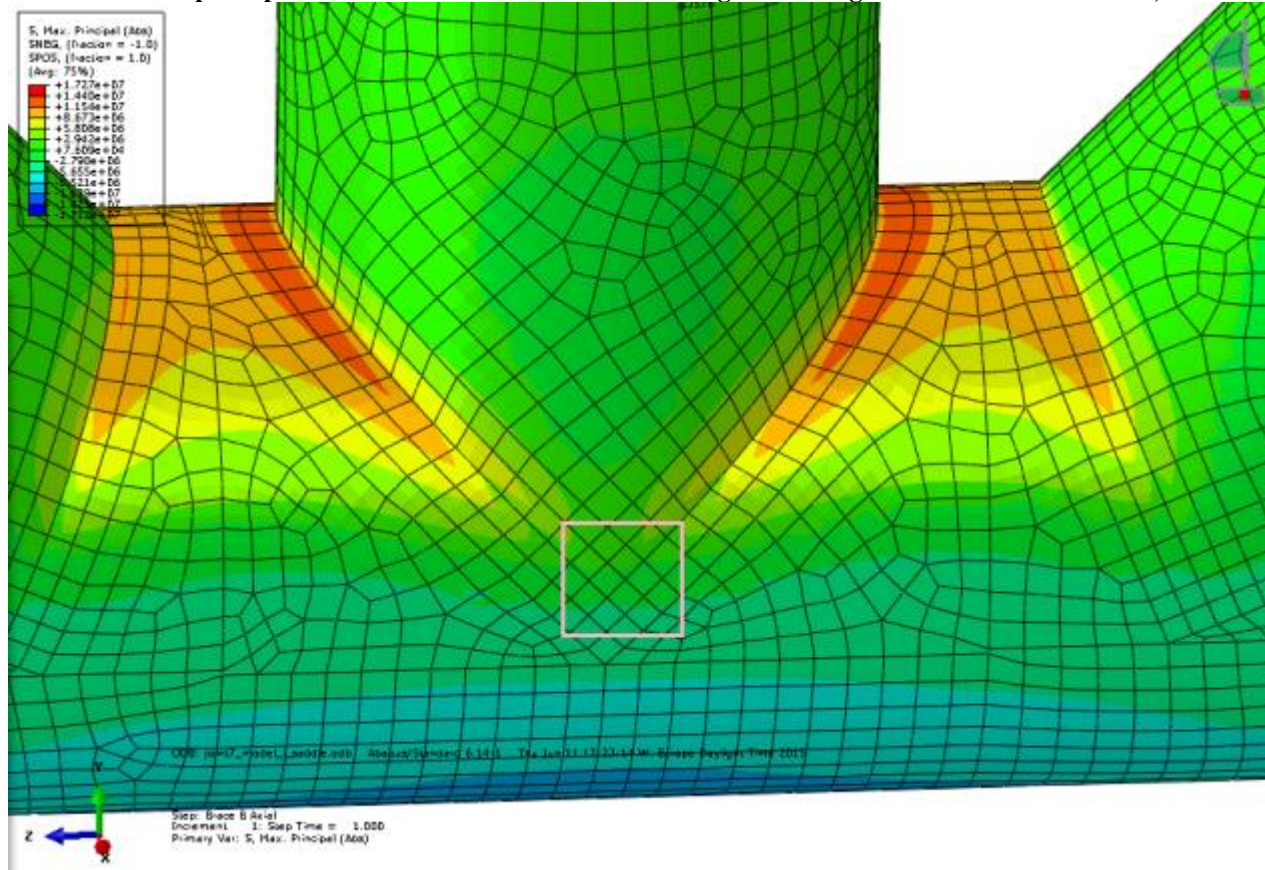
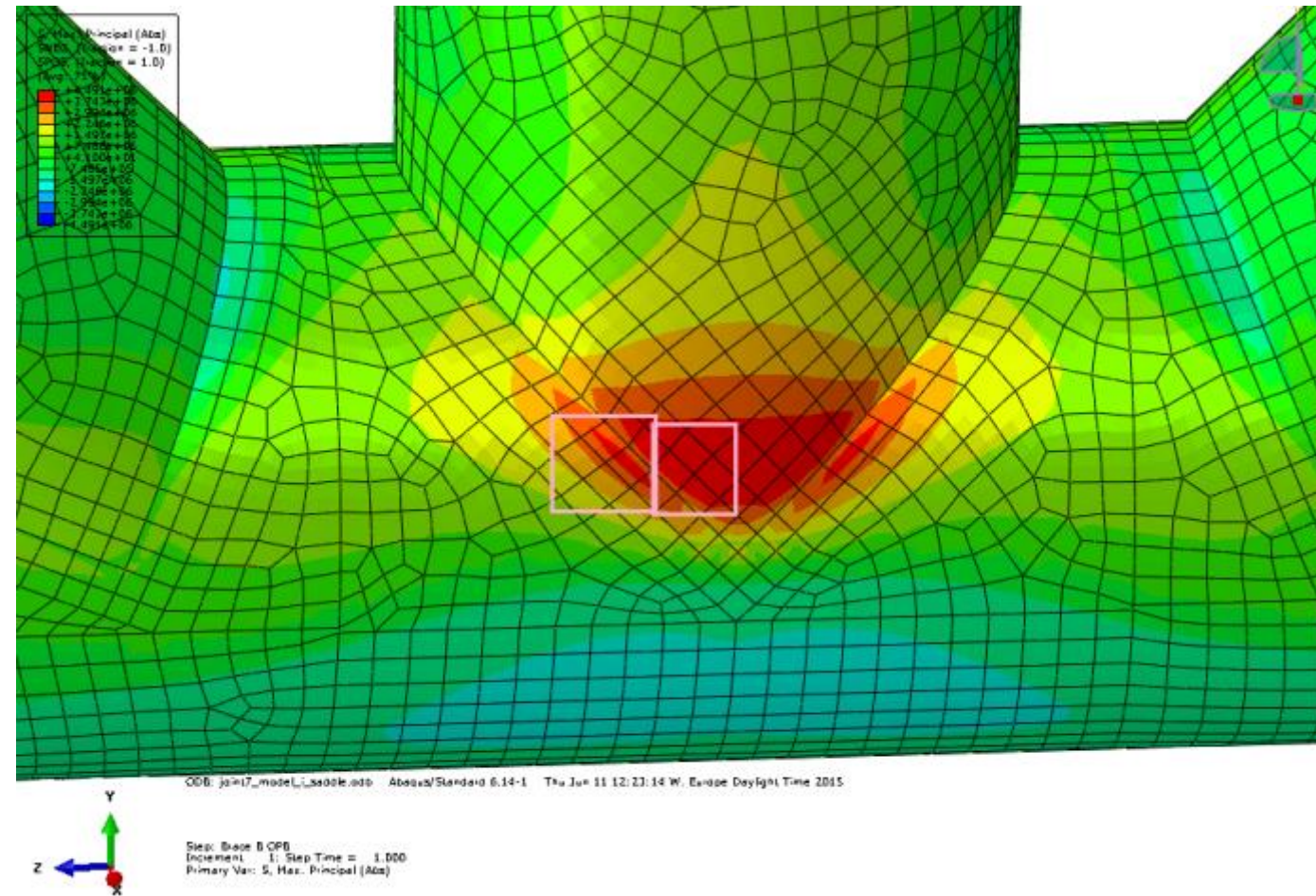


Figure A-5-2: Joint 5 Model I (S8R, t x t, 2 models where mesh is adapted to either saddle or crown position)

Upper left: Abs. max principal stress contour and stress read out region for central brace axial load case, saddle
 Lower left: Abs. max principal stress contour and stress read out region for central brace IPB load case, crown

Upper right: Abs. max principal stress contour and stress read out region for diagonal brace IPB load case, crown
 Lower right: Abs. max principal stress contour and stress read out region for diagonal brace OPB load case, saddle



**Figure A-5-2: Joint 5 Model I (S8R, t x t, 2 models where mesh is adapted to either saddle or crown position)
Abs. max principal stress contour and stress read out region for central brace OPB load case, saddle**

A.6 Joint 6

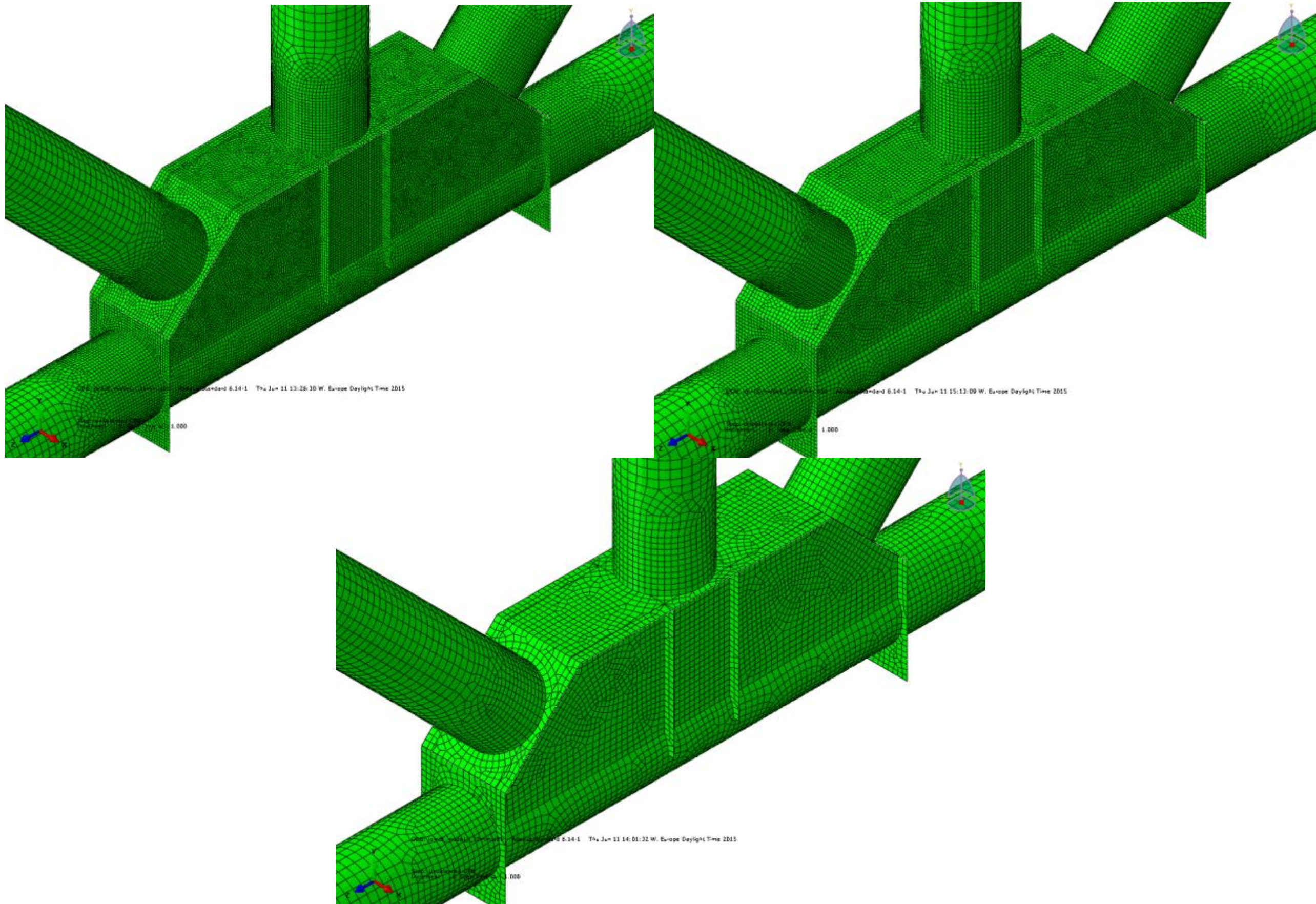


Figure A-6-1: Joint 6 Model I (S8R, t x t, 19.1mm chord/brace, 16mm stiffeners, 30mm top plate)
Upper left: Mesh 16mm density
Upper right: Mesh 19.1mm density
Lower: Mesh 30mm density

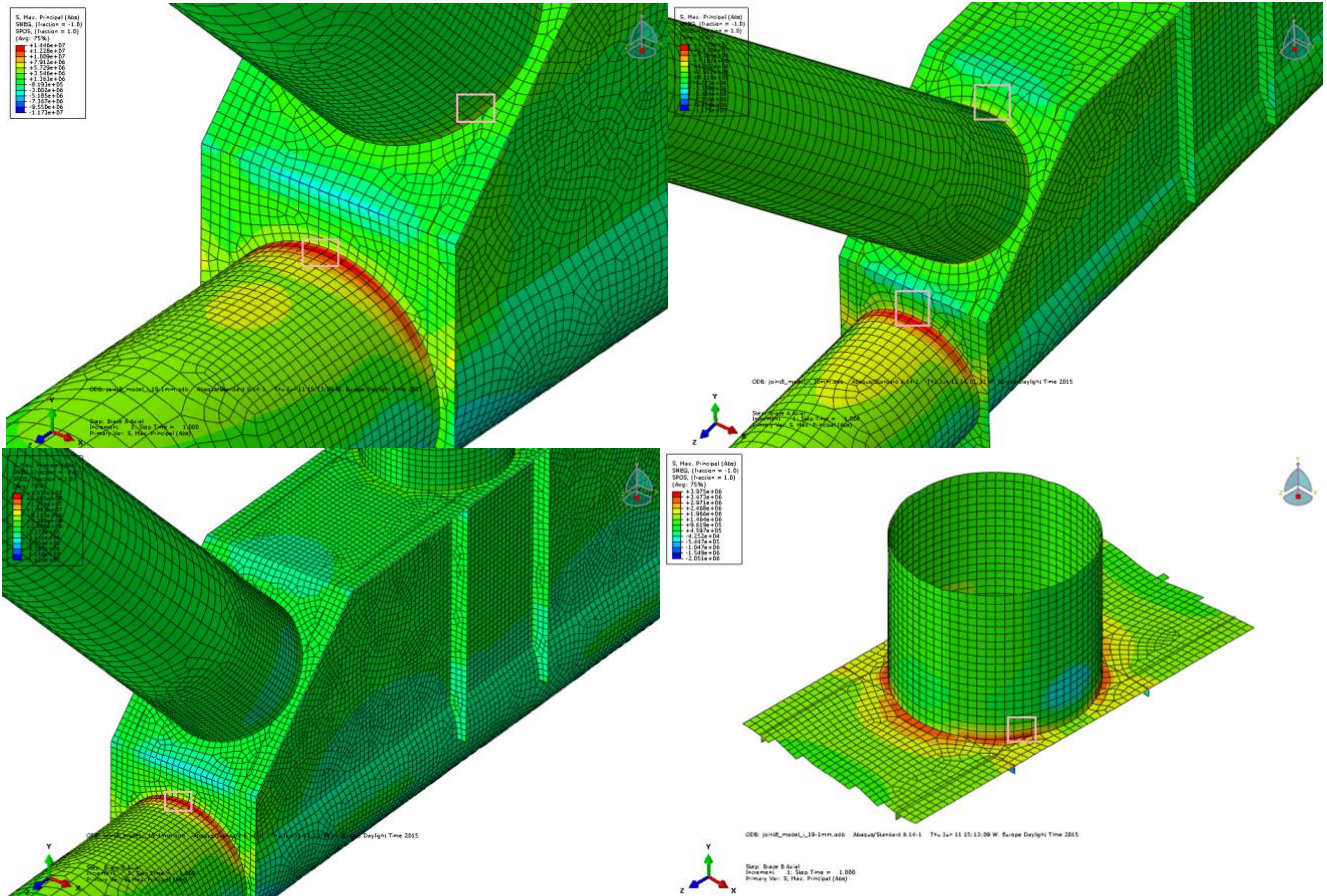


Figure A-6-2: Joint 6 Model I (S8R, 3 models where mesh is adapted to t x t, 19.1mm chord/brace, 16mm stiffeners, 30mm top plate)

Upper left: Abs. max principal stress contour and stress read out region for diagonal brace axial load case, 19.1mm
 Lower left: Abs. max principal stress contour and stress read out region for central brace axial load case, 19.1mm

Upper right: Abs. max principal stress contour and stress read out region for diagonal brace axial load case, 30mm
 Lower right: Abs. max principal stress contour and stress read out region for central brace axial load case, 19.1mm

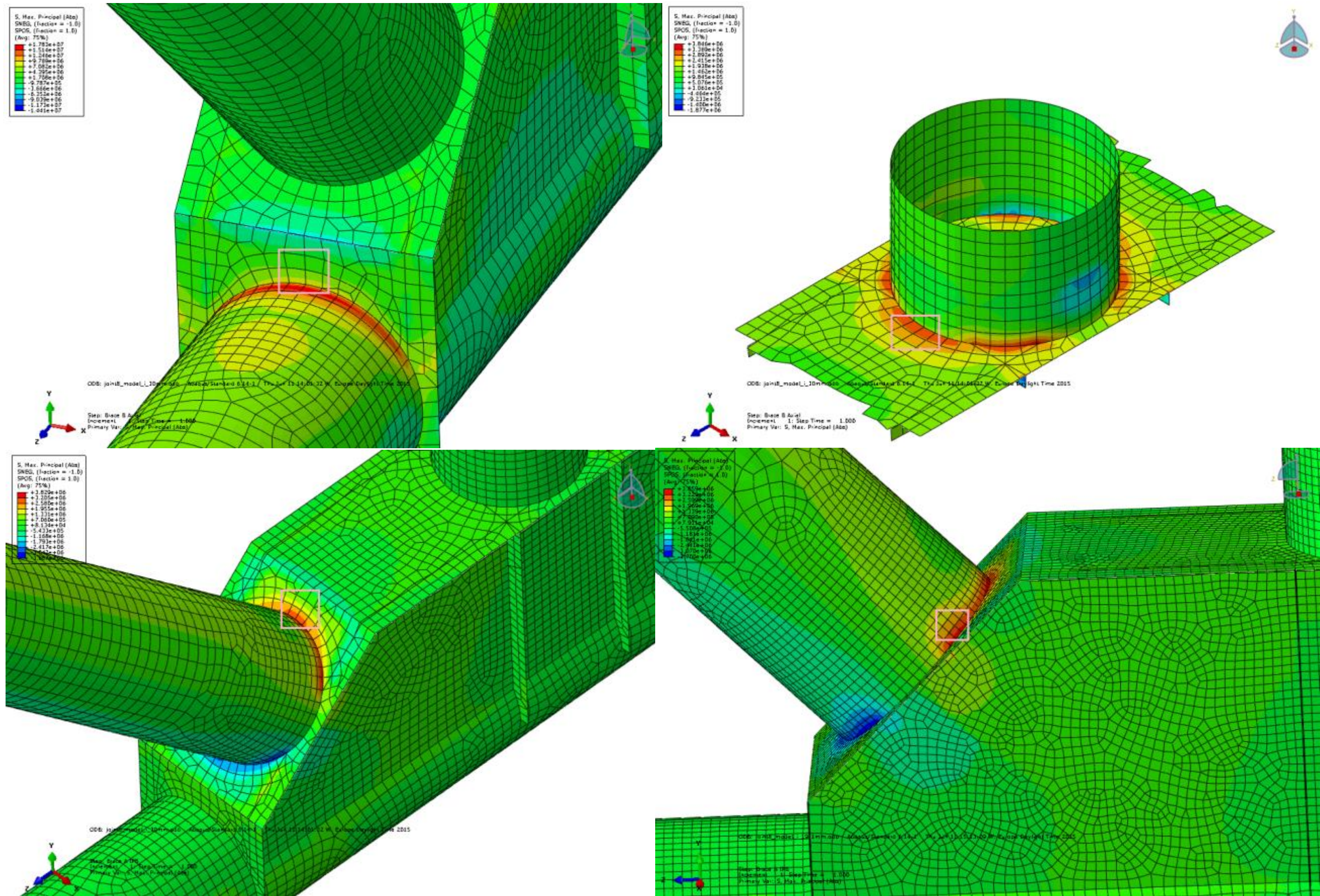


Figure A-6-3: Joint 6 Model I (S8R, 3 models where mesh is adapted to t x t, 19.1mm chord/brace, 16mm stiffeners, 30mm top plate)

Upper left: Abs. max principal stress contour and stress read out region for central brace axial load case, 30mm
 Lower left: Abs. max principal stress contour and stress read out region for diagonal brace IPB load case, 30mm

Upper right: Abs. max principal stress contour and stress read out region for central brace axial load case, 19.1mm
 Lower right: Abs. max principal stress contour and stress read out region for diagonal brace IPB load case, 19.1mm

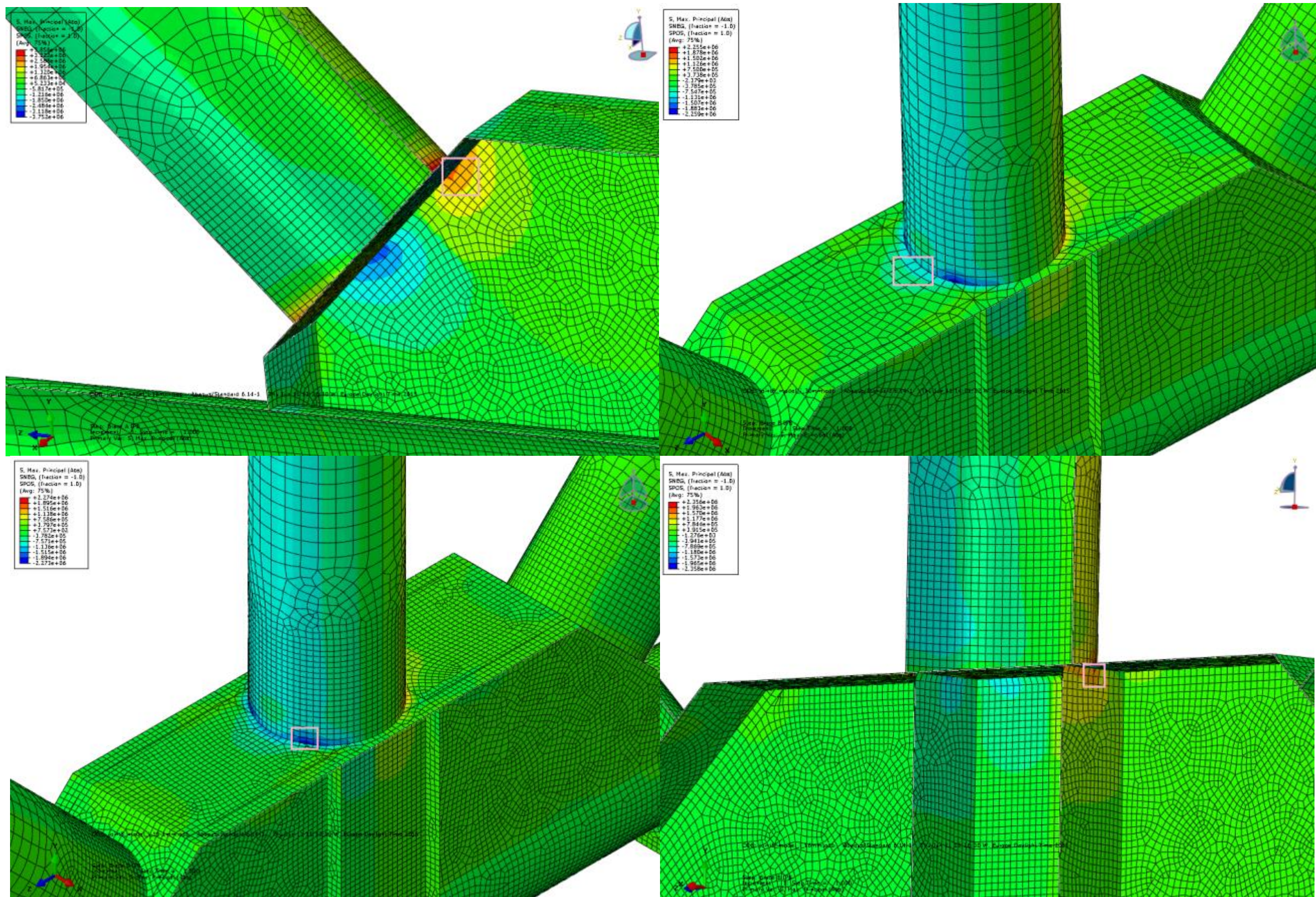


Figure A-6-4: Joint 6 Model I (S8R, 3 models where mesh is adapted to t x t, 19.1mm chord/brace, 16mm stiffeners, 30mm top plate)

Upper left: Abs. max principal stress contour and stress read out region for diagonal brace IPB load case, 16mm
 Lower left: Abs. max principal stress contour and stress read out region for central brace IPB load case, 19.1mm

Upper right: Abs. max principal stress contour and stress read out region for central brace IPB load case, 30mm
 Lower right: Abs. max principal stress contour and stress read out region for central brace IPB load case, 16mm

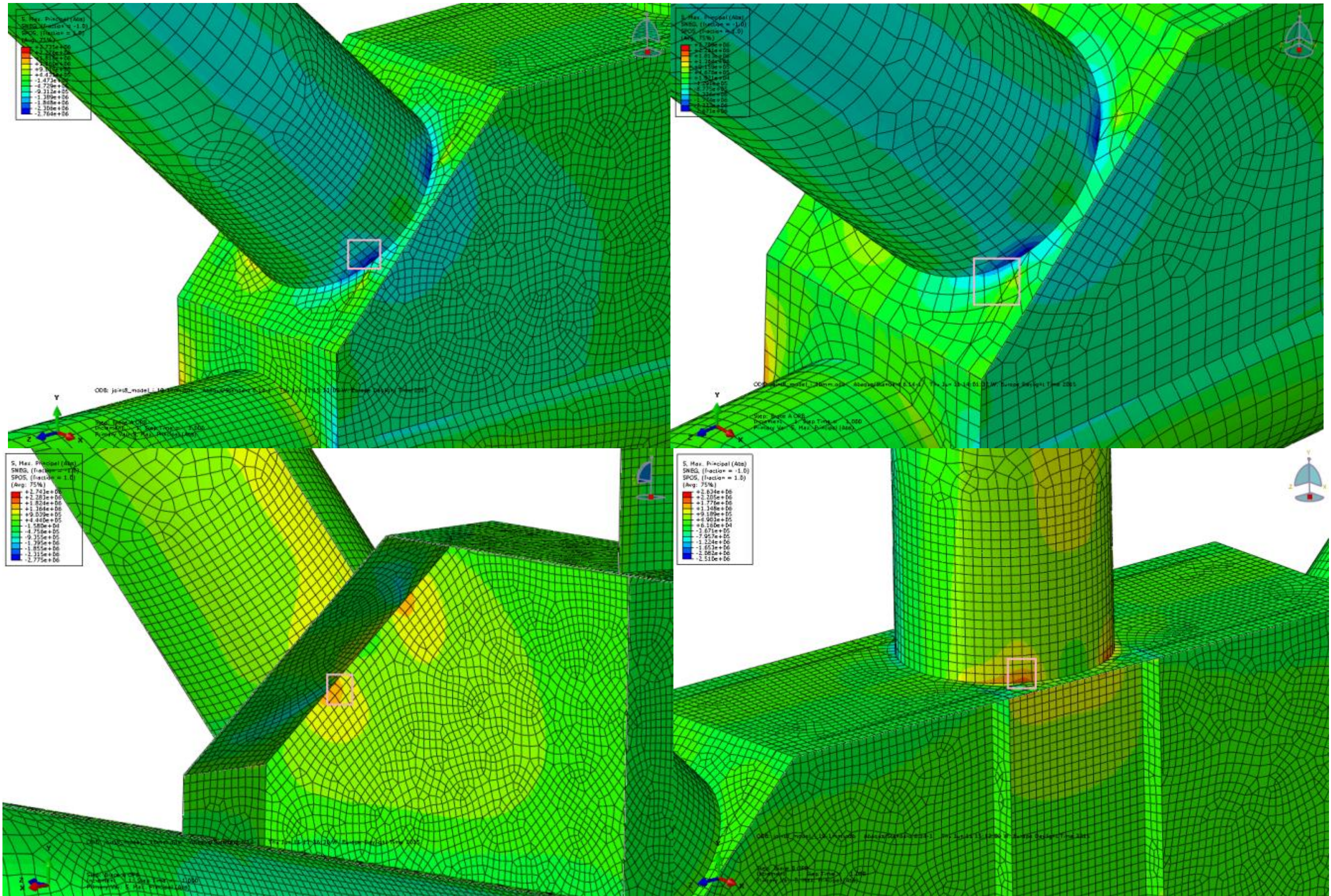


Figure A-6-5: Joint 6 Model I (S8R, 3 models where mesh is adapted to t x t, 19.1mm chord/brace, 16mm stiffeners, 30mm top plate)

Upper left: Abs. max principal stress contour and stress read out region for diagonal brace OPB load case, 19mm
 Lower left: Abs. max principal stress contour and stress read out region for central brace IPB load case, 19.1mm

Upper right: Abs. max principal stress contour and stress read out region for diagonal brace OPB load case, 30mm
 Lower right: Abs. max principal stress contour and stress read out region for central brace OPB load case, 19mm

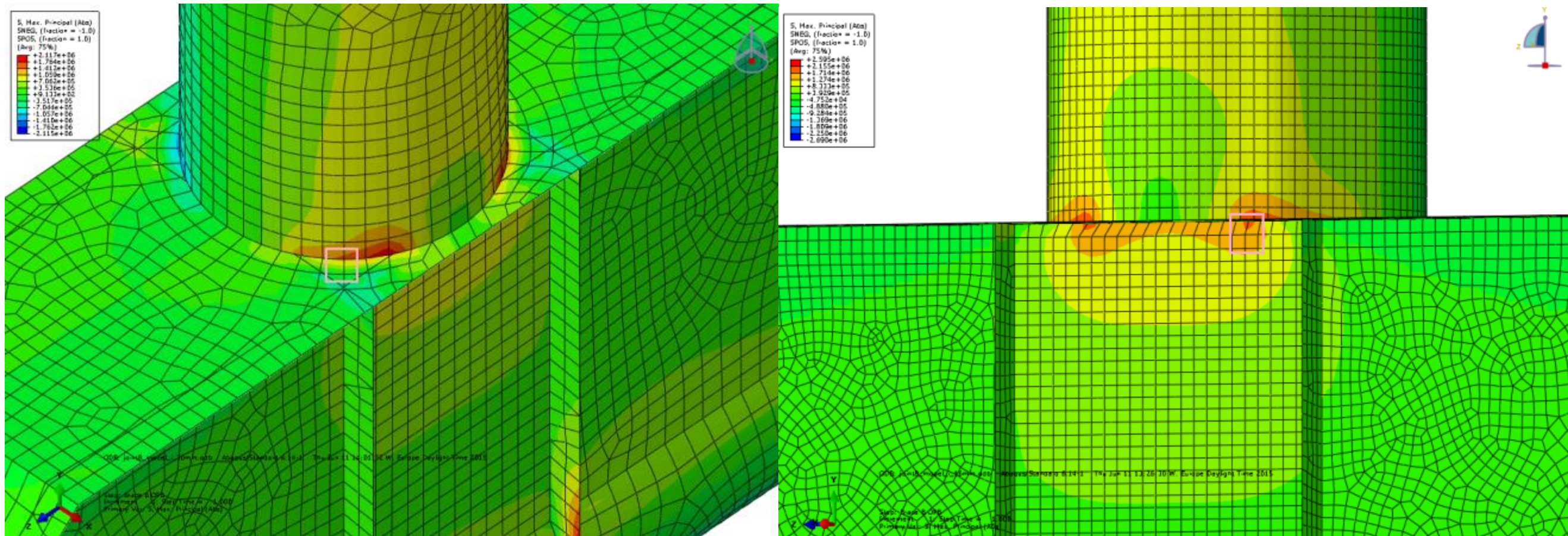


Figure A-6-6: Joint 6 Model I (S8R, 3 models where mesh is adapted to t x t, 19.1mm chord/brace, 16mm stiffeners, 30mm top plate)

Left: Abs. max principal stress contour and stress read out region for central brace OPB load case, 30mm

Right: Abs. max principal stress contour and stress read out region for central brace OPB load case, 16mm

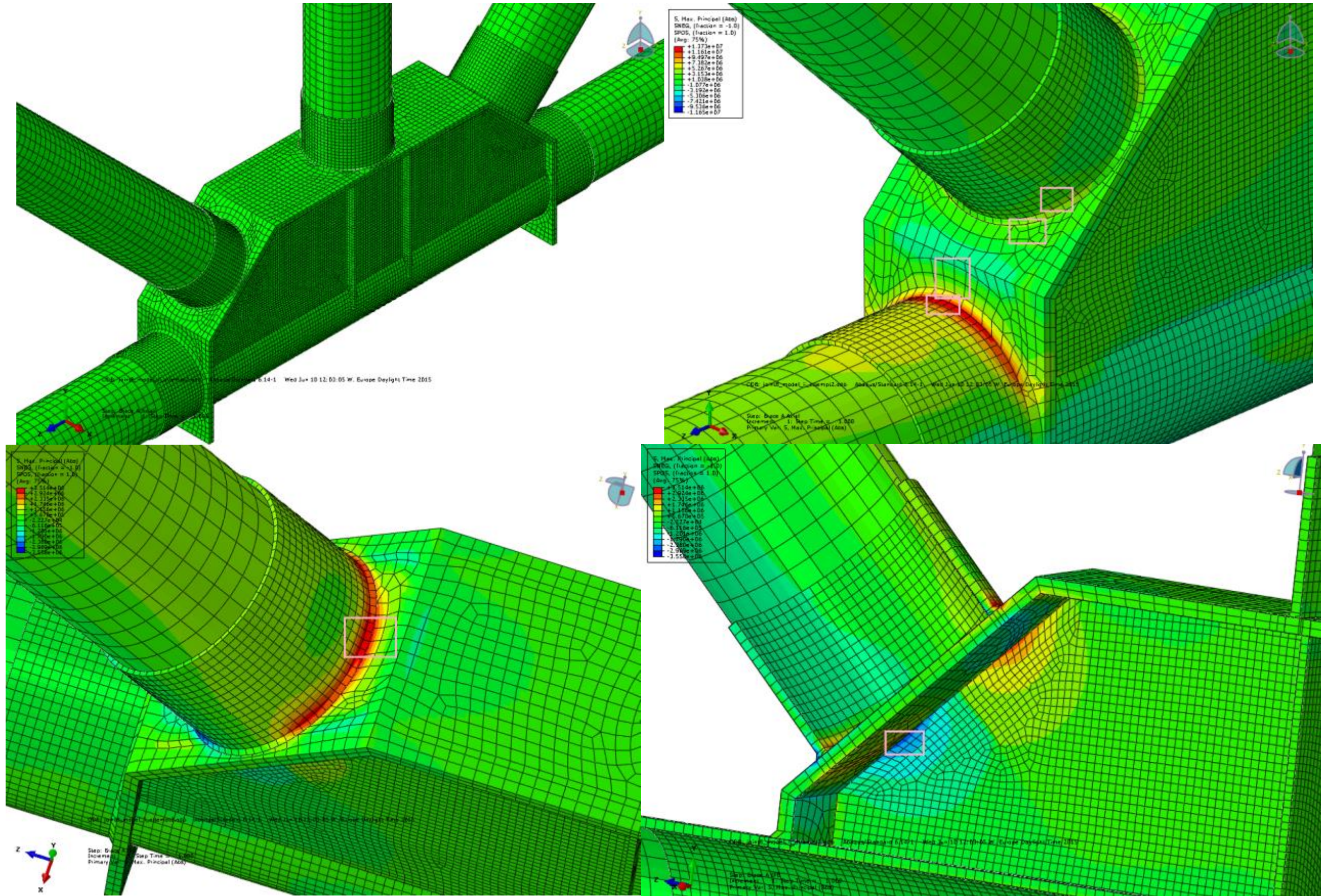


Figure A-6-7: Joint 6 Model II (C3D20R, mesh is adapted to t x t, 19.1mm chord/brace, 16mm stiffeners, 30mm top plate)

Upper left: Mesh

Lower left: Abs. max principal stress contour and stress read out region for diagonal brace IPB load case

Upper right: Abs. max principal stress contour and stress read out region for diagonal brace axial load case

Lower right: Abs. max principal stress contour and stress read out region for diagonal brace IPB load case

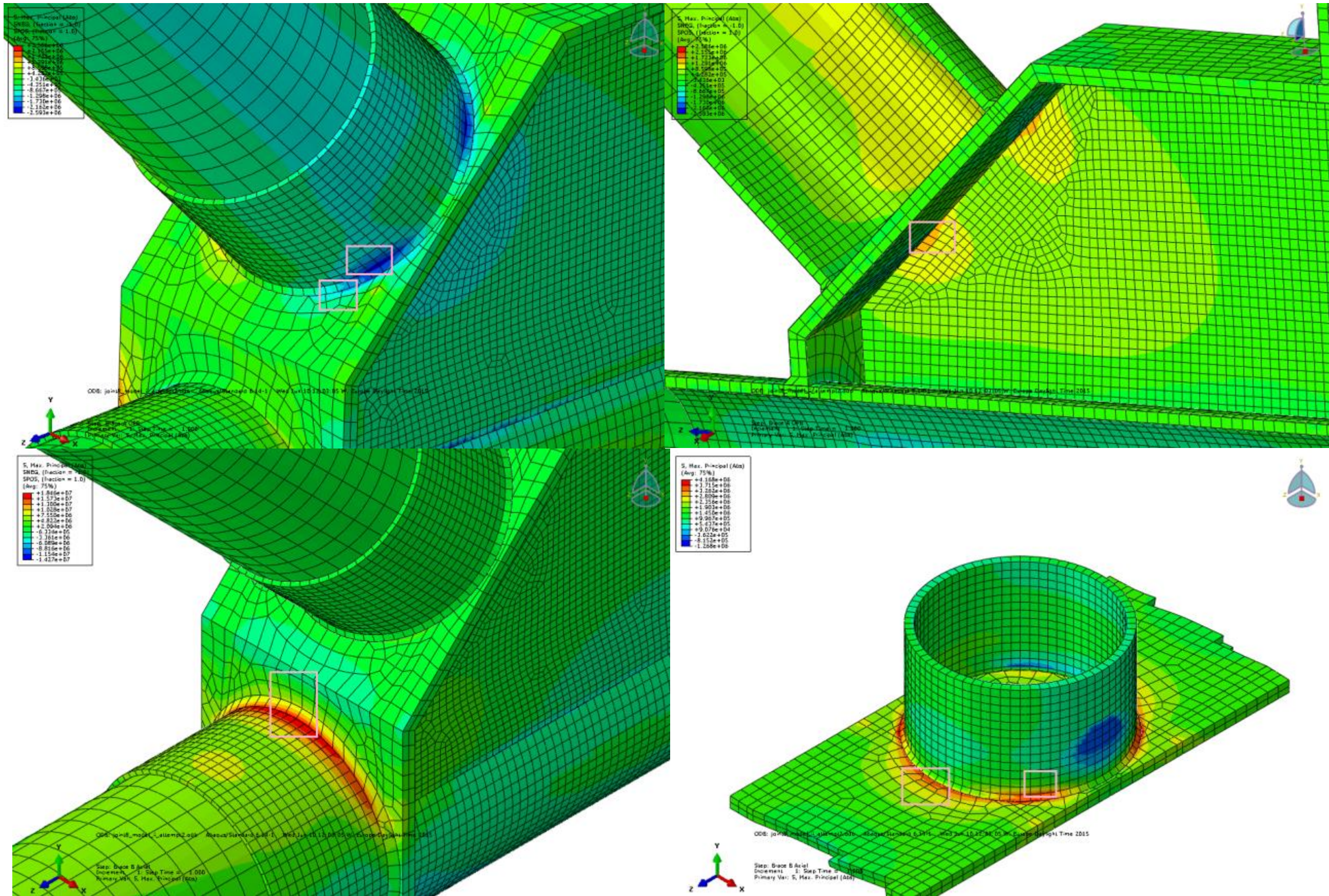


Figure A-6-8: Joint 6 Model II (C3D20R, mesh is adapted to t x t, 19.1mm chord/brace, 16mm stiffeners, 30mm top plate)

Upper left: Abs. max principal stress contour and stress read out region for diagonal brace OPB load case
 Lower left: Abs. max principal stress contour and stress read out region for central brace axial load case

Upper right: Abs. max principal stress contour and stress read out region for diagonal brace OPB load case
 Lower right: Abs. max principal stress contour and stress read out region for central brace axial load case

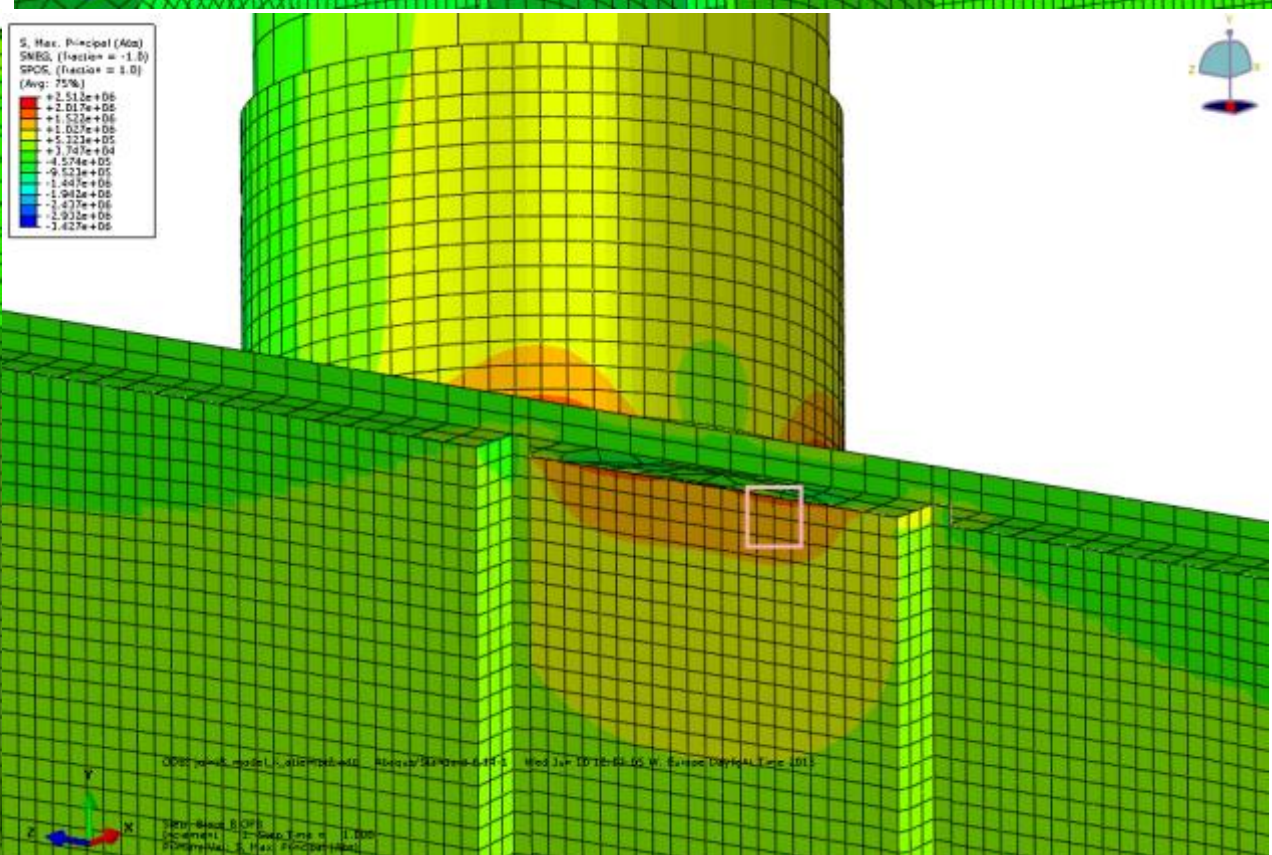
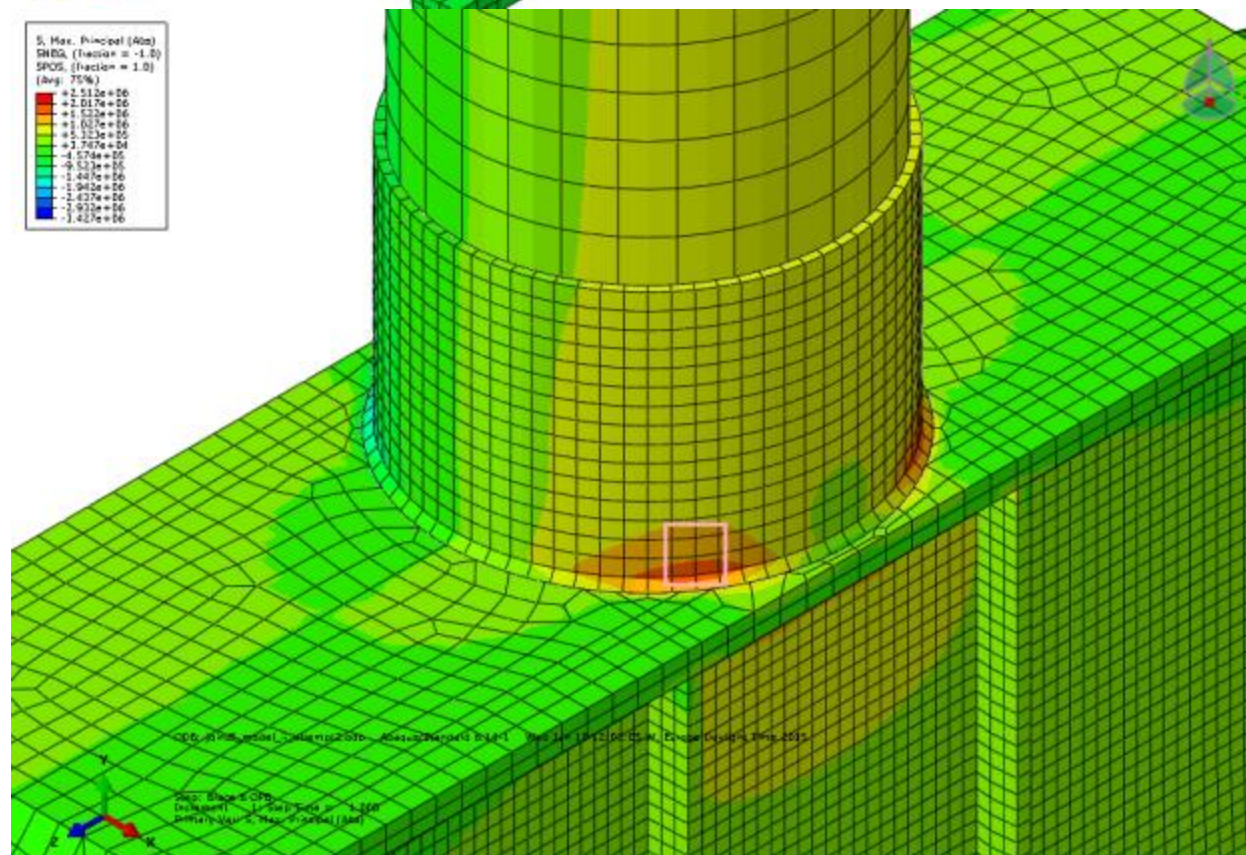
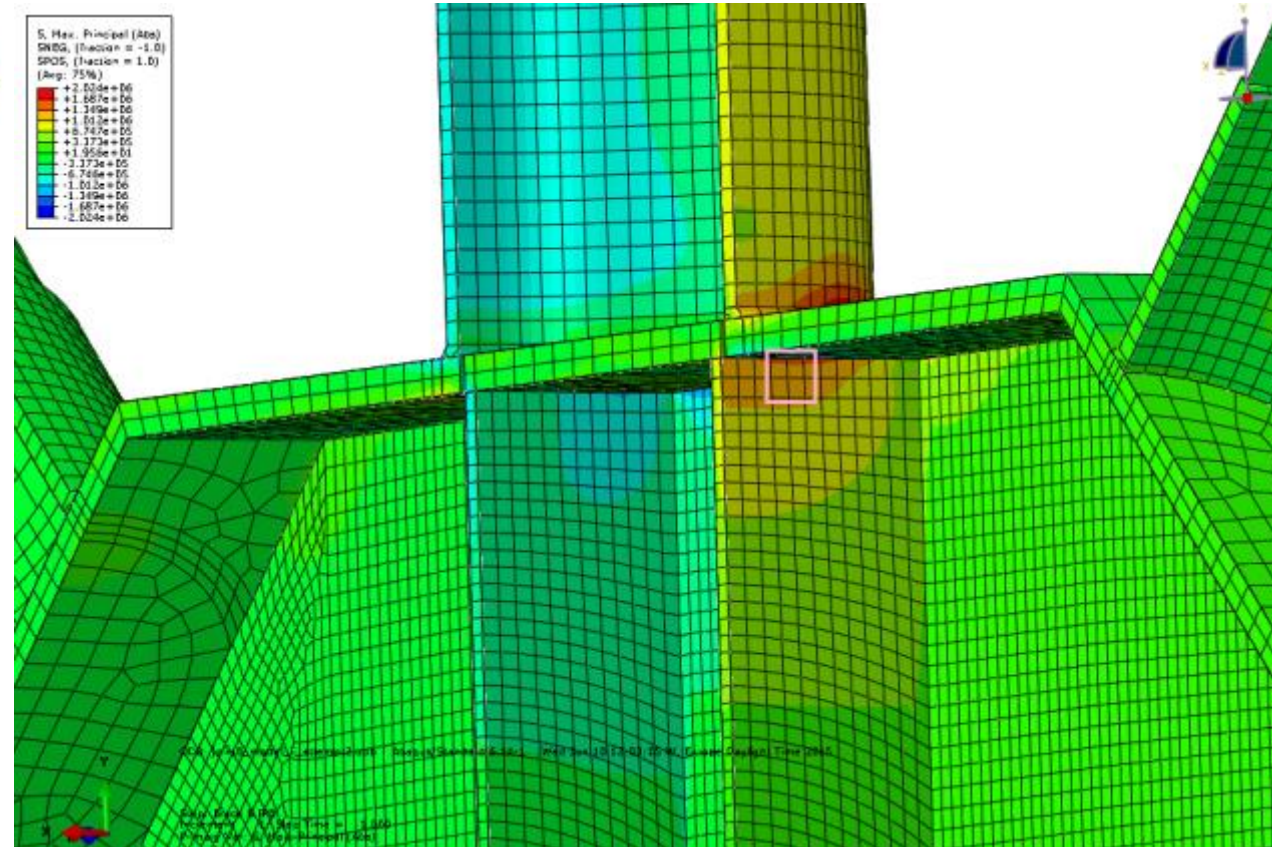
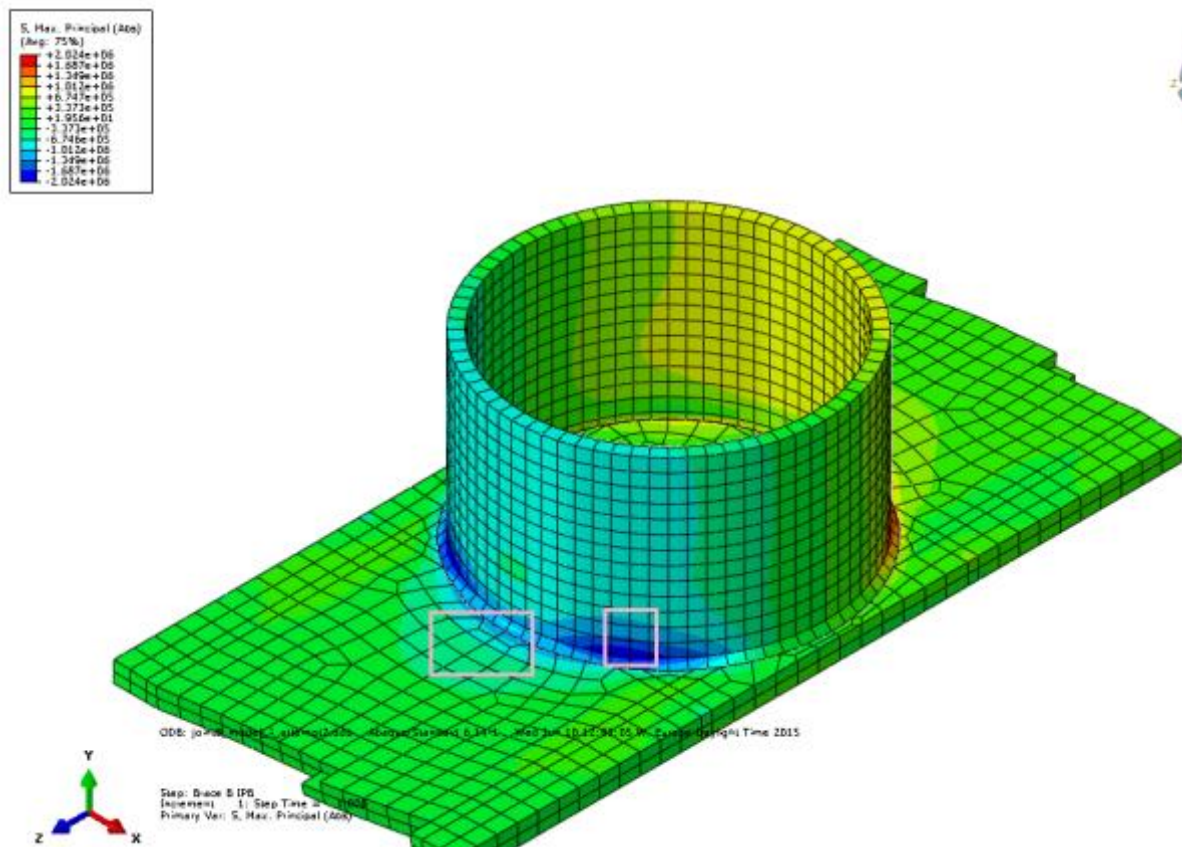


Figure A-6-9: Joint 6 Model II (C3D20R, mesh is adapted to t x t, 19.1mm chord/brace, 16mm stiffeners, 30mm top plate)

Upper left: Abs. max principal stress contour and stress read out region for central brace IPB load case
 Lower left: Abs. max principal stress contour and stress read out region for central brace OPB load case

Upper right: Abs. max principal stress contour and stress read out region for central brace IPB load case
 Lower right: Abs. max principal stress contour and stress read out region for central brace OPB load case

Appendix B – Extrapolation spreadsheets

B.1 Joint 1

Specimen 1 results			Direct stresses						Principal stresses			Effective hot spot stress		
C3D20R_4	Node number	Elements	S11	S22	S33	S12	S13	S23	S1	S2	S3	S.eff	Target	Error %
Hot spot stress (extrapolated)	15	Six	1,26129	-0,1619	0,034045	0	0,00846	0	1,261335	0,034015	-0,1619	1,261335	1,32	-4,65 %
0.5T (read out)	35913	Four	1,21141	-0,13313	0,02279	0	0,00564	0	1,21144	0,02277	-0,13313			
1.5T (read out)	35739	Four	1,11165	-0,07559	0,00028	0	0	0	1,11165	0,00028	-0,07559			
C3D20R_1	Node number	Elements	S11	S22	S33	S12	S13	S23	S1	S2	S3	S.eff	Target	Error %
Hot spot stress (extrapolated)	Edge midpoint	Three	1,405355	-0,0377205	0,3402821	0,185919	0	0,026016	1,405355	0,3414993	0,0389373	1,405355	1,32	6,07 %
0.5T (read out)	Face 4	117	1,30626	-0,0499323	0,220861	0,123946	0	0,015866	1,30626	0,221788	-0,050859			
1.5T (read out)	Face 4	118	1,10807	-0,0743559	-0,0179812	0	0	0,004434	1,10807	0,0176346	0,0747025			
S8R5	Node number	Elements	S11	S22	S12				S1	S2	Angle	S.eff	Target	Error %
Hot spot stress (extrapolated)	33	Five	1,54555	-0,134265	0				1,54555	-0,134265	0		1,32	#DIV/0!
0.5T (read out)	622	Two	1,40766	-0,11261	0				1,40766	-0,11261				
1.5T (read out)	615	Two	1,13188	-0,0693	0				1,13188	-0,0693				
S8R	Node number	Elements	S11	S22	S12				S1	S2	Angle	S.eff	Target	Error %
Hot spot stress (extrapolated)	33	Five	1,625575	-0,0202	0				1,625575	-0,0202	0	1,625575	1,32	18,80 %
0.5T (read out)	622	Two	1,46528	-0,04447	0				1,46528	-0,04447	0			
1.5T (read out)	615	Two	1,14469	-0,09301	0				1,14469	-0,09301	0			
S4	Node number	Elements	S11	S22	S12				S1	S2	Angle	S.eff	Target	Error %
Hot spot stress (extrapolated)	33		1,74	0,0135	0,227				1,766	-0,011	0,1285692	1,766	1,32	25,25 %
0.5T	Int. Pts.	132	1,543	-0,012	0,167				1,561	-0,029	0			
1.5T	Int. Pts.	129	1,149	-0,063	0,047				1,151	-0,065	0			

General notes

Extrapolation formula for 0.5T and 1.5T read out points is $1.5 * s_{0.5t} - 0.5 * s_{1.5t}$, Ref. IIW

Highlighted column is the stress component normal to the weld

Max effective hot spot stress found via 4.3.4 in DNVGL-RP-0005, max of principal stress 1 and 2, and a seemingly empirical formula which uses normal and shear stress

Principal stresses are generally direct read out from postprocessing, except for S4 which is calculated manually

DNV RP and IIW references nodal stresses, which implies averaged results at read out points can be used (this is used where mesh is convenient, C3D20R_4 and S8R)

B.2 Joint 2

Joint 2 model I															
Load case	Position	Read-out point	Node	Element	Direct stresses - top surface			Hot spot stress values			Nominal stress	Max HSS	Efthymiou	Error	
					S11	S22	S12	DNV	S1	S2					
Axial	Chord crown	HS a=7.46mm b=17.4mm	24688		3,620	12,432	0,001	12,432	12,432	3,620	1	Method A	12,432	10,096	23,1 %
			24616		3,343	11,817	0,000								
			13		2,975	10,997	0,000								
	Brace crown	HS a=7.46mm b=24.25mm	24688		1,808	5,077	-0,003	5,077	5,077	1,808	1	Method A	5,077	5,172	-1,8 %
			24725		1,912	4,084	-0,002								
			24683		2,146	1,849	0,000								
	Chord saddle	HS a=7.46mm b=14.13mm	24617		7,655	7,239	0,003	7,655	7,655	7,239	1	Method A	7,655	8,242	-7,1 %
			24804		5,838	6,784	0,000								
15				4,214	6,378	-0,003									
Brace saddle	HS a=7.46mm b=24.25mm	24617		7,655	10,893	0,050	10,893	10,894	7,655	1	Method A	10,894	7,012	55,4 %	
		24587		5,957	8,311	0,033									
		24589		2,131	2,494	-0,005									
IPB	Chord crown	HS a=7.46mm b=17.4mm	24688		-1,906	-3,202	-0,001	3,202	-1,906	-3,202	1	Method A	3,202	2,837	12,9 %
			24616		-1,756	-2,634	-0,001								
			13		-1,555	-1,877	0,000								
	Brace crown	HS a=7.46mm b=24.25mm	24688		-1,390	-2,375	0,000	2,375	-1,390	-2,375	1	Method A	2,375	2,506	-5,2 %
24725				-1,158	-1,927	0,000									
24683				-0,635	-0,917	0,000									
OPB	Chord saddle	HS a=7.46mm b=14.13mm	24617		-7,898	-3,370	0,039	7,898	-3,370	-7,899	1	Method A	7,899	7,565	4,4 %
			24804		-6,460	-2,943	0,019								
			15		-5,174	-2,560	0,001								
	Brace saddle	HS a=7.46mm b=24.25mm	24617		-2,810	-7,050	-0,081	7,050	-2,809	-7,052	1	Method A	7,052	5,238	34,6 %
24587				-2,434	-5,961	-0,049									
24589				-1,585	-3,507	0,023									

B.3 Joint 3

Joint 3 model I															
Load case	Position	Read-out point	Node	Element	Direct stresses - top surface			Hot spot stress values			Nominal stress	Max HSS	Efthymiou	Error	
					S11	S22	S12	DNV	S1	S2					
Axial	Chord crown	HS	1		3,552	14,303	0,000	14,303	14,303	3,552	1	Method A	14,303	13,299	7,5 %
		0.5T - 9,53mm	5313		3,283	13,508	0,000	13,508	13,508	3,283		Method B	15,129		13,8 %
		1.5T - 28,58mm	5329		2,744	11,919	0,000								
	Brace crown	HS	1		0,824	4,597	-0,002	4,597	4,597	0,824	1	Method A	4,597	5,547	-17,1 %
		0.5T - 9,53mm	14478		1,094	3,993	-0,001	3,993	3,993	1,094		Method B	4,472		-19,4 %
		1.5T - 28,58mm	14475		1,633	2,786	-0,001	2,786	2,786	1,633					
	Chord saddle	HS	53		2,361	4,163	1,722	4,442	5,205	1,318	1	Method A	5,205	5,026	3,6 %
		0.5T - 9,53mm	9183		2,004	4,025	1,551	4,261	4,866	1,164		Method B	5,450		8,4 %
		1.5T - 28,58mm	9182		1,290	3,750	1,208	3,905	4,244	0,796					
	Brace saddle	HS	52		2,819	3,835	2,172	4,305	5,558	1,097	1	Method A	5,558	3,699	50,3 %
		0.5T - 9,53mm	15199		2,474	3,733	1,897	4,105	5,102	1,104		Method B	5,715		54,5 %
		1.5T - 28,58mm	15198		1,782	3,527	1,347	3,730	4,260	1,049					
IPB	Chord crown	HS	1		1,706	3,382	0,000	3,382	3,382	1,706	1	Method A	3,382	3,221	5,0 %
		0.5T - 9,53mm	5313		1,575	2,911	0,000	2,911	2,911	1,575		Method B	3,260		1,2 %
		1.5T - 28,58mm	5329		1,314	1,970	0,000								
	Brace crown	HS	1		1,161	1,802	0,000	1,802	1,802	1,161	1	Method A	1,802	2,44	-26,2 %
		0.5T - 9,53mm	14478		1,012	1,487	0,000	1,487	1,487	1,012		Method B	1,666		-31,7 %
		1.5T - 28,58mm	14475		0,716	0,859	0,000	0,859	0,859	0,716					
OPB: 3 possible locations for saddle	Chord saddle	HS	53		4,737	2,752	1,457	3,048	5,507	1,981	1	Method A	5,507	7,8	-29,4 %
		0.5T - 9,53mm	9183		4,314	2,513	1,272	2,762	4,972	1,855		Method B	5,569		-28,6 %
		1.5T - 28,58mm	9182		3,468	2,037	0,902	2,192	3,904	1,601					
	Brace saddle MAX	HS	52		2,093	4,927	1,250	5,054	5,400	1,620	1	Method A	5,400	4,133	30,7 %
		0.5T - 9,53mm	15199		1,868	4,853	1,005	4,937	5,160	1,562		Method B	5,779		39,8 %
		1.5T - 28,58mm	15198		1,419	4,705	0,514	4,728	4,784	1,340					
Brace saddle	53	HS	53		2,190	4,847	1,280	4,982	5,364	1,673	1	Method A	5,364	4,133	29,8 %
		0.5T - 9,53mm	15159		1,973	4,671	1,000	4,757	5,002	1,643		Method B	5,602		35,5 %
		1.5T - 28,58mm	15158		1,540	4,320	0,440	4,338	4,388	1,472					
	51	HS	51		1,610	4,655	1,161	4,771	5,047	1,217	1	Method A	5,047	4,133	22,1 %
		0.5T - 9,53mm	15239		1,474	4,731	0,962	4,809	4,994	1,211		Method B	5,593		35,3 %
		1.5T - 28,58mm	15238		1,204	4,883	0,565	4,909	4,967	1,119					

Joint 4 model II - 16mm stiffeners															
Load case	Position	Read-out point	Node	Model	Direct stresses - top surface			Hot spot stress values			Nominal stress	Max HSS	Efthymiou Joint 3 / Joint 3 result	Error (Method A)	
					S11	S22	S12	DNV	S1	S2					
Axial	Chord crown	HS	71	19,1mm	2,875	15,362	-0,003	15,362	15,362	2,875	1	Method A	15,362	13,299	15,5 %
		0.5T - 9,53mm	122515		2,650	14,373	-0,002	14,373	14,373	2,650		Method B	16,097	14,303	7,4 %
		1.5T - 28,58mm	102787		2,200	12,393	-0,002								
	Stiffener crown (circumferential stiffener)	HS	16	16mm	0,946	9,672	-0,009	9,672	9,672	0,946	1	Method A	9,672	5,547	74,4 %
0.5T - 8mm		153695		0,943	8,403	-0,007	8,403	8,403	0,943	Method B		9,411	4,597	110,4 %	
1.5T - 24mm		153721		0,935	5,864	-0,003		5,864	0,935					(brace crown)	
					0,000	0,000	0,000	0,000	0,000	0,000	1	Method A	0,000		#DIV/0!
					0,000	0,000	0,000	0,000	0,000	0,000		Method B	0,000		#DIV/0!
					0,000	0,000	0,000	0,000	0,000	0,000	1	Method A	0,000		#DIV/0!
					0,000	0,000	0,000	0,000	0,000	0,000		Method B	0,000		#DIV/0!
IPB	Chord crown	HS	71	19,1mm	-0,593	-1,853	-0,002	1,853	-0,593	-1,853	1	Method A	1,853	3,211	-42,3 %
		0.5T - 9,53mm	122515		-0,591	-1,662	-0,002	1,662	-0,591	-1,662		Method B	1,861	3,382	-45,2 %
		1.5T - 28,58mm	102787		-0,588	-1,280	-0,001								
Brace (above circumferential stiffeners)	HS	3193	19,1mm	-0,835	-2,406	0,173	2,411	-0,816	-2,425	1	Method A	2,425	2,44	-0,6 %	
	0.5T - 9,53mm	97539		-0,742	-2,094	0,141	2,098	-0,728	-2,108		Method B	2,361	1,802	34,6 %	
	1.5T - 28,58mm	88146		-0,556	-1,469	0,076		-0,550	-1,475						
Z-steel plate (between stiffener positions)	HS	-	30mm							1			N/A		
0.5T - 15mm	23		1,243	0,722	0,004	1,243	1,243	0,722	Method B		1,392		#VALUE!		
	1.5T - 45mm	-													
OPB	Chord saddle (below circumferential stiffeners)	HS	42	19,1mm	4,942	2,863	-0,151	4,944	4,953	2,852	1	Method A	4,953	7,8	-36,5 %
		0.5T - 9,53mm	101839		3,640	2,086	-0,152	3,642	3,654	2,072		Method B	4,093	5,507	-10,1 %
		1.5T - 28,58mm	101375		1,035	0,533	-0,154								
	Chord saddle (on circumferential stiffeners)	HS	9	16mm	5,293	2,282	2,269	5,673	6,511	1,064	1	Method A	6,511	N/A	#VALUE!
		0.5T - 8mm	154938		3,570	1,432	1,507	3,818	4,348	0,654		Method B	4,870		#VALUE!
		1.5T - 24mm	154936		0,123	-0,269	-0,019		0,124	-0,270					
Brace (above longitudinal stiffeners)	HS	44	19,1mm	-0,808	-2,588	-0,236	2,596	-0,778	-2,618	1	Method A	2,618	4,113	-36,3 %	
	0.5T - 9,53mm	97129		-0,624	-2,228	-0,184	2,234	-0,603	-2,248		Method B	2,518	5,4	-51,5 %	
	1.5T - 28,58mm	97174		-0,256	-1,507	-0,079		-0,251	-1,512						

Joint 4 model III - 12mm stiffeners															
Load case	Position	Read-out point	Node	Model	Direct stresses - top surface			Hot spot stress values			Nominal stress	Max HSS	Efthymiou Joint 3 / Joint 3 result	Error (Method A)	
					S11	S22	S12	DNV	S1	S2					
Axial	Chord crown	HS	71	19,1mm	2,345	13,915	-0,003	13,915	13,915	2,345	1	Method A	13,915	13,299	4,6 %
		0.5T - 9,53mm	122515		2,152	13,198	-0,003	13,198	13,198	2,152		Method B	14,782	14,303	-2,7 %
		1.5T - 28,58mm	102787		1,767	11,764	-0,002								
	Stiffener crown (circumferential stiffener)	HS	16	12mm	0,459	9,081	-0,008	9,081	9,081	0,459	1	Method A	9,081	5,547	63,7 %
0.5T - 6mm		434938		0,498	8,167	-0,009	8,167	8,167	0,498	Method B		9,147	4,597	97,5 %	
1.5T - 18mm		437462		0,576	6,340	-0,009		6,340	0,576					(brace crown)	
					0,000	0,000	0,000	0,000	0,000	0,000	1	Method A	0,000		#DIV/0!
					0,000	0,000	0,000	0,000	0,000	0,000		Method B	0,000		#DIV/0!
					0,000	0,000	0,000	0,000	0,000	0,000	1	Method A	0,000		#DIV/0!
					0,000	0,000	0,000	0,000	0,000	0,000		Method B	0,000		#DIV/0!
IPB	Chord crown	HS	71	19,1mm	-0,777	-1,997	-0,002	1,997	-0,777	-1,997	1	Method A	1,997	3,211	-37,8 %
		0.5T - 9,53mm	122515		-0,750	-1,773	-0,002	1,773	-0,750	-1,773		Method B	1,986	3,382	-41,0 %
		1.5T - 28,58mm	102787		-0,695	-1,326	-0,002								
Brace (above circumferential stiffeners)	HS	3194	19,1mm	-0,812	-2,516	0,142	2,519	-0,800	-2,528	1	Method A	2,528	2,44	3,6 %	
	0.5T - 9,53mm	97537		-0,738	-2,187	0,120	2,189	-0,728	-2,197		Method B	2,460	1,802	40,3 %	
	1.5T - 28,58mm	88143		-0,590	-1,528	0,078		-0,583	-1,534						
Z-steel plate (between stiffener positions)	HS	-	30mm							1			N/A		
0.5T - 15mm	23		1,366	0,767	-0,017	1,366	1,366	0,766			Method B	1,530		#VALUE!	
	1.5T - 45mm	-													
OPB	Chord saddle (below circumferential stiffeners)	HS	42	19,1mm	4,232	2,507	-0,170	4,235	4,249	2,491	1	Method A	4,249	7,8	-45,5 %
		0.5T - 9,53mm	101839		3,080	1,806	-0,172	3,084	3,103	1,784		Method B	3,475	5,507	-22,8 %
		1.5T - 28,58mm	101375		0,776	0,405	-0,175								
	Chord saddle (on circumferential stiffeners)	HS	9	12mm	8,023	2,676	2,490	8,330	9,003	1,696	1	Method A	9,003	N/A	#VALUE!
		0.5T - 6mm	437511		5,646	1,665	1,672	5,843	6,255	1,056		Method B	7,005		#VALUE!
		1.5T - 18mm	437758		0,891	-0,358	0,036		0,892	-0,359					
Brace (above longitudinal stiffeners)	HS	44	19,1mm	-0,804	-2,606	-0,235	2,614	-0,774	-2,636	1	Method A	2,636	4,113	-35,9 %	
	0.5T - 9,53mm	97129		-0,627	-2,247	-0,187	2,253	-0,606	-2,268		Method B	2,540	5,4	-51,2 %	
	1.5T - 28,58mm	97174		-0,274	-1,528	-0,091		-0,268	-1,535						

B.5 Joint 5

Joint 5 model I														
Load case	Position	Read-out point	Node	Element	Direct stresses - top surface			Hot spot stress values		Nominal stress	Max HSS	Efthymiou	Error	
					S11	S22	S12	S1	S2					
Axial	Chord crown, Brace A	HS	7656		4,484	13,437	0,001	13,437	4,484	1	Method A	13,437	10,974	22,4 %
		0.5T - 9,53mm	8533		3,995	12,309	0,000	12,309	3,995		Method B	13,786		25,6 %
		1.5T - 28,58mm	8366		3,016	10,054	0,000							
	Brace A crown	HS	7642		2,546	6,456	0,001	6,456	2,546	1	Method A	6,456	5,547	16,4 %
		0.5T - 9,53mm	8625		2,632	5,256	0,001	5,256	2,632		Method B	5,886		6,1 %
		1.5T - 28,58mm	8531		2,802	2,854	0,000							
	Chord saddle, Brace A	HS	2107		-2,566	-1,198	0,224	-1,162	-2,602	1	Method A	2,602	2,886	-9,8 %
		0.5T - 9,53mm	3321		-2,504	-1,479	0,142	-1,459	-2,524		Method B	2,826		-2,1 %
		1.5T - 28,58mm	3313		-2,380	-2,039	-0,021							
	Brace A between saddle and crown	HS	2532		2,955	6,191	0,562	6,286	2,860	1	Method A	6,286	2,395	162,5 %
		0.5T - 9,53mm	3264		2,554	5,397	0,501	5,483	2,469		Method B	6,141		156,4 %
		1.5T - 28,58mm	3190		1,753	3,809	0,378							
Chord crown, Brace B	HS	18		3,728	15,097	0,000	15,097	3,728	1	Method A	15,097	13,299	13,5 %	
	0.5T - 9,53mm	784		3,448	14,165	0,000	14,165	3,448		Method B	15,864		19,3 %	
	1.5T - 28,58mm	833		2,887	12,301	0,001								
Brace B crown	HS	18		0,917	4,974	0,000	4,974	0,917	1	Method A	4,974	5,547	-10,3 %	
	0.5T - 9,53mm	741		1,208	4,313	0,000	4,313	1,208		Method B	4,830		-12,9 %	
	1.5T - 28,58mm	677		1,789	2,991	0,000								
Chord saddle, Brace B	HS	28		-2,569	-2,114	0,112	-2,088	-2,596	1	Method A	2,596	2,886	-10,1 %	
	0.5T - 9,53mm	1010		-2,786	-2,432	0,101	-2,406	-2,813		Method B	3,150		9,2 %	
	1.5T - 28,58mm	880		-3,219	-3,068	0,079								
Brace B saddle	HS	4		-2,926	-1,826	-0,186	-1,796	-2,956	1	Method A	2,956	3,699	-20,1 %	
	0.5T - 9,53mm	1503		-1,997	-0,816	-0,019	-0,816	-1,997		Method B	2,237		-39,5 %	
	1.5T - 28,58mm	716		-0,139	1,205	0,315								

IPB	Chord crown, Brace A	HS	7656	1,648	3,384	0,000	3,384	1,648	1	Method	3,384	2,520	34,3 %
		0.5T - 9,53mm	8533	1,459	2,892	0,000	2,892	1,459		Method			
		1.5T - 28,58mm	8366	1,083	1,908	0,000				B			
	Brace A crown	HS	7656	1,233	2,061	0,000	2,061	1,233	1	Method	2,061	2,677	-23,0 %
0.5T - 9,53mm		8364	1,074	1,748	0,000	1,748	1,074	Method					
1.5T - 28,58mm		8268	0,758	1,123	0,000			B		1,958			
Chord crown, Brace B	HS	18	-2,143	-4,189	0,000	-2,143	-4,189	1	Method	4,189	3,211	30,4 %	
	0.5T - 9,53mm	784	-1,922	-3,528	0,000	-1,922	-3,528		Method				
	1.5T - 28,58mm	833	-1,479	-2,207	0,000				B				3,952
Brace B crown	HS	18	-1,465	-2,325	0,000	-1,465	-2,325	1	Method	2,325	2,440	-4,7 %	
	0.5T - 9,53mm	741	-1,272	-1,925	0,000	-1,272	-1,925		Method				
	1.5T - 28,58mm	677	-0,886	-1,127	0,000				B				2,157
OPB	Chord, adjacent to Brace A	HS	2414	-3,160	-1,326	0,386	-1,248	-3,238	1	Method	3,238	3,771	-14,1 %
		0.5T - 9,53mm	3661	-2,683	-1,091	0,304	-1,035	-2,739		Method			
		1.5T - 28,58mm	3478	-1,730	-0,621	0,140				B			
	Brace A saddle	HS	2576	-2,287	-2,021	1,074	-1,072	-3,236	1	Method	3,236	1,998	62,0 %
0.5T - 9,53mm		4046	-2,020	-2,037	0,993	-1,036	-3,021	Method					
1.5T - 28,58mm		3962	-1,486	-2,069	0,830			B		3,384			
Chord, adjacent to Brace B	HS	318	4,046	2,416	-1,244	4,718	1,744	1	Method	4,718	6,265	-24,7 %	
	0.5T - 9,53mm	1252	3,544	2,044	-1,037	4,074	1,515		Method				
	1.5T - 28,58mm	1086	2,541	1,301	-0,624				B				4,563
Brace B saddle	HS	317	1,805	4,334	1,083	4,734	1,405	1	Method	4,734	3,320	42,6 %	
	0.5T - 9,53mm	1313	1,508	4,269	0,815	4,491	1,286		Method				
	1.5T - 28,58mm	721	0,915	4,138	0,278				B				5,030

B.6 Joint 6

Joint 6 model I - 16mm stiffeners													
Load case	Position	Read-out point	Node	Model	Direct stresses - top surface			Hot spot stress values			Nominal stress	Max HSS	
					S11	S22	S12	DNV	S1	S2			
Axial, Brace A	Chord crown	HS	1	19,1mm	4,656	16,266	0,000	16,266	16,266	4,656	1	Method A	16,266
		0.5T - 9,53mm	20429		4,384	14,460	0,000	14,460	14,460	4,384		Method B	16,195
		1.5T - 28,58mm	63896		3,839	10,848	0,000						
	Brace A, above stiffeners	HS	329	19,1mm	2,232	5,014	0,327	5,023	5,052	2,194	1	Method A	5,052
		0.5T - 9,53mm	5218		1,866	4,244	0,239	4,249	4,267	1,842		Method B	4,780
		1.5T - 28,58mm	24717		1,134	2,703	0,063						
	Z-steel plate, adjacent to brace A, plate center position	HS	116	30mm	2,032	0,715	-0,153	2,037	2,049	0,698	1	Method A	2,049
		0.5T - 15mm	5058		1,469	0,455	-0,229	0,500	1,518	0,406		Method B	1,700
	Z-steel plate, chord crown	HS	13347		2,241	5,995	0,197	2,248	6,005	2,231	1	Method A	6,005
		0.5T - 15mm	16137		1,960	4,384	0,131	4,386	4,391	1,953		Method B	4,918
		1.5T - 45mm	4501		1,397	1,163	-0,001		1,397	1,163			
	IPB, Brace A	Brace A, above stiffeners	HS	427	19,1mm	-1,260	-3,580	-0,291	3,589	-1,224	-3,616	1	Method A
0.5T - 9,53mm			5402		-1,132	-3,136	-0,337	3,151	-1,077	-3,191	Method B		3,574
1.5T - 28,58mm			24737		-0,877	-2,249	-0,429						
Z-steel plate, top position		HS	17	30mm	1,446	3,375	0,000	3,375	3,375	1,446	1	Method A	3,375
		0.5T - 15mm	4857		1,236	2,659	0,000	2,659	2,659	1,236		Method B	2,978
		1.5T - 45mm	4872		0,817	1,227	0,000						
Longitudinal stiffener, below brace intersection (inside)	HS	16	16mm	2,524	-1,025	-0,846	1,277	2,715	-1,216	1	Method A	2,715	
	0.5T - 8mm	10087		2,279	-0,849	-0,848	1,142	2,495	-1,064		Method B	2,794	
	1.5T - 24mm	9995		1,791	-0,496	-0,854							
OPB, Brace A	Brace A, above stiffeners	HS	329	19,1mm	-0,930	-3,239	-0,226	0,952	-0,909	-3,261	1	Method A	3,261
		0.5T - 9,53mm	5218		-0,765	-2,708	-0,153	0,777	-0,753	-2,720		Method B	3,046
		1.5T - 28,58mm	24717		-0,434	-1,644	-0,009						
	Z-steel plate	HS	304	30mm	-0,615	-1,640	0,038	0,616	-0,613	-1,641	1	Method A	1,641
		0.5T - 15mm	4855		-0,343	-1,103	0,109	0,357	-0,328	-1,119		Method B	1,253
		1.5T - 45mm	4843		0,200	-0,030	0,250						
Longitudinal stiffener, below brace intersection	HS	17	16mm	1,878	1,031	0,562	1,148	2,158	0,750	1	Method A	2,158	
	0.5T - 8mm	10109		1,683	0,888	0,563	1,023	1,975	0,596		Method B	2,212	
1.5T - 24mm	10028		1,293	0,604	0,565								

Joint 6 model I - 16mm stiffeners													
Load case	Position	Read-out point	Node	Model	Direct stresses - top surface			Hot spot stress values			Nominal stress	Max HSS	
					S11	S22	S12	DNV	S1	S2			
Axial, Brace B	Chord crown	HS	1	19,1mm	6,683	21,956	0,000	21,956	21,956	6,683	1	Method A	21,956
		0.5T - 9,53mm	20429		6,220	19,366	0,000	19,366	19,366	6,220		Method B	21,690
		1.5T - 28,58mm	63896		5,294	14,186	0,000						
	Brace B, above stiffeners	HS	261	19,1mm	1,934	3,406	0,625	3,452	3,636	1,705	1	Method A	3,636
0.5T - 9,53mm		5117		1,617	2,826	0,527	2,865	3,023	1,419	Method B		3,386	
1.5T - 28,58mm		21051		0,981	1,665	0,332							
Z-steel plate, adjacent to brace B, plate center position	HS	9	30mm	1,096	3,451	0,000	1,096	3,451	1,096	1	Method A	3,451	
	0.5T - 15mm	4909		1,050	3,170	0,000	3,170	3,170	1,050		Method B	3,550	
	1.5T - 45mm	4887		0,959	2,607	0,000		2,607	0,959				
Z-steel plate, chord crown	HS	13347	30mm	3,880	8,675	0,003	3,880	8,675	3,880	1	Method A	8,675	
	0.5T - 15mm	16137		3,289	6,534	0,002	6,534	6,534	3,289		Method B	7,318	
	1.5T - 45mm	4501		2,107	2,252	-0,001							
IPB, Brace B	Brace B, above stiffeners	HS	448	19,1mm	0,696	2,197	0,053	2,197	2,199	0,694	1	Method A	2,199
		0.5T - 9,53mm	5445		0,594	1,934	0,052	1,935	1,936	0,592		Method B	2,169
		1.5T - 28,58mm	21016		0,389	1,409	0,051						
	Z-steel plate, top position	HS	9	30mm	-0,583	-1,294	0,000	1,294	-0,583	-1,294	1	Method A	1,294
0.5T - 15mm		4909		-0,574	-1,099	0,000	1,099	-0,574	-1,099	Method B		1,231	
1.5T - 45mm		4887		-0,557	-0,710	0,000							
Longitudinal stiffener, below brace intersection (inside)	HS	29669	16mm	0,536	1,673	-0,279	1,692	1,738	0,471	1	Method A	1,738	
	0.5T - 8mm	30142		0,412	1,535	-0,251	1,551	1,588	0,359		Method B	1,779	
	1.5T - 24mm	30142		0,164	1,257	-0,195							
OPB, Brace B	Brace B, above stiffeners	HS	261	19,1mm	0,581	2,034	0,123	0,591	2,044	0,570	1	Method A	2,044
		0.5T - 9,53mm	5117		0,479	1,811	0,114	0,489	1,820	0,469		Method B	2,039
		1.5T - 28,58mm	21051		0,274	1,365	0,098						
	Z-steel plate	HS	203	30mm	1,121	0,451	0,092	1,124	1,134	0,439	1	Method A	1,134
		0.5T - 15mm	4991		0,676	0,198	0,041	0,677	0,679	0,194		Method B	0,761
		1.5T - 45mm	4980		-0,216	-0,308	-0,060						
Longitudinal stiffener, below brace intersection	HS	29744	16mm	0,409	1,417	0,102	1,419	1,427	0,399	1	Method A	1,427	
	0.5T - 8mm	30330		0,296	1,294	0,058	1,295	1,297	0,293		Method B	1,453	
	1.5T - 24mm	30236		0,071	1,049	-0,030		1,050	0,071				

Appendix C – Efthymiou SCFs

C.1 Joint 2

Definition of geometrical parameters

$$d := 2 \cdot r = 219.1 \text{ mm} \quad D := 2 \cdot R = 323.8 \text{ mm}$$

$$L := 10 \text{ m} = 10000 \text{ mm} \quad \vartheta := 90 \text{ deg}$$

$$\beta := \frac{d}{D} = 0.677 \quad \alpha := \frac{\rho L}{D} = 61.767$$

$$\gamma := \frac{D}{2 \cdot T} = 10.182 \quad \tau := \frac{t}{T} = 0.799$$

Chord-end fixity parameter

$$C := 0.7 \quad C_1 := 2 \cdot (C - 0.5) = 0.4 \quad C_2 := \frac{C}{2} = 0.35 \quad C_3 := \frac{C}{5} = 0.14$$

Input for alternative formulations

$$\sigma_{\text{BendingChord}} := 2 \text{ MPa} \quad \sigma_{\text{AxialBrace}} := 1 \text{ MPa} \quad \text{SCF}_{\text{att}} := 1.27$$

Table B-1 Stress concentration factors for simple tubular T/Y-joints

Axial loads - Chord ends fixed

$$\text{Chord saddle} \quad \text{SCF}_{1_axial_fixed_cs} := \gamma \cdot \tau^{1.1} \cdot [1.11 - 3(\beta - 0.52)^2] \cdot \sin(\vartheta)^{1.6} = 8.242$$

$$\text{Chord crown} \quad \text{SCF}_{1_axial_fixed_cc} := \gamma^{0.2} \cdot \tau \cdot [2.65 + 5(\beta - 0.65)^2] + \tau \cdot \beta \cdot (0.25\alpha - 3) \cdot \sin(\vartheta) = 10.096$$

$$\text{Brace saddle} \quad \text{SCF}_{1_axial_fixed_bs} := 1.3 + \gamma \cdot \tau^{0.52} \cdot \alpha^{0.1} \cdot [0.187 - 1.25 \cdot \beta^{1.1} \cdot (\beta - 0.96)] \cdot \sin(\vartheta)^{(2.7 - 0.01 \cdot \alpha)} = 7.012$$

$$\text{Brace crown} \quad \text{SCF}_{1_axial_fixed_bc} := 3 + \gamma^{1.2} \cdot [0.12 \cdot e^{(-4 \cdot \beta)} + 0.011 \cdot \beta^2 - 0.045] + \beta \cdot \tau \cdot (0.1 \cdot \alpha - 1.2) = 5.172$$

In-plane bending

$$\text{Chord crown} \quad \text{SCF}_{1_ipb_cc} := 1.45 \cdot \beta \cdot \tau^{0.85} \cdot \gamma^{(1 - 0.68 \cdot \beta)} \cdot \sin(\vartheta)^{0.7} = 2.837$$

$$\text{Brace crown} \quad \text{SCF}_{1_ipb_bc} := 1 + 0.65 \cdot \beta \cdot \tau^{0.4} \cdot \gamma^{(1.09 - 0.77 \cdot \beta)} \cdot \sin(\vartheta)^{(0.06 \cdot \gamma - 1.16)} = 2.506$$

Out-of-plane bending

$$\text{Chord saddle} \quad \text{SCF}_{1_opb_cs} := \gamma \cdot \tau \cdot \beta \cdot (1.7 - 1.05 \cdot \beta^3) \cdot \sin(\vartheta)^{1.6} = 7.565$$

$$\text{Brace saddle} \quad \text{SCF}_{1_opb_bs} := \tau^{-0.54} \cdot \gamma^{-0.05} \cdot (0.99 - 0.47 \cdot \beta + 0.08 \cdot \beta^4) \cdot \text{SCF}_{1_opb_cs} = 5.238$$

C.2 Joint 3

Definition of geometrical parameters

$$d := 2 \cdot r = 457.2 \text{ mm} \quad D := 2 \cdot R = 457.2 \text{ mm}$$

$$\underline{\underline{L}} := 10m = 10000 \text{ mm} \quad \vartheta := 90 \text{ deg}$$

$$\beta := \frac{d}{D} = 1 \quad \alpha := \frac{2L}{D} = 43.745$$

$$\gamma := \frac{D}{2 \cdot T} = 12 \quad \underline{\underline{\tau}} := \frac{t}{T} = 1$$

Chord-end fixity parameter

$$\underline{\underline{C}} := 0.5 \quad C_1 := 2 \cdot (C - 0.5) = 0 \quad C_2 := \frac{C}{2} = 0.25 \quad C_3 := \frac{C}{5} = 0.1$$

Input for alternative formulations

$$\sigma_{\text{BendingChord}} := 2 \text{ MPa} \quad \sigma_{\text{AxialBrace}} := 1 \text{ MPa} \quad \text{SCF}_{\text{att}} := 1.27$$

Table B-1 Stress concentration factors for simple tubular T/Y-joints

Axial loads - Chord ends fixed

$$\text{Chord saddle} \quad \text{SCF}_{1_axial_fixed_cs} := \gamma \cdot \tau^{1.1} \cdot [1.11 - 3(\beta - 0.52)^2] \cdot \sin(\vartheta)^{1.6} = 5.026$$

$$\text{Chord crown} \quad \text{SCF}_{1_axial_fixed_cc} := \gamma^{0.2} \cdot \tau \cdot [2.65 + 5 \cdot (\beta - 0.65)^2] + \tau \cdot \beta \cdot (0.25\alpha - 3) \cdot \sin(\vartheta) = 13.299$$

$$\text{Brace saddle} \quad \text{SCF}_{1_axial_fixed_bs} := 1.3 + \gamma \cdot \tau^{0.52} \cdot \alpha^{0.1} \cdot [0.187 - 1.25 \cdot \beta^{1.1} \cdot (\beta - 0.96)] \cdot \sin(\vartheta)^{(2.7 - 0.01 \cdot \alpha)} = 3.699$$

$$\text{Brace crown} \quad \text{SCF}_{1_axial_fixed_bc} := 3 + \gamma^{1.2} \cdot [0.12 \cdot e^{(-4 \cdot \beta)} + 0.011 \cdot \beta^2 - 0.045] + \beta \cdot \tau \cdot (0.1 \cdot \alpha - 1.2) = 5.547$$

In-plane bending

$$\text{Chord crown} \quad \text{SCF}_{1_ipb_cc} := 1.45 \cdot \beta \cdot \tau^{0.85} \cdot \gamma^{(1 - 0.68 \cdot \beta)} \cdot \sin(\vartheta)^{0.7} = 3.211$$

$$\text{Brace crown} \quad \text{SCF}_{1_ipb_bc} := 1 + 0.65 \cdot \beta \cdot \tau^{0.4} \cdot \gamma^{(1.09 - 0.77 \cdot \beta)} \cdot \sin(\vartheta)^{(0.06 \cdot \gamma - 1.16)} = 2.44$$

Out-of-plane bending

$$\text{Chord saddle} \quad \text{SCF}_{1_opb_cs} := \gamma \cdot \tau \cdot \beta \cdot (1.7 - 1.05 \cdot \beta^3) \cdot \sin(\vartheta)^{1.6} = 7.8$$

$$\text{Brace saddle} \quad \text{SCF}_{1_opb_bs} := \tau^{-0.54} \cdot \gamma^{-0.05} \cdot (0.99 - 0.47 \cdot \beta + 0.08 \cdot \beta^4) \cdot \text{SCF}_{1_opb_cs} = 4.133$$

C.3 Joint 5

Joint geometry KT joint

Chord diameter	$D := 457.2\text{mm}$	
Brace A diameter	$d_A := 457.2\text{mm}$	
Brace B diameter	$d_B := 457.2\text{mm}$	
Brace C diameter	$d_C := 457.2\text{mm}$	
Chord thickness	$T := 19.05\text{mm}$	
Brace A thickness	$t_A := 19.05\text{mm}$	
Brace B thickness	$t_B := 19.05\text{mm}$	
Brace C thickness	$t_C := 19.05\text{mm}$	
Chord length	$L := 10\text{m}$	
Gap AB	$g_{AB} := 103.95\text{mm}$	
Gap BC	$g_{BC} := 103.95\text{mm}$	
Alfa	$\alpha := \frac{2L}{D} = 43.745$	
Beta A	$\beta_A := \frac{d_A}{D} = 1$	
Beta B	$\beta_B := \frac{d_B}{D} = 1$	
Beta C	$\beta_C := \frac{d_C}{D} = 1$	$\beta := 1$
Tau A	$\tau_A := \frac{t_A}{T} = 1$	
Tau B	$\tau_B := \frac{t_B}{T} = 1$	
Tau C	$\tau_C := \frac{t_C}{T} = 1$	$\tau := 1$
Gamma	$\gamma := \frac{D}{2T} = 12$	
Zeta AB	$\zeta_{AB} := \frac{g_{AB}}{D} = 0.227$	
Zeta BC	$\zeta_{BC} := \frac{g_{BC}}{D} = 0.227$	$\zeta := \zeta_{AB} = 0.227$

Theta A	$\Theta_A := 45\text{deg}$
Theta B	$\Theta_B := 90\text{deg}$
Theta C	$\Theta_C := 45\text{deg}$
Chord fixity parameter	$\underline{C}_w := 0.5$
	$C_1 := 2 \cdot (C - 0.5) = 0$
	$C_2 := \frac{C}{2} = 0.25$
	$C_3 := \frac{C}{5} = 0.1$

Axial load on one brace only

Chord saddle, Brace A, Eqn. (5)

$$SCF_{A,CS,BA} := \gamma \cdot \tau^{1.1} \cdot [1.11 - 3 \cdot (\beta - 0.52)^2] \cdot \sin(\Theta_A)^{1.6} + C_1 \cdot (0.8 \cdot \alpha - 6) \cdot \tau \cdot \beta^2 \cdot (1 - \beta^2)^{0.5} \cdot \sin(2 \cdot \Theta_A)^2 = 2.886$$

Chord crown, Brace A, Eqn. (6)

$$SCF_{A,CC,BA} := \gamma^{0.2} \cdot \tau \cdot [2.65 + 5 \cdot (\beta - 0.65)^2] + \tau \cdot \beta \cdot (C_2 \cdot \alpha - 3) \cdot \sin(\Theta_A) = 10.974$$

Brace saddle, Brace A, Eqn. (3)

$$SCF_{A,BS,BA} := 1.3 + \gamma \cdot \tau^{0.52} \cdot \alpha^{0.1} \cdot [0.187 - 1.25 \cdot \beta^{1.1} \cdot (\beta - 0.96)] \cdot \sin(\Theta_A)^{(2.7 - 0.01 \cdot \alpha)} = 2.395$$

Brace crown, Brace A, Eqn. (7)

$$SCF_{A,BC,BA} := 3 + \gamma^{1.2} \cdot (0.12 \cdot \exp(-4 \cdot \beta) + 0.011 \cdot \beta^2 - 0.045) + \beta \cdot \tau \cdot (C_3 \cdot \alpha - 1.2) = 5.547$$

Chord saddle, Brace B, Eqn. (5)

$$SCF_{A,CS,BB} := \gamma \cdot \tau^{1.1} \cdot [1.11 - 3 \cdot (\beta - 0.52)^2] \cdot \sin(\Theta_B)^{1.6} + C_1 \cdot (0.8 \cdot \alpha - 6) \cdot \tau \cdot \beta^2 \cdot (1 - \beta^2)^{0.5} \cdot \sin(2 \cdot \Theta_B)^2 = 2.886$$

Chord crown, Brace B, Eqn. (6)

$$SCF_{A,CC,BB} := \gamma^{0.2} \cdot \tau \cdot [2.65 + 5 \cdot (\beta - 0.65)^2] + \tau \cdot \beta \cdot (C_2 \cdot \alpha - 3) \cdot \sin(\Theta_B) = 13.299$$

Brace saddle, Brace B, Eqn. (3)

$$SCF_{A,BS,BB} := 1.3 + \gamma \cdot \tau^{0.52} \cdot \alpha^{0.1} \cdot [0.187 - 1.25 \cdot \beta^{1.1} \cdot (\beta - 0.96)] \cdot \sin(\Theta_B)^{(2.7 - 0.01 \cdot \alpha)} = 3.699$$

Brace crown, Brace B, Eqn. (7)

$$SCF_{A,BC,BB} := 3 + \gamma^{1.2} \cdot (0.12 \cdot \exp(-4 \cdot \beta) + 0.011 \cdot \beta^2 - 0.045) + \beta \cdot \tau \cdot (C_3 \cdot \alpha - 1.2) = 5.547$$

In-plane bending

Chord crown position, Loaded through Brace A, Eqn. (8)

$$SCF_{IPB.CC.BA} := 1.45 \cdot \beta \cdot \tau^{0.85} \cdot \gamma^{(1-0.68 \cdot \beta)} \cdot \sin(\Theta_A)^{0.7} = 2.52$$

Chord crown position, Loaded through Brace B, Eqn. (8)

$$SCF_{IPB.CC.BB} := 1.45 \cdot \beta \cdot \tau^{0.85} \cdot \gamma^{(1-0.68 \cdot \beta)} \cdot \sin(\Theta_B)^{0.7} = 3.211$$

Brace crown position, Loaded through Brace A, Eqn. (8)

$$SCF_{IPB.BC.BA} := 1 + 0.65 \cdot \beta \cdot \tau^{0.4} \cdot \gamma^{(1.09-0.77 \cdot \beta)} \cdot \sin(\Theta_A)^{(0.06 \cdot \gamma - 1.16)} = 2.677$$

Brace crown position, Loaded through Brace B, Eqn. (8)

$$SCF_{IPB.BC.BB} := 1 + 0.65 \cdot \beta \cdot \tau^{0.4} \cdot \gamma^{(1.09-0.77 \cdot \beta)} \cdot \sin(\Theta_B)^{(0.06 \cdot \gamma - 1.16)} = 2.44$$

Out-of-plane bending on one brace only

Chord SCF adjacent to diagonal brace A, Eqn. (30)

$$\lambda_{AB} := 1 + \frac{\zeta_{AB} \cdot \sin(\Theta_A)}{\beta_A} = 1.161$$

$$\lambda_{AC} := 1 + \frac{(\zeta_{AB} + \zeta_{BC} + \beta_B) \cdot \sin(\Theta_A)}{\beta_A} = 2.029$$

$$SCF_{OPB.C.BA} := Eqn_{10A} \left[1 - 0.08 \cdot (\beta_B \cdot \gamma)^{0.5} \cdot \exp(-0.8 \cdot x_{AB}) \right] \cdot \left[1 - 0.08 \cdot (\beta_C \cdot \gamma)^{0.5} \cdot \exp(-0.8 \cdot x_{AC}) \right] = 3.771$$

Chord SCF adjacent to diagonal brace B, Eqn. (30)

$$\lambda_{AB} := 1 + \frac{\zeta_{AB} \cdot \sin(\Theta_B)}{\beta_B} = 1.227 \quad P_1 = 1$$

$$\lambda_{BC} := 1 + \frac{\zeta_{BC} \cdot \sin(\Theta_B)}{\beta_B} = 1.227 \quad P_2 = 1$$

$$SCF_{OPB.C.BB} := Eqn_{10B} \left[1 - 0.08 \cdot (\beta_A \cdot \gamma)^{0.5} \cdot \exp(-0.8 \cdot x_{AB}) \right]^{P_1} \cdot \left[1 - 0.08 \cdot (\beta_C \cdot \gamma)^{0.5} \cdot \exp(-0.8 \cdot x_{BC}) \right]^{P_2} = 6.265$$

Brace A SCF, Eqn. (32)

$$SCF_{OPB.BA} := \tau^{-0.54} \cdot \gamma^{-0.05} \cdot (0.99 - 0.47 \cdot \beta + 0.08 \cdot \beta^4) \cdot SCF_{OPB.C.BA} = 1.998$$

Brace B SCF, Eqn. (32)

$$SCF_{OPB.BB} := \tau^{-0.54} \cdot \gamma^{-0.05} \cdot (0.99 - 0.47 \cdot \beta + 0.08 \cdot \beta^4) \cdot SCF_{OPB.C.BB} = 3.32$$

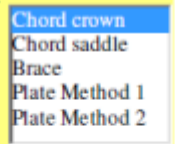
Appendix D – Mathcad extrapolation program

Hot spot stress extrapolation for S4 and S8R elements

Calculation is valid for tubular joints and plate joints.

Input parameters

Select what type component the program will be used for

point :=  point = 1

Chord

$$T_{\text{chord}} := 19.05 \text{ mm}$$

$$R_w := \frac{457.2 \text{ mm}}{2} = 228.6 \text{ mm}$$

Brace

$$t := 19.05 \text{ mm}$$

$$r := \frac{457.2 \text{ mm}}{2} = 228.6 \text{ mm}$$

Plate

$$T_{\text{plate}} := 10 \text{ mm}$$

Location of stress read out points

Chord

$$a_{\text{cc}} := 0.2 \cdot \sqrt{r \cdot t} = 13.2 \text{ mm}$$

$$b_{\text{cc}} := 0.4 \cdot \sqrt[4]{r \cdot t \cdot R \cdot T_{\text{chord}}} = 26.4 \text{ mm}$$

$$a_{\text{cs}} := 0.2 \cdot \sqrt{r \cdot t} = 13.2 \text{ mm}$$

$$b_{\text{cs}} := 2 \cdot \pi \cdot R \cdot \frac{5}{360} = 19.95 \text{ mm}$$

$$a := \begin{cases} a_{\text{cc}} & \text{if point} = 1 \\ a_{\text{cs}} & \text{if point} = 2 \\ a_{\text{b}} & \text{if point} = 3 \\ a_{\text{pl}} & \text{if point} = 4 \\ a_{\text{pl}} & \text{if point} = 5 \end{cases} = 13.198 \text{ mm}$$

Brace

$$a_{\text{b}} := 0.2 \cdot \sqrt{r \cdot t} = 13.2 \text{ mm}$$

$$b_{\text{b}} := 0.65 \cdot \sqrt{r \cdot t} = 42.89 \text{ mm}$$

$$b := \begin{cases} b_{\text{cc}} & \text{if point} = 1 \\ b_{\text{cs}} & \text{if point} = 2 \\ b_{\text{b}} & \text{if point} = 3 \\ b_{\text{pl}} & \text{if point} = 4 \\ b_{\text{pl}} & \text{if point} = 5 \end{cases} = 26.396 \text{ mm}$$

Plate

$$a_{\text{pl}} := 0.5 \cdot T_{\text{plate}} = 5 \text{ mm}$$

$$b_{\text{pl}} := 1.5 \cdot T_{\text{plate}} = 15 \text{ mm}$$

NOTE: Spreadsheet only supports TxT mesh for plate elements.

$$T_w := \begin{cases} T_{\text{chord}} & \text{if point} \leq 2 \\ t & \text{if point} = 3 \\ T_{\text{plate}} & \text{if point} \geq 4 \end{cases} = 19.05 \text{ mm}$$

Check of location of stress read out points (for tubular joints)

The stress read out points usually do not coincide with element nodes, centerlines or other key element points. Interpolation to these points is still possible, but care must be taken to interpolate from the closest integration points, so a check is implemented to see which elements the points are bordering to.

Chord

Element size $T = 19.05 \text{ mm}$

$$\begin{array}{l}
 a_{cc_no} := \begin{cases} 1 & \text{if } 0 \leq a_{cc} < T \\ 2 & \text{if } T \leq a_{cc} \leq 2T \\ 3 & \text{if } 2T \leq a_{cc} \leq 3T \\ \text{"NA"} & \text{otherwise} \end{cases} = 1 \\
 b_{cc_no} := \begin{cases} 1 & \text{if } 0 \leq b_{cc} < T \\ 2 & \text{if } T \leq b_{cc} \leq 2T \\ 3 & \text{if } 2T \leq b_{cc} < 3T \\ 4 & \text{if } 3T \leq b_{cc} < 4T \\ 5 & \text{if } 4T \leq b_{cc} < 5T \\ \text{"NA"} & \text{otherwise} \end{cases} = 2 \\
 a_{cs_no} := \begin{cases} 1 & \text{if } 0 \leq a_{cs} < T \\ 2 & \text{if } T \leq a_{cs} \leq 2T \\ 3 & \text{if } 2T \leq a_{cs} \leq 3T \\ \text{"NA"} & \text{otherwise} \end{cases} = 1 \\
 b_{cs_no} := \begin{cases} 1 & \text{if } 0 \leq b_{cs} < T \\ 2 & \text{if } T \leq b_{cs} \leq 2T \\ 3 & \text{if } 2T \leq b_{cs} < 3T \\ 4 & \text{if } 3T \leq b_{cs} < 4T \\ 5 & \text{if } 4T \leq b_{cs} < 5T \\ \text{"NA"} & \text{otherwise} \end{cases} = 2
 \end{array}$$

Brace

Element size

$t = 19.05 \text{ mm}$

$$\begin{array}{l}
 a_b_no := \begin{cases} 1 & \text{if } 0 \leq a_b < t \\ 2 & \text{if } t \leq a_b \leq 2t \\ 3 & \text{if } 2t \leq a_b \leq 3t \\ \text{"NA"} & \text{otherwise} \end{cases} = 1 \\
 b_b_no := \begin{cases} 1 & \text{if } 0 \leq b_b < t \\ 2 & \text{if } t \leq b_b \leq 2t \\ 3 & \text{if } 2t \leq b_b < 3t \\ 4 & \text{if } 3t \leq b_b < 4t \\ 5 & \text{if } 4t \leq b_b < 5t \\ \text{"NA"} & \text{otherwise} \end{cases} = 3
 \end{array}$$

Plate

$a_{pl_no} := 1$

$b_{pl_no} := 2$

General

$$\begin{array}{l}
 a_{no} := \begin{cases} a_{cc_no} & \text{if point} = 1 \\ a_{cs_no} & \text{if point} = 2 \\ a_b_no & \text{if point} = 3 \\ a_{pl_no} & \text{if point} = 4 \end{cases} \\
 b_{no} := \begin{cases} b_{cc_no} & \text{if point} = 1 \\ b_{cs_no} & \text{if point} = 2 \\ b_b_no & \text{if point} = 3 \\ b_{pl_no} & \text{if point} = 4 \end{cases}
 \end{array}$$

Integration points and numbering

Input required for the following elements:

$$a_{no} = 1$$

$$b_{no} = 2$$

The first number of points in the figure below represents element number (this can continue up to 4 elements for this Mathcad program).

The second number in the picture represents numbering sequence. It is important to input the correct stress in the correct input variable. Stresses from integration points are extrapolated pairwise.

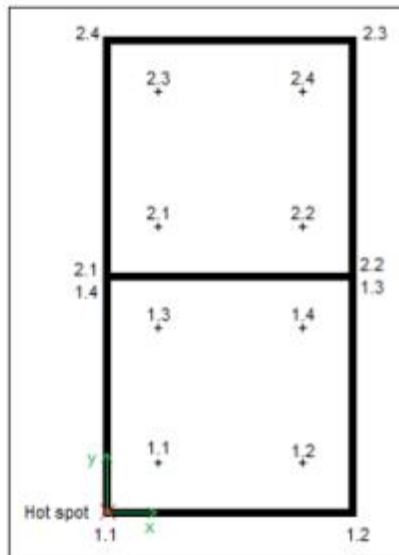


Figure showing integration point numbering and corner node numbering for use in this mathcad spreadsheet.

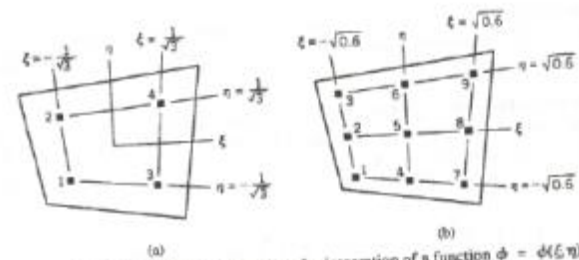


Figure 6.3-3. Sampling point locations for integration of a function $\phi = \phi(\xi, \eta)$, using Gauss rules of orders 2 (four points) and 3 (nine points).

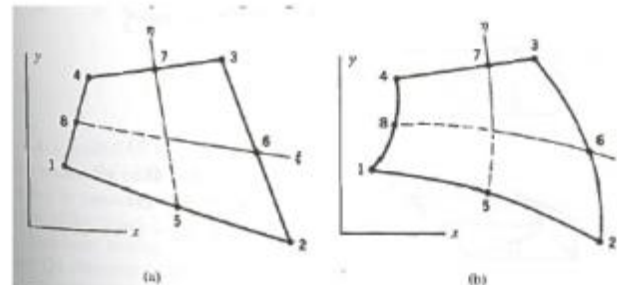


Figure 6.4-1. Eight-node plane serendipity elements in Cartesian coordinates x, y . Elements shown have (a) straight sides and midside nodes, and (b) some curved sides and off-center nodes.

Ref Cook, R. D., Malkus, D. S., Plesha, M. E., & Witt, R. J. (2002). *Concepts and Applications of Finite Element Analysis* (Fourth edition ed.): John Wiley & Sons, Inc.

Integration point stress input

Input should be normal stress, parallel stress and shear stress of each at each integration point. Normal stress has subscript "n", parallel stress has subscript "p". Shear stress is τ .

The stresses are extrapolated to hot spot, and transformed to effective hot spot stress at the hot spot location.

Element 1	Element 2	Element 3	Element 4
$\sigma_{n11} := 3.065\text{MPa}$ $\sigma_{n12} := 3.088\text{MPa}$	$\sigma_{n21} := 3.925\text{MPa}$ $\sigma_{n22} := 3.901\text{MPa}$	$\sigma_{n31} := 1.56\text{MPa}$ $\sigma_{n32} := 1.35\text{MPa}$	$\sigma_{n41} := 1.56\text{MPa}$ $\sigma_{n42} := 1.35\text{MPa}$
$\sigma_{n13} := 2.995\text{MPa}$ $\sigma_{n14} := 3.014\text{MPa}$	$\sigma_{n23} := 3.881\text{MPa}$ $\sigma_{n24} := 3.859\text{MPa}$	$\sigma_{n33} := 1.30\text{MPa}$ $\sigma_{n34} := 1.2\text{MPa}$	$\sigma_{n43} := 1.30\text{MPa}$ $\sigma_{n44} := 1.2\text{MPa}$
$\sigma_{p11} := 3.065\text{MPa}$ $\sigma_{p12} := 3.088\text{MPa}$	$\sigma_{p21} := 3.925\text{MPa}$ $\sigma_{p22} := 3.901\text{MPa}$	$\sigma_{p31} := 1.56\text{MPa}$ $\sigma_{p32} := 1.35\text{MPa}$	$\sigma_{p41} := 1.56\text{MPa}$ $\sigma_{p42} := 1.35\text{MPa}$
$\sigma_{p13} := 2.995\text{MPa}$ $\sigma_{p14} := 3.014\text{MPa}$	$\sigma_{p23} := 3.881\text{MPa}$ $\sigma_{p24} := 3.859\text{MPa}$	$\sigma_{p33} := 1.30\text{MPa}$ $\sigma_{p34} := 1.2\text{MPa}$	$\sigma_{p43} := 1.30\text{MPa}$ $\sigma_{p44} := 1.2\text{MPa}$
$\tau_{11} := 3.065\text{MPa}$ $\tau_{12} := 3.088\text{MPa}$	$\tau_{21} := 3.925\text{MPa}$ $\tau_{22} := 3.901\text{MPa}$	$\tau_{31} := 1.56\text{MPa}$ $\tau_{32} := 1.35\text{MPa}$	$\tau_{41} := 1.56\text{MPa}$ $\tau_{42} := 1.35\text{MPa}$
$\tau_{13} := 2.995\text{MPa}$ $\tau_{14} := 3.014\text{MPa}$	$\tau_{23} := 3.881\text{MPa}$ $\tau_{24} := 3.859\text{MPa}$	$\tau_{33} := 1.30\text{MPa}$ $\tau_{34} := 1.2\text{MPa}$	$\tau_{43} := 1.30\text{MPa}$ $\tau_{44} := 1.2\text{MPa}$

Note: If the "Input" variable does not specify elements 3 and 4 no input is needed here.

Integration point location and element geometry

Two options are offered in this program.

Manual input of nodal corner coordinates. These coordinates are transformed to coordinates for the integration points. Along with the input for integration point stress, this interpolation method can account for any plane geometry. Elements are treated as isoparametric Q4 elements to make the interpolation easier. This is an estimation for the S8R elements, but should not be of significant impact unless there are some special circumstances with the geometry, like significant curvature of element sides.

Quadratic elements assumes all corner angles are 90 degrees, AND element size is TxT. If this is the case, the integration point coordinates will be found automatically without additional input.

M :=

Manual input
Quadratic elements

M = 1

Conversion from abaqus coordinates to reference cartesian coordinate system (optional)

For 4 elements we have 10 nodes, with 2 coordinates (x, y) each.

Node 1 element 1 is reference node / hot-spot

$x_{a.11} := 0.3871\text{m}$	$x_{a.12} := 0.4010\text{m}$	$x_{a.13} := 0.4032\text{m}$	$x_{a.14} := 0.3871\text{m}$
$y_{a.11} := 1.5158\text{m}$	$y_{a.12} := 1.5167\text{m}$	$y_{a.13} := 1.5010\text{m}$	$y_{a.14} := 1.4999\text{m}$
$x_{a.31} := 0.3871\text{m}$	$x_{a.32} := 0.4052\text{m}$	$x_{a.33} := 0.4000\text{m}$	$x_{a.34} := 0.3871\text{m}$
$y_{a.31} := 1.4840\text{m}$	$y_{a.32} := 1.4853\text{m}$	$y_{a.33} := 4.0000\text{m}$	$y_{a.34} := 4.0000\text{m}$
		$x_{a.43} := 0.4000\text{m}$	$x_{a.44} := 0.3871\text{m}$
		$y_{a.43} := 4.000\text{m}$	$y_{a.44} := 4.0000\text{m}$

Manual input of element corner nodes coordinate values (nodal coordinates)

Subscript "c" signifies corner coordinates, "m" signifies manual input. First number is element number, second number is nodal number.

Depending on a_{no} and b_{no} , a number of the yellow fields have to be input. Blue fields are always 0mm (reference coordinate / hot spot location). Values input should match the elements listed in those parameters. Suggested values are computed at the right side of this page if abaqus coordinates have been entered on the page above.

Element 1

$x_{cm11} := 0\text{mm}$	$x_{cm12} := 13.9\text{mm}$	$x_{cm13} := 16.1\text{mm}$	$x_{cm14} := 0\text{mm}$	$x_{r.11} := 0\text{m}$	$x_{r.12} := x_{a.12} - x_{a.11} = 13.9\text{ mm}$
$y_{cm11} := 0\text{mm}$	$y_{cm12} := -0.9\text{mm}$	$y_{cm13} := 14.8\text{mm}$	$y_{cm14} := 15.9\text{mm}$	$y_{r.11} := 0\text{m}$	$y_{r.12} := y_{a.12} - y_{a.11} = 0.9\text{ mm}$
				$x_{r.13} := x_{a.13} - x_{a.11} = 16.1\text{ mm}$	$x_{r.14} := x_{a.14} - x_{a.11} = 0\text{ mm}$
				$y_{r.13} := y_{a.13} - y_{a.11} = -14.8\text{ mm}$	$y_{r.14} := y_{a.14} - y_{a.11} = -15.9\text{ mm}$

Element 2

$x_{cm21} := x_{cm14}$	$x_{cm22} := x_{cm13}$	$x_{cm23} := 18.1\text{mm}$	$x_{cm24} := 0\text{mm}$	$x_{r.23} := x_{a.32} - x_{a.11} = 18.1\text{ mm}$	$x_{r.24} := x_{a.31} - x_{a.11} = 0\text{ mm}$
$y_{cm21} := y_{cm14}$	$y_{cm22} := y_{cm13}$	$y_{cm23} := 30.5\text{mm}$	$y_{cm24} := 31.8\text{mm}$	$y_{r.23} := y_{a.32} - y_{a.11} = -30.5\text{ mm}$	$y_{r.24} := y_{a.31} - y_{a.11} = -31.8\text{ mm}$

Element 3

$x_{cm31} := x_{cm24}$	$x_{cm32} := x_{cm23}$	$x_{cm33} := 12.9\text{mm}$	$x_{cm34} := 0\text{mm}$	$x_{r.33} := x_{a.33} - x_{a.11} = 12.9\text{ mm}$	$x_{r.34} := x_{a.34} - x_{a.11} = 0\text{ mm}$
$y_{cm31} := y_{cm24}$	$y_{cm32} := y_{cm23}$	$y_{cm33} := 3\text{T}$	$y_{cm34} := 3\text{T}$	$y_{r.33} := y_{a.33} - y_{a.11} = 2484.2\text{ mm}$	$y_{r.34} := y_{a.34} - y_{a.11} = 2484.2\text{ mm}$

Element 4

$x_{cm41} := x_{cm34}$	$x_{cm42} := x_{cm33}$	$x_{cm43} := \text{T}$	$x_{cm44} := 0\text{mm}$	$x_{r.43} := x_{a.43} - x_{a.11} = 12.9\text{ mm}$	$x_{r.44} := x_{a.44} - x_{a.11} = 0\text{ mm}$
$y_{cm41} := y_{cm34}$	$y_{cm42} := y_{cm33}$	$y_{cm43} := 4\text{T}$	$y_{cm44} := 4\text{T}$	$y_{r.43} := y_{a.43} - y_{a.11} = 2484.2\text{ mm}$	$y_{r.44} := y_{a.44} - y_{a.11} = 2484.2\text{ mm}$

For quadratic elements

Elements are assumed quadratic with dimensions $T \times T$. Reference elements are of dimensions $2\xi \times 2\eta$. The center of the reference element has coordinate 0,0

in the ξ - η coordinate system. Integration points are located at $\pm \frac{1}{\sqrt{3}}\xi$ and $\pm \frac{1}{\sqrt{3}}\eta$.

The locations in cartesian coordinates compared to the hot spot are determined below.

Subscript "q" signifies quadratic elements, first number is element number, second number is nodal number.

Nodal coordinates for quadratic TxT elements

Subscript "c" signifies corner coordinates, subscript "q" signifies quadratic elements. First number is element number, second number is nodal number.

Element 1

$$x_{cq11} := 0mm \quad x_{cq12} := T \quad x_{cq13} := T \quad x_{cq14} := 0mm$$

$$y_{cq11} := 0mm \quad y_{cq12} := 0mm \quad y_{cq13} := T \quad y_{cq14} := T$$

Element 2

$$x_{cq21} := 0mm \quad x_{cq22} := T \quad x_{cq23} := T \quad x_{cq24} := 0mm$$

$$y_{cq21} := T \quad y_{cq22} := T \quad y_{cq23} := 2T \quad y_{cq24} := 2T$$

Element 3

$$x_{cq31} := 0mm \quad x_{cq32} := T \quad x_{cq33} := T \quad x_{cq34} := 0mm$$

$$y_{cq31} := 2T \quad y_{cq32} := 2T \quad y_{cq33} := 3T \quad y_{cq34} := 3T$$

Element 4

$$x_{cq41} := 0mm \quad x_{cq42} := T \quad x_{cq43} := T \quad x_{cq44} := 0mm$$

$$y_{cq41} := 3T \quad y_{cq42} := 3T \quad y_{cq43} := 4T \quad y_{cq44} := 4T$$

Nodal coordinates are selected based on choice of manual input or quadratic elements.

Element 1

$$x_{c11} := \begin{cases} x_{cm11} & \text{if } M = 1 \\ x_{cq11} & \text{if } M = 2 \end{cases} \quad x_{c12} := \begin{cases} x_{cm12} & \text{if } M = 1 \\ x_{cq12} & \text{if } M = 2 \end{cases}$$

$$x_{c13} := \begin{cases} x_{cm13} & \text{if } M = 1 \\ x_{cq13} & \text{if } M = 2 \end{cases} \quad x_{c14} := \begin{cases} x_{cm14} & \text{if } M = 1 \\ x_{cq14} & \text{if } M = 2 \end{cases}$$

$$y_{c11} := \begin{cases} y_{cm11} & \text{if } M = 1 \\ y_{cq11} & \text{if } M = 2 \end{cases} \quad y_{c12} := \begin{cases} y_{cm12} & \text{if } M = 1 \\ y_{cq12} & \text{if } M = 2 \end{cases}$$

$$y_{c13} := \begin{cases} y_{cm13} & \text{if } M = 1 \\ y_{cq13} & \text{if } M = 2 \end{cases} \quad y_{c14} := \begin{cases} y_{cm14} & \text{if } M = 1 \\ y_{cq14} & \text{if } M = 2 \end{cases}$$

Element 2

$$x_{c21} := \begin{cases} x_{cm21} & \text{if } M = 1 \\ x_{cq21} & \text{if } M = 2 \end{cases} \quad x_{c22} := \begin{cases} x_{cm22} & \text{if } M = 1 \\ x_{cq22} & \text{if } M = 2 \end{cases}$$

$$x_{c23} := \begin{cases} x_{cm23} & \text{if } M = 1 \\ x_{cq23} & \text{if } M = 2 \end{cases} \quad x_{c24} := \begin{cases} x_{cm24} & \text{if } M = 1 \\ x_{cq24} & \text{if } M = 2 \end{cases}$$

$$y_{c21} := \begin{cases} y_{cm21} & \text{if } M = 1 \\ y_{cq21} & \text{if } M = 2 \end{cases} \quad y_{c22} := \begin{cases} y_{cm22} & \text{if } M = 1 \\ y_{cq22} & \text{if } M = 2 \end{cases}$$

$$y_{c23} := \begin{cases} y_{cm23} & \text{if } M = 1 \\ y_{cq23} & \text{if } M = 2 \end{cases} \quad y_{c24} := \begin{cases} y_{cm24} & \text{if } M = 1 \\ y_{cq24} & \text{if } M = 2 \end{cases}$$

Element 3

$$x_{c31} := \begin{cases} x_{cm31} & \text{if } M = 1 \\ x_{cq31} & \text{if } M = 2 \end{cases} \quad x_{c32} := \begin{cases} x_{cm32} & \text{if } M = 1 \\ x_{cq32} & \text{if } M = 2 \end{cases}$$

$$x_{c33} := \begin{cases} x_{cm33} & \text{if } M = 1 \\ x_{cq33} & \text{if } M = 2 \end{cases} \quad x_{c34} := \begin{cases} x_{cm34} & \text{if } M = 1 \\ x_{cq34} & \text{if } M = 2 \end{cases}$$

$$y_{c31} := \begin{cases} y_{cm31} & \text{if } M = 1 \\ y_{cq31} & \text{if } M = 2 \end{cases} \quad y_{c32} := \begin{cases} y_{cm32} & \text{if } M = 1 \\ y_{cq32} & \text{if } M = 2 \end{cases}$$

$$y_{c33} := \begin{cases} y_{cm33} & \text{if } M = 1 \\ y_{cq33} & \text{if } M = 2 \end{cases} \quad y_{c34} := \begin{cases} y_{cm34} & \text{if } M = 1 \\ y_{cq34} & \text{if } M = 2 \end{cases}$$

Element 4

$$x_{c41} := \begin{cases} x_{cm41} & \text{if } M = 1 \\ x_{cq41} & \text{if } M = 2 \end{cases} \quad x_{c42} := \begin{cases} x_{cm42} & \text{if } M = 1 \\ x_{cq42} & \text{if } M = 2 \end{cases}$$

$$x_{c43} := \begin{cases} x_{cm43} & \text{if } M = 1 \\ x_{cq43} & \text{if } M = 2 \end{cases} \quad x_{c44} := \begin{cases} x_{cm44} & \text{if } M = 1 \\ x_{cq44} & \text{if } M = 2 \end{cases}$$

$$y_{c41} := \begin{cases} y_{cm41} & \text{if } M = 1 \\ y_{cq41} & \text{if } M = 2 \end{cases} \quad y_{c42} := \begin{cases} y_{cm42} & \text{if } M = 1 \\ y_{cq42} & \text{if } M = 2 \end{cases}$$

$$y_{c43} := \begin{cases} y_{cm43} & \text{if } M = 1 \\ y_{cq43} & \text{if } M = 2 \end{cases} \quad y_{c44} := \begin{cases} y_{cm44} & \text{if } M = 1 \\ y_{cq44} & \text{if } M = 2 \end{cases}$$

Determination of global coordinates of integration points

Element length, width and thickness

$$T = 19.05 \cdot \text{mm}$$

Integration point distance from element center

$$\xi := \frac{1}{\sqrt{3}}$$

in reference coordinate system ξ -direction

Integration point distance from element center

$$\eta := \frac{1}{\sqrt{3}}$$

in reference coordinate system η -direction

First shape function of Q4 element

$$N_1(\xi, \eta) := \frac{1}{4}(1 - \xi) \cdot (1 - \eta)$$

Second shape function of Q4 element

$$N_2(\xi, \eta) := \frac{1}{4}(1 + \xi) \cdot (1 - \eta)$$

Third shape function of Q4 element

$$N_3(\xi, \eta) := \frac{1}{4}(1 + \xi) \cdot (1 + \eta)$$

Fourth shape function of Q4 element

$$N_4(\xi, \eta) := \frac{1}{4}(1 - \xi) \cdot (1 + \eta)$$

The shape functions are used to interpolate the coordinates of a point within the elements from the coordinates of the nodes. Thus:

$$\begin{pmatrix} x \\ y \end{pmatrix} = \begin{bmatrix} \sum_i (N_i \cdot x_i) \\ \sum_i (N_i \cdot y_i) \end{bmatrix} = N \cdot c \quad \text{where}$$

$$c = (x_1 \ y_1 \ x_2 \ y_2 \ x_3 \ y_3 \ x_4 \ y_4)^T$$

$$N = \begin{pmatrix} N_1 & 0 & N_2 & 0 & N_3 & 0 & N_4 & 0 \\ 0 & N_1 & 0 & N_2 & 0 & N_3 & 0 & N_4 \end{pmatrix}$$

So to find the global coordinates for 4 points within each element we have

$$\begin{pmatrix} x_{11} \\ y_{11} \\ x_{12} \\ y_{12} \\ x_{13} \\ y_{13} \\ x_{14} \\ y_{14} \end{pmatrix} = \begin{pmatrix} N_1(-\xi, -\eta) & 0 & N_2(-\xi, -\eta) & 0 & N_3(-\xi, -\eta) & 0 & N_4(-\xi, -\eta) & 0 \\ 0 & N_1(-\xi, -\eta) & 0 & N_2(-\xi, -\eta) & 0 & N_3(-\xi, -\eta) & 0 & N_4(-\xi, -\eta) \\ N_1(\xi, -\eta) & 0 & N_2(\xi, -\eta) & 0 & N_3(\xi, -\eta) & 0 & N_4(\xi, -\eta) & 0 \\ 0 & N_1(\xi, -\eta) & 0 & N_2(\xi, -\eta) & 0 & N_3(\xi, -\eta) & 0 & N_4(\xi, -\eta) \\ N_1(\xi, \eta) & 0 & N_2(\xi, \eta) & 0 & N_3(\xi, \eta) & 0 & N_4(\xi, \eta) & 0 \\ 0 & N_1(\xi, \eta) & 0 & N_2(\xi, \eta) & 0 & N_3(\xi, \eta) & 0 & N_4(\xi, \eta) \\ N_1(-\xi, \eta) & 0 & N_2(-\xi, \eta) & 0 & N_3(-\xi, \eta) & 0 & N_4(-\xi, \eta) & 0 \\ 0 & N_1(-\xi, \eta) & 0 & N_2(-\xi, \eta) & 0 & N_3(-\xi, \eta) & 0 & N_4(-\xi, \eta) \end{pmatrix} \begin{pmatrix} x_{c11} \\ y_{c11} \\ x_{c12} \\ y_{c12} \\ x_{c13} \\ y_{c13} \\ x_{c14} \\ y_{c14} \end{pmatrix}$$

$$\begin{pmatrix} x_{21} \\ y_{21} \\ x_{22} \\ y_{22} \\ x_{23} \\ y_{23} \\ x_{24} \\ y_{24} \end{pmatrix} = \begin{pmatrix} N_1(-\xi, -\eta) & 0 & N_2(-\xi, -\eta) & 0 & N_3(-\xi, -\eta) & 0 & N_4(-\xi, -\eta) & 0 \\ 0 & N_1(-\xi, -\eta) & 0 & N_2(-\xi, -\eta) & 0 & N_3(-\xi, -\eta) & 0 & N_4(-\xi, -\eta) \\ N_1(\xi, -\eta) & 0 & N_2(\xi, -\eta) & 0 & N_3(\xi, -\eta) & 0 & N_4(\xi, -\eta) & 0 \\ 0 & N_1(\xi, -\eta) & 0 & N_2(\xi, -\eta) & 0 & N_3(\xi, -\eta) & 0 & N_4(\xi, -\eta) \\ N_1(\xi, \eta) & 0 & N_2(\xi, \eta) & 0 & N_3(\xi, \eta) & 0 & N_4(\xi, \eta) & 0 \\ 0 & N_1(\xi, \eta) & 0 & N_2(\xi, \eta) & 0 & N_3(\xi, \eta) & 0 & N_4(\xi, \eta) \\ N_1(-\xi, \eta) & 0 & N_2(-\xi, \eta) & 0 & N_3(-\xi, \eta) & 0 & N_4(-\xi, \eta) & 0 \\ 0 & N_1(-\xi, \eta) & 0 & N_2(-\xi, \eta) & 0 & N_3(-\xi, \eta) & 0 & N_4(-\xi, \eta) \end{pmatrix} \begin{pmatrix} x_{c21} \\ y_{c21} \\ x_{c22} \\ y_{c22} \\ x_{c23} \\ y_{c23} \\ x_{c24} \\ y_{c24} \end{pmatrix}$$

$$\begin{pmatrix} x_{31} \\ y_{31} \\ x_{32} \\ y_{32} \\ x_{33} \\ y_{33} \\ x_{34} \\ y_{34} \end{pmatrix} = \begin{pmatrix} N_1(-\xi, -\eta) & 0 & N_2(-\xi, -\eta) & 0 & N_3(-\xi, -\eta) & 0 & N_4(-\xi, -\eta) & 0 \\ 0 & N_1(-\xi, -\eta) & 0 & N_2(-\xi, -\eta) & 0 & N_3(-\xi, -\eta) & 0 & N_4(-\xi, -\eta) \\ N_1(\xi, -\eta) & 0 & N_2(\xi, -\eta) & 0 & N_3(\xi, -\eta) & 0 & N_4(\xi, -\eta) & 0 \\ 0 & N_1(\xi, -\eta) & 0 & N_2(\xi, -\eta) & 0 & N_3(\xi, -\eta) & 0 & N_4(\xi, -\eta) \\ N_1(\xi, \eta) & 0 & N_2(\xi, \eta) & 0 & N_3(\xi, \eta) & 0 & N_4(\xi, \eta) & 0 \\ 0 & N_1(\xi, \eta) & 0 & N_2(\xi, \eta) & 0 & N_3(\xi, \eta) & 0 & N_4(\xi, \eta) \\ N_1(-\xi, \eta) & 0 & N_2(-\xi, \eta) & 0 & N_3(-\xi, \eta) & 0 & N_4(-\xi, \eta) & 0 \\ 0 & N_1(-\xi, \eta) & 0 & N_2(-\xi, \eta) & 0 & N_3(-\xi, \eta) & 0 & N_4(-\xi, \eta) \end{pmatrix} \begin{pmatrix} x_{c31} \\ y_{c31} \\ x_{c32} \\ y_{c32} \\ x_{c33} \\ y_{c33} \\ x_{c34} \\ y_{c34} \end{pmatrix}$$

$$\begin{pmatrix} x_{41} \\ y_{41} \\ x_{42} \\ y_{42} \\ x_{43} \\ y_{43} \\ x_{44} \\ y_{44} \end{pmatrix} = \begin{pmatrix} N_1(-\xi, -\eta) & 0 & N_2(-\xi, -\eta) & 0 & N_3(-\xi, -\eta) & 0 & N_4(-\xi, -\eta) & 0 \\ 0 & N_1(-\xi, -\eta) & 0 & N_2(-\xi, -\eta) & 0 & N_3(-\xi, -\eta) & 0 & N_4(-\xi, -\eta) \\ N_1(\xi, -\eta) & 0 & N_2(\xi, -\eta) & 0 & N_3(\xi, -\eta) & 0 & N_4(\xi, -\eta) & 0 \\ 0 & N_1(\xi, -\eta) & 0 & N_2(\xi, -\eta) & 0 & N_3(\xi, -\eta) & 0 & N_4(\xi, -\eta) \\ N_1(\xi, \eta) & 0 & N_2(\xi, \eta) & 0 & N_3(\xi, \eta) & 0 & N_4(\xi, \eta) & 0 \\ 0 & N_1(\xi, \eta) & 0 & N_2(\xi, \eta) & 0 & N_3(\xi, \eta) & 0 & N_4(\xi, \eta) \\ N_1(-\xi, \eta) & 0 & N_2(-\xi, \eta) & 0 & N_3(-\xi, \eta) & 0 & N_4(-\xi, \eta) & 0 \\ 0 & N_1(-\xi, \eta) & 0 & N_2(-\xi, \eta) & 0 & N_3(-\xi, \eta) & 0 & N_4(-\xi, \eta) \end{pmatrix} \begin{pmatrix} x_{c41} \\ y_{c41} \\ x_{c42} \\ y_{c42} \\ x_{c43} \\ y_{c43} \\ x_{c44} \\ y_{c44} \end{pmatrix}$$

Global coordinates of integration points

Number refers to element number, subscripts "n" and "p" signifies positive or negative of ξ and η respectively. I.e np means negative ξ and positive η , pn means positive ξ and negative η .

Element 1

$$\begin{pmatrix} x_{11} \\ y_{11} \\ x_{12} \\ y_{12} \\ x_{13} \\ y_{13} \\ x_{14} \\ y_{14} \end{pmatrix} = \begin{pmatrix} 3.036 \\ 3.161 \\ 11.329 \\ 2.617 \\ 12.331 \\ 11.706 \\ 3.304 \\ 12.316 \end{pmatrix} \cdot \text{mm}$$

Element 2

$$\begin{pmatrix} x_{21} \\ y_{21} \\ x_{22} \\ y_{22} \\ x_{23} \\ y_{23} \\ x_{24} \\ y_{24} \end{pmatrix} = \begin{pmatrix} 3.492 \\ 19.019 \\ 13.031 \\ 18.359 \\ 13.942 \\ 27.448 \\ 3.736 \\ 28.174 \end{pmatrix} \cdot \text{mm}$$

Element 3

$$\begin{pmatrix} x_{31} \\ y_{31} \\ x_{32} \\ y_{32} \\ x_{33} \\ y_{33} \\ x_{34} \\ y_{34} \end{pmatrix} = \begin{pmatrix} 3.593 \\ 36.94 \\ 13.408 \\ 36.348 \\ 11.041 \\ 51.576 \\ 2.958 \\ 51.735 \end{pmatrix} \cdot \text{mm}$$

Element 4

$$\begin{pmatrix} x_{41} \\ y_{41} \\ x_{42} \\ y_{42} \\ x_{43} \\ y_{43} \\ x_{44} \\ y_{44} \end{pmatrix} = \begin{pmatrix} 3.001 \\ 61.176 \\ 11.199 \\ 61.176 \\ 13.999 \\ 72.174 \\ 3.751 \\ 72.174 \end{pmatrix} \cdot \text{mm}$$

Extrapolation of stresses to center line

For element 1

Node 1 and 2 extrapolated to centerline

$$\begin{pmatrix} \sigma_{n.cl.1.12} \\ \sigma_{p.cl.1.12} \\ \tau_{cl.1.12} \end{pmatrix} := \begin{bmatrix} \sigma_{n11} + \frac{(\sigma_{n11} - \sigma_{n12})}{(x_{11} - x_{12})} \cdot (0 - x_{11}) \\ \sigma_{p11} + \frac{(\sigma_{p11} - \sigma_{p12})}{(x_{11} - x_{12})} \cdot (0 - x_{11}) \\ \tau_{11} + \frac{(\tau_{11} - \tau_{12})}{(x_{11} - x_{12})} \cdot (0 - x_{11}) \end{bmatrix} = \begin{pmatrix} 3.057 \\ 3.057 \\ 3.057 \end{pmatrix} \cdot \text{MPa}$$

Node 3 and 4 extrapolated to centerline

$$\begin{pmatrix} \sigma_{n.cl.1.34} \\ \sigma_{p.cl.1.34} \\ \tau_{cl.1.34} \end{pmatrix} := \begin{bmatrix} \sigma_{n13} + \frac{(\sigma_{n13} - \sigma_{n14})}{(x_{14} - x_{13})} \cdot (0 - x_{14}) \\ \sigma_{p13} + \frac{(\sigma_{p13} - \sigma_{p14})}{(x_{14} - x_{13})} \cdot (0 - x_{14}) \\ \tau_{13} + \frac{(\tau_{13} - \tau_{14})}{(x_{14} - x_{13})} \cdot (0 - x_{14}) \end{bmatrix} = \begin{pmatrix} 2.988 \\ 2.988 \\ 2.988 \end{pmatrix} \cdot \text{MPa}$$

For element 2

Node 1 and 2 extrapolated to centerline

$$\begin{pmatrix} \sigma_{n.cl.2.12} \\ \sigma_{p.cl.2.12} \\ \tau_{cl.2.12} \end{pmatrix} := \begin{bmatrix} \sigma_{n21} + \frac{(\sigma_{n21} - \sigma_{n22})}{(x_{21} - x_{22})} \cdot (0 - x_{21}) \\ \sigma_{p21} + \frac{(\sigma_{p21} - \sigma_{p22})}{(x_{21} - x_{22})} \cdot (0 - x_{21}) \\ \tau_{21} + \frac{(\tau_{21} - \tau_{22})}{(x_{21} - x_{22})} \cdot (0 - x_{21}) \end{bmatrix} = \begin{pmatrix} 3.934 \\ 3.934 \\ 3.934 \end{pmatrix} \cdot \text{MPa}$$

Node 3 and 4 extrapolated to centerline

$$\begin{pmatrix} \sigma_{n.cl.2.34} \\ \sigma_{p.cl.2.34} \\ \tau_{cl.2.34} \end{pmatrix} := \begin{bmatrix} \sigma_{n23} + \frac{(\sigma_{n23} - \sigma_{n24})}{(x_{24} - x_{23})} \cdot (0 - x_{24}) \\ \sigma_{p23} + \frac{(\sigma_{p23} - \sigma_{p24})}{(x_{24} - x_{23})} \cdot (0 - x_{24}) \\ \tau_{23} + \frac{(\tau_{23} - \tau_{24})}{(x_{24} - x_{23})} \cdot (0 - x_{24}) \end{bmatrix} = \begin{pmatrix} 3.889 \\ 3.889 \\ 3.889 \end{pmatrix} \cdot \text{MPa}$$

For element 3

Node 1 and 2 extrapolated to centerline

$$\begin{pmatrix} \sigma_{n.cl.3.12} \\ \sigma_{p.cl.3.12} \\ \tau_{cl.3.12} \end{pmatrix} := \begin{bmatrix} \sigma_{n31} + \frac{(\sigma_{n31} - \sigma_{n32})}{(x_{31} - x_{32})} \cdot (0 - x_{31}) \\ \sigma_{p31} + \frac{(\sigma_{p31} - \sigma_{p32})}{(x_{31} - x_{32})} \cdot (0 - x_{31}) \\ \tau_{31} + \frac{(\tau_{31} - \tau_{32})}{(x_{31} - x_{32})} \cdot (0 - x_{31}) \end{bmatrix} = \begin{pmatrix} 1.637 \\ 1.637 \\ 1.637 \end{pmatrix} \cdot \text{MPa}$$

Node 3 and 4 extrapolated to centerline

$$\begin{pmatrix} \sigma_{n.cl.3.34} \\ \sigma_{p.cl.3.34} \\ \tau_{cl.3.34} \end{pmatrix} := \begin{bmatrix} \sigma_{n33} + \frac{(\sigma_{n33} - \sigma_{n34})}{(x_{34} - x_{33})} \cdot (0 - x_{34}) \\ \sigma_{p33} + \frac{(\sigma_{p33} - \sigma_{p34})}{(x_{34} - x_{33})} \cdot (0 - x_{34}) \\ \tau_{33} + \frac{(\tau_{33} - \tau_{34})}{(x_{34} - x_{33})} \cdot (0 - x_{34}) \end{bmatrix} = \begin{pmatrix} 1.337 \\ 1.337 \\ 1.337 \end{pmatrix} \cdot \text{MPa}$$

For element 4

Node 1 and 2 extrapolated to centerline

$$\begin{pmatrix} \sigma_{n.cl.4.12} \\ \sigma_{p.cl.4.12} \\ \tau_{cl.4.12} \end{pmatrix} := \begin{bmatrix} \sigma_{n41} + \frac{(\sigma_{n41} - \sigma_{n42})}{(x_{41} - x_{42})} \cdot (0 - x_{41}) \\ \sigma_{p41} + \frac{(\sigma_{p41} - \sigma_{p42})}{(x_{41} - x_{42})} \cdot (0 - x_{41}) \\ \tau_{41} + \frac{(\tau_{41} - \tau_{42})}{(x_{41} - x_{42})} \cdot (0 - x_{41}) \end{bmatrix} = \begin{pmatrix} 1.637 \\ 1.637 \\ 1.637 \end{pmatrix} \cdot \text{MPa}$$

Node 3 and 4 extrapolated to centerline

$$\begin{pmatrix} \sigma_{n.cl.4.34} \\ \sigma_{p.cl.4.34} \\ \tau_{cl.4.34} \end{pmatrix} := \begin{bmatrix} \sigma_{n43} + \frac{(\sigma_{n43} - \sigma_{n44})}{(x_{44} - x_{43})} \cdot (0 - x_{44}) \\ \sigma_{p43} + \frac{(\sigma_{p43} - \sigma_{p44})}{(x_{44} - x_{43})} \cdot (0 - x_{44}) \\ \tau_{43} + \frac{(\tau_{43} - \tau_{44})}{(x_{44} - x_{43})} \cdot (0 - x_{44}) \end{bmatrix} = \begin{pmatrix} 1.337 \\ 1.337 \\ 1.337 \end{pmatrix} \cdot \text{MPa}$$

Determination of y-coordinate of extrapolated stress on centerline

Assuming an arbitrary isoparametric Q4 geometry, the global y coordinate of the interpolated stress value on the centerline must be determined. This is the point on the centerline which has the extrapolated stress value. All values of global x coordinate will be 0 on the centerline, so this parameter is dismissed in the calculations.

The y coordinate of the extrapolated stress value has reference coordinates $(-1, +\frac{1}{\sqrt{3}})$. Like before the global coordinates at this point is interpolated over the element by use of the element shape functions.

$y_{cl.1.1}$ is the point on element 1 interpolated to from nodes 1 and 2. "cl" signifies centerline, the first number signifies element number, second number refers to node pairs (1 = node 1 and 2, 2 = node 3 and 4).

Reference coordinates are $\xi = -1$ and $\eta = \frac{1}{\sqrt{3}}$

Element 1

$$\begin{pmatrix} y_{cl.1.1} \\ y_{cl.1.2} \end{pmatrix} := \begin{pmatrix} N_1(\xi, \eta) & N_2(\xi, \eta) & N_3(\xi, \eta) & N_4(\xi, \eta) \\ N_1(\xi, -\eta) & N_2(\xi, -\eta) & N_3(\xi, -\eta) & N_4(\xi, -\eta) \end{pmatrix} \begin{pmatrix} y_{c11} \\ y_{c12} \\ y_{c13} \\ y_{c14} \end{pmatrix} = \begin{pmatrix} 3.36 \\ 12.54 \end{pmatrix} \cdot \text{mm}$$

Element 2

$$\begin{pmatrix} y_{cl.2.1} \\ y_{cl.2.2} \end{pmatrix} := \begin{pmatrix} N_1(\xi, \eta) & N_2(\xi, \eta) & N_3(\xi, \eta) & N_4(\xi, \eta) \\ N_1(\xi, -\eta) & N_2(\xi, -\eta) & N_3(\xi, -\eta) & N_4(\xi, -\eta) \end{pmatrix} \begin{pmatrix} y_{c21} \\ y_{c22} \\ y_{c23} \\ y_{c24} \end{pmatrix} = \begin{pmatrix} 19.26 \\ 28.44 \end{pmatrix} \cdot \text{mm}$$

Element 3

$$\begin{pmatrix} y_{cl.3.1} \\ y_{cl.3.2} \end{pmatrix} := \begin{pmatrix} N_1(\xi, \eta) & N_2(\xi, \eta) & N_3(\xi, \eta) & N_4(\xi, \eta) \\ N_1(\xi, -\eta) & N_2(\xi, -\eta) & N_3(\xi, -\eta) & N_4(\xi, -\eta) \end{pmatrix} \begin{pmatrix} y_{c31} \\ y_{c32} \\ y_{c33} \\ y_{c34} \end{pmatrix} = \begin{pmatrix} 37.157 \\ 51.793 \end{pmatrix} \cdot \text{mm}$$

Element 4

$$\begin{pmatrix} y_{cl.4.1} \\ y_{cl.4.2} \end{pmatrix} := \begin{pmatrix} N_1(\xi, \eta) & N_2(\xi, \eta) & N_3(\xi, \eta) & N_4(\xi, \eta) \\ N_1(\xi, -\eta) & N_2(\xi, -\eta) & N_3(\xi, -\eta) & N_4(\xi, -\eta) \end{pmatrix} \begin{pmatrix} y_{c41} \\ y_{c42} \\ y_{c43} \\ y_{c44} \end{pmatrix} = \begin{pmatrix} 61.176 \\ 72.174 \end{pmatrix} \cdot \text{mm}$$

Determining stresses at read-out points and extrapolation to hot-spot

For interpolation/extrapolation of stresses to read out points it is assumed that a and b can be located on several elements (1 to 4), and on an arbitrary location along the line intersecting the hot spot and the stress read out points. Because of this several interpolations are performed, but only the relevant ones are used further in calculations. This is done by if/else arguments.

Read out points are

a = 13.198·mm at element no a_{no} = 1 b = 26.396·mm at element no b_{no} = 2 T = 19.05·mm

Stresses at locations are

$\begin{pmatrix} \sigma_{n.cl.1.12} \\ \sigma_{p.cl.1.12} \\ \tau_{cl.1.12} \end{pmatrix} = \begin{pmatrix} 3.057 \\ 3.057 \\ 3.057 \end{pmatrix} \cdot \text{MPa}$	at location	$y_{cl.1.1} = 3.36 \cdot \text{mm}$	$\begin{pmatrix} \sigma_{n.cl.2.12} \\ \sigma_{p.cl.2.12} \\ \tau_{cl.2.12} \end{pmatrix} = \begin{pmatrix} 3.934 \\ 3.934 \\ 3.934 \end{pmatrix} \cdot \text{MPa}$	at location	$y_{cl.2.1} = 19.26 \cdot \text{mm}$
$\begin{pmatrix} \sigma_{n.cl.1.34} \\ \sigma_{p.cl.1.34} \\ \tau_{cl.1.34} \end{pmatrix} = \begin{pmatrix} 2.988 \\ 2.988 \\ 2.988 \end{pmatrix} \cdot \text{MPa}$	at location	$y_{cl.1.2} = 12.54 \cdot \text{mm}$	$\begin{pmatrix} \sigma_{n.cl.2.34} \\ \sigma_{p.cl.2.34} \\ \tau_{cl.2.34} \end{pmatrix} = \begin{pmatrix} 3.889 \\ 3.889 \\ 3.889 \end{pmatrix} \cdot \text{MPa}$	at location	$y_{cl.2.2} = 28.44 \cdot \text{mm}$
$\begin{pmatrix} \sigma_{n.cl.3.12} \\ \sigma_{p.cl.3.12} \\ \tau_{cl.3.12} \end{pmatrix} = \begin{pmatrix} 1.637 \\ 1.637 \\ 1.637 \end{pmatrix} \cdot \text{MPa}$	at location	$y_{cl.3.1} = 37.157 \cdot \text{mm}$	$\begin{pmatrix} \sigma_{n.cl.4.12} \\ \sigma_{p.cl.4.12} \\ \tau_{cl.4.12} \end{pmatrix} = \begin{pmatrix} 1.637 \\ 1.637 \\ 1.637 \end{pmatrix} \cdot \text{MPa}$	at location	$y_{cl.4.1} = 61.176 \cdot \text{mm}$
$\begin{pmatrix} \sigma_{n.cl.3.34} \\ \sigma_{p.cl.3.34} \\ \tau_{cl.3.34} \end{pmatrix} = \begin{pmatrix} 1.337 \\ 1.337 \\ 1.337 \end{pmatrix} \cdot \text{MPa}$	at location	$y_{cl.3.2} = 51.793 \cdot \text{mm}$	$\begin{pmatrix} \sigma_{n.cl.4.34} \\ \sigma_{p.cl.4.34} \\ \tau_{cl.4.34} \end{pmatrix} = \begin{pmatrix} 1.337 \\ 1.337 \\ 1.337 \end{pmatrix} \cdot \text{MPa}$	at location	$y_{cl.4.2} = 72.174 \cdot \text{mm}$

if a is between the hot spot and second pair of integration points (the case for plate, 0.5T)

$$\begin{pmatrix} \sigma_{n,a1} \\ \sigma_{p,a1} \\ \tau_{a1} \end{pmatrix} = \begin{pmatrix} \frac{\sigma_{n,cl.1.12} - \sigma_{n,cl.1.34}}{y_{cl.1.1} - y_{cl.1.2}} (a - y_{cl.1.1}) + \sigma_{n,cl.1.12} \\ \frac{\sigma_{p,cl.1.12} - \sigma_{p,cl.1.34}}{y_{cl.1.1} - y_{cl.1.2}} (a - y_{cl.1.1}) + \sigma_{p,cl.1.12} \\ \frac{\tau_{cl.1.12} - \tau_{cl.1.34}}{y_{cl.1.1} - y_{cl.1.2}} (a - y_{cl.1.1}) + \tau_{cl.1.12} \end{pmatrix} = \begin{pmatrix} 2.983 \\ 2.983 \\ 2.983 \end{pmatrix} \text{MPa}$$

if a is between the second and third pairs of integration points

$$\begin{pmatrix} \sigma_{n,a2} \\ \sigma_{p,a2} \\ \tau_{a2} \end{pmatrix} = \begin{pmatrix} \frac{\sigma_{n,cl.1.34} - \sigma_{n,cl.2.12}}{y_{cl.1.2} - y_{cl.2.1}} (a - y_{cl.1.2}) + \sigma_{n,cl.1.34} \\ \frac{\sigma_{p,cl.1.34} - \sigma_{p,cl.2.12}}{y_{cl.1.2} - y_{cl.2.1}} (a - y_{cl.1.2}) + \sigma_{p,cl.1.34} \\ \frac{\tau_{cl.1.34} - \tau_{cl.2.12}}{y_{cl.1.2} - y_{cl.2.1}} (a - y_{cl.1.2}) + \tau_{cl.1.34} \end{pmatrix} = \begin{pmatrix} 3.081 \\ 3.081 \\ 3.081 \end{pmatrix} \text{MPa}$$

if a is between the third pair of integration points and the far edge of element 2

$$\begin{pmatrix} \sigma_{n,a3} \\ \sigma_{p,a3} \\ \tau_{a3} \end{pmatrix} = \begin{pmatrix} \frac{\sigma_{n,cl.2.12} - \sigma_{n,cl.2.34}}{y_{cl.2.1} - y_{cl.2.2}} (a - y_{cl.2.1}) + \sigma_{n,cl.2.12} \\ \frac{\sigma_{p,cl.2.12} - \sigma_{p,cl.2.34}}{y_{cl.2.1} - y_{cl.2.2}} (a - y_{cl.2.1}) + \sigma_{p,cl.2.12} \\ \frac{\tau_{cl.2.12} - \tau_{cl.2.34}}{y_{cl.2.1} - y_{cl.2.2}} (a - y_{cl.2.1}) + \tau_{cl.2.12} \end{pmatrix} = \mathbf{\cdot} \text{MPa}$$

if b is between the hot spot and second pair of integration points

$$\begin{pmatrix} \sigma_{n.b1} \\ \sigma_{p.b1} \\ \tau_{b1} \end{pmatrix} := \begin{bmatrix} \frac{\sigma_{n.cl.1.12} - \sigma_{n.cl.1.34}}{y_{cl.1.1} - y_{cl.1.2}} \cdot (b - y_{cl.1.1}) + \sigma_{n.cl.1.12} \\ \frac{\sigma_{p.cl.1.12} - \sigma_{p.cl.1.34}}{y_{cl.1.1} - y_{cl.1.2}} \cdot (b - y_{cl.1.1}) + \sigma_{p.cl.1.12} \\ \frac{\tau_{cl.1.12} - \tau_{cl.1.34}}{y_{cl.1.1} - y_{cl.1.2}} \cdot (b - y_{cl.1.1}) + \tau_{cl.1.12} \end{bmatrix} = \begin{pmatrix} 2.885 \\ 2.885 \\ 2.885 \end{pmatrix} \cdot \text{MPa}$$

if b is between the second and third pairs of integration points

$$\begin{pmatrix} \sigma_{n.b2} \\ \sigma_{p.b2} \\ \tau_{b2} \end{pmatrix} := \begin{bmatrix} \frac{\sigma_{n.cl.1.34} - \sigma_{n.cl.2.12}}{y_{cl.1.2} - y_{cl.2.1}} \cdot (b - y_{cl.1.2}) + \sigma_{n.cl.1.34} \\ \frac{\sigma_{p.cl.1.34} - \sigma_{p.cl.2.12}}{y_{cl.1.2} - y_{cl.2.1}} \cdot (b - y_{cl.1.2}) + \sigma_{p.cl.1.34} \\ \frac{\tau_{cl.1.34} - \tau_{cl.2.12}}{y_{cl.1.2} - y_{cl.2.1}} \cdot (b - y_{cl.1.2}) + \tau_{cl.1.34} \end{bmatrix} = \begin{pmatrix} 4.938 \\ 4.938 \\ 4.938 \end{pmatrix} \cdot \text{MPa}$$

if b is between the third and fourth pairs of integration points (the case for plate, 1.5T)

$$\begin{pmatrix} \sigma_{n.b3} \\ \sigma_{p.b3} \\ \tau_{b3} \end{pmatrix} := \begin{bmatrix} \frac{\sigma_{n.cl.2.12} - \sigma_{n.cl.2.34}}{y_{cl.2.1} - y_{cl.2.2}} \cdot (b - y_{cl.2.1}) + \sigma_{n.cl.2.12} \\ \frac{\sigma_{p.cl.2.12} - \sigma_{p.cl.2.34}}{y_{cl.2.1} - y_{cl.2.2}} \cdot (b - y_{cl.2.1}) + \sigma_{p.cl.2.12} \\ \frac{\tau_{cl.2.12} - \tau_{cl.2.34}}{y_{cl.2.1} - y_{cl.2.2}} \cdot (b - y_{cl.2.1}) + \tau_{cl.2.12} \end{bmatrix} = \begin{pmatrix} 3.899 \\ 3.899 \\ 3.899 \end{pmatrix} \cdot \text{MPa}$$

if b is between the fourth and fifth pairs of integration points

$$\begin{pmatrix} \sigma_{n.b4} \\ \sigma_{p.b4} \\ \tau_{b4} \end{pmatrix} := \begin{pmatrix} \frac{\sigma_{n.cl.2.34} - \sigma_{n.cl.3.12}}{y_{cl.2.2} - y_{cl.3.1}} \cdot (b - y_{cl.2.2}) + \sigma_{n.cl.2.34} \\ \frac{\sigma_{p.cl.2.34} - \sigma_{p.cl.3.12}}{y_{cl.2.2} - y_{cl.3.1}} \cdot (b - y_{cl.2.2}) + \sigma_{p.cl.2.34} \\ \frac{\tau_{cl.2.34} - \tau_{cl.3.12}}{y_{cl.2.2} - y_{cl.3.1}} \cdot (b - y_{cl.2.2}) + \tau_{cl.2.34} \end{pmatrix} = \begin{pmatrix} 4.417 \\ 4.417 \\ 4.417 \end{pmatrix} \cdot \text{MPa}$$

if b is between the fifth and sixth pairs of integration points

$$\begin{pmatrix} \sigma_{n.b5} \\ \sigma_{p.b5} \\ \tau_{b5} \end{pmatrix} := \begin{pmatrix} \frac{\sigma_{n.cl.3.12} - \sigma_{n.cl.3.34}}{y_{cl.3.1} - y_{cl.3.2}} \cdot (b - y_{cl.3.1}) + \sigma_{n.cl.3.12} \\ \frac{\sigma_{p.cl.3.12} - \sigma_{p.cl.3.34}}{y_{cl.3.1} - y_{cl.3.2}} \cdot (b - y_{cl.3.1}) + \sigma_{p.cl.3.12} \\ \frac{\tau_{cl.3.12} - \tau_{cl.3.34}}{y_{cl.3.1} - y_{cl.3.2}} \cdot (b - y_{cl.3.1}) + \tau_{cl.3.12} \end{pmatrix} = \begin{pmatrix} 1.858 \\ 1.858 \\ 1.858 \end{pmatrix} \cdot \text{MPa}$$

if b is between the sixth and seventh pairs of integration points

$$\begin{pmatrix} \sigma_{n.b6} \\ \sigma_{p.b6} \\ \tau_{b6} \end{pmatrix} := \begin{pmatrix} \frac{\sigma_{n.cl.3.34} - \sigma_{n.cl.4.12}}{y_{cl.3.2} - y_{cl.4.1}} \cdot (b - y_{cl.3.2}) + \sigma_{n.cl.3.34} \\ \frac{\sigma_{p.cl.3.34} - \sigma_{p.cl.4.12}}{y_{cl.3.2} - y_{cl.4.1}} \cdot (b - y_{cl.3.2}) + \sigma_{p.cl.3.34} \\ \frac{\tau_{cl.3.34} - \tau_{cl.4.12}}{y_{cl.3.2} - y_{cl.4.1}} \cdot (b - y_{cl.3.2}) + \tau_{cl.3.34} \end{pmatrix} = \begin{pmatrix} 0.524 \\ 0.524 \\ 0.524 \end{pmatrix} \cdot \text{MPa}$$

if b is between the seventh pair of integration points
and the far edge of element 4

$$\begin{pmatrix} \sigma_{n.b7} \\ \sigma_{p.b7} \\ \tau_{b7} \end{pmatrix} := \begin{pmatrix} \frac{\sigma_{n.cl.4.12} - \sigma_{n.cl.4.34}}{y_{cl.4.1} - y_{cl.4.2}} \cdot (b - y_{cl.4.1}) + \sigma_{n.cl.4.12} \\ \frac{\sigma_{p.cl.4.12} - \sigma_{p.cl.4.34}}{y_{cl.4.1} - y_{cl.4.2}} \cdot (b - y_{cl.4.1}) + \sigma_{p.cl.4.12} \\ \frac{\tau_{cl.4.12} - \tau_{cl.4.34}}{y_{cl.4.1} - y_{cl.4.2}} \cdot (b - y_{cl.4.1}) + \tau_{cl.4.12} \end{pmatrix} = \begin{pmatrix} 2.586 \\ 2.586 \\ 2.586 \end{pmatrix} \cdot \text{MPa}$$

Selection of correct stress values

Stress at read-out point $a = 13.198\text{-mm}$

$$\sigma_{n,a} := \begin{cases} \sigma_{n,a1} & \text{if } 0\text{mm} \leq a \leq y_{cl,1,2} = 3.081\text{-MPa} \\ \sigma_{n,a2} & \text{if } y_{cl,1,2} \leq a \leq y_{cl,2,1} \\ \sigma_{n,a3} & \text{if } y_{cl,2,1} \leq a \leq y_{24} \end{cases}$$

$$\sigma_{p,a} := \begin{cases} \sigma_{p,a1} & \text{if } 0\text{mm} \leq a \leq y_{cl,1,2} = 3.081\text{-MPa} \\ \sigma_{p,a2} & \text{if } y_{cl,1,2} \leq a \leq y_{cl,2,1} \\ \sigma_{p,a3} & \text{if } y_{cl,2,1} \leq a \leq y_{24} \end{cases}$$

$$\tau_a := \begin{cases} \tau_{a1} & \text{if } 0\text{mm} \leq a \leq y_{cl,1,2} = 3.081\text{-MPa} \\ \tau_{a2} & \text{if } y_{cl,1,2} \leq a \leq y_{cl,2,1} \\ \tau_{a3} & \text{if } y_{cl,2,1} \leq a \leq y_{24} \end{cases}$$

Stress at read out point $b = 26.396\text{-mm}$

$$\sigma_{n,b} := \begin{cases} \sigma_{n,b1} & \text{if } 0\text{mm} \leq b \leq y_{cl,1,2} = 3.899\text{-MPa} \\ \sigma_{n,b2} & \text{if } y_{cl,1,2} \leq b \leq y_{cl,2,1} \\ \sigma_{n,b3} & \text{if } y_{cl,2,1} \leq b \leq y_{cl,2,2} \\ \sigma_{n,b4} & \text{if } y_{cl,2,2} \leq b \leq y_{cl,3,1} \\ \sigma_{n,b5} & \text{if } y_{cl,3,1} \leq b \leq y_{cl,3,2} \\ \sigma_{n,b6} & \text{if } y_{cl,3,2} \leq b \leq y_{cl,4,1} \\ \sigma_{n,b7} & \text{if } y_{cl,4,1} \leq b \leq y_{44} \end{cases}$$

$$\sigma_{p,b} := \begin{cases} \sigma_{p,b1} & \text{if } 0\text{mm} \leq b \leq y_{cl,1,2} = 3.899\text{-MPa} \\ \sigma_{p,b2} & \text{if } y_{cl,1,2} \leq b \leq y_{cl,2,1} \\ \sigma_{p,b3} & \text{if } y_{cl,2,1} \leq b \leq y_{cl,2,2} \\ \sigma_{p,b4} & \text{if } y_{cl,2,2} \leq b \leq y_{cl,3,1} \\ \sigma_{p,b5} & \text{if } y_{cl,3,1} \leq b \leq y_{cl,3,2} \\ \sigma_{p,b6} & \text{if } y_{cl,3,2} \leq b \leq y_{cl,4,1} \\ \sigma_{p,b7} & \text{if } y_{cl,4,1} \leq b \leq y_{44} \end{cases}$$

$$\tau_b := \begin{cases} \tau_{b1} & \text{if } 0\text{mm} \leq b \leq y_{cl,1,2} = 3.899\text{-MPa} \\ \tau_{b2} & \text{if } y_{cl,1,2} \leq b \leq y_{cl,2,1} \\ \tau_{b3} & \text{if } y_{cl,2,1} \leq b \leq y_{cl,2,2} \\ \tau_{b4} & \text{if } y_{cl,2,2} \leq b \leq y_{cl,3,1} \\ \tau_{b5} & \text{if } y_{cl,3,1} \leq b \leq y_{cl,3,2} \\ \tau_{b6} & \text{if } y_{cl,3,2} \leq b \leq y_{cl,4,1} \\ \tau_{b7} & \text{if } y_{cl,4,1} \leq b \leq y_{44} \end{cases}$$

Extrapolation of stresses to hot spot

Stress components at hot spot

$$\begin{pmatrix} \sigma_n \\ \sigma_p \\ \tau \end{pmatrix} := \begin{pmatrix} \frac{\sigma_{n,a} - \sigma_{n,b}}{a - b} \cdot (0\text{mm} - a) + \sigma_{n,a} \\ \frac{\sigma_{p,a} - \sigma_{p,b}}{a - b} \cdot (0\text{mm} - a) + \sigma_{p,a} \\ \frac{\tau_a - \tau_b}{a - b} \cdot (0\text{mm} - a) + \tau_a \end{pmatrix} = \begin{pmatrix} 2.262 \\ 2.262 \\ 2.262 \end{pmatrix} \text{MPa}$$

at location $y = 0\text{mm}$
(intersection)

Principal stresses

$$\sigma_1 := \frac{\sigma_n + \sigma_p}{2} + \frac{1}{2} \sqrt{(\sigma_n - \sigma_p)^2 + 4 \cdot \tau^2} = 4.525 \text{ MPa}$$

$$\sigma_2 := \frac{\sigma_n + \sigma_p}{2} - \frac{1}{2} \sqrt{(\sigma_n - \sigma_p)^2 + 4 \cdot \tau^2} = 0 \text{ Pa}$$

$$\sqrt{\sigma_n^2 + 0.81 \tau^2} = 3.044 \text{ MPa}$$